A study of the variability in the molecular structure of the human pancreas with age and its effect on islet isolation and transplantation outcomes





Rebecca Marie Spiers (BSc)
St Edmund Hall
University of Oxford

Thesis submitted for DPhil Examination
Trinity Term 2019

Supervisors: Prof. Paul RV Johnson and Dr. Sarah E Cross

Student number: 840918

Words: 48,321

Abstract

Pancreatic islet transplantation is a minimally invasive treatment that has the potential to reverse Type 1 Diabetes Mellitus in selected patients. Islets of Langerhans are isolated (extracted) from the pancreatic exocrine tissue using a collagenase and supplementary protease enzyme blend, which digests the extracellular matrix (ECM) scaffold surrounding human islets. However, the inefficiency of current enzyme blends to digest the pancreatic ECM from younger donors (those aged ≤35 years) has led to the underutilisation of donor pancreases from this age group. The hypothesis is that suboptimal digestion in younger donors is a likely consequence of age-related differences in the pancreatic ECM. However, this has not been previously studied in detail at the molecular level. The studies described in this thesis therefore aimed to define how the composition of the native pancreatic ECM is influenced by age and how this in turn affects the enzyme-mediated digestion of this structure.

Initially, the UK donor data set was analysed to determine the impact of different donor factors on islet isolation and transplantation outcomes. Whilst the success of islet isolation was clearly shown to increase with donor age, islets from younger donors demonstrated enhanced post-transplantation graft function.

High-throughput proteomics was then used to identify quantitative differences in native pancreatic matrix protein expression between younger (≤35 years old) and older (≥45 years old) donors. These novel studies identified substantial age-related differences in the pancreatic matrisome and demonstrated that a number of key matrix proteins, including several collagen and laminin chains, were significantly more highly expressed in younger donors.

Subsequently, the impact of donor age on pancreatic matrix digestion was studied through the development of a slide-based digestion assay. This involved the treatment of pancreatic tissue sections with collagenase and neutral protease, at clinically relevant concentrations. Following enzyme treatment, immunostaining was used to assess the digestion of specific matrix proteins. Once assay reproducibility was confirmed, this technique successfully demonstrated that age significantly influenced the digestion of several key matrix proteins. These results were confirmed by using Raman microspectroscopy (RMS) as a novel label-free technology to study ECM digestion. Furthermore, RMS indicated that age affected the action of collagenase to a greater extent than neutral protease.

The studies detailed in this thesis provide novel insights into the impact of donor age on the composition and digestion of the pancreatic ECM. Continued detailed analysis will aid in the development of targeted donor-specific enzyme blends to dramatically improve the overall efficiency of human islet isolation and transplantation.

Work done in collaboration

Some aspects of the work presented within this thesis were performed in collaboration with others. The Glucose Dependent Insulin Secretion Rate (GDISR) described in Chapter 2 was created by Dr John Spiliotis and colleagues at the University of Oxford. Dr Spiliotis assisted me with the calculation of the GDISR scores presented within this thesis and he performed the deconvolution of the C-peptide scores. The assessment of the C-peptide and glucose concentrations from the blood samples, obtained during and prior to the mixed meal tolerance tests, were performed by a reference laboratory in Cambridge. The data was kindly provided by the UK Islet Transplant Consortium, which our Research Group are a part of.

In Chapter 3, the Mass Spectrometry was performed under the supervision of Dr Sarah Bonham at the Target Drug Institute (TDI), University of Oxford. Dr Roman Fischer (also TDI) assisted with the analysis of these results, through the operation of the Progenesis software.

I performed all experiments and data analysis within Chapter 4. This Chapter formed the basis of a published manuscript and the co-authors of the manuscript assisted in the study design and the preparation of the manuscript for publication. In addition, I am grateful to Ms Helen Brown, who served as the 'second operator' during the validation of the described assay.

I generated the data in Chapter 6 whilst visiting the laboratory of Prof Katja Schenke-Layland at the University of Tubingen, Germany. The research presented within this Chapter was supported by Prof Schenke-Layland and other members of her research team. Specifically, Ms Julia Marzi assisted in the analysis and interpretation of the Raman imaging experiments. Dr Eva Brauchle assisted with the interpretation of the Raman spectra, from the pancreatic tissue digestion experiments.

Although I performed all of the statistical analyses contained within this thesis, statistical advice and support was provided by Dr Daniel Lunn, via the University of Oxford's Statistics Consultancy Service.

Table of Contents

Abstract 2

Work done in collaboration 3

Abbreviations 10

CHAPTER 1: General Introduction 13

1.1 Type 1 Diabetes Mellitus 14

1.2 Current Treatment Options for Restoring Normoglycaemia in T1DM 15

1.2.1 Islet Morphology 15

1.2.2 β-cell Physiology 17

1.2.3 Use of Intensive Insulin Regimes for Restoring Normoglycaemia 19

1.2.4 Insulin Pumps and Continuous Glucose Monitoring Systems 21

1.2.5 Replacement of Insulin Producing Tissue by Transplantation 22

1.2.5.1 Whole Pancreas Transplantation 23

1.2.5.2 Islet Transplantation 24

1.3 Islet Isolation and Transplantation 25

1.3.1 Islet Isolation 25

1.3.2 The History of Islet Transplantation 28

1.3.3 Islet Transplantation: Current Clinical Outlook 30

1.4 Ongoing Challenges in Islet Transplantation 34

1.4.1 Optimising Density-gradient Purification 34

1.4.2 Optimisation of Islet Culture 36

1.4.3 Immune Tolerance 37

1.4.4 Pancreas Digestion 40

1.5 Role of Exogenous Enzymes in the Isolation of Islets 41

1.6 The Pancreatic ECM; the Substrate for Enzyme Digestion 44

1.6.1 The Islet BM 46

1.6.1.1 Collagen IV 47

1.6.1.2 Laminin 48

1.6.1.3 Nidogen 50

1.6.1.4 Heparan Sulphate Proteoglycans 51

1.6.2 Interstitial Matrix 53
1.6.2.1 Collagenous components 53
1.6.2.2 Non-collagenous components 55

1.7 The Impact of Donor Factors on Islet Isolation Outcome 56
1.7.1 Cold Ischemia Time 57
1.7.2 Donor Size 58
1.7.3 Donor Age 59

1.8 The Impact of Donor Age on Pancreatic ECM Structure 63

1.9 Tailoring Isolation Blends to Younger Donor Pancreases 67

Aims of Thesis 70

CHAPTER 2: Analysis of Donor Factors on Islet Isolation and Transplantation Outcomes in the UK 71

2.1 Introduction 72

2.2 Methods 75
2.2.1 Impact of Donor and Pancreas Factors on Isolation Outcome 75
2.2.1.1 NHSBT Human Islet Isolation Data 75
2.2.1.2 Statistical Analysis for Isolation Data 76
2.2.2 Impact of donor and pancreas factors on islet transplantation outcomes 77
2.2.2.1 UKITC Islet Transplant Data 77
2.2.2.2 Statistical analysis for transplant data 78

2.3 Results 78
2.3.1 Influence of Donor and Pancreas Factors on Islet Isolation Outcomes in the UK 79
2.3.1.1 General Description of Explanatory Variables and Islet Isolation Outcome Measures 79
2.3.1.2 Factors Influencing IEQ as a Continuous Outcome Measure 79
2.3.1.3 Factors Influencing the Ability to Achieve a Transplantable Yield 81
2.3.2 Influence of Donor and Pancreas Factors on Islet Transplantation Outcomes in the UK 83
2.3.2.1 General Description of Explanatory Variables and Islet Transplantation Outcome Measures 83

2.3.2.2 Factors influencing transplantation outcome as measured by the Beta-2 score 87

2.3.2.3 Factors Influencing Transplantation Outcome as Measured by the GDISR 89

2.4 Discussion 98

2.4.1 Influence of Donor Factors on Isolation Outcomes 98

2.4.2 Influence of Donor Factors on Transplantation Outcomes 101

2.5 Conclusions 103

CHAPTER 3: The Impact of Donor Age on ECM Protein Expression in the Native Pancreas 104

3.1 Introduction 105

3.2 Methods 108

3.2.1 Determination of Experimental Age Groups 108

3.2.2 Sampling Technique 109

3.2.3 Pancreatic Tissue Homogenisation and ECM Enrichment 109

3.2.3.1 Whole Tissue Lysate 109

3.2.3.2 ECM Enrichment 110

3.2.4 Digestion of Proteins into Peptides for Mass Spectrometry 111

3.2.5 Sample Desalting and MS Injection 112

3.2.6 Proteomic Data and Statistical Analysis 112

3.2.7 Immunofluorescent staining of pancreatic Tissue Sections for ECM Proteins and Insulin 113

3.2.8 ELISA Validation 113

3.3 Results 114

3.3.1 ECM Extraction vs Whole Tissue Lysate for the Detection of Matrix Proteins 114

3.3.2 Characterisation of the Pancreatic Matrisome – Final Cohort 115

3.3.2.1 Identification of Proteins by LC-MS/MS 115

3.3.2.2 Localisation of Core Matrix Proteins to the Islet-exocrine Interface Using Immunofluorescence 117

3.3.3 Donor Age-related Differences in the Pancreatic Matrisome 120

3.3.4 ELISA Validation of Donor Age-related Changes in ECM Expression 123

3.4 Discussion 124

3.5 Conclusion 130

CHAPTER 4: Development and Validation of a Slide-based Assay for Monitoring Enzyme Digestion of Pancreatic Tissue 131

4.1 Introduction 132

4.2 Methods 133

4.2.1 Sampling Technique 133

4.2.2 Enzymatic Treatment and Immunolabelling of Tissue Sections 133

4.2.3 Quantitative Analysis of Digestion 134

4.2.4 Assay Reproducibility 136

4.2.5 Statistical Analysis 136

4.3 Results 136

4.3.1 Donor Demographics 136

4.3.2 Mixed Linear Modelling 137

4.3.3 Quantitative Analysis of Digestion 138

4.3.4 Assay Reproducibility 140

4.4 Discussion 143

4.5 Conclusion 146

CHAPTER 5: The Impact of Donor Age on Enzymatic Digestion of ECM Proteins; a Study Using Slide-based Digestion and Conventional Immuno-labelling 147

5.1 Introduction 148

5.2 Methods 149

5.2.1 Sampling Technique 149

5.2.2 Quantitative Analysis of ECM Digestion Using Slide-based Digestion and Immunostaining 149

5.2.3 Statistical Analysis for Slide-based Digestion Assay Experiments 150

5.2.4 Purified Protein Digestion 150

5.2.5 Sample Loading and Protein Electrophoresis 151

5.2.6 Gel Transfer to Nitrocellulose Membrane 151
5.2.7 Membrane Blocking and Immunostaining 152
5.2.8 Densitometry 152

5.3 Results 153
5.3.1 Donor Demographics 153
5.3.2 Mixed Linear Modelling for slide-based Digestion Assay Experiments 153
5.3.3 Digestion of ECM Proteins in Native Pancreatic Tissue and Purified Form 154
5.3.3.1 Interstitial Proteins 156
5.3.3.2 Basement Membrane Proteins 161

5.4 Discussion 167

5.5 Conclusion 172

CHAPTER 6: Raman Microspectroscopy: a Novel Approach for Comparing Digestion of the Pancreatic ECM in Different Aged Donors 173

6.1 Introduction 174

6.2 Methods 178
6.2.1 ECM Reference Standards and Digestion 178
6.2.2 Human Tissue Sampling and Preparation of Cryosections 178
6.2.3 Digestion of Pancreatic Tissue Sections and Immunofluorescent Labelling 179
6.2.4 Raman Microspectrometer set-up 180
6.2.4.1 Purified Protein Reference Standards and Enzyme-treated Proteins 180
6.2.4.2 Measurements from Native Human Tissue 180
6.2.4.3 Measurements from Digested Human Tissue 181
6.2.5 Spectral Analysis 181
6.2.6 Statistical Analysis 183

6.3 Results 183
6.3.1 Raman Spectra for Purified Matrix Proteins 183
6.3.2 Changes of ECM Fingerprint Spectra due to Enzymatic Digestion 184
6.3.3 Identification of the ECM Spectra in Human Pancreatic Tissue 187
6.3.4 Raman Detects Age-related Differences in the Digestion of the Pancreatic ECM 190

6.4 Discussion 194

6.5 Conclusion 197

CHAPTER 7: Conclusions and Proposed Future Research 199

7.1 Introduction 200

7.2 Thesis Conclusions 201

7.2.1 Overall Thesis Conclusions 201

7.2.2 The Influence of Donor Factors on Isolation and Transplantation Outcomes 202

7.2.3 Aging Causes Molecular Changes in the Composition of the Native Human Pancreas 203

7.2.4 The Pancreatic ECM is Differentially Digested Depending on Donor Age 205

7.3 Ongoing Work 207

7.3.1 Development of a Simple 'in vitro' Islet Isolation Technique 207

7.3.2 Collection of Undigested Pancreatic Tissue from Clinical Isolations 215

7.4 Conclusion 215

References 216

Publications and Awards Arising from DPhil 245

Adknowlegements 247

Appendices 248

Appendix A (Chapter 2) 249

Appendix B (Chapter 3) 256

Appendix C (Chapter 4) 266

Appendix D (Chapter 5) 267

Appendix E (Chapter 6) 270

Abbreviations

Acronym	Full Name
AGE	Advanced glycation end products
AMBIC	Ammonium bicarbonate
BM	Basement membrane
BSA	Body surface area
CBD	Collagen binding domains
CCD	Charged coupled device
CGM	Continuous glucose monitoring system
CID	Collision induced dissociation
CIT	Cold ischemia time
CLS	Closed-loop system
CMRL	Connaught Research Medical Laboratories (media)
DBD	Donation after brain death
DCCT	Diabetes Control and Complications Trials
DCD	Donation after cardiac death
DM	Diabetes mellitus
DMCU	Dimethylcasein unit
DTT	Dithiothretiol
ECM	Extracellular matrix
EDIC	Epidemiology and diabetes interventions and complications trial
EGF	Epidermal growth factor
ESI	Electrospray ionisation
FACIT	Fibril-associated collagens with interrupted triple helicases
GDISR	Glucose Dependent Insulin Secretion Rate
GSIS	Glucose stimulated insulin secretion
HbA1c	Glycated haemoglobin
HPLC	High Performance Liquid Chromatography
HS	Heparan sulphate
HSA	Human serum albumin

HSPG	Heparan sulphate proteoglycans
IAA	Iodoacetamide alkylating
IEQ	Islet equivalent
IHC	Immunohistochemistry
IM	Interstitial matrix
ISR	Insulin Secretion Rate
ITA	Islet transplant alone
LC-MS/MS	Liquid chromatography tandem mass spectrometry
LOX	Lysyl Oxidase
m/z	Mass/charge (ratio)
MALG	Minnesota Antilymphoblast Globulin
MMP	Matrix metalloproteinases
MMT	Mixed meal test
MS	Mass spectrometry
MSC	Mesenchymal stem cells
NADH	Nicotinamide adenine dinucleotide
NAIDS	North American Islet Donor Score
NP	Neutral Protease
PAK	Pancreas after kidney (transplant)
PC	Principle component
PCA	Principle component analysis
PDX-1	Pancreatic duodenal homeobox-1
PGs	Proteoglycans
PIC	Protease inhibitor cocktail
PKD	Polycystic kidney disease like-domains
PTA	Pancreas transplant alone
PTFE	Polytetrafluoroethylene
PTM	Post translational modification
PZU	4-phenyl-azo benzyl-oxycarbonyl-Pro-Leu-Gly-Pro-D-Arg Unit
Q-Q	Quantile-quantile (plot)
r.t	Room temperature

RGD	Arginine-glycine-aspartic acid
RMS	Raman microspectroscopy
SD	Standard deviation
SEM	Standard error of the mean
SPK	Simultaneous pancreas and kidney (transplant)
T1DM	Type 1 diabetes mellitus
T2DM	Type 2 diabetes mellitus
TCA	Tricarboxylic acid
TLM	Two Layer Method
T-regs	T-regulatory cells
UKITC	UK Islet Transplant Consortium
UW	University of Wisconsin (solution)
VDCC	Voltage dependent Ca^{2+} channels
VEGF	Vascular endothelial growth factor
WIT	Warm ischemia time

CHAPTER 1

General Introduction

1.1 Type 1 Diabetes Mellitus

Diabetes mellitus (DM) is a group of metabolic diseases characterised by hyperglycaemia resulting from defects in insulin secretion, insulin action, or both [1]. Two main forms of DM are recognised, namely Type 1 DM (T1DM) and Type 2 DM (T2DM). T1DM results from a deficiency of insulin secretion through the irreversible autoimmune targeted destruction of insulin-producing β-cells within the pancreatic islets of Langerhans [1], whereas T2DM is characterised by insulin resistance and a lack of supplementary insulin response. DM is a growing pandemic. According to the 7th edition of the International Diabetes Federations "Diabetes Atlas" 415 million people worldwide suffer from DM, of which 5-10% are classified as having T1DM [2]. It is also predicted that the number of individuals living with T1DM in the UK is set to increase from 400,000 (2010/2011 period) to an estimated 650,000 by 2035 [3].

The mainstay treatment for T1DM to date is insulin replacement therapy. Indeed, the Nobel Prize winning discovery of insulin made by the Canadian born physicians Charles Best and Frederick Banting at the University of Toronto in 1922 [4] transformed T1DM from a fatal disease to one that could be managed with frequent exogenous insulin injections. However, despite the effectiveness of exogenous insulin regimes in treating the acute metabolic complications of the disease, the challenge remains to prevent the life-changing chronic secondary complications. Such complications result from years of persistent or fluctuating hyperglycaemia [1]. The secondary complications of T1DM are usually divided into 2 broad categories: microvascular complications and macrovascular complications. Microvascular complications include conditions such as retinopathy, neuropathy and nephropathy, which can retrospectively result in loss of vision, loss of limbs, and renal failure [1]. Cardiovascular disease is the most common macrovascular complication of diabetes, with individuals with T1DM displaying a ten-fold increased risk of developing cardiovascular related disorders, when compared with their non-diabetic counterparts [5]. Not only do these chronic complications severely impact on the quality of life of people with diabetes, but

they also have a significant economic impact on health care provision. In the 2010/2011 period the UK National Health Service (NHS) spent around £720 million in the treatment of secondary associated disorders that resulted from T1DM [3]. This is estimated to increase to £1.3 billion by 2035 [3]. These figures highlight the desperate need to improve the control of diabetes, and importantly, to reduce the incidence of these chronic complications. An unequivocal body of evidence has shown that controlling blood glucose concentrations near the normal physiological range can prevent the onset, as well as slow the progression, of chronic complications associated with T1DM [6]. The translational challenge is to know how best to do this, balancing the promise of novel treatments, with their risks to the patient. There are several different approaches to restoring normoglycaemia in T1DM, and these are each reviewed in the next Section.

1.2 Current Treatment Options for Restoring Normoglycaemia in T1DM

1.2.1 Islet Morphology

Before discussing the different ways of achieving normal glucose control in people with T1DM, it is first helpful to understand the complex process of normal insulin secretion from pancreatic islets. First described in the doctoral thesis of Paul Langerhans in 1869 [7], islets are multi-celled structures located within the pancreas. The pancreas performs both endocrine and exocrine functions. The exocrine portion comprises about 98% of the pancreas and it is composed of acinar and ductal cells. Acinar cells synthesise, store and secrete digestive enzymes, which are transported towards the duodenum by the pancreatic ductal network [8]. The endocrine portion of the pancreas is comprised of the islets of Langerhans ('islets'), which are essential in maintaining normal glucose homeostasis. Islets are clusters of endocrine cells that are dispersed throughout the exocrine pancreas, making up around 1-2% of the total pancreatic mass. The human pancreas contains within the vicinity of 3.2 million islets, comprising a total volume of around 2ml [9]. The average human islet diameter is 150µm. This fact underpins the theory behind the standardised

methods used for counting human islets that try to adjust for differential islet function. One Islet Equivalent (IEQ) is deemed a standard size islet measuring 150µm in diameter, and all counted islets are compared with this standard, converted to a volume, and expressed as a proportion of it. For example, a 50µm islet is one third of an IEQ and a 300µm islet is the equivalent of two IEQs. One IEQ contains around 1,500 individual cells [10]. Importantly, these cells fall into 5 main categories: glucagon secreting α cells, insulin secreting β cells, somatostatin secreting δ cells, pancreatic polypeptide secreting PP cells and epsilon cells secreting ghrelin [11, 12]. Together these cells control glucose homeostasis within a tight range (around 4-7 mmol/l in the human). Insulin and glucagon are counter-regulatory hormones. Briefly, whilst insulin lowers blood glucose levels by initiating the cellular uptake of glucose, glucagon raises blood glucose by stimulating glycogenolysis and gluconeogenesis [13]. Somatostatin is known to regulate both the secretion of insulin and glucagon, whereas pancreatic polypeptide is thought to be important in inhibiting glucagon secretion [13, 14].

The complex cytoarchitecture of islets, both in terms of cell composition and arrangement, is species dependent. In mouse islets, β-cells make up approximately 80% of the islet, with α-cells and δ-cells comprising the remaining 14 and 6%, respectively [15]. Murine islets have a distinct β-cell core, with the non-insulin producing cells surrounding the periphery [11, 15]. In contrast, human islets, (and islets from non-human primates) have far fewer β-cells than murine islets but a higher percentage of α-cells. As such, human islets are estimated to be comprised of approximately 50-60% β-cells, 30-50% α-cells and around 10% δ-cells [10, 11, 16]. Indeed, these estimations are made based on cell number; the proportion of each cell type changes if assessments are made on the basis of cell volume [10]. Further differences between human and mouse islets are observed in the arrangement of the distinct cell types; in human islets there is a lack of an organised β-cell core or other subdivisions, with cell types heterogeneously scattered throughout the islet [11, 16]. Such an arrangement facilitates paracrine interactions and allows islets (i.e. α-cells) to respond to lower glucose concentrations than murine islets [11]. Islet density is affected by anatomical region, and

is higher in the body and tail regions of the pancreas, as opposed to the head and neck [9, 17]. Islets are richly vascularised. The pancreas receives around 1% of the total cardiac output [18], and despite only comprising around 1-2% of the total pancreatic mass, islets receive up to 20% of this arterial blood flow [19, 20]. The islet capillary network is well adapted to the high degree of blood flow, and is often likened to that of the glomerular network of the kidney; several afferent arterioles penetrate the islet interior, exiting through efferent venules that eventually empty into the larger veins [12]. The capillaries are also richly fenestrated, allowing the endocrine cells to efficiently release hormones into the blood stream, in response to current blood glucose levels [21]. In addition to a large capillary network, human islets are innervated by autonomic nerves. Using high resolution confocal imaging, Rodriguez-Diaz and colleagues were able to show that sympathetic nerves enter the interior of human islets, where they were co-localised with intra-islet blood vessels. This suggests that the sympathetic nervous system excises its control over islets by modulating the adjacent blood flow, as opposed to a direct cellular interaction/innervation that is present in murine islets [22]. Although parasympathetic nerves were also detected, few penetrated the islet interior [22].

1.2.2 β-cell Physiology

The pancreatic β-cell is electrically excitable, with changes in membrane action potential resulting from glucose stimulation, which lead to insulin secretion. The overall mechanisms of insulin secretion are complex, and for the purpose of this thesis are only briefly summarised (see also Figure 1).

The rapid diffusion of glucose across the β-cell is facilitated by members of the GLUT family of glucose membrane transporter proteins. GLUT 2 is responsible for glucose diffusion in rodents, and until recently it was also referenced as facilitating the passage of glucose in human β-cells [23, 24]. However, GLUT-2 expression is low on human islets [25, 26]. Recent studies examining the mRNA and protein expression of GLUT transporters on human islets show strong expression of GLUT 1

and 3, suggesting that these are the main transporter proteins in humans [25]. Once inside the cell glucokinase phosphorylates glucose to glucose-6-phospate, which is believed to be a rate limiting step to insulin secretion [26, 27]. The phosphorylated glucose is then metabolised by glycolysis (in the cytosol) and the tricarboxylic acid (TCA) cycle and electron transport chain (in the mitochondria), leading to an increase in cellular ATP. This results in the closure of the ATP dependent K^+ gated channels, with the elevated concentration of cytoplasmic K^+ causing depolarisation of the β-cell membrane [28]. The positive increase in membrane action potential causes a cellular influx of Ca^{2+}, by facilitating the opening of voltage dependent Ca^{2+} channels (VDCC) [29]. An increase in cytoplasmic Ca^{2+} concentration initiates the movement of vesicles containing pre-stored insulin granules to the membrane, where they fuse with the cell membrane and become released by exocytosis [30]. Upon release, insulin enters the portal circulation where up to 80% of the secreted insulin is degraded during the first liver passage [31]. The remnant insulin enters the arterial circulation, where it binds to insulin receptors on the surface of target cells [32]. Through complex signalling cascades, this binding leads to the translocation of the GLUT 4 glucose transporter protein from the cytoplasm to the cell membrane, facilitating the diffusion of glucose across the cell membrane and into the cytoplasm of the cell. Here, glucose can either be used for the generation of ATP, or converted to glycogen for storage [32].

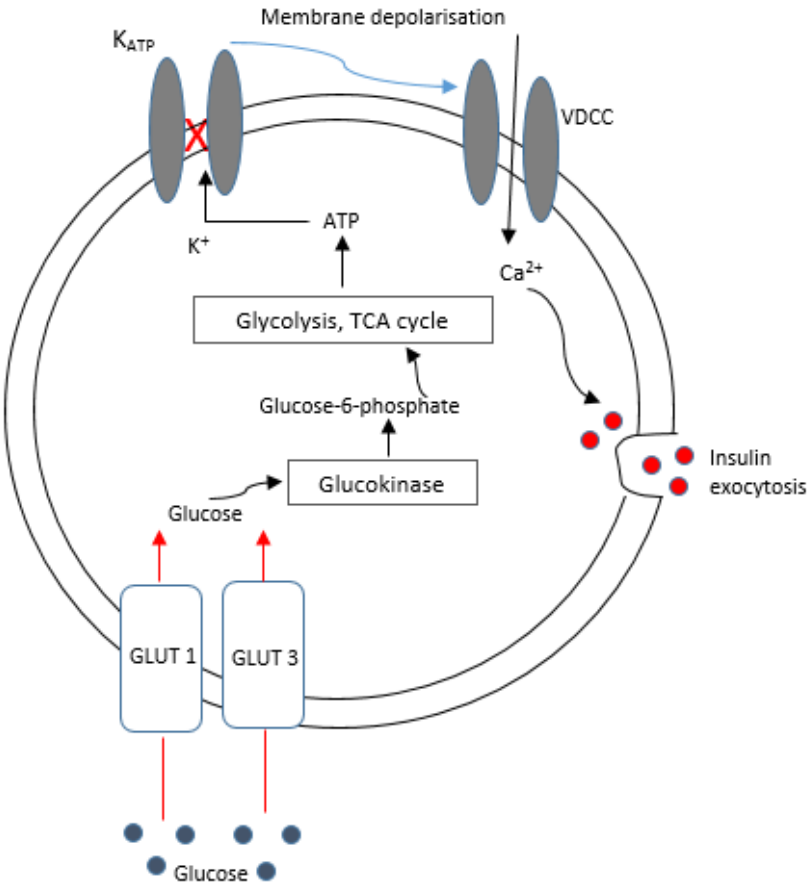


Figure 1: Glucose mediated insulin secretion from the human pancreatic β-cell
Influx of glucose across the cell membrane is facilitated by glucose transporter proteins GLUT 1 and 3. Inside the cell, glucose is phosphorylated to glucose-6-phospate by glucokinase. Glucose-6-phosphate is metabolised by glycolysis and the TCA cycle to produce ATP, which closes the K_{ATP} channels resulting in membrane depolarisation. Voltage dependent calcium channels (VDCC) open, leading to an increase in cytoplasmic Ca^{2+} and leading to exocytosis of insulin granules.

1.2.3 Use of Intensive Insulin Regimes for Restoring Normoglycaemia

An indisputable body of evidence has now demonstrated that the administration of intensive insulin regimes significantly reduces the incidence and development of the secondary complications associated with T1DM. Central to these findings were the results from the Diabetes Control and Complications Trials (DCCT) performed in the early 1990's [6]. 1441 participants with T1DM were recruited into the study and followed up over a mean duration of 6.5 years. Participants

were divided into one of four groups, primarily based on the absence or presence of mild retinopathy (respectively termed the 'primary intervention cohort' and 'secondary intervention cohort'). Each intervention group was further divided, with half the participants receiving 'conventional' or 'intensive' insulin therapies. Whereas conventional therapy entailed 1-2 daily insulin injections, the intensive group received 3 or more insulin doses daily, or an external insulin pump. The exact dosage of insulin was frequently modified following intensive self-regulatory testing of blood glucose levels. Strict criteria for maintaining glycaemic control within tight ranges were a prerequisite of intensive therapy. In the primary prevention cohort intensive insulin therapy reduced the average risk of developing retinopathy by 76% and decreased the progression of retinopathy by 54% in the secondary intervention group. Nephropathy risk was reduced by 34% and 43% in the primary and secondary groups respectively, whereas neuropathy risk was reduced by 69% and 57%. The combined reduction in macrovascular complications was 34% in the intensive groups [6]. During the subsequent Epidemiology and Diabetes Interventions and Complications (EDIC) follow-up study, 93% of the original DCCT patients were observed over a 30-year period [33]. The EDIC study demonstrated that DCCT patients in the intensive insulin therapy group benefitted from a 30% reduced risk of cardiovascular disease. This was facilitated through the maintained reduction in glycated haemoglobin (HbA1c). As a biomarker of glucose homeostasis, HbA1c is a commonly used for determining the likelihood of a patient developing secondary complications [34]. HbA1c is the product on a non-enzymatic reaction between glucose and the beta chain of haemoglobin, which provides an estimate of the average glucose levels over a 3-month period. Levels of 6.5% or higher indicate diabetes, whereas between 4 - 5.6% is considered a normal range. Therefore, the reduction in HbA1c seen in this trial substantiates the effectiveness of intensive insulin regimes in maintaining long term health [33].

Despite the clear advantages of using intensive insulin regimes to prevent and control the chronic complications of T1DM, there were several risk factors associated with their usage, the most marked of which was a significant increase in severe hypoglycaemic episodes [6, 35]. Such episodes

were defined at those requiring third party intervention and were approximately three-fold higher in the group receiving the intensive as opposed to conventional therapy [6, 35]. The enhanced risk of suffering from life-threatening hypoglycaemic incidents cannot be ignored when considering the efficacy of intensive insulin regimes in reducing and stabilising the secondary complications of T1DM. In addition, the requirement to obtain frequent blood glucose readings and perform frequent insulin injections may become intolerable for some patients.

1.2.4 Insulin Pumps and Continuous Glucose Monitoring Systems

Insulin pumps, or continuous subcutaneous insulin infusion (CSII) devices, operate by secreting continuous amounts of basal insulin, as well as variable post-prandial boluses. The use of an insulin pump negates the need to administer frequent daily insulin injections, and as such has transformed the management of T1DM for many patients. However, although favourable for many, isolated use of an insulin pump has not demonstrated a clear benefit over utilising multiple insulin injections for improving glycaemic control [36]. Alternatively, coupling an insulin pump with a continuous glucose monitoring system (CGM) has demonstrated clear advantages over frequent injections for promoting tight glycaemic control [37, 38]. Such devices work based with a closed-loop system (CLS), where insulin delivery from the pump occurs in response to the blood glucose measurements obtained from the interstitial fluid. Measurements are automatically and continuously transmitted to a connected blood glucose monitoring device [39]. As such the basal insulin infusion from the pump is gradually modified, based on glycaemic variation [39]. Due to the parallels between these devices and the physiological working mechanism of the pancreas, the devices are often likened to an 'Artificial Pancreas'. Several studies have tested the efficacy of CLS. One such trial investigated the effects of a CLS on glycaemic control, enrolling 30 adolescent and 94 adult participants with T1DM [37]. The study was able to show a significant reduction in HbA1c over the study period (7.7% to 7.1% and 7.3% to 6.8%, for adolescents and adults respectively). Although promising, the absence of a control group (i.e. a cohort receiving standard insulin injections), made it impossible

to conclude that such a device is beneficial over more conventional therapies. Furthermore, the relatively short term 3-month follow-up period of the study does not provide evidence for long term efficacy [37]. Another study showed that CLS was superior to a standard insulin pump for reducing hypoglycaemia in 18 adult participants with T1DM, however, once more, the study duration was short, with the intervention only covering a 40 hour period [38]. The next generation of devices introduced the concept of CLS dual-hormonal systems; secreting glucagon in addition to insulin, which is beneficial for avoiding hypoglycaemia. In a randomised cross over study, preadolescent children were treated with either a conventional insulin pump, or with a dual-hormone CLS. The dual-CLS was not only superior for lowering blood glucose levels to a more normal range, but also reduced hypoglycaemia [40]. Although the 'Artificial Pancreas' offers an attractive treatment option for those with T1DM, their use is not without limitations. Such limitations include the 5-6 minute lag between blood and interstitial fluid glucose levels [41], which may result in inaccurate insulin dosing. In addition, CLS devices have been associated with dermatological complications (including eczema and skin legions), which presented in one third of adult participants [42]. Furthermore, owed to the mechanical nature of pump devices, there is always an inherent risk of failure [43].

1.2.5 Replacement of Insulin Producing Tissue by Transplantation

As T1DM results from the destruction of the endocrine portion of the pancreas, another attractive treatment option is to reverse this process by replacing the tissue by transplantation. β-cell replacement (a misnomer because all islet cells are replaced), can be performed either by whole pancreas transplantation, or by specifically isolating and infusing the islet tissue alone (islet transplantation). β-cell replacement by transplantation is currently the only treatment option that truly restores the intricate balance of normal glucose homeostasis, owed to the islets inherent ability to respond instantaneously to current blood glucose levels [43]. However, given the present life-long immunosuppression that is a prerequisite for any allogeneic transplant, a careful

assessment must be made of the risk versus benefit for the patient. Therefore, indications for transplantation are limited to a subset of patients. The choice between an islet and a pancreas transplant is then tailored based on recipient needs. For whole pancreas transplantation the main indication is the progression of secondary complications (mainly renal failure), whereas for islet transplant recipients the main target is to restore glycaemic control in patients who are liable to glycaemic instability and hypoglycaemic unawareness [44].

1.2.5.1 Whole Pancreas Transplantation

Whole pancreas transplantation has been practised for over 50 years, with the first simultaneous pancreas and kidney (SPK) transplant having been performed at the University of Minnesota, Minneapolis, in 1966 [45]. However, these early procedures were associated with a high risk of mortality, with a report from 1970 showing an SPK recipient survival rate of less than 50% [46]. With this said, pancreas transplantation outcomes have improved greatly over the last few decades, with an 88% 5-year post-op patient survival rate in the UK [47]. This coincides with a 79% 5-year graft survival rate for SPKs (2009-2013 period; graft failure defined as permanent return to insulin dependence) [47]. These figures are in line with international data from the International Pancreas Transplant Registry, which show a 71% SPK graft survival rate at 5 years (2007-2011 period) [48].

However, whole pancreas transplantation still remains a major surgical intervention, with significant morbidity resulting from graft thrombosis and pancreatitis [43]. Given that these complications often result from the implanted exocrine tissue, and that T1DM is characterised by the targeted loss of islet function, it can be argued that transplanting the entire gland is in fact surplus to requirements, unless a simultaneous renal graft is required to justify it. Isolating and infusing the 1-2% endocrine component of the pancreas is clearly an attractive alternative.

1.2.5.2 Islet Transplantation

Islet transplantation is a minimally invasive treatment that is well tolerated. Islets are extracted (isolated) from a donor pancreas and infused into the recipients portal vein, under a local anaesthetic using radiological techniques [49]. Throughout the infusion, frequent portal vein pressure monitoring occurs. The islets become lodged in the liver, where they engraft and begin to secrete insulin in response to glucose stimulation. Given the simplicity and non-invasiveness of an islet transplant, the incidence of associated complications is low and mortality negligible [43, 44]. Since the first reported case of insulin independence following allogenic islet transplantation in 1990 [50], islet transplantation has become an established procedure for the treatment of T1DM, with the procedure becoming government-funded in several countries, including the UK [51]. The gap between the efficiency of islet and pancreas transplantation, in terms of clinical outcome, continues to close. However, it is important to acknowledge that it can be challenging to compare clinical outcomes between the two types of transplant due to significant variations in procedure and indication. Whilst transplantation of isolated islets is usually performed alone (islet transplant alone; ITA), pancreas transplantation is usually performed either as an SPK, or proceeding a kidney transplant (pancreas after kidney; PAK). Although it is less common to perform a pancreas transplant without combining it with a kidney (pancreas transplant alone; PTA), a recent study completed in San Francisco compared the efficacy and cost efficiency of ITA and PTA, in nonuremic patients [52]. Interestingly, insulin independence rates were comparable between the two groups (90% and 93% at 1 year, and 70% and 64% at 3 years, for ITA and PTA respectively), as was glycaemic control. Although the authors reported that the over-all total costs of the two procedures were comparable (which, for the ITA, included isolation costs for up to two infusions) the authors fail to mention the number of isolations that were required to achieve islet yields suitable for transplantation. The recipients were also significantly older in the ITA group, with a significantly longer duration of T1DM [52]. Regardless, the promising clinical outcomes, together with the low associated incidences of morbidity and mortality, make islet transplantation an attractive

treatment option for a subset of patients with T1DM. In the next Section the history and current outlook of islet isolation and transplantation are considered.

1.3 Islet Isolation and Transplantation

1.3.1 Islet Isolation

The main prerequisite for any successful islet transplantation procedure is the requirement to isolate a sufficient number of intact and viable islets from the donated human pancreas. Islet isolation is a multi-step sequential process, which takes an average of 5-6 hours to complete. The key components of the islet isolation procedure are summarised in Figure 2 (page 32) and include: donor organ procurement, continuous enzymatic and mechanical pancreas dissociation to liberate islets, islet purification and islet culture. Transplantable cells are then infused into the recipients' liver. Indeed, in the current era of islet transplantation it is possible to isolate transplantable yields from around 50% of pancreases processed worldwide [43], although this achievement has been only reached through continued protocol optimisation, facilitated by collaborative efforts throughout the global islet community, which are summarised below.

Historically, although the separation of the endocrine and exocrine pancreas dates back to the early 1900s [53], the only means of achieving this separation at that time was through manual microdissection. This separation technique proved laborious and technically challenging, due to the islets firm attachment to the surrounding exocrine tissue [54]. The introduction of collagenase for the dissociation of the guinea pig pancreas by Moskalewski in 1965 led to the liberation of many more morphologically intact free islets, which could then be microscopically handpicked from the pancreatic digest [55]. This method was adapted to the rodent pancreas, with modifications including the distension of the pancreas with cold saline prior to enzyme digestion, and the use of a discontinuous sucrose density gradient to separate the islets from the acinar tissue as opposed to islet handpicking [56]. Subsequent attenuations incorporated the use of dialysed Ficoll, as an

alternative to sucrose for discontinuous density purification, owed to its improved osmotic environment [57, 58]. However, although efficient in isolating islets from the rodent pancreas, these protocols remained largely ineffective for the human pancreas, preventing the advancement of human islet transplantation. It wasn't until the establishment of several revolutionary protocols during the 1980s that the efficiency of human islet isolation improved. Novel developments included the introduction of intra-ductal collagenase infusion, which following its success in canine models [59], was adapted to the human pancreas by Gray and colleagues at The University of Oxford [60]. The method involved the injection of pre-warmed collagenase solution, containing calcium chloride, through the pancreatic duct, with the enzyme infused organ held at 37°C for 20 minutes in HBSS, with gentle shaking. Tissue was disrupted by mechanical teasing before being passed through different sized meshes to separate the sufficiently cleaved islets from those that remained embedded in exocrine tissue. Purification was achieved using discontinuous Ficoll based gradients, taking advantage of the differential densities of islets and exocrine tissue [60]. On average this method liberated 1,000 islets per gram of pancreas, with preparation purity ranging from 10-40%. The superiority of enzyme ductal injection was highlighted, as well as the importance of pre-warming the enzyme solution, and the use of calcium chloride for enhancing enzyme activity. Despite the improvement in enzyme delivery protocols, islet isolation continued to involve implementation of techniques that were mechanically traumatic to islets, including teasing tissue apart with forceps and passing the digest through needles and tissues macerators [60-62], all of which pose a significant risk of islet fragmentation. A breakthrough came in 1988 when researchers at the University of Missouri proposed a semi-automated approach for human islet isolation [63]. Enzyme pancreatic infused tissue was placed into a heated bioreactor chamber with mechanical digestion facilitated by glass marbles and external shaking. Cleaved islets were small enough in size to progressively pass through the 280μm wire mesh at the top of the chamber, where they exited through an outlet port into a cooling circuit. Recirculation of the fluid continued until free islets were detected in biopsies obtained from a sample port, promoting a switch to an open circuit for

islet collection, which bypassed the heating circuit. Fresh HBSS was introduced during the islet collection phase, to further reduce the enzyme activity, and the free islets collected into cooled flasks. Isolations were successfully performed on 10 pancreases using this method, obtaining an average yield of 160,000 islets per organ, with an average purity of 78% [63]. The success was attributed to the use of a continuous digestion circuit, which allowed uniform pancreas digestion through the liberation of free islets with the continued extraction from undigested tissue. The complete digestion was also reflected in the chamber at the end of the procedure, when only the intact fibrous network of vessels and ducts remained. The minimal traumatic action of the procedure was demonstrated by good islet morphology, and insulin response to glucose, measured following overnight culture [63]. The semi-automated method greatly increased the quality and quantity of islets that could be extracted from the human pancreas, and it still remains an integral part of the isolation procedure today. The following year, the islet purification process was further improved and up-scaled by incorporating the use of a Cobe 2991 cell processor, a device routinely used at the time for separation of blood products [64, 65]. Although the Cobe system continued to be used alongside a discontinuous gradient, it enabled rapid high-throughput processing of large volumes of pancreatic digest, substantially improving the efficiency of human islet isolation [66]. Separation of cells occurred within a rotating bag, located on top of a drum containing hydraulic fluid. The expansion of hydraulic fluid forces the cells out of the bag in a controlled manner, allowing islets to be separated from the exocrine tissue based on their differing densities [67]. However, when utilising a discontinuous gradient, the migration of cells throughout the system is limited, preventing an efficient separation [67]. The implementation of a continuous gradient system overcame this issue [67]. Continuous gradients are achieved by mixing ‘low’ and ‘high’ density gradient medium, with continuous delivery into the Cobe bag. The resulting linear continuous density gradient, unlike a discontinuous system, contains multiple density interfaces [67]. The pancreatic digest is then loaded from the top, and following centrifugation up to 10 fractions are collected for purity assessment [67]. Due to its efficiency, continuous density

purification using a Cobe remains the universally accepted method for separating islets from exocrine tissue for human islet transplantation.

1.3.2 The History of Islet Transplantation

In 1972, Ballinger and Lacy performed the first successful islet transplant procedure in rodents, successfully ameliorating hyperglycaemia in a streptozotocin induced diabetic rat model. Islets that had been successfully isolated from healthy rats of the same strain were transplanted into the peritoneal cavity [68]. Research was also underway to determine the optimal transplantation site for islets. The benefits of intraportal infusion were demonstrated when normoglycemia was restored in rats receiving isografts to the liver, but not when islets were placed into subcutaneous and intraperitoneal cavities [69]. This study was responsible for introducing the concept of islet infusion into the liver, which still remains the universally accepted transplantation site. The success of islet transplantation in rodent models encouraged trials in larger animal models [59, 70, 71], before the first reported human trials in the 1980s. Seven recipients with T1DM received islet grafts following a kidney transplant from unrelated donors at the University of Minnesota [72]. All recipients remained insulin dependent, although there was evidence of transient islet function in some of the patients [72]. The increase in quantity and quality of islets produced by the semi-automated method, led to the first case of insulin independence following islet transplantation in 1990 [50]. The 36-year-old recipient received 800,000 IEQs, isolated from 1.4 pancreases. The islets were transplanted into the liver through the portal vein, secondary to a kidney transplant. Cyclosporin was already being taken to prevent rejection of the kidney transplant, but in addition a weeks' worth of Minnesota Antilymphoblast Globulin (MALG) was prescribed. All exogenous insulin therapy was stopped at 10 days post-transplant, with the recipient maintaining good glycaemic control. The insulin independence continued to the end of the reported follow-up period of 22 days [50]. Warnock and colleagues shared their experiences of achieving normoglycaemia

and insulin independence in an islet after kidney transplant recipient, following the infusion of 10,000 IEQ/Kg. This incorporated a combination of freshly isolated islets (1 donor) in addition to those that had been cryopreserved (pooled from 4 donors). The immunosuppressive regime consisted of a mixture of cyclosporin, MALG, prednisolone and azathioprine. The graft continued to function during the 3-month follow-up period, with insulin treatment withdrawn at day 69 post-transplant [73]. The same year insulin independence was reported for the first time in a recipient who received a transplant comprised of islets from a single donor. The recipient had previously received a kidney transplant from an unrelated donor, and remained insulin independent for five months, before exogenous insulin therapy was resumed [74]. Human islet transplantation trials continued to be performed throughout the 1990s, but to only moderate success. A report from The Islet Transplantation Registry in 1999 (http://www.med.uni-giessen.de/itr/) summarised the results from 267 allogenic islet transplants, which had been reported from 1990 to 1998. Only 12% of recipients achieved insulin independence, which dropped to 8% at one-year follow-up.

The turn of the century welcomed a new era for islet transplantation, with the introduction of the 'Edmonton protocol', by James Shapiro and Jonathon Lakey, at the University of Alberta, Canada [75]. This modified protocol achieved insulin independence in seven consecutive recipients who received an islet transplant alone, and included the introduction of a new steroid-free immunosuppressive regime. Conventionally used immunosuppressant agents at the time (cyclosporin, MALG, and azathioprine) were replaced with glucocorticoid free drugs: sirolimus, low dose tacrolimus and daclizumab (an interleukin-2 receptor antibody). Further modifications included the infusion of a larger islet mass (on average 11,547 IEQ/Kg of recipient), augmented by using two or more donors, and the use of human albumin in place of animal derived serums during processing. All seven recipients remained insulin independent during the 1-year follow-up, which resulted in a huge resurgence of interest in islet transplantation.

Despite these initially promising results, only 58% of patients achieved insulin independent in the multicentre international trial of the Edmonton protocol, with just 31% retaining this insulin independence for the full 2-year study period [76]. However, despite the lower than anticipated levels of insulin independence, 67% of recipients retained at least partial graft function [76].

1.3.3 Islet Transplantation: Current Clinical Outlook

Islet transplantation can significantly enhance quality of life, even if insulin independence is not achievable. Indeed, the primary indication for ITA worldwide remains life-threatening hypoglycaemia. Hypoglycaemic unawareness is characterised by the loss of autonomic ability to detect low blood glucose levels, which usually proceeds unstable glycaemic control (sometimes termed 'brittle' diabetes). The resulting lack of preventive action may lead to a severe hypoglycaemic event, requiring third party intervention [77].

Islet transplantation has been shown to reduce the number of annual severe hypoglycaemic events by, on average, 98% at 2 years post-transplantation [51]. Hypoglycaemic awareness is also significantly improved [51], which has been shown to be maintainable even if an islet graft was to later fail [78]. As such, life-threatening hypoglycaemic unawareness has become the primary indication for islet transplantation in many centres around the world [79, 80]. A small amount of data also suggests that islet transplantation is capable of reducing the progression of secondary complications [81].

Due to the continued refinements in isolation and transplantation protocols, both the short and long term outcomes of clinical islet transplantation continue to improve. Between 1999 and 2015, 1086 allogenic islet graft recipients were reported to the Collaborative Islet Transplant Registry (CITR). This data, received from 37 participating centres, totalled 2150 infusions from 2619 donors [82]. 877 recipients received an ITA, whereas 209 also received a kidney. At 1-year post-transplant approximately 50% of all patients remained insulin independent, which was maintained in 30% of

the patients for up to 5 years. Importantly, the absence of severe hypoglycaemic events was achieved in 90% of patients, during the five-year follow-up period [82], further substantiating the effectiveness of islet transplantation for the treatment of 'brittle' diabetes. Recent clinical trials further justify islet isolation as a treatment option for T1DM, which include a multi-centre licence enabling phase III trial, completed by the Clinical Islet Transplant (CIT) consortium [80]. This trial involved 8 centres across North America, with results indicating that 87.5% of the 48 enrolled participants met the primary study endpoint, defined as maintaining a HbA1C ≤7% and remaining free of severe hypoglycaemic events during the first year post-transplant. This dropped to 71% after two years. Insulin independence, though not an endpoint measurement, was achieved in 52% of patients at 1 year [80]. Similar results were achieved in the multicentre Australian trial using the same endpoints, with 82% of the 17 recipients meeting the primary endpoint across 3 centres. In addition, insulin independence was achieved in 53% of participants, for a median duration of 26 months [79]. Clinical outcomes reported by the Swiss/French 'GRAGIL' network were also comparable, with 83% of the 24 recipients reaching the primary endpoint (as defined above) at one year. This study also provided evidence for long term graft function, showing that 58% of patients continued to meet the clinical endpoint at the end of the five-year study follow up period [83]. However, it must be noted that transplantation of a relatively large islet mass was necessary to achieve these results in all three trials (on average approximately 12,000, 15,000 and 9,000 IEQ/Kg for the US and Australian, and GRAGIL trials respectively). In all instances, to achieve this islet mass up to three infusions were required, utilising up to three donor organs per recipient. Taken together with the fact that transplantable yields are only obtainable from approximately half of the pancreases that are processed [43], it becomes clear that sub-optimal islet isolation outcomes are preventing islet transplantation from being more widely available as a treatment option for patients with unstable T1DM.

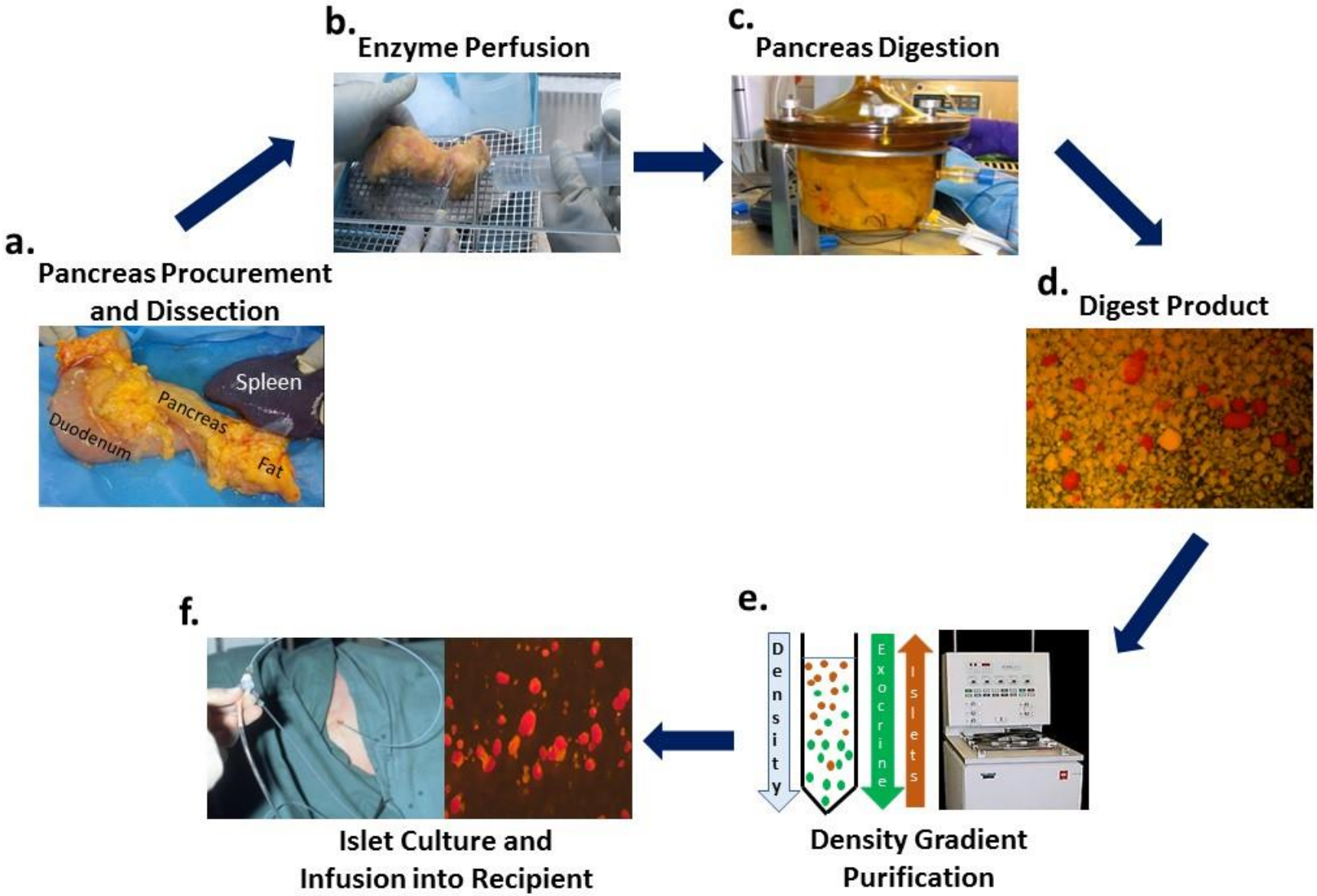

a.
Pancreas Procurement and Dissection
Spleen
Pancreas
Duodenum
Fat
b.
Enzyme Perfusion
c.
Pancreas Digestion
d.
Digest Product
e.
Density
Exocrine
Islets
Density Gradient Purification
f.
Islet Culture and Infusion into Recipient

Figure 2: Schematic overview of the human islet isolation process
Islet isolation is depicted from receipt of the donor pancreas to the infusion of islets into the recipient. **a)** Pancreas is retrieved from the donor *en-bloc.* The spleen, duodenal segment and exogenous fat are removed; **b)** commercially available collagenase-based enzymes are infused via cannulation of the pancreatic duct; **c)** the enzyme infused pancreas is loaded into a bioreactor device; the 'Ricordi chamber', where the pancreas is digested both enzymatically and mechanically in a continuous sterile closed-loop circuit; **d)** the resulting digest contains a mixture of islets (seen in red, stained with dithizone) and exocrine tissue; **e)** the digest is purified using a continuous density gradient purification system on a COBE 2991 cell processor. Islets are isolated from exocrine tissue based on the differing densities; **f)** the purified islets are cultured for up to 48 hours, allowing sterility and quality tests to be performed, as well as allowing transplant logistics to be arranged. Following this the islets are infused into the recipient under local anaesthetic via cannulation of the portal vein using interventional radiological techniques. The islets engraft into the liver, where they begin to produce insulin.
Images from the DRWF Human Islet Isolation Facility in Oxford, UK

1.4 Ongoing Challenges in Islet Transplantation

The steady increase in the number of islet transplant recipients (7% increase from 2013 to 2015; CITR 10th Annual Report [82]), ensures that the production demand for large numbers of highly purified and viable islets continues to rise. Although islet isolation has progressed tremendously over the last two decades, the progress remains insufficient to meet this augmentation. As the extraction of islets from the pancreas is a multi-stage sequential process, many of the procedural steps have been targeted in an attempt to maximise isolation outcomes. Strategies include improving density-gradient purification systems to further enhance separation of the islets from the exocrine tissue [84-88] and the optimisation of tissue culture conditions to minimalize loss of islets during culture [89-92]. Current research efforts also aim to renounce the need for immunosuppression by developing immunoisolation (i.e. islet encapsulation) [93-95] or immunomodulation (using ex-vivo expanded T-regulatory cells) strategies [96, 97]. Successfully removing the need for immunosuppression has the potential to make islet transplantation available to children, which is a highly important ongoing goal in the field [43].

Pivotally, there is also the critical need to maximise the utilisation of donor organs for islet transplantation, by enhancing the efficiency of the islet extraction process. To achieve this, current research aims to optimise the clinical enzyme blends that are used in the digestion of the human pancreas [98-100]. Below each of these strategies is considered, including the current progress and ongoing efforts.

1.4.1 Optimising Density-gradient Purification

Although continuous density purification, using a Cobe 2991 cell processor, is the universally accepted method for purifying human islets, there are a few scenarios for which this method is sub-optimal. The main instance is when islets remain partially embedded in exocrine tissue, a phenomenon that is caused by incomplete pancreas digestion, and is prevalent in younger pancreatic donors [101, 102]. Indeed, although extracellular matrix (ECM) attachment is critical for

preventing anoikis (cell apoptosis initiated through matrix detachment [103, 104]), trapped islets have densities that are indistinguishable from exocrine tissue, and hence are lost during Cobe purification. To improve post-purification islet recovery, attempts have been made to optimise the purification of trapped islets. In one study, 500ml bottles were used to create continuous density gradients, following the addition of the pancreatic digest by either top or bottom loading [105]. Post-purification recovery was significantly improved by top-loading, and the method was also superior in recovering a higher percentage of trapped islets than standard Cobe purification, although the mechanisms behind the enhanced recovery of trapped islets are not clear [105]. The method also relies on the operator creating the continuous gradients within the bottle, and as only a quarter of the pancreatic digest could be loaded per bottle, this process has the potential to become laborious.

The inclusion of additional processing steps on fractions containing high percentages of embedded islets have also been investigated. One report incubated fractions that contained >50% trapped islets, following standard purification, in high osmolality University of Wisconsin (UW) solution. The authors speculate that the significant decline in the number of embedded islets following incubation was due to the exocrine surrounding the islet shrinking and allowing the islet to detach under gentle agitation. However, prolonged incubation of islets (>30 minutes) in the high osmolality solution also resulted in a decline in viability and IEQ [106]. Others have incorporated discontinuous 'test gradients', to enable the selection of the most appropriate density gradient prior to purification, by allowing the approximate density of the exocrine and islet tissue to be determined [107]. This is particularly advantageous for recovering embedded islets, such as those that are produced from younger donor pancreases. Another strategy is to include extra Cobe runs, using alternative continuous density and osmolarity gradients [108], or discontinuous density gradients [85]. Both methods appear to be beneficial for improving the recovery of trapped islets, without impacting on islet viability or function.

Despite these promising results, incorporating additional purification stages to enhance the recovery of trapped islets will undoubtedly incur additional costs, time and labour. Arguably, if isolation protocols can be optimised to reduce the number of islets that remain incompletely digested in the first instance, islet recovery post-purification will in turn improve. Strategies to enhance pancreas digestion (particularly those from younger donors) therefore require careful consideration.

1.4.2 Optimisation of Islet Culture

Prior to their release for clinical transplantation islets undergo a period of tissue culture, usually at 37˚C for 24-48 hours. Culturing islets offers several clear benefits, including: allowing quality tests to be performed, enabling the islets to recover from the isolation process and stabilise, as well as providing logistical benefits for organising the transplant and mobilising the recipient. This said, the decline in islet number during the pre-transplant culture period can be substantial, with losses reported as high as 20-30% [109, 110]. The most commonly utilised media for human islet culture is Connaught Research Medical Laboratories (CMRL), containing supplementary additives such as Hepes, antibiotics, glutamine and serum [111, 112]. As human islet preparations must conform to strict manufacturing criteria, animal serums cannot be used. Instead the majority of isolation centres incorporate human serum albumin (HSA) into their culture systems, despite several studies demonstrating that human AB serum is superior to HSA for maintaining islet function and survival [111, 113, 114]. Other groups have shown that culture temperature is important for maintaining islets, with post-culture recovery enhanced by culturing islets at low temperatures (i.e. 4°C), as opposed to the standard 37°C [115, 116]. In addition, current efforts are investigating the potential of media additives for improving islet function and survival during culture, with particular reference to sustaining islets in hypoxia, given the low oxygen concentration in the portal vein [117]. Research includes the co-culturing of islets with ECM proteins/sequences [91, 118, 119] or mesenchymal

stem cells (MSC) (or MSC preconditioned media) [89, 120, 121], both of which have shown benefits to islet function and survival.

1.4.3 Immune Tolerance

As with any allogeneic transplant, recipients receiving an islet graft are required to take lifelong immunosuppression to prevent the risk of donor cell rejection by the host. The landmark introduction of a steroid-free immunosuppressive regime by the Edmonton group in 2000 greatly reduced the toxic effects of immunosuppressive drugs on islets [75]. However, immunosuppressive therapy is still associated with risks, including malignancies and organ damage [122], which prevents islet transplantation from being a treatment option for children and restricts its use to adult patients with life threatening hypoglycaemic unawareness or with renal failure [44]. Currently, two strategies to address immunotolerance are being explored: immunomodulation and immunoisolation.

Immunomodulation exploits the existence of a heterogeneous sub-population of lymphocytes called T-regulatory cells (T-regs), which are capable of maintaining immune homeostasis by promoting host tolerance to foreign and self-antigens [97, 123]. T-regs suppress the immune response through a variety of mechanisms. They can secrete a number of suppressive cytokines, such as interleukin-10, or interact directly with T-effector cells [124]. Although T-regs are present at low numbers in the peripheral blood, they can be isolated and expanded *ex-vivo* [97]. Several routes of T-regs administration have been investigated in the context of islet transplantation. One study investigated the effect of intravenous delivery of *ex vivo* expanded T-regs in humanised diabetic mice receiving allogeneic islets [125]. The T-regs migrated to the engrafted human islets and significantly prolonged graft survival by suppressing the infiltration of innate immune cells [125]. Recent exciting advancements include the direct coating of islets with T-regs, utilising biotin-based conjugates [96, 126]. Such coatings do not affect the viability or function of human islets, and have been shown to decrease islet immunogenicity *in vitro* [96]. Indeed, utilising T-regs also

has the clear advantage of potentially supressing the recurrence of autoimmunity in patients with T1DM [97].

An alternative approach for reducing the need for immunosuppression is to segregate islets from the host immune system by utilising encapsulation technologies. Indeed, this strategy may be paramount in the future with advancements in xenogeneic or islet stem cell transplantation, which require complete isolation from the immune system. Currently, a number of phase 1/2 trials investigating the feasibility and efficacy of islet encapsulation are underway [127]. However, as well as isolating islets from the immune system, islet encapsulation also prevents islet engraftment (i.e. islet re-vascularisation and re-innervation). Passive diffusion of oxygen and nutrients, as well as glucose and insulin, across a semi-permeable membrane are therefore paramount for islet survival and function [122]. Islets can either be encapsulated in micro or macro devices. Where microencapsulation involves the encapsulation of single islets, macroencapsulation consists of incorporating the islets into a larger, usually single, device. The performance and efficacy of several macroencapsulation devices are currently being trialled clinically, including the βair [93]. This device consists of a polytetrafluoroethylene (PTFE) and alginate-based shell, with the islets immobilised inside the device in alginate. To overcome issues of hypoxia (due to the large diffusion area across the device membrane to the islets), an external gas reservoir delivering oxygen is integrated into the device, which undergoes daily replenishment. A βair device, containing around 2,000 IEQ/kg, was transplanted into the peritoneal cavity of a 63 year old patient with long standing T1DM. Although there was evidence of basal and stimulated C-peptide, the levels were much lower than those observed physiologically. Furthermore, there was only a modest decrease in HbA1c [93]. Given that most clinical protocols transplant a minimum of 5,000 IEQ/Kg, with in excess of 10,000 IEQ/Kg required to achieve insulin independence [75], the lower than anticipated C-peptide levels may result from the implantation of an insufficient islet mass. That said, increasing the IEQ by transplanting more than one device does not appear to enhance C-peptide response [128]. The poor graft response may result from the large diffusion distance between the outside and inside of

the device. This theory is supported by the enhanced insulin response when high levels of glucose were specifically delivered to the device region [93]. In contrast, microencapulsation devices have the added benefit of a smaller diffusion distance, but as each cell is encapsulated individually it is difficult to standardise the membrane and pore size for each capsule. However, current efforts to standardise the thickness of each membrane appear promising [129]. The diameter of the encapsulation device also requires careful consideration to ensure an adequate insulin response [130, 131]. Recent microencapsulation strategies involve the layering of charged polymers around the surface of islets [94, 95]. Although the negligible increase in islet size is beneficial for molecular diffusion, human studies demonstrating the long-term survival of these devices *in vivo* are lacking. Encapsulation offers the possibility to incorporate additional molecules into the scaffolds, which can enhance graft performance. The signalling interactions that occur between the pancreatic ECM and islets *in vivo* are known to be critical for islet survival and function [100]. The isolation process leads to a substantial loss of islet:ECM, interrupting these interactions [112]. Therefore, incorporating ECM molecules into encapsulation devices offers an attractive option for replenishing the islet:ECM interaction and may prevent early graft loss by avoiding anoikis. The addition of collagen IV to microporous polymer scaffolds was beneficial for restoring normoglycaemia in a syngeneic diabetic mouse model. Histology indicated an increased islet area and vessel density in the excised grafts compared to controls [132]. Similarly, incorporating collagen IV and laminin into poly-ethylene glycol (PEG) hydrogels increased insulin response in mouse islets [133]. Other groups have focused on the creation of capsules made from elastin-like-molecules [134]. Research exploring the potential of these capsules within the field of islet transplantation should be considered. The incorporation of ECM molecules into encapsulation devices is also an important aspect of the ongoing European DRIVE project (Diabetes Reversing Implants for enhanced Viability and long term Efficacy). This project aims to create a 'panceo-mimetic' environment for transplanted islets, by suspending them within a novel β-gel, housed within an outer immune-isolating capsule. The β-gel is reported to not only contain oxygen producing components, but also

ECM molecules. The exact composition of the device, and the incorporated ECM molecules, remains yet to be disclosed (http://www.drive-project.eu/).

Finally, as with any encapsulation device the lag between blood glucose elevation and insulin response, owed to the time that it takes for the molecules to diffuse across the membrane, must be considered carefully [122]. In addition, when islets are encapsulated the insulin secretory response duration is prolonged [122], which may result in hypoglycaemia.

1.4.4 Pancreas Digestion

The efficient liberation of islets from the surrounding pancreatic architecture is a prerequisite to any successful islet isolation procedure. The extraction of islets from their *in situ* environment occurs during the critical pancreas digestion phase of the isolation process, which involves the infusion of commercially available collagenase based enzymes through the main pancreatic duct [60]. The enzymes then become distributed at the regional interface that separates the islet from the general exocrine tissue (the 'islet-exocrine interface'). Aided by mechanical shaking, the enzymes digest the ECM proteins within this region [112], to release 'free' (devoid of exocrine tissue) islets. Successfully achieving the correct balance between sufficient exocrine and endocrine dissociation, without causing islet fragmentation, is an ongoing caveat in the field of islet transplantation. Central to this issue is not only the variability between commercially available batches of collagenase [135], but our incomplete understanding of the composition of the ECM and the mechanisms behind its digestion with exogenous enzymes. This issue is further exacerbated by inter-pancreatic variability, with pancreatic digestion affected by donor variables such as age. The assumed insufficient cleavage of the proteins constituting the islet-exocrine interface in pancreases retrieved from younger donors results in high percentages of exocrine embedded islets, which are technically challenging to purify [101, 102]. Sub-optimal pancreas digestion most likely results from donor related changes in the pancreatic ECM. However, in spite of this, current efforts to optimise

pancreas digestion in particular donor groups have relied on the empirical attenuation of enzyme blends [98, 99, 136]. Such adjustments have been made without first understanding how donor variables influence the pancreatic matrisome surrounding the islet. Defining donor specific changes in the molecular structure of the pancreas has the potential to allow enzymes to be tailored to specific donor substrates, and improve isolation success rates from the full pool of donors.

This Chapter continues with a specific focus on the collagenase digestion phase of islet isolation, with a view to improve enzyme-mediated pancreas digestion. The structure and working mechanism of collagenase is considered in the next Section.

1.5 Role of Exogenous Enzymes in the Isolation of Islets

As discussed above, the first documented use of collagenase in the isolation of islets dates to the 1960s, when Moskalewski successfully extracted large numbers of islets from the guinea pig pancreas using crude collagenase blends [55]. Due to its success, this technique quickly superseded manual microdissection as the preferred method for separating the endocrine and exocrine pancreas [54]. Collagenase is an endopeptidase that is capable of cleaving peptide bonds within the triple helical region of native collagen [137]. Bacterial collagenases have a broader substrate specificity than mammalian collagenases, as well as a more potent collagenolytic activity. Where mammalian collagenases cleave collagens into only two fragments [138, 139], bacterial collagenases are capable of hydrolysing the triple helix at multiple locations to create small peptides [140]. Early screenings of multiple types of bacterial cultures revealed collagenase and proteinases produced by the gram-positive bacteria *Clostridium histolyticum* to be the most potent at digesting both native and denatured collagens [141], making it the clear specie of choice for the production of collagenases for islet isolation. Characterisation of collagenase from *C. histolyticum* (defined from here within as 'collagenase') revealed the presence of two genetically distinct sub-classes, which are characterised based on their specificity for native and synthetic substrates [142].

Both collagenase Class I (C1) and Class II (C2) are 116KDa, and are controlled by the genes *colG* and *colH*, respectively [142].

The two subclasses of collagenase work synergistically to digest triple helical collagen into multiple small peptides, with each targeting different regions of the molecule. When collagen I is treated with crude collagenase, CI first cleaves all three chains close to the C-terminus, to produce fragments of approximately 88KDa. The fragments are then cleaved near the N-terminus, reducing their weight to 80KDa. Alternatively, C2 collagenase targets the triple helix interior, producing N and C terminal fragments that are 35KDa and 62KDa respectively. The C-terminal fragment undergoes multiple further cleavages to produce 59KDa and 24KDa fragments [140]. Less is known about the working mechanism of collagenase. Originally, it was suggested that collagenase 'unwound' the triple helix, implying inherent triple helicases capabilities [143, 144]. More recently it has been argued that collagen naturally undergoes thermal fluctuations, which causes areas to adopt a partially unwound conformation [145, 146]. Collagenase then enters these vulnerable regions and stabilises the structure, before hydrolysing the scissile bond [146]. Indeed, this reaction scheme appears more plausible, given that the unwinding of a triple helix is an energetically costly task, and collagenolysis does not require energy input [147, 148].

Prior to the availability of commercially available purified enzymes, crude collagenase blends were used in islet isolation [55, 56, 149]. Highly heterogeneous, these collagenase based mixtures contained at least 12 different components, including neutral protease, clostripain, trypsin and elastase [150]. Although several of these components (particularly neutral protease) are essential for successful islet isolation, the inconsistencies in collagenase activity in these crude enzyme blends, particularly across different batches, resulted in the production of highly variable yields [149, 151].

The introduction of the first commercially available purified collagenase blend by Roche in 1995 caused a decline in the use of these crude un-purified enzymes. Liberase contained both classes of

collagenase from *C. histolyticum* and the neutral protease thermolysin (produced from the gram positive bacteria *Bacillus thermoproteolyticus*) [152, 153]. The use of Liberase significantly reduced lot to lot variability, resulting in the production of more consistent and reproducible islet yields across different batches of enzymes [154, 155]. Owed to the success of Liberase, other companies such as Serva [156] and Vitacyte [157] began to produce their own enzyme mixtures. These two manufactures began to dominate the field post-2007, following the discontinuation of Liberase, due to potential contamination with bovine neuronal tissue, used during the fermentation processes of enzyme production.

Although greatly improved, the use of purified enzyme blends did not completely eliminate issues of batch to batch variability, and inconsistent islet yields remained an issue [43, 158]. As the ratio of C1 and C2 collagenase is known to be important for successful islet isolation [159, 160], it has been suggested that degradation of C1 may be responsible for the variability seen in different batches of collagenase, and indeed from vials of the same lot [135].

Structurally, intact C1 collagenase contains five domains. The first two domains, the activator and peptidase domains, are situated at the N terminus. As the catalytic activity is dependent on the presence of both of these domains, together they make up the collagenous module of the molecule [143]. Downstream of this region are the polycystic kidney disease like-domains (PKD) and the collagen binding domains (CBD). The number of these domains varies depending on the collagenase type; C1 collagenase has two CBD and one PKD. The CBD is positioned at the C-terminus of the molecule, with the PKD domains situated upstream, linking the catalytic region with the CBD domains [143]. When degraded, C1 collagenase loses one of its two CBD domains, reducing the molecular weight from 116KDa to 100KDa (Figure 3). This truncated isoform can be separated by High Performance Liquid Chromatography (HPLC), and has a ten-fold lower collagen degradation activity than intact C1 collagenase [161]. Indeed, although it has been shown that neutral protease can compensate for diminished intact C1 content [162], this variability in collagenase activity

between different batches likely contributes to the unpredictability of human islet isolation yields. The unstandardized nature of enzyme activity between different batches means that at present isolation centres must 'batch test' the performance of new enzyme lots on incoming clinical organs every time the current batch is exhausted.

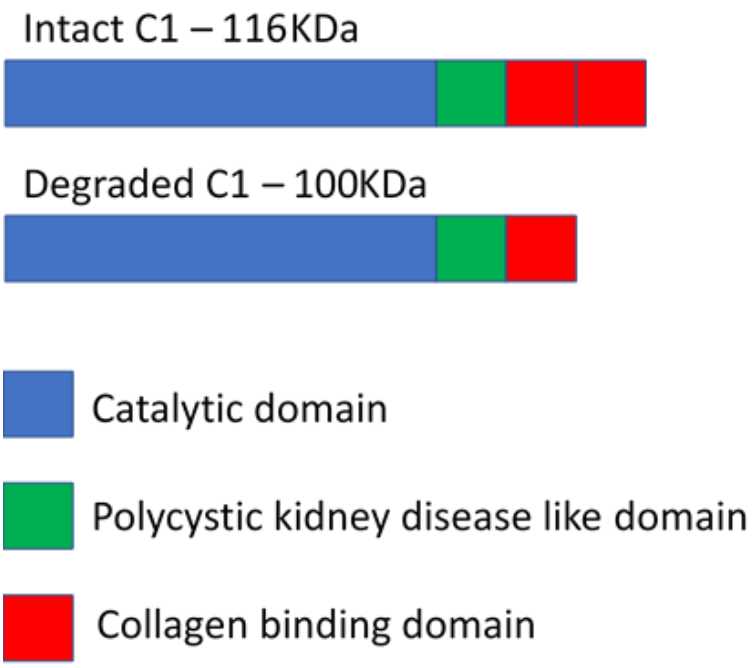


Figure 3: Structure of intact and degraded Class I collagenase from *Clostridium histolyticum* Class I (C1) collagenase has a molecular weight of 116KDa. It contains a catalytic domain, a polycystic kidney disease like domain, and two collagen binding domains (CBD). C1 commonly becomes degraded and loses one of its CBD domains. The molecular weight of degraded C1 is 100KDa.

1.6 The Pancreatic ECM; the Substrate for Enzyme Digestion

The ECM surrounding the human islet is comprised of both a peri-islet basement membrane (BM) and an interstitial matrix (IM), which are linked adjacently through the interaction of specific proteins within this network. During the pancreas digestion phase of the isolation process these ECM structures form the substrate for enzyme digestion, which is facilitated by the collagenase-

based enzymes delivered through the pancreatic ductal network (Figure 4). Although the efficient enzymatic cleavage of the ECM at the region separating the islet from the exocrine tissue is essential for releasing free islets, investigations into the enzyme mediated digestion of the ECM within the human pancreas are lacking. In a recent proteomic characterisation of the decellularised human pancreas, Sackett *et al.* identified 120 ECM associated proteins [163]. The fully characterised pancreatic matrisome contained 19 of the known 28 collagens, and 7 of the 16 currently discovered laminin chains. This emphasises the complexity of the pancreatic ECM, and highlights the importance of accurately defining the composition and structure of the native matrix prior to undertaking investigations into matrix digestion. In this Section, the composition of both the islet BM and IM are considered, as well as the mechanisms behind the critical islet-ECM interactions.

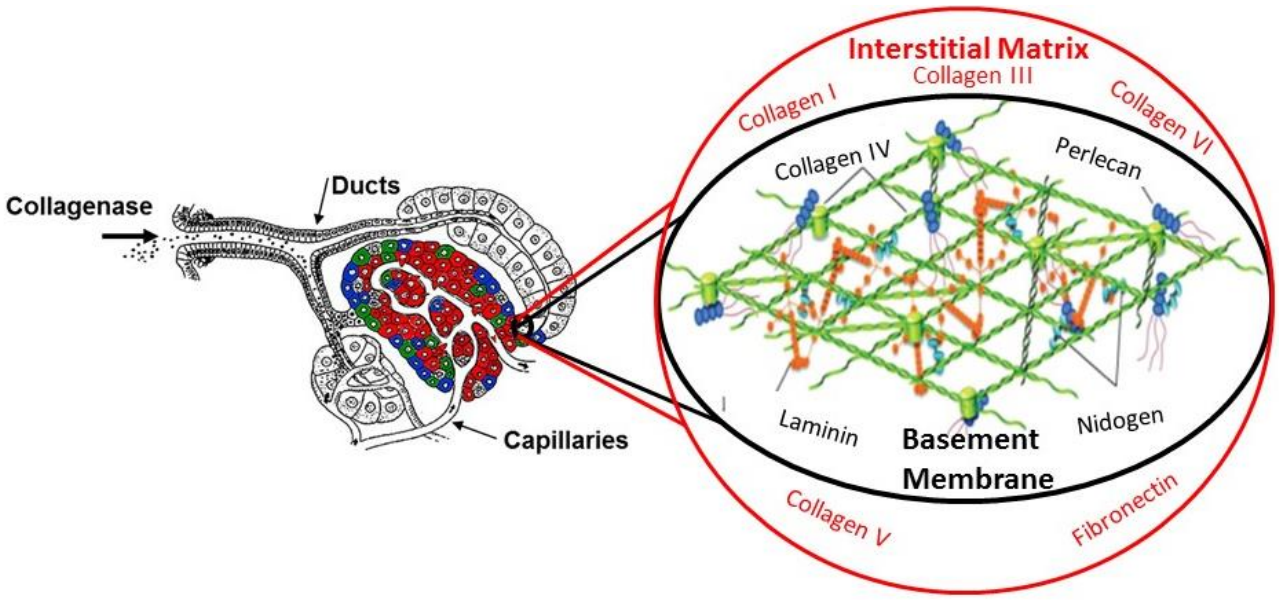


Figure 4: Enzyme delivery to the islet-exocrine interface
Collagenase based enzymes are infused through the pancreatic duct, where they become distributed at the islet-exocrine interface. Here they digest the components of the ECM to release free islets from the surrounding exocrine tissue. The pancreatic ECM surrounding the islet is composed of a double layered BM and adjacent to this is an interstitial matrix (in red). Figure adapted from Figure 1 in Cheng *et al*. 2011 [164].

1.6.1 The Islet BM

BMs are specialised sheets of ECM that are located on the basal side of every epithelium. They offer mechanical support, as well as allowing for compartmentalisation and facilitating cell adherence. Transmission Electron Microscopy (TEM) has shown that the average BM is around 100nm thick, but this can increase to 10µm in certain tissues [165]. Whilst murine β-cells have demonstrated to be incapable of forming a BM, they do so by attracting matrix secreting endothelial cells, through the secretion of vascular endothelial growth factor (VEGF). The endothelial cells then form a vascular BM adjacent to the endocrine cells [166]. Investigations into the composition of the human islet BM has revealed a unique duplex BM structure that surrounds the intra-islet vasculature [167]. This structure results from a secondary BM associated with endocrine cells, in addition to the standard vascular BM surrounding the endothelium. In murine islets this duplex structure is lacking, resulting in the endocrine cells interacting directly with the endothelial BM [167].

The interaction between islets and the surrounding BM is not only essential in preventing anoikis, but is important in facilitating many important aspects of cellular function. Islet-ECM interactions are mediated through both integrin and non-integrin receptors. Integrins are a diverse family of transmembrane receptors, with 18 α and 8 β subunits comprising a total of 24 different heterodimers [168]. A large extracellular domain exists, which usually spans the length of the membrane, before tailoring into a shorter cytoplasmic domain. Upon ligand binding to the extracellular portion various signals are transduced to the cell interior [168]. The exact composition of the integrin receptors expressed on human islets is somewhat controversial. However, there is a general consensus that both human islets and isolated human β-cells express the integrin subunits α3, αv and β1 [167, 169, 170], as well as α5 [169, 170]. Although the integrin subunit α6 was expressed in whole islets, expression was low on isolated β-cells [169], which is supported by data demonstrating that the presence of this integrin is limited to the islet vasculature [167, 170]. Integrins α2 and β3 are not expressed on human islets [167, 170], despite α2 being expressed on porcine islets [170].

BM are capable of self-assembling, with collagen IV functioning as the major scaffold network. Other BM components such as specific laminin isoforms and perlecan integrate with this framework. Below, the structure and assembly of the main BM components are considered in the context of the islet BM structure and function.

1.6.1.1 Collagen IV

Collagen IV is a major component of all BMs, and is expressed in the human islet BM [112, 167, 171-173]. Collagen IV forms the basis of the BM scaffold, by self-assembling into a 2-D network and allowing other matrix components to integrate into this framework to form a supramolecular architecture [174]. Structurally, six highly homogenous genetically distinct α chains exist, which assemble into one of only three heterotrimers *in vivo*; [α1(IV)$_2$α2(IV)], [α3(IV)α4(IV)α5(IV)] or [α5(IV)$_2$α6(IV)]. Whereas α1 and α2 are ubiquitously expressed in all tissues, the presence of α5 and α6 are thought to be restricted to specific tissues [175]. Each α chain has three structurally distinct regions, the 7S domain, the helical region, and the non-collagenous domain (NC1). The 7S domain lies at the N-terminal. The length of this domain varies through the 6 α-chains, ranging from 157 (α2) to 13 (α3) amino acids [176]. All 7S domains are rich in cysteine, lysine and hydroxylysine residues, which facilitates inter and intramolecular lysine derived crosslinking, and disulphide bonding. As such, the 7S is domain highly resistant to collagenase treatment, and thus it can be isolated following extensive digestion of the BM with bacterial collagenase [177, 178]. The helical domain of collagen IV contains the standard collagenous repeated triplicate of amino acids (Glycine, X, Y), with the X and Y positions often occupied by proline and hydroxyproline. The length of the collagenous domain ranges from 1271 to 1416 amino acids (α1 and α5, respectively) [176]. As opposed to other members of the collagen family, the helical domain of collagen IV has between 21 and 26 interruptions in the repeating triplicate amino acid sequence [176]. These interruptions vary from the absence of either the X or Y amino acid, to the deletion of several glycine residues.

The longer interruptions correspond well to 'kinks' seen in collagen IV via electron microscopy, suggesting that the non-helical regions are responsible for the flexibility of the molecular within the BM [177]. The C terminal NC1 domain contain a high proportion of cysteine residues, as well as hydrophobic amino acids, which helps to facilitate interactions with other regions of the molecule [177]. It is also the domain that displays the most homogeneity in length across the six α chains and contains 229 amino acids on average [176]. Collagen polymerisation begins by the assembly of three separate chains into heterotrimers. Two heterotrimers then join to form a dimer. The final stage is the association of four distinct dimers [179, 180]. The collagen IV networks are further stabilised by intramolecular disulphide bonding, as well as lysine derived crosslinking, making them highly insoluble [177]. The final resulting structure is a loose hexagonal network that is often likened to 'chicken-wire'. The isoforms detected in the human islet BM include α chains 1-5 [112, 163, 167].

Collagen IV integrin binding is assumed to be mainly facilitated through integrin receptor α1β1. Insulin secretion was promoted in human fetal β-cells that were cultured on collagen IV, which was lost following the blockage of the α1 subunit of the receptor. In the same study adhesion of both adult and fetal β-cells to collagen IV was prevented by blocking the α1 and β1 receptor units [181]. Although it well established that specific regions of collagen IV bind to the α1β1 integrin [182, 183], the expression of the α1 receptor on human islets remains controversial [170]. It has been suggested that whilst collagen IV contains arginine-glycine-aspartic acid (RGD) sequences, this is unlikely to facilitate integrin binding due to the inaccessible nature of these sequences in native collagen [183].

1.6.1.2 Laminin

Laminins are heterotrimeric glycoproteins, which take on a cruciform appearance following the assembly of their α, β and ϒ chains. Along with collagen IV they are major components of the BM.

Electron microscopy and rotary shadowing revealed the presence of one long (~ 70nm) and three shorter arms (~ 36nm), with the long arm terminating in a globular like domain [184]. Due to the increasing discovery of different laminin chains and their various combinations of heterotrimeric assembly, in 1994 a universal nomenclature for laminin was proposed [185]. This nomenclature assigned a number to each laminin, based on its chronological discovery, rather than on a compositional basis. For example, laminin-1 was assigned to the original Engelbreth-Holm-Swarm extracted laminin, despite it having the composition of α1, β1, ϒ1. The universal nomenclature of the different laminins was revisited in 2005, devising a simplified system defining each laminin by each chain composition. For example, laminin-1 is now referred to as laminin 111 [186]. To date, 16 laminins have been biochemically characterised, devised from 11 genetically distinct peptide chains, including; 5 α, 3 β and 3 ϒ chains [187]. Laminin is capable of self-assembling, with the three chains connecting in the long arm region. Here, they coil into a triple helical structure, initiated by the dimerization of the β and ϒ chains, followed by the incorporation of the α chain [188]. Five laminin globular (LG) domains are present at the end of the molecule, from an extension of the α chain at the C-terminus [189]. Polymerisation of each laminin trimer occurs through the N-terminal region of the three shorter arms, which interact to form a quasi-hexagonal network. All three arms are required to be present in order for laminin to re-polymerise following restricted proteolysis [190]. Sophisticated studies using high magnification confocal laser scanning microscopy revealed the distinct arrangement of the different laminin subtypes in the islet BM [167]. Expression of laminins α2 and α4 were limited to the BM of the exocrine tissue, and the endothelial vascular channels of the intra-islet blood vessels, respectively. In contrast, laminins α5, β1 and Y1 were found not only in the peri-islet BM, but also in both layers of the duplex BM surrounding the intra-islet blood vessels. The β2 chain was also expressed in the duplex membrane but was absent from the peri-insular region surrounding the islet. Expression of laminins α1 and α3 were not detected in the pancreas, whereas β3 and Y2 were restricted to the ductal network. Taken together, this work suggests that although both laminin 411/421 and 511/521 are found in the endothelial region

of the duplex BM, laminin 511/521 is also expressed in the endocrine membrane, making it the only laminin isoform to be expressed in both layers of the double BM [167]. Further studies on human pancreatic tissue sections have supported the finding that laminin, with particular reference to the α5 chain, is a major constituent of the human islet BM [112, 173]. In their full proteomic characterisation Sackett *et al.* identified the following laminin chains: α 2, 3 and 5, β 1 and 2 and Y1 and 3 [163].

Attachment of human β-cells to laminin-511 is prevented upon incubation with monoclonal antibodies against the integrin subunits α3 and β1 [167]. Adherence is also blocked by soluble Lutheran, suggesting that Lutheran glycoprotein, which is highly expressed at the periphery of the islet BM, is also a receptor for laminin-511 [167]. Islet interaction with laminin is reported to be important for β-cell survival and insulin secretion. When human islets are encapsulated in alginate micro-scaffolds containing collagen IV and specific laminin sequences, both necrosis and apoptosis were significantly decreased upon exposure to cytokines for 72 hours [119]. The ECM proteins reduced nitric oxide (NO) induction and prevented a decline in islet oxygen consumption rate (OCR), suggesting that islet-matrix interactions, including that with laminin, are able to protect again cytokine toxicity [119].

1.6.1.3 Nidogen

Nidogen exists as two immunologically distinct isoforms, which share a 46% sequence homology [191]. Nidogen-1 was originally identified as a 150KDa protein synthesised by parietal endoderm cells [192], with nidogen-2 identified some 20 years later, as a 200KDa protein with a similar overall composition [191]. Structurally, the study of recombinant nidogen-1 revealed the presence of three globular domains (G1-G3), present at the terminal ends of the molecule and in the central position. G1 and G2 were linked by a flexible protease susceptible segment, with a firm rod linking G2 to G3. The total molecule measured around 30nm [193]. Production of a recombinant nidogen-2 revealed

a similar structure, albeit the molecule was around 20nm longer [191]. Nidogen is capable of linking collagen IV and laminin, as well as integrating perlecan. Where laminin binding has been localised to the G3 domain of nidogen-1 [193], collagen IV and perlecan binding are facilitated through the G2 domain [194]. Although nidogen-2 is capable of binding collagen IV and perlecan to a comparable level to nidogen-1, the affinity for laminin is around 1,000 fold lower [191]. Unlike nidogen-1, nidogen-2 was unable to bind the glycoprotein fibulin [191].

Due to its role in linking the two major BM networks *in vitro*, nidogen is thought to be important in normal BM assembly, where it acts to stabilise the structure. Both nidogen isoforms have been detected in the BM of murine and human islets [163, 167, 173, 195]. Although the role of nidogen in β-cell function has not been reported, deletion of both nidogen isoforms in knock-out mice is lethal. This is assumed to be due to loss of BM integrity, with heart vessels in nidogen knock-out mice showing abnormal staining for collagen IV and laminin, as compared to controls [196].

1.6.1.4 Heparan Sulphate Proteoglycans

Heparan sulphate proteoglycans (HSPG) are defined as core proteins that contain one or more covalently linked heparan sulphate (HS) carbohydrate side chains [197]. HS itself is a highly charged polysaccharide composed of repetitive units of the disaccharides uronic acid and glucosamine, assembled in a linear fashion [197]. Broadly speaking, HSPGs fall into two main categories: membrane proteins and secreted ECM proteins. The secreted ECM proteins are important constituents of BMs [197].

Perlecan is the most well characterised BM HSPG and is regulated by the gene *HSPG2.* The core protein of perlecan is around 470KDa and contains 5 distinct protein domains, each providing distinct bio-functional properties [198]. The N-terminal positioned sequence of the first domain is highly conserved to perlecan, and lacks homology with other proteins [198]. It also provides the main site for HS side chain attachment, which are important for initiating binding to other proteins,

facilitated through electrostatic interaction. The second and third domains share sequence homologies with the low density lipoprotein (LDL) receptor and laminin respectively, in turn providing perlecan with lipid retention and cell attachment properties [198, 199]. The fourth and largest domain facilitates the binding of several other matrix components such as nidogen and fibronectin, making it crucial in BM and ECM assembly. The C-terminal fifth domain of the molecule is often termed endorepellin due to its demonstrated anti-angiogenic properties. It is composed of laminin and epidermal growth factor (EGF) like repeats [198]. Two additional HSPG have been discovered in the BM: agrin and collagen VXIII. Agrin possesses a smaller 210KDa core protein, but like perlecan, it has several laminin and EGF like regions [200, 201]. Collagen XVIII was the final BM HSPG protein to be discovered, which also marked the discovery of the first collagen that possessed HS side chains [202]. The core component of collagen XVIII has a molecular weight of 180KDa, with the heparin sulphate side chains adding an additional 120KDa to this weight [202]. Similar to perlecan, the C-terminal region of the molecule possesses anti-angiogenic properties. This domain can be released from the core protein by proteolytic cleavage, resulting in a 20KDa fragment termed endostatin [203].

Perlecan [112, 163, 173], agrin [163] and collagen XVIII [163, 204] are all present in the human pancreas. Although they are known to be important in stabilising the laminin and collagen IV networks [187], the functional role of HSPGs in the islet BM has not been fully elucidated. Interestingly, collagen XVIII has been localised to the intracellular region of both mouse and human pancreatic β-cells, which correlates with the internal expression of HS [204, 205]. During islet isolation there is a significant reduction in intracellular HS, but not of the core proteins, in murine islets [204]. Treating islets with antioxidants significantly reduced islet death and increased intracellular HS content, suggesting that reactive oxygen species (ROS) generated during the islet isolation process may be responsible for the loss of HS [205]. Replenishment of the internal HS in isolated human β-cells, by culturing with a heparin mimetic, protected islets from experiencing diminished viability when exposed to H_2O_2. The authors also found a progressive *in situ* loss of both

collagen XVIII core protein and HS in β-cells from donors with T1DM, which correlated with a progressive loss of insulin content. Heperanase (a HS degrading enzyme) co-localised to invading leukocytes, suggesting that loss of HS may contribute to the pathogenesis of T1DM [204]. However, it is worth noting that culturing human islets with heparin has been shown to promote amyloid production, which is toxic to β-cells. Although heparin cultured islets displayed decreased apoptosis they were also significantly inferior in reversing diabetes in a diabetic mouse model [206].

1.6.2 Interstitial Matrix

The IM lies adjacent to the BM and is composed of a variety of integrated proteins that are responsible for providing mechanical support and flexibility to tissues. The IM surrounding the human islet is known to contain many collagen isoforms, in addition to non-collagenous glycoproteins such as fibronectin and vitronectin, and members of the proteoglycan family, including decorin and lumican [163]. Inter and intra-molecular collagen crosslinking, mediated through the enzyme Lysyl Oxidase (LOX), confers mechanical strength and stabilises the matrix structure [207]. Certain IM proteins have demonstrated beneficial effects on islet function and survival, particularly collagen I and fibronectin. Interaction between the IM and BM has been shown to be mainly facilitated by collagen VI, which anchors the two networks through interaction with the major BM protein collagen IV [208].

1.6.2.1 Collagenous Components

To be classified as a collagen, three polypeptide chains must be capable of forming the characteristic supramolecular triple helical domain. As with collagen IV, the helical domain of the IM collagens contains the standard collagenous repeated triplicate of amino acids (Gly, Xaa, Yaa), which is a pre-requisite for triple helix assembly. The number of triplicate repeats varies depending on the collagen subtype [209]. On the basis of structure and organisation, collagens are further divided into additional categories. Whereas BM collagen specifically pertains to collagen type IV,

the IM collagens are further divided into a number of categories including: fibril forming collagens, fibril-associated collagens with interrupted triple helicases (FACIT), microfibrillar collagens, anchoring fibrils, network forming collagens, multiplexins and transmembrane collagens. Each of these collagen types has a unique structure, which aids in their bio-function. For example, the interrupting 'non-helical' repeats found within the collagenous domain of FACIT collagens allow this collagen type to confer important flexible properties to tissue. Alternatively, the well characterised fibril forming collagens offer tensile strength and load bearing properties to tissues, formulated through the highly organised supramolecular fibre aggregates [209].

Early studies using immunohistochemistry to characterise the protein composition of the IM surrounding human islets identified the presence of collagens I, III, V [210] and VI [171]. Interestingly, the semi-quantified content of collagen V and VI was found to be significantly higher than that of collagens I or IV, although potential differences in antibody binding affinities cannot be excluded [171]. The reported high content of collagen VI is of particular interest for human islet isolation, as this particular collagen subtype has been shown to be resistant to collagenase digestion [211]. The resistance to proteolytic degradation likely resides from the high degree of disulphide linkage within the molecule [212]. A recent in depth proteomic investigation of the pancreatic matrix identified a further 13 IM collagens present in the human pancreas: collagens II, VII, VIII, IX, X, XI, XII, XIII, XIV, XV, XVI , XXI, XXVIII (Table 1) [163]. However, the lack of accompanying histology data prevents the identification of these proteins at the islet-exocrine interface [163]. Determining the location of these proteins, in relation to the islet, would dictate their importance in the enzymatic digestion phase of the human islet isolation procedure.

Interestingly, although the main role of the IM is to confer structural support, isolated human islets that are cultured on purified collagen I adhere and display significantly enhanced viability, compared to controls [91]. Table 1 lists the IM collagens that have been detected in the human pancreas.

1.6.2.2 Non-Collagenous Components

Non-collagenous components present in the human pancreatic IM include the glycoproteins fibronectin [99, 163] and vitronectin, in addition to proteoglycans decorin and lumican [163]. Fibronectin has been shown to positively influence islet function and survival *in vitro* through interaction with its integrin receptors, facilitated through the RGD binding sequence present within fibronectin. This sequence is known to bind the αv integrin subunit [213], which is present on human β-cells. In rodent islets apoptosis is significantly reduced following culture with RGD sequences, mediated through activation of specific anti-apoptotic proteins [214].

TYPE	MOLECULAR COMPOSITION	COLLAGEN TYPE	REFERENCES
I	$[a1(I)]_2$, a2(I)	Fibril-forming	[210], [171], [99], [163]
II	$[a1(II)]_3$	Fibril-forming	[163]
III	$[a1(III)]_3$	Fibril-forming	[210], [99], [163]
V	a1(V), a2(V), a3(V)	Fibril-forming	[210], [171], [163], [99]
VI	a1(VI), a2(VI), a3(VI)	Micro-fibrillar	[171], [163], [99]
VII	$[a1(VII)]_3$	Anchoring fibrils	[163]
VIII	$[a1(VIII)]_2$, a2(VIII)	Hexagonal network-forming collagens	[163]
IX	a1(IX), a2(IX), a3(IX)	FACIT forming	[163]
X	$[a3(X)]_3$	Hexagonal network-forming collagens	[163]
XI	a1(XI), a2(XI), a3(XI)	Fibril-forming	[163]
XII	$[a1(XII)]_3$	FACIT forming	[163]

XIII	[a1(XIII)]$_3$	Transmembrane collagen	[163]
XIV	[a1(XIV)]$_3$	FACIT forming	[163]
XV	[a1(XV)]$_3$	Multiplexin	[163]
XVI	[a1(XVI)]$_3$	Multiplexin	[163]
XXI	[a1(XXI)]$_3$	FACIT forming	[163]
XXVIII	[a1(XXVIII)]$_3$	Multiplexin	[163]

Table 1: Interstitial matrix collagens present in the human pancreas
Collagen type, molecular composition of polypeptide chains, and assembly type are listed. References listed are for the sources citing the presence of the protein in the human pancreas. Adapted from Table 1 in Gelse *et al.* 2003 [209]. FACIT; fibril forming associated collagens with interrupting triple helicases.

1.7 The Impact of Donor Factors on Islet Isolation Outcome

As any successful islet isolation begins with the acceptance of a suitable donor organ, many islet centres have attempted to determine how donor related factors impact on isolation outcome. An extensive literature review highlighted 27 studies that have attempted to determine the impact of donor, pancreas, and retrieval factors on isolation success (Table 2). Whilst these analyses have the potential to inform future organ acceptance criteria, the incompatibility of these studies can be appreciated when reviewing the definition of a 'successful' isolation, which has ranged from 100,000 to 400,000 IEQ [215, 216]. 'Success' is of course dependent on the centres pre-defined islet release criteria for transplantation, which is usually based on the minimum IEQ required per Kg of the recipient's body weight (in the UK this is 5,000 IEQ/Kg for a first transplant). Transplantable islet yields therefore vary depending on recipient requirements, which arguably renders a universal definition of success/failure inappropriate in this context. Other reports have used IEQ as a continuous variable [217], or utilised a composite measure, encompassing other assessment parameters such as islet viability, purity or function [218, 219]. The use of such vast

outcome measures make studies largely incomparable and may be responsible for the inconsistencies in factors that are reported to significantly affect isolation outcome (Table 2).

Of the donor/pancreas factors identified in the literature, a number were only investigated in a small amount of studies, making it challenging to be conclusive about their impact on islet isolation. Such factors included: warm ischemia time (WIT), donation type (donation after cardiac death (DCD) or donation after brain death (DBD)), as well as a number of socio-economic factors including past smoker and alcohol history (Table 2).

Rather surprisingly, despite amylase being a marker of pancreas inflammation, only 1 study detected a significant negative correlation between blood amylase and isolation outcome, with a further 10 studies reporting that amylase levels are not indicative of isolation outcome (Table 2). One study identified that donor acute insulin response to arginine (a surrogate marker of β-cell mass) was highly successful in predicting isolation outcome. In this particular study, no other donor parameters (including age and BMI) were significantly predictive of yield [220].

Critical factors, that were identified across numerous studies, include donor age [215, 221, 222], cold ischemia time (CIT), BMI [101, 222-224], body surface area (BSA), weight, height and gender [225]. Below the impact of each of these variables on isolation success is discussed, and the underlying cause of the association considered.

1.7.1 Cold Ischemia Time

The calculation of pancreas cold ischemia interval varies between different isolation centres. Although the commencement of cold ischemia is taken from aortic cross-clamp at retrieval, the duration is defined as ranging to either: the commencement of pancreas dissection [224], collagenase injection [217, 226], or the placement of the pancreas in the Ricordi chamber for digestion [227]. Regardless of these subtle variations, a number of studies have demonstrated that isolation yield is negatively influenced by the duration of cold ischemia (Table 2). Furthermore, CIT

negatively influences islet recovery post-culture [109]. A number of studies also demonstrated the significant benefits of local organ procurement, which is likely to indicate shorter CIT for these donors (Table 2).

Although islets only make up around 2% of the total pancreatic mass, they are highly vascularised and receive up to 20% of the total arterial blood flow [228]. Indeed, owed to this native oxygen rich environment, prolonging pancreas cold storage is likely to cause irreversible islet damage [229]. It is therefore unsurprising that a number of studies have reported that CIT negatively affects isolation outcome. That said, it is worth noting that many of these reports included pancreases with very prolonged CIT, which in the majority of countries, would be classed as outside the criteria for clinical isolation. For example, the pancreas CIT in the Zeng *et al.* study reached 19 hours [221], whereas Wang *et al.* included pancreases that had CITs of 24 hours [216]. Within the UK, to meet clinical guidelines, CIT must fall within 10 hours for a DBD, or 6 hours for a DCD. Limiting the variability in the duration of pancreas cold ischemia, by controlling it within a tight range, is likely to reduce the impact of CIT on isolation outcome [219, 230]. Furthermore, current strategies have been successful in reducing the detrimental effects of organ cold storage. Such methods include the implementation of the Two Layer Method (TLM), a system that introduces oxygen to a solution during cold storage using oxygen carriers such as perfluorocarbons (PFC). The TLM had been used to successfully reduce the impact of organ ischemia on islet yield during both short [231] and more prolonged storage [232].

1.7.2 Donor Size

Donor size is assessed via several parameters. Height and weight are routinely used, both in raw data form, and as part of composite measurements such as BMI and body surface area (BSA, calculated as described by Mosteller [233]). The vast majority of these studies have reported a positive relationship between BMI and islet yield (Table 2). Although assessed less frequently than

BMI, both donor weight and BSA also have significant positive impacts on isolation outcome. This is with the exception of one study, which found that higher islet yields are obtained from donors weighing <110Kg, as opposed to >110Kg [221]. However, as only 3 donors were assigned to the heavier group it is likely that this study was statistically underpowered, and therefore provides little argument against the overwhelming body of evidence showing a positive correlation between donor size and isolation yield. Data also suggests that male donors yield significantly more islets than their female counterparts (Table 2). However, it is likely that gender may be a surrogate marker of donor size, given that male donors are also often associated with a larger body weight.

There are several explanations for the relationship between donor size and isolation outcome. Firstly, it is possible that donor size is a surrogate marker for pancreas weight. The positive relationship between pancreas weight and BMI has been reported previously [234], and attempts have been made to use measurements of donor size, along with age and gender, to estimate pancreas weight prior to retrieval [235]. However, this argument is contradicted by studies that fail to demonstrate a relationship between pancreas weight and islet yield (Table 2). It is also feasible to suggest that islet mass increases in line with body size and the associated increased metabolic demand, though evidence supporting a correlation between increased BMI and elevated islet mass is controversial [236-239]. Finally, increased isolation success from larger donors may result from changes in the structure of the pancreatic ECM located at the islet-exocrine interface (the 'substrate' for enzyme digestion). It has been hypothesised that obesity causes this structure to 'loosen' [112], perhaps making the matrix more accessible to enzymes. However, this theory has not been investigated at the pancreatic ultrastructural level, and therefore remains unsupported.

1.7.3 Donor Age

Along with body size, age is a donor variable strongly associated with isolation outcome, both in terms of islet yield and function. Functionally, islets from younger donors are superior, and loss of insulin secretory function in non-diabetic individuals is a consequence of the normal aging process

[240, 241]. This is supported by an age related decline in insulin secretion capacity, when islets are challenged with glucose *in vitro* [215, 242-244]. Metabolic data, obtained from islet recipients post-transplantation following a meal tolerance test, also demonstrates that islets from younger donors have superior graft function. Niclauss *et al.* reported higher rates of C-peptide, as well as insulin independence, in recipients who had received islet grafts from donors <45 years old [102]. This finding was supported by data from Ihm *et al.* who investigated seven islet graft recipients 3 months post-transplant and showed superior C-peptide results were obtained in the recipients who had received islets from younger donors. However, the mechanism for decreased β-cell function with aging has not been fully elucidated. Maedler *et al*. showed that β-cell expression of the transcription factor pancreatic duodenal homeobox (PDX)-1 (important for β-cell replication and function [245]), decreased in an age dependent manner in humans, which led to decreased proliferation and insulin secretory capacity in islets from older donors [243]. Decrease in PDX-1 with age was confirmed in human pancreas tissue sections using immunohistochemistry [246]. Significant reduction in islet ATP content (a likely indicator of mitochondrial dysfunction), was also detected in islets from donors >40 years old, which also corresponded to a lower insulin response to glucose in this group [242].

Despite their functional superiority, islets from younger donors are currently underutilised, due to the technical challenges encountered when processing pancreases from this donor type. Where the literature generally demonstrates that younger donors produce lower islet yields, not all data have demonstrated this (Table 2). Nevertheless, despite detecting no difference in post-purification yields, a number of studies did show that younger donors are associated with a high numbers of trapped islets, which remain partially embedded in exocrine tissue post-digestion [101, 102]. Indeed, it is important to note that groups that have reported obtaining good islet yields from younger donors (<35 years old) often tend to receive donors with elevated BMIs (>30) [247]. This therefore suggests that age and BMI are indeed co-factors; with the positive effect of an elevated BMI decreasing the negative impact of a younger age. However, in many countries, including the

UK, the majority of donors possess lower BMIs. This most likely results in donor age having a larger impact on islet isolation outcome.

It is likely that age-related differences in pancreas digestion result from compositional differences in the ECM, which results in a suboptimal digestion from younger donors. Therefore, enhancing islet yields from younger donors can be achieved by first gaining an improved understanding of how the pancreatic ultrastructure is affected by age.

The next Section considers the effect of donor age on the structure and composition of the native pancreatic ECM.

Factor	Significant (number of studies)	Reference(s)	Not significant (number of studies)	Reference(s)
Age (years)	11	[224], [215], [221], [222], [136], [217], [248], [219], [249], [242], [250]	10	[223], [225], [101], [102], [226], [216], [218], [230], [251], [220]
BMI (Kg/m^2)	12	[224], [215], [222], [217], [248], [223], [101], [216], [218], [230], [252], [250]	5	[219], [225], [226], [251], [220]
Height (cm)	2	[136], [216]	0	
Weight (Kg)	7	[224], [221], [136], [101], [216], [252], [250]	1	[220]
BSA	4	[136], [216], [218], [250]	0	
Gender (male)	5	[136], [225], [216], [230], [226]	9	[224], [221], [222], [217], [219], [223], [218], [251], [250]
Ethnicity	0		2	[230], [250]
Time spent in hospital/ ICU prior to donation	2	[226], [218]	7	[222], [136], [217], [219], [216], [251], [250]
Donation after cardiac death (DCD)	1	[253]	4	[224], [254], [255], [256]
Traumatic cause of death	2	[224], [221]	11	[221], [222], [136], [217], [225], [216], [218], [230], [251], [250], [220]

Factor	Significant (number of studies)	Reference(s)	Not significant (number of studies)	Reference(s)
Occurrence of cardiac arrest	3	[215], [226], [216]	3	[219], [230], [251]
History of alcohol abuse	0		2	[224], [216]
Past smoker/history	1	[257]	2	[224], [250]
History of drug abuse	0		1	[224]
History of hypertension	0		3	[224], [216], [250]
Amylase (Ui/l)	1	[224]	10	[221], [222], [217], [248], [219], [223], [216], [218], [230], [251]
Insulin used	0		1	[223]
Steroid(s) used	2	[101], [230]	1	[223]
Vasopressor(s) used	4	[215], [216], [218], [230]	3	[136], [217], [223]
Pancreas fibrotic	0		4	[136], [223], [218], [230]
Pancreas damage	1	[223]	2	[224], [136]
Local procurement team	6	[215], [222], [136], [226], [216], [230]	4	[223], [224], [221], [251]
Pancreas weight (g)	4	[215], [222], [224], [230]	6	[136], [218], [219], [223] [250], [220]
Cold ischemia time (hrs)	8	[101], [215], [216], [217], [218], [221], [224], [251]	8	[136], [219], [222], [223], [226], [230] [250], [220]
Warm ischemia (hrs)	1	[217]	1	[219]
Presence of surface fat	1	[224]	1	[230]
Presence of fatty infiltration	4	[136], [222], [224], [250]	2	[218], [230]
High blood glucose	4	[215], [216], [221], [226]	4	[217], [218], [222], [251]

Table 2: Overview of donor factors reported in the literature to affect isolation outcome
References in red represent negative associations. Definition of 'isolation outcome' varies depending on the study, however the Table has been constructed based primarily on outcome of islet yield, as opposed to other parameters (i.e. preparation purity/viability/islet function).

1.8 The Impact of Donor Age on Pancreatic ECM Structure

The ECM is a dynamic structure, which is constantly being remodelled through a series of enzymatic and non-enzymatic mechanisms [258]. Part of this process is characterised by a general transition towards ECM deterioration, as a part of the normal aging process. Age dependent ECM degeneration is considered to be a two-fold process, resulting from a decrease in new matrix formation by fibroblasts, in addition to enhanced degradation [258]. ECM breakdown is modulated by tissue specific matrix metalloproteinases (MMPs), which are fundamental enzymes involved in normal tissue remodelling. However, in the aging matrix there is a progressive upregulation of specific MMPs, resulting in enhanced matrix breakdown [259, 260].

Somewhat paradoxically, despite the decrease in new matrix accumulation, many BM are reported to thicken with age, mediated through the accumulation of Advanced Glycation End products (AGEs). AGEs are a heterogeneous group of molecules formed in a non-enzymatic biochemical reaction between non-reducing sugars and amino acids. AGEs production results in a high degree of non-specific intra and intermolecular crosslinking between long lived ECM molecules. AGEs accumulation increases in line with biological aging, with these adducts identified in a variety of tissues [261-264]. Once created, AGEs formation is irreversible and can lead to significant tissue changes, including loss of ECM binding properties [265, 266], which may contribute to enhanced age-related matrix fragility. AGEs have also been shown to initiate cellular apoptosis through interaction with the receptor for AGEs (RAGE) [267]. In addition to an age-related increase, the persistent hyperglycaemia resulting from diabetes leads to elevated AGEs formation, which have been shown to contribute towards the development of many of the secondary complications of T1DM, such as retinopathy [268, 269].

In spite of the above, when reviewing the effects of aging on human tissues, changes in ECM quantity have been largely inconsistent (Table 3). In addition to age, in some tissues, ECM content also appears to be influenced by gender; in cardiac tissue there was an age dependent decrease in

collagens I, III and VI, whereas all three proteins increased with age in female subjects [270]. It is also apparent that changes in collagen content in response to the normal aging process are tissue specific (Table 3). For example, collagen content in the kidney increases with age [271, 272], but is reduced in the invertebral disc of older donors [273].

As the relationship between ECM content and age appears to be tissue specific, before determining how donor age affects pancreas digestion it is first important to determine how the pancreatic ECM is affected by age. Bedossa *et al*. attempted to quantify total collagen content in pancreases from 11 donors using Sirius Red staining. The results indicated that collagen content was significantly higher in donors aged over 50. However, the age range of the donors in this study was very limited; only 4 donors were aged under 50, and the youngest donor was 48 [274]. Using the same detection method, Tons *et al*. determined the content of collagen in 60 human pancreases, from a wide age range of donors. Collagen content was assessed in the peri-islet region, as well as in the total pancreatic region. The results indicate a slight increase in total pancreatic collagen content with age, but the authors did not assess if this was statistically significant [275]. Hughes *et al.* aimed to determine if collagen type VI was differentially expressed between younger (aged 4-28 years, n=7) and older (aged 40-62, n=7) donors. The authors found no age related difference in peri-islet collagen VI content, which was semi-quantified morphometrically [171].

In the most complete characterisation of age-related changes in the pancreatic ECM to date, Loganathan and colleagues investigated quantitative differences in pancreases from younger (<34 years old, n=19) and older (>35 years old, n=25) donors [99]. Total ECM content and collagen contents were investigated. In addition, the matrix proteins: collagens I, III, IV, VI, laminin and fibronectin, were quantified via morphometrical assessment. Measurements were not localised to specific morphological areas of pancreatic tissue (i.e. the peri-islet region). The results indicated that total ECM content was significantly higher in the younger donor pancreas. There was also a decrease in total collagen content with age, though this did not reach significance. Although the

expression of the majority of specific proteins was not affected by age, there was a significant age-related decrease in BM proteins laminin and collagen IV [99].

Increased matrix expression in younger donors has the potential to explain why a high percentage of trapped islets are produced during the pancreas digestion of this donor type. It is possible that the effectiveness of the currently utilised isolation blends (optimised to digest pancreases from older donors) is reduced due to an increase in matrix protein quantity. However, current studies investigating age-related changes in the pancreatic matrix have focused on a restricted group of ECM proteins. Complete characterisation of the pancreatic matrisome has revealed that it is a highly complex environment, composed of over 100 proteins [163]. It can therefore be argued that investigating a select subset of proteins is oversimplifying this complex system, whilst creating the potential to overlook ECM proteins that are significantly affected by age. Instead, what is required is a complete characterisation of the ECM of both younger and older donors, enabling the full list of proteins that are differentially expressed between the two groups to be identified.

ECM Protein	Tissue	Measurement Type	Age Definition	Age Related Change	Reference
Collagens I & III	Cardiac	• Picrosirus staining & convention light microscopy • Transition Electron Microscopy (TEM)	• *Younger subjects:* (20-25 years old; n=6) • *Older subjects:* (67-87 years old; n=6)	• Significant increase in total collagen staining with age (particularly collagen I) • Increase in collagen fibre diameter with age	[276]
Collagens I, III & VI	Cardiac	• Western Blotting	• *Younger subjects:* (17-40 years old; n=14) • *Older subjects:* (50-68 years old; n=17)	• Age related changes in ECM content were gender dependent • In male donors all three proteins decrease with age • In female donors all three proteins increase with age	[270]

ECM Protein	Tissue	Measurement Type	Age Definition	Age Related Change	Reference
Collagen & proteoglycans (PGs)	Invertebral Disc	• Dimethylmethylene Blue Stain (PGs estimate) • Western blotting for specific PGs • Hydroxyproline determination by HPLC (collagen estimate)	Age stratification: • 41-50 years • 51-60 years • 61-70 years • 71-80 years	• At age 51 plus there was a significant reduction in total PGs and collagen content • Specific PGs decorin and lumican were significantly reduced in subjects aged 71 plus	[273]
PGs	Skin	• Western Blotting	• Fetal: 80 and 120 days • Adult: 33 and 82 years	• PGs expression affected by age • Versican expression increased with age, whereas decorin expression decreased	[277]
Collagen	Skin	• Hydroxyproline assessment	• 53 subjects aged 15-93 years	• Males have higher collagen content than females • Gender independent decline of collagen content with age	[278]
Collagens I and IV	Kidney	• IHC	• 18 subjects aged 19 – 92 years	• Collagen I expression increased with age • Collagen IV content was unaffected by age	[271]
Collagen IV and laminin	Kidney	• Radioimmunoassay • IHC • Hydroxyproline assessment	• 20 subjects aged 2-89 years	• Significant increase in collagen IV with age • Decrease in laminin with age	[272]
Collagen IV	Cerebral microvess-els	• Immunofluorescence	• *Younger subjects:* (27-47 years old; n=11) • *Older subjects:* (67-82 years old; n=16)	• Collagen IV expression associated with microvessels significantly increased with age	[279]
Collagen	Cervix	• Hydroxyproline assessment	• 57 subjects aged 29-49 years	• Collagen content significantly increased with age	[280]

ECM Protein	Tissue	Measurement Type	Age Definition	Age Related Change	Reference
Collagen	Pancreas	• Sirius red staining	• 11 subjects aged 48-82 years	• Collagen content significantly increased in donors over 50	[274]
Collagen	Pancreas	• Sirius red staining	• 60 donors. Approx. 20 to 70 years	• Slight increase in total collagen content with age, but significance not confirmed by statistical testing	[275]
Collagen VI	Pancreas	• IHC	• *Younger donors:* (4-28 years; n=7) *Older donors:* (40-62 years; n=7)	• Peri-islet collagen VI content was not affected by donor age	[171]
Total ECM, total collagen. Specific matrix proteins: collagens I, III, IV, V, VI, laminin and fibronectin	Pancreas	• Masson's trichrome staining (total ECM) • Hydroxyproline assessment (total collagen) • IHC (specific matrix proteins)	• *Younger donors:* (<34 years; n=19) *Older donors:* (>35 years; n=25)	• Total ECM content was significantly higher in younger donors • Collagen content decreased with age, but didn't reach significance • Collagen IV and laminin significantly higher in younger donors	[99]

Table 3: Age-related differences in ECM composition in a variety of human non-diseased tissues
IHC; immunohistochemistry

1.9 Tailoring Isolation Blends to Younger Donor Pancreases

Several studies have attempted to optimise islet isolation protocols from younger donors, to allow the full potential of these donors to be realised. This has included efforts to enhance the purification of trapped islets [88], in addition to modifying aspects of the semi-automated digestion phase, which included utilising a larger pore size and reducing the mechanical shaking of the digestion chamber [87]. Balamurugan and colleagues were successfully able to obtain mantle free islets from donors aged as young as 6 months, by reducing mechanical shaking and introducing

additional filter systems to prevent the release of mantled islets into the collection flask [281]. Early intra-ductal injection of collagenase has also been shown to be beneficial for improving isolation yields from younger donors (<30 years) [282]. In this study, collagenase was injected within 45 minutes of retrieval, followed by an additional dose upon reaching the isolation facility. The control group only received the second injection of collagenase. Although the increased collagenase dose cannot be eliminated as the reason for the superior outcome, the authors propose that the enhanced distal distribution of collagenase throughout the pancreas is achieved when using the early injection method. They suggest that the fragility of the pancreatic ductal architecture in younger donors makes distal ducts predisposed to collapse. Although an intriguing argument, the authors did not use an older aged group to show that early injection of collagenase is specifically beneficial for younger donors. Indeed, it is well established that ductal preservation can enhance isolation yields [283-285], but based on the current evidence this phenomenon cannot be specifically assigned to the younger donor.

As the embedded islets are produced during the enzymatic digestion phase of the procedure, some studies have attempted to enhance isolation from younger donors by attenuating enzyme blends. Doubling collagenase concentrations has been shown to significantly reduce the percentage of trapped islets in donors aged under 30 [98]. Although using a more concentrated collagenase slightly improved post-purification yield this did not reach significance, suggesting that modification of collagenase concentration may not be the best method for increasing islet yields from younger donors [98]. In a recent report by Loganathan *et al*. the authors experimented with attenuating the ratio of collagenase to protease, to improve isolation outcome for younger donor pancreases (aged 15-34 years) [99]. Using Vitacyte enzyme, three enzyme combinations were created:

a) Standard enzyme concentration (SEC);

b) Increased collagenase concentration (ICC), containing three-fold more collagenase than SEC;

c) Increased protease concentration (IPC), containing four-fold more protease than SEC.

The authors were able to test all three enzyme combinations on a single pancreas, by dividing the pancreas into the head, body and tail portions. Using the semi-automated isolation method, separate islet isolation procedures were performed for each of the three pancreatic regions, and the anatomical region used for each enzyme combination was rotated for each of the six organs studied. Interestingly, the IPC enzyme combination significantly reduced the percentage of mantled islets by 43%, as well increasing the islet recovery percentage by 22% post-purification. Increasing the protease concentration did not have any significant adverse effects on viability or insulin response following glucose stimulation. In contrast, the ICC enzyme was less successful and only reduced the percentage of mantled islets by 5%, and increased total islet recovery by 3%, when compared to SEC [99]. To test the effectiveness of the IPC blend in a clinical scenario, 5 full scale isolations using whole pancreases from donors aged 19-30 years old were used. Not only were the percentage of mantled islets, and islet recovery, similar to the split pancreas results, but were comparable to those from a 55 year old donor, isolated using the IPC [99]. Another study showed that significantly increased post-purification yields were obtainable from donors aged <25 years when an enzyme with significantly enhanced caseinase activity was used (caseinase is used as a marker for measuring protease activity) [136].

These studies highlight the potential importance of protease, in enhancing islet yields from younger donors. However, these improvements are based on the empirical attenuation of enzyme blends. An alternative approach would aim to understand how isolation enzymes components target the ECM for digestion, and how this process is influenced by donor age. Although this approach would allow enzyme blends to be tailored to specific pancreatic substrates/donor types this concept is lacking in the current literature.

Aims of this Thesis

Key to enhancing the success of human islet isolation is the creation of donor-specific enzyme blends. Donor age is a factor extensively reported to impact islet yields, with high percentages of trapped islets produced when processing younger donor pancreases that have been controlled for BMI. Previous research has attempted to optimise pancreas digestion from this donor type by attenuating clinical enzyme blends. However, these modifications are implemented with a lack of knowledge about the interaction of enzyme components with the ECM. As exocrine free islets are readily isolated from older human donors, it is reasonable to assume that trapped islets are produced from younger donors due to differences in ECM composition.

Therefore, the research project contained in this thesis aimed to test the hypothesis that **Donor age affects the molecular structure of the human pancreas, which influences the ability of current enzyme blends to digest the peri-islet ECM**

This was achieved by:

1. Confirming the impact of donor variables on islet isolation outcomes, utilising UK isolation data (Chapter 2)
2. Characterising age-related differences in the expression of ECM proteins in the native pancreas (Chapter 3)
3. Determining how donor age affects the digestion of the peri-islet ECM, by studying specific enzyme and ECM interactions, in pancreases from different aged donors (Chapters 4-6)

CHAPTER 2

Analysis of Donor Factors on Islet Isolation and Transplantation Outcomes in the UK

2.1 Introduction

In order to help inform decisions about pancreas acceptance criteria, and increase the overall success of human islet isolation, many islet groups have investigated the impact of pancreas donor factors on islet isolation outcomes (see Chapter 1, Table 2). This has led to the development of several novel scoring systems, such as the North American Islet Donor Score (NAIDS). Designed by examining 1,056 isolations, the NAIDS predicts the likelihood of obtaining a transplantable islet yield (>400K IEQ), based on a combination of donor factors [216]. The NAIDS score ranges from 0-100, with an increasing score associated with a higher likelihood of obtaining a transplantable islet yield. Whilst only 7% of donors with scores <50 achieved a transplantable yield, this increased to 54% for those that scored ≥80 [216]. An increased NAIDS was associated with an elevated BMI and body surface area (BSA), whilst an increased amylase, and the use of vasopressors, reduced the overall score. More recently, the NAIDS was validated by a medium volume clinical islet isolation facility, at the University of Chicago [286]. In this study, 0% of the isolations that incurred scores <50 went on to produce a transplantable yield, which was increased to 40% for isolations that scored ≥80. However, unlike the original study, this group defined a transplantable yield as being >300K IEQ [286]. The NAIDS is reminiscent of the 2005 donor scoring system produced by the Edmonton group, which correctly predicted transplantable yields from 15/15 of pancreases that had donor scores of 90-100 [287]. Interestingly, in this scoring system, donor age was determined to have the largest impact on isolation outcome, where it accounted for 20% of the overall score weighting [287]. Another study reported that donor age, sex, and the duration of enzyme digestion could predict isolation outcome with an accuracy of 72% [136]. However, as the efficiency of enzyme digestion cannot be determined prior to the commencement of the isolation procedure, the predictive power of this model is limited.

Although these studies have demonstrated that donor factors have a substantial impact on isolation outcomes, there has been significant study-to-study variation in the factors that are reported to be most influential. For example, whilst a number of reports have demonstrated that

donor age is significantly inversely proportional to isolation success [215, 221, 222, 249], not all studies have supported this relationship [102, 223, 225]. The impact of cold ischemia time (CIT) is also disputed, with some reports showing that increasing CIT is significantly detrimental to yield [101, 215, 221], whereas others have shown no effect [136, 222, 230]. Such inconsistencies likely result from the fact that many of these studies are retrospective and are determined by the variations in the pancreas donor acceptance criteria for each country (or islet transplant network). For example, the age of donors accepted for clinical islet isolation have ranged from 5-77 years [216] to 19-65 years [215]. Currently, within the UK, only pancreases from donors aged between 25-60 years are accepted for clinical isolation. Variations in these basic donor demographics prevent the meaningful transference of results outside of a specific country or network. Therefore, when considering how organ donor characteristics influence UK islet isolations, it is critical to examine UK isolation data. However, to date, no one has undertaken a large-scale analysis of this nature on a UK cohort.

Of equal importance to determining the effect of donor factors on islet isolation, is understanding their impact on post-transplant islet graft function. The few studies that have attempted to explore this relationship have focused mainly on the influence of donor age, and have shown that donor islets become less metabolically potent with age [102, 242]. In addition, an increasing pancreas warm ischemia time (WIT) has demonstrated to be detrimental to islet function, post-infusion [288].

In recent years, based on the indication for transplantation, there has been a shift in many centres from defining islet transplantation success on the basis of achieving insulin independence [75], to its ability to improve glycaemic control, and reverse life threatening hypoglycaemic unawareness [79, 80]. The achievement of these endpoints is reliant on the functionality of the islet graft, which can be studied with a series of metabolic tests [289]. This can include measuring insulin or C-peptide, in response to various stimuli such as glucose, arginine [242, 290], or following an oral

mixed meal test (MMT) [291]. A MMT is a standardised liquid based meal that, in addition to carbohydrates, contains a known amount of lipids and proteins, thus providing a more physiological based challenge for the islets [291]. Furthermore, the use of integrated graft scoring systems enables multiple variables to be assessed in tandem, as opposed to measuring single parameters. Currently, the most well utilised composite assessment tool is the Beta score [292]. This is a categorical based scoring system that incorporates the fasting glucose, the 90-minute stimulated C-peptide (following a MMT), the HbA1c and the daily insulin requirement. A score of between 0-8 is assigned, with 8 representing excellent graft function, and 0 a failed graft. The Beta score correlates well with the 90-minute stimulated glucose concentration, validating its ability to measure graft function [292]. However, due to its categorical nature, its ability to detect subtle changes in a graft have been questioned, which prompted the revision of the score in 2016 [289]. The 'Beta-2' score not only estimates graft function as a continuous variable, but the measurements are made on the basis of a single fasting blood sample [289]. Scores range from 0-42, with a score >15 considered to indicate insulin independence. In line with the original Beta score, it is well correlated with the 90-minute stimulated glucose [289]. The Beta-2 score was validated externally, demonstrating excellent reproducibility [293]. Finally, our group has recently developed a novel graft assessment scoring system, termed the 'Glucose Dependent Insulin Secretion Rate' (GDISR) [294]. Using deconvolution-based technology, the GDISR predicts the pre-hepatic insulin secretion rate (ISR), from the plasma C-peptide measurements [294]. The GDISR is then taken as the slope of linear regression, when plotting the ISR against the corresponding glucose concentrations, throughout the course of the MMT [294]. The GDISR has demonstrated to be significantly superior for predicting a failed vs functioning graft, when compared with the Beta and Beta 2 scores (failed graft defined as 90-minute stimulated C-peptide <50pmol/L) [294].

The aim of this Chapter was to determine the impact of donor factors on isolation and transplantation outcomes within the UK. Two isolation outcome measures were investigated, which included the analysis of IEQ as a continuous variable, in addition to the determining how

each factor affected the ability to achieve a transplantable yield (≥200K IEQ). Post-transplant graft function was measured via the Beta-2 score, and the GDISR.

2.2 Methods

2.2.1 Impact of Donor and Pancreas Factors on Isolation Outcome

2.2.1.1 NHSBT Human Islet Isolation Data

Between January 2011 and December 2017, 736 pancreases were retrieved for human islet isolation after appropriate informed consent, as part of the UK Nationwide Islet Transplantation Programme. The organs were transported to one of the three clinical isolation facilities licenced by the UK regulators (Oxford, Kings and Edinburgh). 4 organs were rejected after receipt at the lab, on the basis of extensive fibrosis, a prolonged CIT, pancreas weight <50g and organ damage at retrieval. The remaining 732 organs were processed for islet isolation using standard protocols. In summary, this involved semi-automated enzymatic and mechanical digestion followed by density gradient purification using a Cobe 2991 processor. Post-purification, the number of islet equivalents (IEQ) were determined by staining with dithizone and manual counting. Isolation outcome data from all three isolation centres was reported centrally to NHS Blood and Transplant (NHSBT). Following appropriate consent and ethical approval, isolation data was obtained from NHSBT, which included islet yield (in the form of IEQs) and 41 donor and pancreas related factors. Raw data was obtained for: donor age, sex, height, and weight, past socio-economic history, blood chemistry, and information regarding pancreas condition. Donor BMI (Kg/m^2) and BSA were determined from the height and weight data. BSA was calculated based on the method described by Mosteller [233].

2.2.1.2 Statistical Analysis for Isolation Data

Regression analysis was used to determine the effect of donor and pancreas related factors on islet yield. Yield was investigated as both a continuous outcome measure and as a dichotomised variable. For the dichotomised analysis, isolations were separated into two groups based on whether or not a transplantable yield was obtained. A 'transplantable' yield was defined as ≥200K IEQ, as per the guidelines of the UK-wide PAG-ISG (Pancreas Advisory Group - Islet Study Group). For the analysis performed with IEQ as a continuous variable, linear regression was used. Binary logistical regression was selected for analysing the dichotomised outcome measure. For both outcome measures univariate analysis was performed, followed by multivariate analysis. Factors with a data completeness of >50%, and with a *p* value ≤0.25 following univariate analysis, were selected for the multivariate analysis. The presence of collinearity was explored. For factors that were considered to be correlated, the explanatory variable that best described the outcome variable (i.e. the factor with the most significant *p* value) was entered into the multi model. The set of explanatory variables that had the largest impact on islet yield were identified by performing backwards stepwise linear regression. Briefly, all selected explanatory variables were added to the multivariate model, and the least significant variable (i.e. that with the highest *p* value) was removed. The model was then refitted, and the step-by-step elimination continued to be performed until all remaining factors had a *p* value of ≤0.1.

The predictive capabilities of the final multivariate models were investigated. For the model generated with IEQ as a continuous variable, the predicted IEQ values for each isolation were determined from the regression equation. The predicted IEQ values were correlated against the actual IEQ values that were produced following islet isolation. Receiver operating characteristic (ROC) curves were used to determine the diagnostic capabilities of the binary model, designed to predict the likelihood of obtaining a transplantable yield. SPSS was used for the statistical analysis (IBM Corp, Version 22, Armonk, NY).

2.2.2 Impact of Donor and Pancreas Factors on Islet Transplantation Outcomes

2.2.2.1 UKITC Islet Transplant Data

The UK Islet Transplantation Consortium (UKITC) kindly provided data from 84 follow-up MMTs, attended by 45 recipients who had received a single (i.e. first) islet transplant at one of six UK transplant centres (Edinburgh, Newcastle, Royal Free, Oxford, Manchester and Bristol) between October 2009 and October 2014. Prior to transplantation all recipients were proven C-peptide negative and had life-threatening hypoglycaemic unawareness and unstable glycaemic control, despite optimised conventional insulin treatment. Follow-up appointments occurred every 3 months, up until one-year post-transplant. Not all recipients attended every follow-up appointment. During the MMT blood samples were obtained every 30 minutes, over a 3-hour period (including collection of a fasting sample). Samples were analysed at a central reference laboratory in Cambridge (UK), where the C-peptide and glucose concentrations were measured. Two composite measurements of graft efficiency were calculated. The first was the validated Beta-2 score, which was calculated using the fasting C-peptide and glucose, in addition to the recipient's insulin dose and HbA1c, as described previously (Figure 5) [289]. The GDISR was also used, developed by our team in Oxford [294]. The GDISR was calculated as the slope of the linear regression, which resulted from plotting the deconvoluted ISR (pmol/kg/min) against the corresponding glucose concentration (mmol/L), over the course of the MMT [294]. The islet recipients were linked with their respective donors through the anonymised UKT numbers. Prior to 2014, limited amounts of donor data was stored centrally. Therefore, only 5 donor factors were selected for investigation. This included donor age, sex, BMI, donor type (DBD/DCD) and pancreas CIT. In addition, the purity (%), viability (%) and the size of the graft (IEQ/Kg) were investigated, as well as the duration of time since transplantation (months).

$$\text{BETA-2 score} = \frac{\left(\sqrt{\text{fasting C-peptide (nmol/L)}} \times (1 - \text{insulin dose [units/kg]})\right)}{\text{Fasting plasma glucose (mmol/L)} \times \text{HbA1c}(\%)} \times 1000$$

Figure 5: Calculation of the Beta-2 score
As described by Forbes *et al.* [289]

2.2.2.2 Statistical analysis for Transplant Data

Linear modelling was used to determine the statistical impact of each explanatory variable on graft outcome (assessed via the Beta-2 and GDISR scores). As the experimental design contained repeated measurements (i.e. multiple measurements were obtained from each donor at different time points), a mixed linear modelling approach was selected. As with the isolation outcome data, univariate analysis was first performed, followed by multivariate analysis. Factors with a *p* value ≤0.25 were selected for multivariate modelling. Backwards stepwise analysis was used to determine which variables had the largest impact on transplantation outcome. A final *p* value cut-off of ≤0.1 was used. The predictive capabilities of the resulting multivariate models were investigated. The predicted Beta-2 and GDISR scores for each recipient visit were determined from the regression equation. These were then correlated against the actual values. Mixed linear modelling was performed in the software package 'R' (R Core Team (2016). R: A language and environment for statistical computing. R Foundation for Statistical Computing, Vienna, Austria.) This statistical programme was selected as it allows for the straightforward incorporation of random effects into linear models.

2.3 Results

All results tables, unless specified to be located within the Appendix, can be found at the end of this results section (page 92). Figures are integrated within the text.

2.3.1 Influence of Donor and Pancreas Factors on Islet Isolation Outcomes in the UK

2.3.1.1 General Description of Explanatory Variables and Islet Isolation Outcome Measures

Data was available for 732 donors, whose pancreases were retrieved and accepted for islet isolation at one of the three UK licenced islet isolation facilities. In total, 41 different donor and pancreas factors were examined for each donor. General data exploration was performed, to determine the characteristics of each explanatory variable (Table A1, Appendix). Only 6 of the 41 explanatory variables contained data from all 732 donors (age, sex, weight, height, BMI and BSA). In addition, 5 variables contained >50% missing values (cardiac arrest duration, administration of insulin or dopamine, ITU stay and AST levels; (Table A1, Appendix). The mean age of the donors was 45.7±9.8 years and the mean BMI was 28.3±4.4. 54% of the donors were male, and almost 84% of organs were donated following brain death certification (DBD), as opposed to donation following cardiac death (DCD; 16%). The mean CIT was 6.9± 2.1 hours, and approximately 13% of pancreases were reported to be received with at least one haematoma (Table A1, Appendix). A transplantable islet yield was achieved in 53% of the pancreases processed (≥200K IEQ). On average, 223,400± 26,200 IEQs were produced per pancreas (Table A1, Appendix).

2.3.1.2 Factors Influencing IEQ as a Continuous Outcome Measure

The impact of each explanatory variable on islet yield was first examined independently using univariate linear regression (Table 4). The 'B' value presented in Table 4 represents the coefficient for each explanatory variable, which allows changes in the dependent variable (i.e. IEQ) to be predicted. For example, for each yearly increase in age, there would be a predicted 2,311 increase in IEQ. Pancreases from female donors were predicted to produce 18,502 more IEQs than their male counterparts (Table 4). The 95% confidence intervals for B are also displayed. The R^2 value indicates the extent to which each explanatory variable can explain the overall variation in IEQ. For example, around 1.6% of the overall variation in IEQ can be explained by donor age. The *p* value

tests if the coefficient is significantly different from zero (Table 4). Factors that had a significant positive impact on yield included: age, weight, BMI, BSA, abdominal girth, confirmed presence of past hypertension, and a fatty pancreas. Factors that had a significant negative impact on yield included: past smoker history (but not amount of cigarettes/day), presence of donor cardiac arrest (but not duration of arrest), a hypoxia related cause of death, being a DCD donor, and the presence of pancreatic fibrosis or haematomas (Table 4). Past alcohol abuse, pancreas CIT, and pancreas weight were three of the explanatory factors that had no significant impact on final islet yield. 14 factors with *p* values ≤0.25 and a completeness of >50% were selected for multivariate analysis (Table 4). There was a high degree of collinearity between donor weight, BSA and BMI. Therefore, as the most significant factor, only BMI was selected to be entered into the multivariate model. After performing backwards stepwise linear regression, 5 factors remained with *p* values ≤0.1 (Table 5). Of these factors, donor age and BMI positively influenced isolation outcome, whereas a history of past smoking, and the presence of pancreatic fibrosis and haematomas, reduced islet yield. Overall, the model was able to explain around 7% of the overall variability in IEQ (Table 5). This was demonstrated further by plotting the model predicted IEQ values against the IEQ values actually obtained following islet isolation (Figure 6).

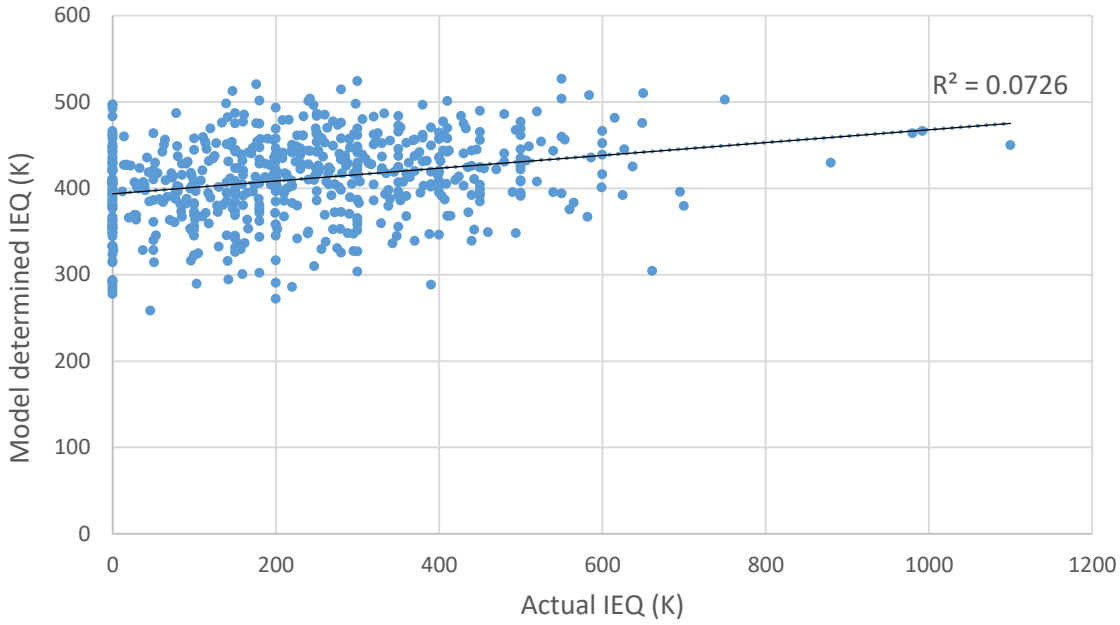


Figure 6: Correlation between the IEQ predicted by the model and the actual IEQ
The model developed in Table 5 was used to predict the IEQ values for 618 isolations. The predicted values were compared with the actual IEQ value, produced following islet isolation. The R^2 value was 0.07.

2.3.1.3 Factors Influencing the Ability to Achieve a Transplantable Yield

Univariate binary logistical regression was used to determine which explanatory variables affected the likelihood of obtaining a transplantable yield (≥200K IEQ) (Table 6). This type of regression analysis is interpreted as an odds ratio, which predicts the likelihood that the explanatory variable will cause the dependent variable (i.e. IEQ) to fall into one of two categories (i.e. a transplantable vs a non-transplantable yield). An odds ratio >1 suggests that the explanatory variable has a positive impact on yield (i.e. the higher the value of the variable, the more likely that a transplantable yield will be obtained). The reverse is true for an odds ratio <1, which indicates that the variable has a negative impact on isolation outcome. For example, for each yearly increase in age, it is predicted that likelihood of achieving a transplantable yield will increase by a factor of 1.024 (Table 6). For the dichotomous explanatory variables the direction of the relationship is indicated in the 'factor'

box in Table 6. For example, when a pancreatic haematoma was present (indicated by the (Y) in this box) the odds ratio was 0.434 (Table 6). Therefore the presence of a haematoma decreased the likelihood of obtaining a transplantable yield by a factor of 2.3 (1/0.434). Procurement of pancreases following cardiac death (DCD) produced an odds ratio of 0.661, indicating that DCD donation reduced the chance of obtaining a transplantable yield by a factor of 1.5 (1/0.661). Table A2 in the thesis Appendix provides an overview of the explanatory variable characteristics within the two outcome groups.

Overall, the factors that had a significant positive impact on the likelihood of obtaining a transplantable yield included: age, weight, BMI, abdominal girth, confirmed presence of past hypertension, and being administered insulin during hospital stay. Factors that had a significant negative impact on yield included: DCD donation, hypoxia related cause of death and the presence of pancreatic haematomas (Table 6). 11 factors with *p* values ≤0.25 and a completeness of >50% were selected for multivariate analysis (Table 6). Following backwards stepwise regression, 5 factors remained with a *p* value ≤0.1 (Table 7). Of these factors, donor age, BMI and the presence of past hypertension positively influenced isolation outcome, whereas not surprisingly, the presence of pancreatic fibrosis and haematomas, reduced the likelihood of obtaining a transplantable islet yield. Overall, the model was able to explain around 8% of the overall variability in IEQ (Table 7). ROC curves were generated on the basis of this model (Figure 7 a). The area under the ROC (AUROC) was 0.65 (Figure 7 b). The cut-off value of 0.563 resulted in a test sensitivity (i.e. true positive) of 0.61, and a 1-specificity (i.e. false positive) of 0.39. Therefore, overall, 61% of isolation outcomes were correctly predicted using the model (Figure 7 b).

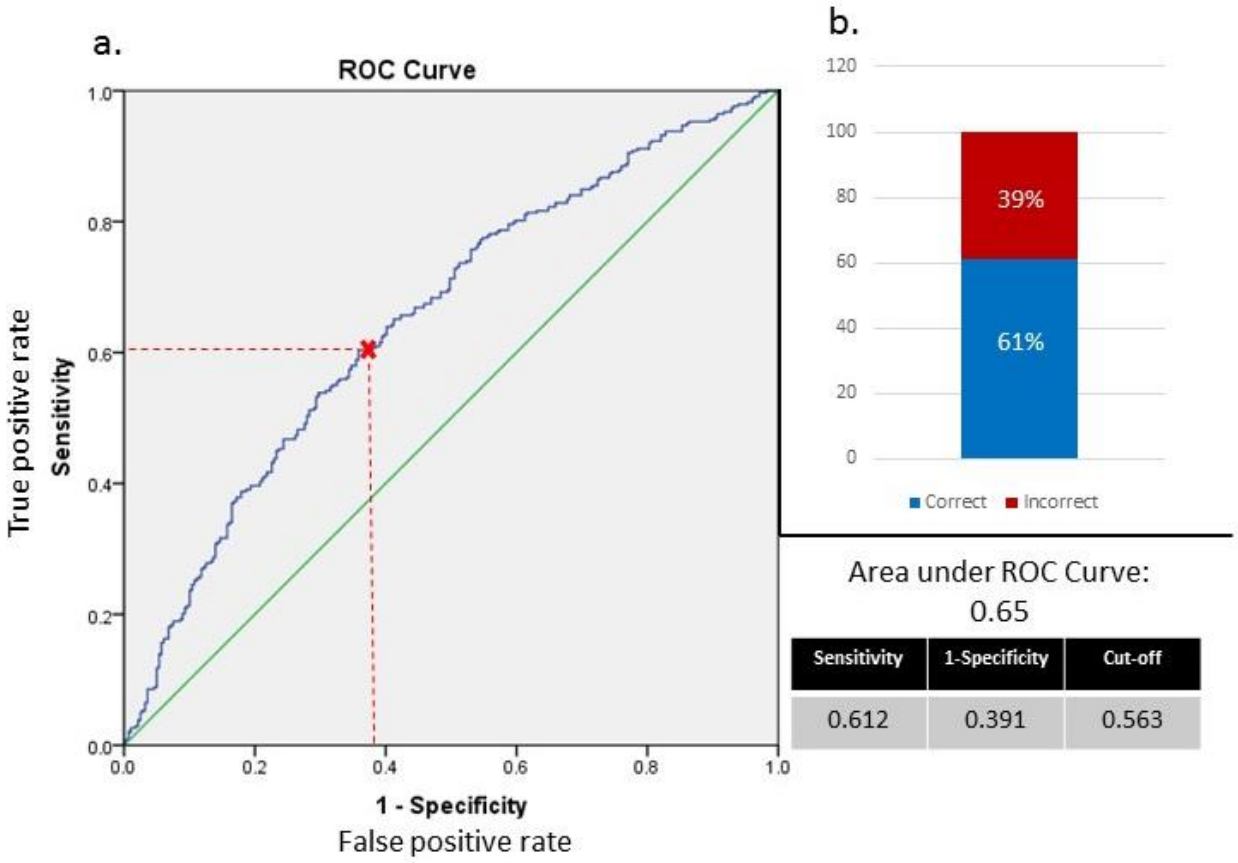


Figure 7: ROC curve of the devised multivariate binary model for predicting islet isolation outcome

a) ROC curves were generated based on the multivariate model (Table 7). A cut-off value of 0.563 resulted in a maximal test sensitivity of 0.61 and a 1-specifiity of 0.39

b) Overall, 61% of isolation outcomes were correctly predicted using the model

2.3.2 Influence of Donor and Pancreas Factors on Islet Transplantation Outcomes in the UK

2.3.2.1 General Description of Explanatory Variables and Islet Transplantation Outcome Measures

84 MMT were analysed from 45 first islet transplant recipients, over a four-year period. Analysis was restricted to first islet transplant recipients only, to enable post-transplant graft function to be attributed to specific donors. MMT were administered at 1, 3, 6, 9 and 12 months post-transplantation. Not all recipients had an MMT at each time point (Table A3, Appendix). Only one recipient completed all 5 MMT (2%). 7 of the recipients had 3 MMT (16%), 21 had 2 MMT (47%), and 16 were only administered a single MMT (35%). Following islet transplantation, 2 recipients

were insulin independent at 1 and 3 months (6.25 and 6.8%, respectively), which decreased to only 1 recipient at 12 months (16%). 1 graft failed within the first month (defined as 90-minute C-peptide <50pmol/L), but still benefited from a reduction in hypoglycaemic events. Only two recipients did not see an improvement in hypoglycaemia during the first month (Table A3, Appendix). Interestingly, both of these recipients had functioning grafts (Table A3, Appendix). Both recipient insulin requirement and HbA1c were improved by islet transplantation (Figure 8). The mean insulin dose prior to transplantation was 0.53±0.19 U/Kg, which significantly reduced to 0.32±0.23 U/Kg at 1 month (p<0.05 as compared to pre, Figure 8 a). By 9 and 12 months the insulin dose was not significantly different from the pre-dosage, although the cohort had greatly diminished by this time (Figure 8 a). HbA1c was also significantly reduced from 8.4±1.5% pre-transplantation to 7.2±1.2% at one-month post-transplantation (p<0.01 as compared to pre, Figure 8 b). Although the average HbA1c decreased further at 3 and 6 months, by 12 months it had returned to the one-month post-transplant level (7.3±2%, Figure 8 b). For both the HbA1c and insulin dose, the spike at 9-months reflected the limited number of data points for this particular visit (Figure 8).

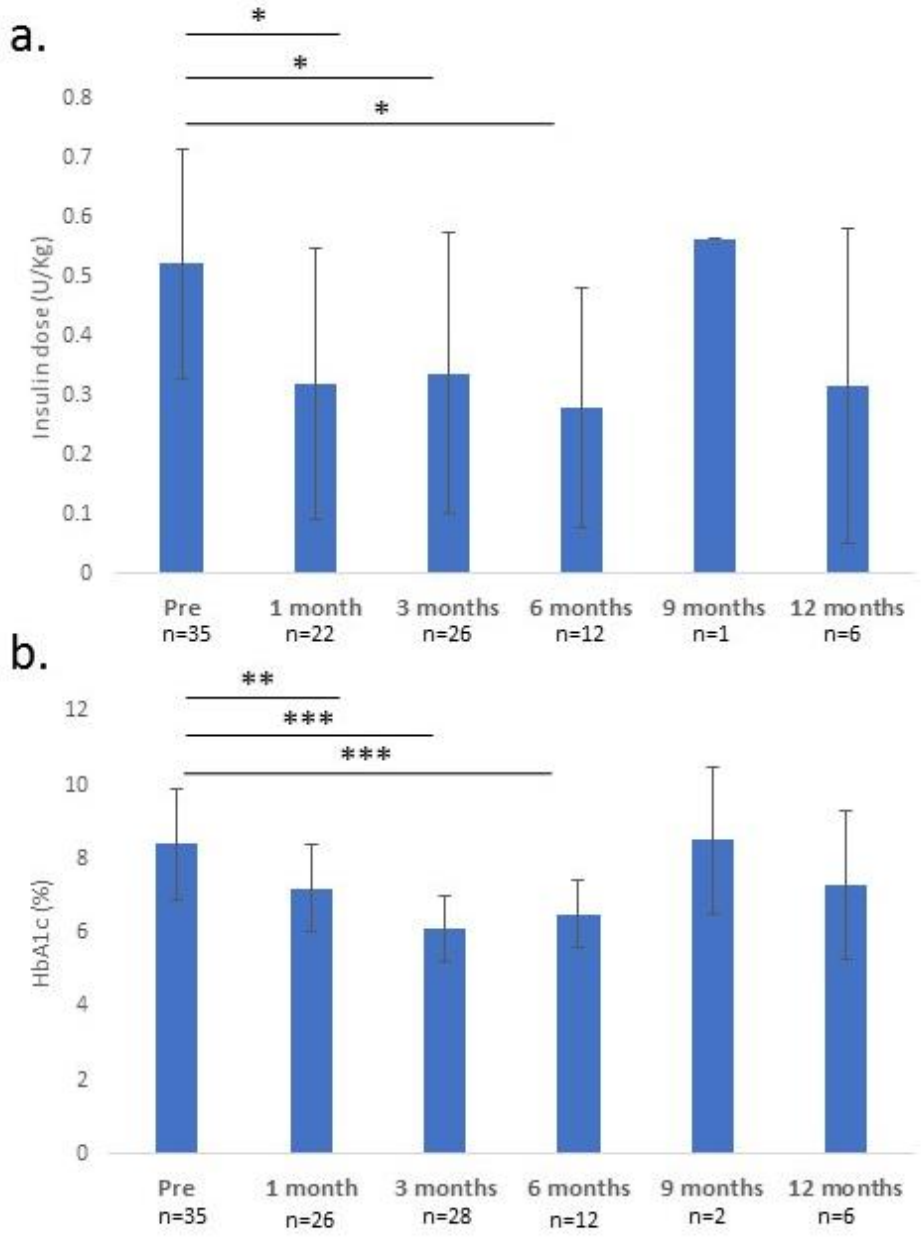


Figure 8: Average recipient insulin dose and HbA1c prior to, and following, first islet transplant a) Average insulin dose (U/Kg) for recipients' pre and post islet transplantation. b) Average HbA1c (%) for recipient pre and post islet transplantation. Both Insulin dose and HbA1c significantly declined following first transplant, which was maintained up until 6 months. From 9 months onwards recipient insulin dose and HbA1c were not significantly different from the pre-transplant levels. Mean and standard deviations are displayed. Data were analysed by ANOVA.
* p<0.05, ** p<0.01, *** p<0.001

On average, the transplanted islets were procured from donors with a mean age of 45.9±10.1 years, and a BMI of 29.4±4.6 (Table A4, Appendix). 48% of the donors were male, and 82% of the organs

were retrieved from donors following brain death (DBD; Table A4, Appendix). The mean pancreas CIT was 7.1±1.9 hours. Following isolation and culture, the mean preparation purity and viability were 73.4±16.1% and 88.4±5.7% respectively. The number of IEQs transplanted ranged from 3,108 to 11,429 IEQ/Kg of recipient body weight, with 6,153.6±1825.8 IEQ/Kg transplanted on average (Table A4, Appendix). The Beta-2 score was calculated using the fasting C-peptide and glucose, in addition to the recipient's insulin dose and HbA1c (Figure 5) [289]. Due to the absence of daily insulin dose requirements for 18 recipients, it was only possible to calculate the Beta-2 scores for 66 of the visits. The mean Beta-2 score was 6.102±5.188 (Table A4, Appendix). The GDISR was calculated from the deconvoluted ISR (pmol/Kg/min) and the corresponding glucose concentration (mmol/L), over the course of the 3 hour MMT [294]. The mean GDISR obtained from all visits was 0.261±0.326 (Table A4, Appendix). To confirm how accurate the scoring systems were at predicting graft function, correlations were performed against the stimulated 90-minute C-peptide. Both the Beta-2 score and the GDISR displayed strong correlations with this measurement (Figure 9).

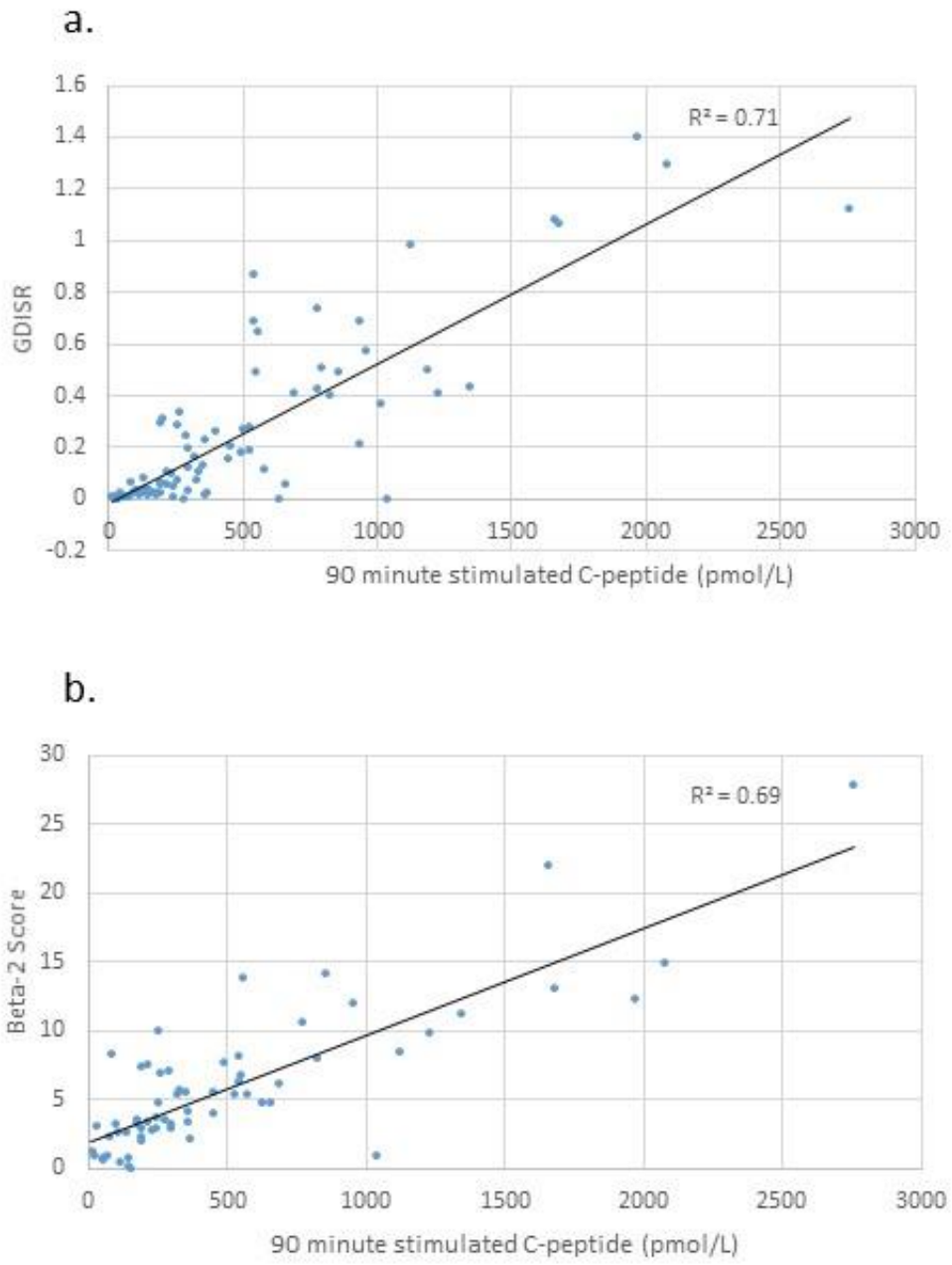


Figure 9: Correlation of Composite Scoring Systems with the 90-minute C-peptide
Correlation between the 90-minute C-peptide and the a) GDISR and b) Beta-2 score. Both scoring methods are well correlated to the 90-minute stimulated C-peptide (pmol/L).

2.3.2.2 Factors Influencing Transplantation Outcome as Measured by the Beta-2 Score

Mixed linear modelling was used to determine the impact of each explanatory variable on the calculated Beta-2 scores. Interestingly, there was a negative, but non-significant, trend between donor age and graft efficiency (B= -0.008, *p*=0.09; Table 8, and Figure 10 a). To ensure that this

result was independent of the number of islets that had been transplanted, donor age was correlated against graft size (IEQ/Kg). A negative correlation did exist, but this did not reach significance (r= -0.170, *p*=0.26, data not shown). A positive trend was noted between the Beta-2 score and donor BMI and CIT, but in both cases, this did not reach statistical significance (Table 8). Donor type and sex, in addition to the preparation purity and viability, did not affect graft outcome (Table 8). The Beta-2 score did not significantly change over the course of the 12-month follow-up period (*p*=0.464; Table 8). Not surprisingly, the best predictor of Beta-2 score was the number of islets transplanted, for which there was a significantly positive relationship (B=0.00008, *p*=0.004; Table 8 and Figure 10 b).

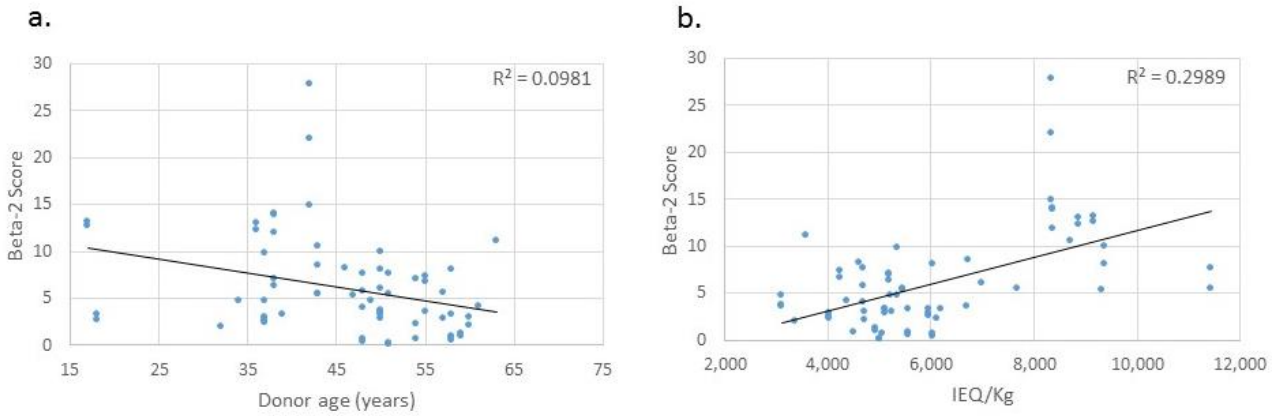


Figure 10: Factors influencing the Beta-2 score
Correlations were performed between the Beta-2 score and a) donor age, b) islet graft size (IEQ/Kg). Donor age showed a negative correlation, whereas IEQ/Kg was positively correlated with the Beta-2.

The 4 factors with a *p* values ≤0.25 were added to the multivariate model (donor age, BMI, CIT and IEQ/Kg). CIT was removed during stepwise backwards regression, which resulted in a final model containing donor age, BMI and IEQ/Kg (Table 9). The model was used to predict the value of Beta-2 scores. The predicted Beta-2 scores were well correlated to the actual Beta-2 scores (R^2=0.79; Figure 11).

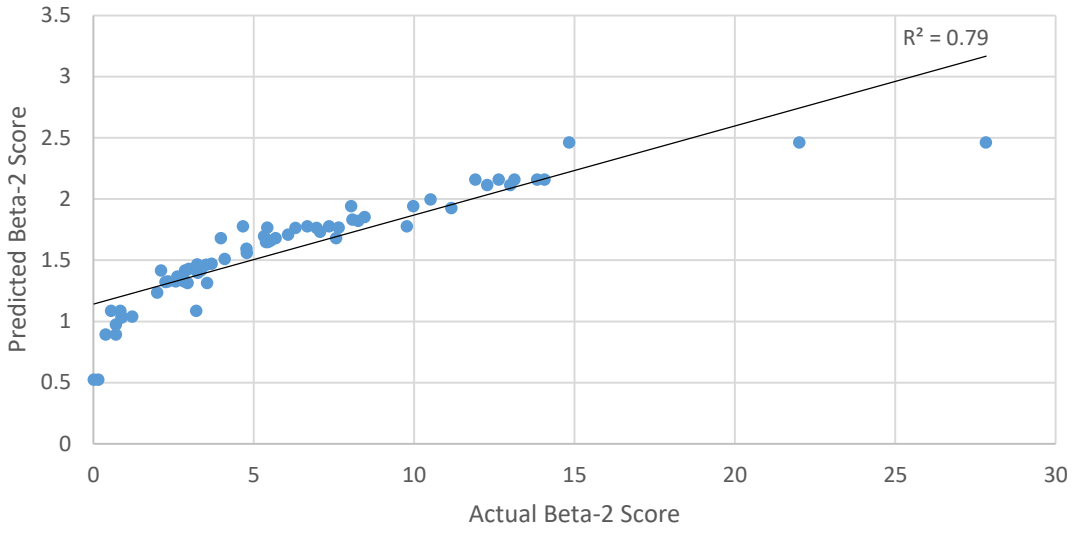


Figure 11: Correlation between the Beta-2 Predicted by the Multivariate Model and the Actual Beta-2 Score
The Beta-2 score that was predicted by the multivariate model (Table 9) was well associated with the actual Beta-2 score that was calculated following each visit

2.3.2.3 Factors Influencing Transplantation Outcome as Measured by the GDISR

As was observed with the Beta-2 score, a negative trend existed between donor age and the GDISR, although this did not reach significance (B=-0.007, *p*=0.141; Table 10 and Figure 12 a). The GDISR was unaffected by donor sex, BMI, donor type or pancreas CIT (Table 10). In addition, the preparation purity and viability prior to transplantation did not affect the score. Interestingly, unlike the Beta-2 score, the GDISR significantly decreased over the post-transplantation period (B=-0.016, *p*=0.014; Table 10). As with the Beta-2 score, the explanatory variable that most significantly affected the GDISR was the number of islets transplanted (IEQ/Kg; B=0.00007, *p*=0.003; Table 10 and Figure 12 b).

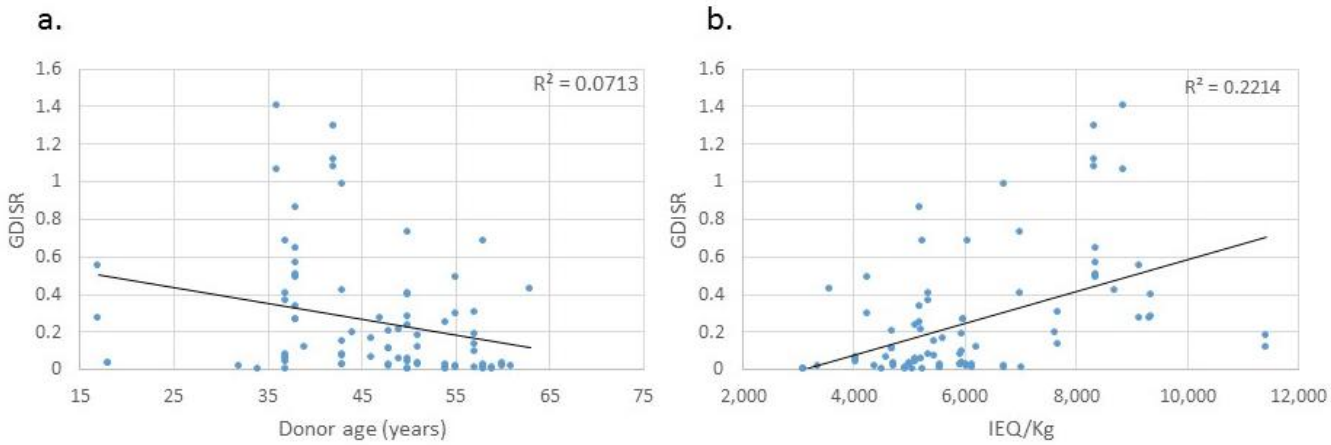


Figure 12: Factors influencing the GDISR
Correlations were performed between the GDISR score and a) donor age, b) islet graft size (IEQ/Kg). Donor age showed a negative correlation, whereas IEQ/Kg was positively correlated with the GDISR.

Donor age, time since transplantation and IEQ/Kg were included in the multivariate model. Donor age was however, eliminated during the stepwise regression, to leave the IEQ/Kg and the time since transplantation as the only factors in the model (Table 11). The model was used to predict the GDISR scores, which were then correlated against the actual GDISR. The R^2 for this correlation was 0.23 (Figure 13).

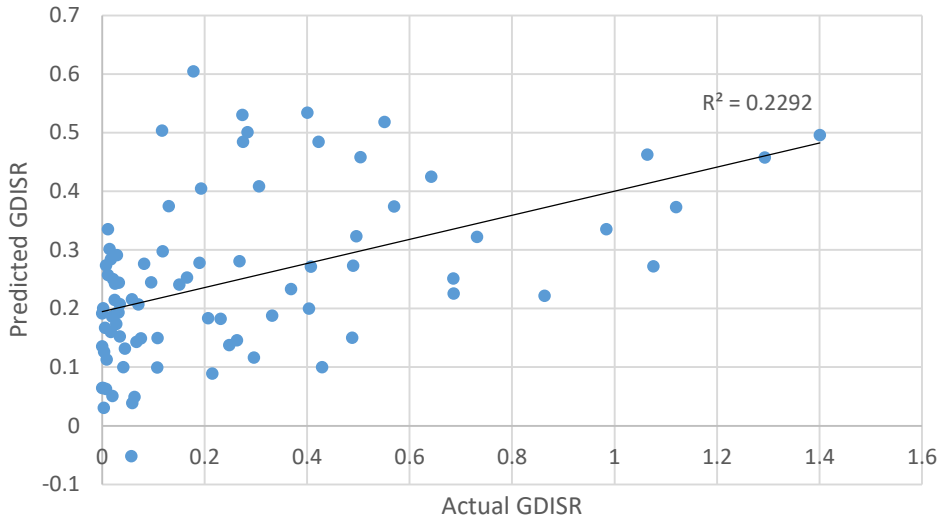


Figure 13: Correlation between the GDISR predicted by the multivariate model and the actual GDISR scores

Although the GDISR that was predicted by the multivariate model (Table 11) was associated with the actual GDISR that was calculated following each visit, it was poorer than the predictive power of the Beta-2 model (seen in Figure 11).

The GDISR model was refitted using only the 66 data points that had a corresponding Beta-2 score available. No substantial change in the results was observed, and a significant decline in the GDISR over the 12-month follow up period was still present (Table A5 Appendix).

Results Tables for Chapter 2

Factor	B (95% CI)	R^2	*p* value	Included in multi-model?
Age (years)	2.311 (1.012 - 3.611)	0.016	0.001	Yes
Sex (Female)	18.502 (-7.260 - 44.263)	0.003	0.159	Yes
Height (cm)	-0.496 (-1.791 - 0.799)	0.001	0.452	No (*p*>0.25)
Weight (Kg)	1.266 (0.408 - 2.123)	0.011	0.004	No –high degree of collinearity with BMI
BMI (Kg/m^2)	5.937 (3.059 - 8.815)	0.022	0.000	Yes
Body surface area (BSA) (As per Mosteller **[233]**)	68.088 (7.523 - 128.653)	0.007	0.028	No –high degree of collinearity with BMI
Abdominal girth (cm)	1.823 (0.920 - 2.727)	0.022	0.000	Yes
Past hypertension (Y)	36.274 (5.995 - 66.554)	0.008	0.019	Yes
Past alcohol abuse (Y)	-13.832 (-68.316 – 40.653)	0.001	0.618	No (*p*>0.25)
Past smoker (Y)	-39.455 (-65.284 - -13.627)	0.012	0.003	Yes
Past smoker amount (cigarettes/day)	-0.626 (-1.845 – 0.592)	0.001	0.313	Yes
Traumatic cause of death (Y)	8.055 (-50.586 - 66.696)	0.000	0.787	No (*p*>0.25)
Cardiac arrest? (Y)	-34.641 (-63.617 - -5.655)	0.008	0.019	Yes
Cardiac arrest duration (minutes)	-0.173 (-1.381 - 1.035)	0.000	0.778	No (*p*>0.25)
Hypoxia related cause of death (Y)	-49.486 (-84.372 - -4.601)	0.011	0.005	Yes
Donor type (DCD)	-39.168 (-73.883 - -4.453)	0.007	0.027	Yes
Blood Urea (mmol/l)	-2.189 (-7.713 – 3.335)	0.001	0.437	No (*p*>0.25)
Alanine aminotransferase (ALT; iu/l)	-0.29 (-0.135 – 0.77)	0.000	0.590	No (*p*>0.25)
Amylase (iu/l)	0.24 (-0.137 – 0.185)	0.000	0.768	No (*p*>0.25)
Aspartate aminotransferase (AST; iu/l)	-0.33 (-0.264 – 0.198)	0.000	0.777	No (*p*>0.25)

Factor	B (95% CI)	R^2	*p* value	Included in multi-model?
Bilirubin (µmol/l)	0.785 (-0.695 - 2.266)	0.002	0.298	No (*p*>0.25)
Glucose (mmol/l)	-1.325 (-7.014 - 4.365)	0.000	0.648	No (*p*>0.25)
Insulin (Y)	83.601 (-26.174 - 193.377)	0.062	0.131	No (<50% complete)
Methylprednisolone administered? (Y)	-2.346 (-33.535 - 28.843)	0.000	0.883	No (*p*>0.25)
Dopamine administered? (Y)	161.977 (-13.209 - 337.162)	0.016	0.070	No (<50% complete)
Dobutamine administered? (Y)	-24.730 (-100.456 - 50.996)	0.001	0.522	No (*p*>0.25)
Adrenaline administered? (Y)	25.907 (-45.781- 97.594)	0.001	0.478	No (*p*>0.25)
Noradrenaline administered? (Y)	7.351 (-27.355 - 42.056)	0.000	0.678	No (*p*>0.25)
Vasopressin administered? (Y)	-12.872 (-43.386 – 17.642)	0.001	0.408	No (*p*>0.25)
Triliodotryronine administered? (Y)	18.658 (-19.957 – 57.274)	0.002	0.343	No (<50% complete)
Duration in intensive treatment unit (ITU) (days)	-5.904 (-12.868 - 1.059)	0.013	0.096	No (<50% complete)
Pancreas cold ischemia time (CIT) (hours)	-1.717 (-8.657 – 5.223)	0.000	0.627	No (*p*>0.25)
Pancreas weight (g)	-0.050 (-0.583 – 0.482)	0.000	0.853	No (*p*>0.25)
Pancreas fibrosis (Y)	-80.090 (-152.446 - 7.733)	0.007	0.030	Yes
Pancreas nodular (Y)	-98.825 (-220.159 – 22.508)	0.004	0.110	Yes
Pancreas haematomas (Y)	-73.761 (-112.698 - -34.824)	0.021	0.000	Yes
Pancreas oedema (Y)	-55.763 (-195.915-84.389)	0.001	0.435	No (*p*>0.25)
Pancreas inflammation (Y)	-50.508 (-190.412-89.397)	0.001	0.479	No (*p*>0.25)
Pancreas fatty (Y)	38.216 (10.879 – 65.553)	0.012	0.006	Yes
Capsular damage (Y)	18.193 (-36.770 – 73.165)	0.001	0.516	No (*p*>0.25)
Parenchymal damage (Y)	21.172 (-42.379 – 84.723)	0.001	0.513	No (*p*>0.25)

Table 4: Univariate linear regression with IEQ as a continuous variable

Note: IEQ is presented as K (i.e. thousand)

Factor	*B* (95% CI)	*p* value
Age (years)	1.978 (0.591 – 3.366)	0.005
BMI (Kg/m^2)	5.497 (2.410 – 8.585)	0.001
Past Smoker (Y)	-35.622 (-62.802 - -8.443)	0.01
Haematomas (Y)	-73.725 (-113.271 - -34.180)	0.000
Fibrosis (Y)	-77.518 (-149.682 - -5.353)	0.035

Table 5: Final multivariate linear model produced using stepwise regression with IEQ as a continuous variable
R^2 of model 0.073
n=618

Factor	Odds ratio (95% CI)	R^2	*p* value	Included in multi-model?
Age (years)	1.024 (1.008-1.039)	0.017	0.002	Yes
Sex (Female)	1.304 (0.973-1.746)	0.006	0.075	Yes
Height (cm)	0.994 (0.980-1.009)	0.001	0.456	No (*p*>0.25)
Weight (Kg)	1.012 (1.002-1.022)	0.010	0.018	No –high degree of collinearity with BMI
BMI (Kg/m^2)	1.061 (1.026-1.097)	0.022	0.001	Yes
Body surface area (BSA) (As per Mosteller **[233]**)	1.918 (0.960-3.833)	0.006	0.065	No –high degree of collinearity with BMI
Abdominal girth (cm)	1.017 (1.066-1.028)	0.018	0.003	Yes
Past hypertension (Y)	1.642 (1.158-2.328)	0.015	0.005	Yes
Past alcohol abuse (Y)	0.849 (0.488-1.584)	0.001	0.668	No (*p*>0.25)
Past smoker (Y)	0.012 (0.592-1.140)	0.003	0.240	Yes
Past smoker amount (cigarettes/day)	0.994 (0.980-1.007)	0.002	0.371	No (*p*>0.25)
Traumatic cause of death (Y)	1.212 (0.626-2.350)	0.001	0.568	No (*p*>0.25)
Cardiac arrest? (Y)	0.822 (0.592-1.140)	0.003	0.240	Yes
Cardiac arrest duration (minutes)	0.994 (0.978-1.009)	0.005	0.404	No (*p*>0.25)
Hypoxia related cause of death (Y)	0.583 (0.391-0.870)	0.01	0.008	Yes
Donor type (DCD)	0.661 (0.446-0.982)	0.008	0.041	Yes
Blood Urea (mmol/l)	1.137 (0.966-1.098)	0.002	0.363	No (*p*>0.25)
Alanine aminotransferase (ALT; iu/l)	1.000 (0.999-1.001)	0.000	0.80	No (*p*>0.25)
Amylase (iu/l)	1.000 (0.998-1.002)	0.000	0.843	No (*p*>0.25)

Factor	Odds ratio (95% CI)	R^2	*p* value	Included in multi-model?
Aspartate aminotransferase (AST; iu/l)	1.000 (0.998-1.003)	0.000	0.813	No (*p*>0.25)
Bilirubin (µmol/l)	1.001 (0.984-1.018)	0.000	0.911	No (*p*>0.25)
Glucose (mmol/l)	0.979 (0.919-1.043)	0.001	0.509	No (*p*>0.25)
Insulin (Y)	5.067 (1.193-21.513)	0.175	0.028	No (<50% complete)
Methylprednisolone administered? (Y)	1.084 (0.764-1.538)	0.000	0.651	No (*p*>0.25)
Dopamine administered? (Y)	0.618 (0.055-6.927)	0.001	0.696	No (*p*>0.25)
Dobutamine administered? (Y)	0.721 (0.307-1.696)	0.001	0.453	No (*p*>0.25)
Adrenaline administered? (Y)	0.943 (0.423-2.104)	0.000	0.887	No (*p*>0.25)
Noradrenaline administered? (Y)	0.839 (0.566-1.243)	0.002	0.839	No (*p*>0.25)
Vasopressin administered? (Y)	0.844 (0.599-1.189)	0.000	0.332	No (*p*>0.25)
Triliodotryronine administered? (Y)	0.924 (0.598-1.426)	0.000	0.720	No (*p*>0.25)
Duration in intensive treatment unit (ITU) (days)	0.961 (0.871-1.060)	0.004	0.428	No (*p*>0.25)
Pancreas cold ischemia time (CIT) (hours)	0.975 (0.901-1.054)	0.001	0.522	No (*p*>0.25)
Pancreas weight (g)	0.996 (0.990-1.002)	0.003	0.996	No (*p*>0.25)
Pancreas fibrosis (Y)	0.436 (0.182-1.043)	0.008	0.062	Yes
Pancreas nodular (Y)	0.495 (0.117-2.088)	0.002	0.338	No (*p*>0.25)
Pancreas haematomas (Y)	0.434 (0.273-0.691)	0.026	0.000	Yes
Pancreas oedema (Y)	0.797 (0.160-3.980)	0.000	0.782	No (*p*>0.25)
Pancreas inflammation (Y)	1.616 (0.294-8.885)	0.001	0.581	No (*p*>0.25)
Pancreas fatty (Y)	1.168 (0.851-1.604)	0.002	0.336	No (*p*>0.25)
Capsular damage (Y)	1.305 (0.683-2.494)	0.001	0.420	No (*p*>0.25)
Parenchymal damage (Y)	1.409 (0.660-3.012)	0.002	0.376	No (*p*>0.25)

Table 6: Binary logistical regression with 'transplantable' yield set to 200K IEQ
The direction of the relationship is indicated in the factor column (i.e. when a haematoma is present the odds ratio is negative, suggesting that this feature predicts that a donor with a pancreatic haematoma is more likely to yield an IEQ of <200K IEQ).
(Y); Yes

Factor	Odds Ratio (95% CI)	*p* value
Age (years)	1.021 (1.003 – 1.039)	0.020
BMI (Kg/m^2)	1.053 (1.014 – 1.095)	0.008
Past Hypertension (Y)	1.455 (0.968 – 2.188)	0.071
Haematomas (Y)	0.421 (0.296 – 0.681)	0.000
Fibrosis (Y)	0.428 (0.171 – 1.064)	0.068

Table 7: Multivariate binary regression with 'transplantable' yield set to 200K IEQ
R^2 of model 0.084
n=611

Factor	*B* (95% CI)	*p* value	Included in multi-model?
Donor Age (years)	-0.008 (-0.018 – 0.001)	0.092	Yes
Donor Sex (Female)	0.093 (-0.144 – 0.330)	0.431	No *p* >0.25
Donor BMI (Kg/m^2)	0.029 (-0.002 – 0.048)	0.103	Yes
Donor type (DCD)	0.028 (-0.270 – 0.325)	0.852	No *p* >0.25
Pancreas cold ischemia time (hours)	0.054 (-0.040 – 0.148)	0.241	Yes
Preparation viability (%)	-0.005 (-0.180 – 0.169)	0.950	No *p* >0.25
Preparation purity (%)	0.0744 (-0.194 – 0.116)	0.590	No *p* >0.25
Time since transplantation (months)	-0.005 (-0.018 – 0.009)	0.464	No *p* >0.25
Number of islets transplanted/Kg of recipient (IEQ/Kg)	0.00008 (0.00002 – 0.0001)	0.004	Yes

Table 8: Univariate analysis by mixed linear modelling for factors influencing transplantation outcome, measured using the Beta-2 score

Factor	*B* (95% CI)	*p* value
Donor Age	-0.009 (-0.019 – 0.002)	0.100
Donor BMI	0.029 (0.004 – 0.057)	0.047
IEQ/Kg	0.00008 (0.00002 – 0.0001)	0.009

Table 9: Multivariate analysis by mixed linear modelling for factors influencing transplantation outcome, measured using the Beta-2 score

Factor	*B* (95% CI)	*p* value	Included in multi-model?
Donor Age (years)	-0.007 (-0.0153 – 0.002)	0.141	Yes
Donor Sex (Female)	0.021 (-0.182 – 0.223)	0.849	No *p* >0.25
Donor BMI (Kg/m^2)	0.011 (-0.010 – 0.031)	0.305	No *p* >0.25
Donor type (DCD)	0.042 (-0.216 – 0.300)	0.750	No *p* >0.25
Pancreas cold ischemia time (hours)	-0.005 (-0.056 – 0.045)	0.830	No *p* >0.25
Preparation viability (%)	0.004 (-0.156 – 0.164)	0.961	No *p* >0.25
Preparation purity (%)	-0.024 (-0.166 – 0.117)	0.726	No *p* >0.25
Time since transplantation (months)	-0.016 (-0.029 – -0.004)	0.014	Yes
Number of islets transplanted/Kg of recipient (IEQ/Kg)	0.00007 (0.00002 – 0.0001)	0.003	Yes

Table 10: Univariate analysis by mixed linear modelling for factors influencing transplantation outcome, measured using the GDISR score

Factor	*B* (95% CI)	*p* value
IEQ/Kg	0.000075 (0.000030 – 0.000120)	0.0018
Time since transplantation	-0.0167 (-0.0294 - -0.0044)	0.0095

Table 11: Multivariate analysis by mixed linear modelling for factors influencing transplantation outcome, measured using the GDISR

2.4 Discussion

This Chapter aimed to examine the impact of donor and pancreas factors on the outcome of clinical islet isolation, within a UK dataset. In addition, MMT data from 45 first UK islet transplant recipients were examined, to determine the effect of donor and islet preparation factors on transplantation outcomes.

2.4.1 Influence of Donor Factors on Isolation Outcomes

The donor factors that are reported to influence isolation outcomes, are subject to the intrinsic regional variations in pancreas inclusion/acceptance criteria. This Chapter represents the first analysis of this type to be performed on UK data. 732 isolations were analysed, from pancreases that were accepted at one of the three clinical isolation centres over a six-year period. 41 donor and pancreas factors were examined, and the impact of each factor on isolation outcome was determined. Outcome was measured both in terms of the generated islet yield (IEQ), and on the basis of obtaining a transplantable yield. Only 8 factors significantly affected both outcome measures. Of these 8 factors, donor age, weight, BMI, abdominal girth, and past hypertension significantly enhanced isolation outcome, whereas as DCD donation, a hypoxia related cause of death and the presence of pancreatic haematomas, had a negative impact.

Age is one of the most reported donor factors known to influence isolation success [136, 215, 221, 222, 249]. Poor isolation yields from younger donors likely result from the production of trapped islets following collagenase-based digestion, which are then lost during density gradient purification [101, 102]. In the current study, there was an average increase of over 2,000 IEQs for each yearly increase in donor age. Therefore, in the UK, donor age alone could result in yield variations of up to 70,000 IEQ (based on the UK-wide age acceptance criteria of 25-60 years). In addition to age, an increasing donor BMI, weight and abdominal girth, were significantly beneficial for isolation outcome, in agreement with previous reports [136, 215, 216, 224].

Interestingly, past donor hypertension significantly increased the chances of obtaining a transplantable yield by a factor of 1.6. Although hypertension has been previously reported to have no effect on isolation outcome, these studies utilised a 'successful isolation' cut-off value of up to two-fold higher than that used in the current study [216, 224, 250]. It is not entirely clear why hypertension would result in a larger islet yield, though it is likely acting as a surrogate marker to another, yet to be considered, variable.

DCD donation reduced the likelihood of obtaining a transplantable yield by a factor of 1.5, when compared to pancreases that had been retrieved following DBD donation. DCD donation proceeds an unavoidable period of additional warm ischemia, which is the variable interval from the cessation of cardiac output to the perfusion of organs with cold preservative solution. Warm ischemia has been previously associated with low islet yield [217], and therefore it is unsurprising that DCD donation would also affect isolation outcome [253]. The potential detrimental impact of warm ischemia is further emphasised through the negative effect that cardiac arrest has on isolation outcome, observed both in this current study and a series of other reports [215, 216, 226]. Interestingly, the duration of cardiac arrest did not affect outcome, which may result from inaccurate reporting's, especially when cardiac arrest is 'out of hospital'.

Cause of death was identified as a significant contributing factor to islet yield. Previously, studies have focused on whether death resulted from trauma, which has been found to negatively impact yield [221, 224]. In the current Chapter, isolation outcome was not affected by trauma. Instead, death that resulted from hypoxia significantly affected islet recovery, and reduced the chances of obtaining a transplantable yield by a factor of 1.7. Due to their high metabolic activity, islets have substantial oxygen demands. Despite only comprising 2% of the overall pancreatic mass, islets receive up to 20% of the arterial pancreatic blood flow [19]. In low oxygen environments (such as following transplantation into the liver) islets are prone to suffer from hypoxia-induced apoptosis [295]. In addition, larger islets have been demonstrated to develop a 'hypoxic core', which results

in central necrosis [296]. Hypoxia-induced necrosis in larger islets may account for the significant reduction in IEQ, following a hypoxia related cause of death, and prolonged ischemia. Tobacco smoke has also been shown to reduce the availability of oxygen in tissues [297], and therefore may explain why a history of past smoking significantly reduced the number of IEQs that could be recovered. In addition, Lakey and colleagues speculated that ischemia may lead to the collapse of the distal ductal system of the pancreas [298]. This could result in the inefficient delivery of enzymes to the islet-exocrine interface. Indeed, ductal injection at the time of retrieval maintains the structural integrity of ducts, and is beneficial for improving collagenase distribution and islet yields [283, 284].

Although trauma itself did not affect isolation outcome, pancreases that contained haematomas yielded significantly less islets than those without and reduced the likelihood of obtaining a transplantable yield. A haematoma is a localised bleeding that occurs outside a blood vessel, which can result from trauma, but can also form during organ retrieval. The presence of a haematoma reduced islet yield by 73,000 IEQ. The significant risk associated with haematomas questions the suitability of these organs for clinical islet isolation and transplantation. However, pancreases with haematomas only comprised a modest proportion of the overall organ pool (13%).

Multivariate models were created to determine which factors had the greatest impact on isolation outcome. The final models for predicting total yield and a transplantable yield were similar, but both were able to explain less than 10% of the net variation in yield. The high percentage of unexplained variance can be at least partly explained by the enzymes that were used for islet isolation. Although NHSBT do not collect enzyme specific information, it is acknowledged that different enzyme products are used across the UK. For example, the isolation centres in Oxford and Kings College London tend to favour Serva/Nordmark products, whereas Edinburgh use Roche's Liberase. Differences in the efficiency of collagenases produced by each manufacturer have been reported [299, 300]. In addition, there is known to be batch to batch variability that occurs between

different lots of the same product [135]. Therefore, enzyme selection is likely to account for a proportion of the variation in islet yield, which cannot be explained by the models developed in this Chapter. Indeed, for full validation these models should be tested on a cohort that is independent from the one in which they were developed. Further data will be requested from NHSBT for this purpose (i.e. from the 2018-2019 period).

2.4.2 Influence of Donor Factors on Transplantation Outcomes

Following a single islet transplant, recipients benefitted from a reduction in HbA1c, and insulin dose requirements. There was a gradual time dependent increase of HbA1c and insulin requirement over the 12 months post transplantation period (excluding 9-months, which was statistically underpowered). One recipient retained insulin independence at 12 months (16%). In the majority of cases islet transplantation resulted in a functioning graft, with only 3 of the 45 recipients displaying no residual function. Even following graft failure, recipients have been shown to retain protection from hypoglycaemia [78], which was demonstrated in the current dataset (i.e. recipient RF015 at 1 month).

In this study, analysis of islet transplantation outcomes was limited to first transplant recipients, to control for the influence of multiple donors, and to allow the impact of donor variables on graft efficiency to be investigated. This almost certainly explains why insulin independence rates at 1-year were substantially lower than those reported by other countries, when recipients have received multiple infusions [80, 83]. Graft efficiency was measured via the Beta-2 score and the GDISR. Both of these measurements associated well with the stimulated 90-minute C-peptide, demonstrating that they can accurately measure graft function. Although there is limited research regarding the effect of donor factors on transplantation outcomes, the impact of donor age [102, 242] and WIT [288] have been investigated. The data in this Chapter support a reduction in graft efficiency with age, measured by the Beta-2 score and the GDISR, by mixed linear modelling.

However, in both cases this trend did not reach significance (p = 0.09 and 0.14 for Beta-2 and GDISR respectively). This age-related reduction was irrespective of the graft size (IEQ/Kg). It is not surprising that a trend existed between decreasing graft function and an increasing donor age, as in non-diabetic individuals loss of insulin secretory capacity occurs as part of the normal aging process [240, 241]. This age related decline in insulin secretory capacity has been linked to a reduction in PDX-1 expression [243, 246], in addition to a decrease in ATP content [242]. Donor type (DCD/DBD), gender and pancreas CIT had little impact on transplantation outcome. However, there was a trend towards improved graft efficiency with an increasing BMI, measured via the Beta-2 score (p=0.10. BMI had limited effect on the GDISR). Interestingly, insulin secretion has been shown to significantly increase in non-diabetic obese patients [301, 302]. In addition, insulin content (ng/IEQ), and *in vitro* secretion, significantly increase with donor BMI [303]. This said, these benefits should be interpreted with caution, as obesity associated hyper-insulin secretion could be linked to early onset insulin resistance. Overall, the best determinant of graft function was the number of islets that were transplanted per Kg of recipient weight. The 12 recipients (14%) that were transplanted with grafts that fell below the minimum recommended 5,000 IEQ/Kg accounted for 50% (2/4) of the failed grafts, emphasising the importance of adhering to these minimum criteria. Purity and viability had no significant effect on graft outcome, which most likely reflects the strict release criteria adopted by UK islet centres, in relation to these parameters.

The GDISR, but not the Beta-2 score, significantly declined over the post-transplantation period. This suggests that the GDISR is more sensitive to detecting early graft deterioration. The failure for the Beta-2 score to detect this decline likely results from the way in which each outcome measure is assessed; the Beta-2 score is comprised from fasting data, whereas the GDISR is calculated following a MMT. Although the Beta-2 score correlates well with 90-minute C-peptide data, subtle changes in graft function may be lost when assessing graft function on non-stimulated measurements. This said, an assessment that can be made on the basis of a single fasting blood sample has clear economical and logistical benefits. It is also worth noting that the final multivariate

model for the Beta-2 score, which contained donor age, BMI and IEQ/Kg, had more accurate predictive powers than the multivariate model for the GDISR, which only contained the IEQ/Kg and duration of time since transplantation. This reduction in predictive power may reflect the absence of donor factors, which were removed during the stepwise elimination process. This further emphasises the importance of donor factors, when predicting transplantation outcomes.

One criticism of this study is the lack of consideration given to the recipient characteristics, when assessing how donor factors influence islet graft outcomes. This caveat is also apparent in previous studies of this nature [102, 242]. Although all current study patients were C-peptide negative prior to transplantation, the duration and stability of diabetes, as well as the age of the recipient, may impact on graft function. Indeed, islet transplantation has previously been shown to be more effective in recipients aged over 35 [82]. Future efforts should be made to obtain this information, and incorporate this into a multilevel model, alongside the corresponding donor characteristics.

2.5 Conclusions

This Chapter represents the first investigation into the impact of donor and pancreas factors on isolation and transplantation outcomes, within the UK. Whilst the study highlighted several factors that were significantly influential for liberating islets, the negative impact that donor age has on isolation outcome is especially problematic, given the fact that islets from younger donors have enhanced post-transplantation graft function. The high percentages of trapped islets in younger donors likely arise from the insufficient cleavage of the pancreatic ECM that is present at the islet-exocrine interface. As exocrine free islets are readily extractable from older donors, changes to ECM composition most likely occur with age. This may render current isolation enzyme blends suboptimal when applied to younger donors. On the basis of these important observations, this thesis will continue with a focus on donor age and will aim to determine how age affects the composition and enzyme mediated digestion of the pancreatic ECM.

CHAPTER 3

The Impact of Donor Age on ECM protein Expression in the Native Pancreas

3.1 Introduction

The hypothesis is that the high percentages of trapped islets that are produced when digesting pancreases from younger human donors result from age-related changes in the pancreatic ECM. Therefore, to improve digestion outcomes from younger donors, age-related changes in the native pancreatic matrix need to be accurately defined. Although the impact of age on the composition of the pancreatic ECM has been studied previously, investigations have been restricted to conventional histology and immunostaining methods [99, 171, 275, 304]. Indeed, as with any antibody-based detection, the identification of matrix proteins is limited to those preselected by the investigator, and any quantification performed will be restricted to the areas of the protein recognised by the antibodies. It is also not possible to rule out the influences of tissue quality on antibody binding efficiency.

High-throughput proteomics offers an alternative approach for characterising the pancreatic matrisome. Conceptually, proteomics aims to identify (or 'screen') the entire proteome, offering the potential for complete characterisation, whilst eliminating any pre-selected user bias. Liquid chromatography tandem mass spectrometry (LC-MS/MS) enables the separation, identification and quantification of complex protein mixtures. Mass spectrometry methodology falls into two broad categories: top-down or bottom-up protein detection. Where the top-down approach involves the analysis of intact proteins, bottom-up detection analyses peptide fragments, following restricted proteolysis, usually with trypsin [163, 305-307]. As larger proteins are very insoluble, and therefore less amenable to MS analysis [308], bottom-up (or 'shotgun') proteomics is generally preferred. Following the extraction and the digestion of proteins into peptides, the general work flow of LC-MS/MS involves peptide injection into a high-performance liquid chromatography column, followed by the elution of the separated peptides into the first mass spectrometer via an interface. A standard MS analyser contains three principle components: an ionisation source, a mass analyser and a detector [308, 309]. The role of the ionisation source is to convert the incoming

peptides into gaseous phase ions under a vacuum, which are then accelerated in a magnetic field towards the analyser. The analyser separates the ions on the basis on their m/z (mass/charge) ratios, before they enter the detector, which records the intensity of each individual ion [309]. Electrospray ionisation (ESI) is the ionisation source most compatible with liquid chromatography [309]. ESI involves dissolving the analyte in a solvent, followed by the high pressured, high voltage injection of the mixture through a fine needle, leading to the production of a fine spray of highly charged ions [309]. Commonly used mass analysers include the Quadrupole, which separates ions based on their voltage dependent deflection throughout a linear flight path, encompassed by 4 voltage dependent metal rods. Attenuation of the voltage facilitates the sorting of ions on the basis of their m/z ratios [309]. In tandem MS, more than one analyser is used. Identification of a parent ion is completed in the first MS (MS1 scans), followed by the further fragmentation of this parent ion by collision induced dissociation (CID). The resulting fragments are then separated in a second MS, before being sent to the detector (MS2 scans) [309]. Generally speaking, the most abundant parent ions are often selected for CID and the subsequent MS2 analysis. Tandem MS maximises successful protein identification; specific peptides will have unique fragmentation fingerprints following CID, allowing the discrimination of abundant parent ions that have the same m/z. Although several types of MS detectors exist commercially, an ion trap detector (such as Orbitrap) is often used for protein-based applications [163, 306, 307]. Following the peptide mass identification, complex bioinformatic strategies are used to infer information about the originating proteins. Briefly, the experimentally determined peptide masses are compared with the mass of the theoretical peptide that would be produced from a protein following restricted digestion. The comparison occurs against all of the proteins that are located within a defined sequence database (i.e. Swissprot) [309]. A minimum of 2 unique peptide matches are often required for a positive protein identification [309]. Post-translational modifications (such as hydroxylation and oxidation) can be added to the search, to enhance the chance of a positive identification. Finally, following identification, proteins can be quantified via label or label-free MS methods. Stable isotopes are

routinely used in label-based quantification studies, but such methods incur large costs, in addition to limiting the number of proteins that can be quantified [308]. Alternatively, label-free proteomics can be performed by integrating all of the chromatographic elution peaks that are confirmed to belong to a specific protein. The integrated and normalised ion abundance is then measured [308, 310]. On this basis, label-free quantification is presented as a relative change in protein quantity between two or more experimental groups, rather than an absolute concentration.

LC-MS/MS based characterisation of the ECM is by no means a new concept. In the past, comprehensive 'atlases' have been developed to determine the composition of the matrisome in different tissues and disease states [311]. In addition, the creation of a matrix database public resource (http://matrixdb.univ-lyon1.fr/) [312] allows the rapid annotation of matrix-based datasets, based on previously identified matrix proteins. The matrix proteins are listed in categories, which distinguish core-matrix proteins (i.e. collagens, laminins and perlecans) from matrix associated proteins (such as affiliated, regulatory, and secreted proteins) [311].

Proteomics has also been performed on pancreas and islet tissue from mice [305, 306, 313]. This has led to the identification of 120 ECM and ECM-associated proteins in murine islets, including 28 collagen chains, 9 laminin chains and 8 proteoglycans [305]. In a recent study, Sackett and colleagues performed the first in-depth proteomic based characterisation of the human pancreatic matrisome, which identified 120 ECM proteins [163]. However, despite an age-varied cohort (13-58 years), determination of age-related changes in matrix composition fell outside the scope of this study. Nonetheless, the data produced highlights the huge complexity of the pancreatic matrix, and further emphasises the limitations of restricting matrix investigations to single proteins [99, 171]. Indeed, obtaining a complete characterisation of the age-related changes that occur in the matrix, is the first step towards understanding why digestion outcomes are sub-optimal from younger donors.

Therefore, the aim of the study outlines in this Chapter was to use high-throughput proteomics to comprehensively characterise the pancreatic matrisome in younger and older pancreatic donors and determine quantitative differences in protein expression. In addition, immunofluorescent staining was used to determine the location of a sub-set of the identified proteins, in relation to islets.

3.2 Methods

3.2.1 Determination of Experimental Age Groups

For investigations into the impact of donor age on the molecular structure of the human pancreas, two distinct age groups were defined, which will be used throughout the remainder of this thesis. Pancreatic donors were divided into 'younger' (≤35 years) and 'older' (≥45 years) age groups. Indeed, within the literature the classification of what constitutes a 'younger' pancreatic donor has been widely variable and defined somewhat arbitrarily. The upper age limit of a 'younger' donor has ranged from 20 to 40 years [88, 98, 99, 249]. In this study, the selected 'cut-off' between the two groups aims to reflect the age at which collagenase-based digestion of the pancreas transitions from being suboptimal (with high percentages of trapped islets) to more effective (with good islet-exocrine cleavage). The age groups were defined based on the combined clinical isolation expertise at the DRWF Human Islet Isolation Centre in Oxford, where trapped islets are commonly reported in donors aged 35 and under and are rare from donors aged 45 and over. In addition, this classification was made based on the age range of the donors that are accepted into the clinical Islet Programme. As part of the UK Joint Donor Pancreas Allocation Scheme, pancreases from donors aged 24 and under are solely allocated to the Whole Pancreas Programme. As a result, the Islet Programme does not receive pancreases from any clinical grade donors under the age of 25. The maximum age of donors accepted into the clinical islet programme is 60 years.

3.2.2 Sampling Technique

With appropriate consent and ethical approval, human pancreases from older (≥45 years old; n=12) and younger (≤35 years old; n=12) multi-organ donors were procured for islet isolation (Table 12). Organs were transported in UW solution (Bridge to Life, London, UK) on ice to the DRWF Human Islet Isolation Facility, at the Churchill Hospital in Oxford. 0.5cm^3 tissue samples were taken from the head of the pancreas, snap frozen in liquid nitrogen, and stored at -80°C until use.

	Younger Donors ≤ 35 years (n=12)	**Older Donors ≥ 45 years (n=12)**	***p* value**
Age, y (Mean ± SEM)	29.4±1	53.8±1.2	<0.001
Age, y (Median (Range))	29.5 (25-35)	54 (46-60)	<0.001
Gender (M:F)	9:3	8:4	0.5
BMI (Mean ± SEM)	26.4±1.2	27.7±0.6	0.3
CIT, h (Mean ± SEM)	6±0.4	6.4±0.4	0.4
Donor Type (DBD:DCD)	12:0	9:3	0.06

Table 12: Donor demographics for Chapter 3
CIT, cold ischaemia time; DBD, donation after brain death; DCD, donation after cardiac death
Statistical analysis was performed by independent samples t-test.

3.2.3 Pancreatic Tissue Homogenisation and ECM Enrichment

For proteomics, two different sample preparation methods were investigated. The first was a whole tissue extract, and the second was an ECM enriched fraction. Although ECM enrichment is commonly used prior to the proteomic analysis of the matrisome [311], it utilises a larger amount of tissue than standard tissue homogenisation. Therefore the aim was to determine the extent of its benefits.

3.2.3.1 Whole Tissue Lysate

Approximately 20mg of frozen pancreatic tissue were homogenised in 250µl of RIPA buffer (Sigma Aldrich) containing protease inhibitor cocktail (PIC; cOmplete™ Mini Protease Inhibitor Cocktail,

Roche). The Eppendorf tubes selected for the homogenisation were low protein binding (Thermofisher Scientific). One steel homogenisation ball was added to each tube (Retsch UK limited, Hope Valley, UK). Homogenisation was completed using a Retsch mixer mill (Retsch UK limited). Four x 60 second homogeniser cycles were completed, at a frequency of 25. Between each cycle the tissue was cooled on dry ice for 30 seconds. Samples were centrifuged at 14,000g for 5 minutes, before being frozen at -20°C until use.

3.2.3.2 ECM Enrichment

ECM enrichment was performed using the commercially available tissue compartment protein extraction kit by Millipore (catalogue number: 2145, Watford, UK). The extraction process works by exploiting the insolubility of ECM proteins, following the sequential incubation of the homogenised tissue in buffers that contain different pH, salt and detergent concentrations. The protocol described by Naba *et al.* was followed, which details how the kit is used to separate tissues into five progressive protein based fractions: cytosolic, nuclear, membrane, cytoskeletal and ECM [314]. Approximately 50mg of frozen pancreatic tissue was used for ECM enrichment. As the protocol details the processing steps for 100mg of tissue, all volumes were halved. Tissue homogenisation occurred as detailed above for the whole tissue lysate, with the exception of replacing the RIPA buffer with solution 'C' contained within the commercial kit. Following homogenisation, the extraction procedure involved progressively treating the homogenised tissue in the buffer solutions outlined in the Naba *et al.* protocol [314], which were all present within the tissue compartmentalisation kit. A protocol amendment was made following the extraction of the nuclear proteins, which involved an additional incubation step in buffer 'M'. This aimed to improve the extraction of membrane-based proteins. At the end of each incubation period the samples were centrifuged (16,000g) and the supernatants, containing each of the protein fractions, were collected. Each fraction was snap frozen in liquid nitrogen and stored at -80°C. At the end of the

procedure, the ECM pellet was washed 5 times in 1 X PBS containing PIC. All liquid was removed and the dry pellets were snap frozen and stored at -80°C.

3.2.4 Digestion of Proteins into Peptides for Mass Spectrometry

8M urea/2M thiourea stock solution was produced by dissolving 480mg of urea and 152mg of thiourea in 100mM ammonium bicarbonate (Urea/AMBIC; all Sigma-Aldrich, Gillingham, UK). The ECM pellets were dissolved in 50µl of the Urea/AMBIC solution and incubated with continuous agitation for 1 hour at 37°C. Samples were reduced using dithiothretiol (DTT, Sigma-Aldrich), adjusted to a final concentration of 5mM, and shaken at 1400rpm for 30 minutes at room temperature (rt). Iodoacetamide alkylating reagent (IAA, Sigma-Aldrich) was added, to a final concentration of 20mM. Samples were vortexed thoroughly to ensure that IAA had fully dissolved, following incubation at room temperature for 30 minutes at 1400rpm. At the end of the incubation period 1µg (5µl) of the enzyme LyS C (Promega UK, ref: V1671, Southampton, UK) was added to each sample, to commence the digestion of proteins into peptides. Samples were incubated for 2 hours at 37°C on a rotator platform set to 1,400rpm. At the end of the incubation period the samples were diluted with the addition of 150µl of Urea/AMBIC solution and 15µl of trypsin was added (3µg per sample; Promega ref: V5111). Samples were incubated at 37°C overnight, with 1400rpm rotation. The following day a second aliquot of trypsin was added (7.5 µl/1.5µg per sample). The samples were incubated at 1400rpm, for 2 hours, at 37°C. Samples were acidified with 1% formic acid (2.5µl; Sigma), to quench the enzyme reaction. 30µl aliquots were obtained from each sample, and a peptide quantification was performed, as per the manufacturer's protocol (Pierce Quantitative colorimetric peptide assay, Thermofisher Scientific). The samples were stored short term, at 4°C.

3.2.5 Sample Desalting and MS injection

Sample desalting was performed on C18 solid-phase extraction cartridges (SOLA HRP C18 Cartridge, Thermofisher Scientific), dried and re-suspended in 2% acetonitrile and 0.1% formic acid. On the basis of the peptide quantification, 1.86µg of peptide was injected, in the total volume of 1µl. LC-MS/MS analysis was performed using a Dionex Ultimate 3000 nano-ultra high pressure reverse phase chromatography coupled on-line to a Q Exactive mass spectrometer (Thermofisher Scientific). Samples were separated on an EASY-Spray PepMap RSLC C18 column (500mm x 75µm, 2µm particle size, Thermofisher Scientific) over a 60 minute gradient of 2-35% acetonitrile in 5% dimethyl sulfoxide (DMSO), 0.1% formic acid at 250 nl/min. MS1 scans were acquired at a resolution of 70,000 at 200 m/z and the top 15 most abundant precursor (parent) ions were selected for CID fragmentation (MS2 scans).

3.2.6 Proteomic Data and Statistical Analysis

Samples were searched using Mascot (V2.5.1. Matrix Science, London, UK) against the Human Swissprot database, using an ion cut off score of 20 and a 1% false discovery rate (FDR). Trypsin was selected as the enzyme, and a maximum of one missed cleavage site was allowed. Post translational modifications included hydroxylation (+15.99 Da), carbamidomethylation (+57.02 Da), deamidation (+0.98 Da) and oxidation (+15.99 Da). ≥2 unique peptide matches were required for positive protein identification. Label-free quantification was performed using Progenesis (non-linear dynamics, Newcastle, UK). Ions were quantified following the alignment of ion chromatographs. Matrix proteins were identified based on the lists available on MatrixDB (www.matrixdb.univ-lyon1.fr/) [312]. The multivariate analysis technique, principle component analysis (PCA), was performed in Progenesis. This enabled the effect of donor age on the overall variability of the proteome to be visualised. PCA is interpreted as a scores plot, with each donor represented by an individual dot on this plot. Donors that have similar proteomes cluster together on the plot, whereas those that are very dissimilar are separated. The Progenesis software was also

used to determine the maximum fold change of the proteins between the two age groups. The statistical significance of these changes was determined using ANOVA.

3.2.7 Immunofluorescent Staining of Pancreatic Tissue Sections for ECM Proteins and Insulin

Pancreatic tissue cryosections (n=6) were used to determine the location of a sub-set of ECM proteins in relation to islets. Frozen tissue sections (10µm thickness) were prepared using a Cryostat (Leica, Milton Keynes, UK) and collected onto Superfrost Plus glass slides (Thermofisher Scientific), before storage at -20ºC until use. Sections were thawed in 1 X TBS (Thermofisher Scientific) and fixed with 2.5% paraformaldehyde (Sigma Aldrich). Details of the blocking serum, primary and secondary antibodies for each protein can be found in the Appendix (Table B1). Briefly, post-thawing, sections were incubated with the appropriate animal serum for 30 minutes at r.t. Sections underwent double immunofluorescent labelling for insulin and the selected ECM protein for 1.5 hours at r.t. Sections were then incubated with secondary antibodies for 30 minutes at r.t. Slides were mounted with ProLong Diamond Antifade mounting media without DAPI (ThermoFisher Scientific) and cured overnight at 4ºC. Islets were identified by immunofluorescent labelling of insulin. A minimum of eight islets (and the corresponding ECM stain) were imaged per donor, using an Axioskop 40 microscope and Axiovision software (Carl Zeiss, Jena, Germany).

3.2.8 ELISA Validation

The results of the proteomics experiments were validated using ECM specific ELISAs. A subset of proteins were selected for investigation, including: collagens I, IV, V, VI, laminin (total), laminin α2 and α5, perlecan and nidogen 1 (Appendix, Table B2). For each ELISA, 10µg of pancreatic homogenate was loaded per well, as determined by BCA assay (Pierce BCA protein quantification kit, Thermofisher Scientific). All ELISAs were ran as per the manufacturer's instructions. Statistics were performed in Prism/Graphpad (San Diego, USA). The normality of the data was confirmed,

followed by the performance of independent t-tests to determine significant differences in protein quantity between the two age groups.

3.3 Results

3.3.1 ECM Extraction vs Whole Tissue Lysate for the Detection of Matrix Proteins

ECM enrichment utilises a large amount of tissue. As limited clinical grade pancreatic tissue was available for these experiments, the benefit of performing ECM enrichment for the enhanced identification of matrix proteins was examined. Two donors from the final experimental cohort were used, and the number of matrix proteins that were detected in a whole tissue lysate vs the ECM extract following LC-MS/MS analysis were compared. On average 863 and 192 proteins were detected in the whole tissue lysate and ECM extract conditions respectively. In the whole tissue lysate condition, only 12 of these proteins were classified as ECM, which was increased to 61 in the ECM extract group. Using ECM extraction therefore increased the matrix proteins detected from 1% to 32% (Figure 14 a). The five-fold increase in the total number of ECM proteins detected (Figure 14 b), included a four-fold increase in collagen chain detection (Figure 14 c) and almost an eight-fold increase in laminin detection (Figure 14 d). Performing ECM extraction did not result in the loss of any matrix proteins, and all ECM proteins that were detected in the whole tissue lysates were also present in the ECM extract for both donors. Due to these clear benefits, ECM enrichment was incorporated into the final sample protocol.

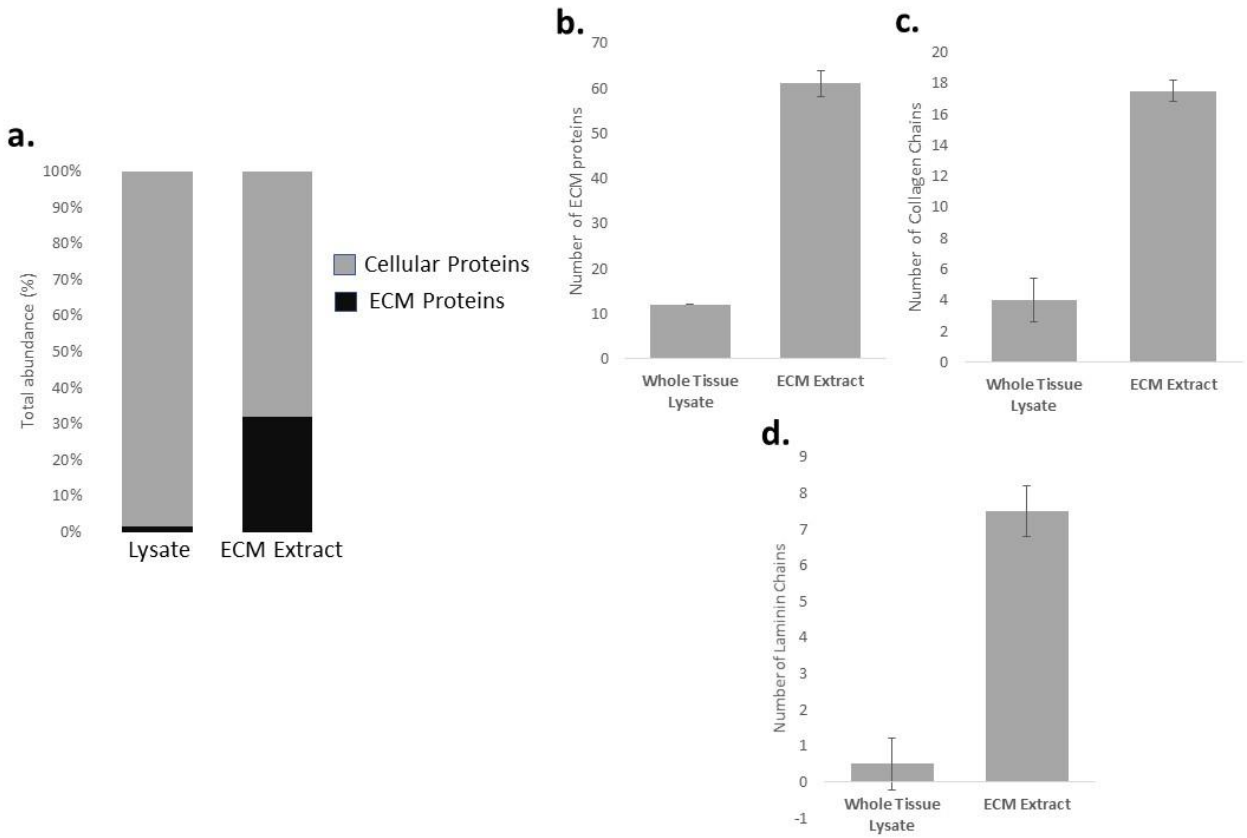


Figure 14: Comparison of matrix protein identification in whole tissue lysate vs ECM enriched samples
a. Proteomic analysis of the percentage of the total abundance represented by ECM associated or cellular proteins, in whole tissue lysate and ECM enriched pancreas samples. Comparisons of the number of proteins identified in the whole tissue lysate and ECM extract were performed for b. total ECM proteins, c. collagen chains and d. laminin chains.
Mean and SD are displayed (n=2, each group).

3.3.2 Characterisation of the Pancreatic Matrisome – Final Cohort

3.3.2.1 Identification of Proteins by LC-MS/MS

For the final sample run, following homogenisation, cloudy suspensions were observed in 4 samples. Due to limited sample availability the ECM extraction process was continued on these samples. As the extraction process progressed the cloudiness of the suspensions was lost, and by the end of the procedure the ECM pellets of these four samples were indistinguishable from the other six samples. However, when the matrisome of each donor was analysed by PCA, these four samples formed a scattered separate population in the positive region of principle component 1

(PC1). The other six donors remained tightly clustered towards the negative region of the plot (Figure 15). These 4 outliers were removed, which resulted in 3 remaining donors in each age group. The groups remained BMI, CIT and gender matched. 709 proteins were identified within these six samples. 81 of these proteins were classified as matrix (65; 80%) or matrix associated (16; 20%) proteins. A full list of the identified matrix proteins is available in the Appendix (Table B3). Matrix associated proteins consisted of those that were regulatory, affiliated or secretory in nature, and respectively included: serpin H1, members of the Annexin family, and 'calcium binding proteins' (such as Protein S100 A10). Of the remnant 65 proteins that made up the core matrisome, 34% were classified as collagen chains (I-VI, XII, XIV, XV, XVI, XVIII, XXI, XXVIII), 12% as proteoglycans (including, perlecan, decorin and biglycan), 14% were laminin chains (α1-5, β1-2, Y1&3) and the remnant 40% were classified as non-laminin glycoproteins including nidogens 1, 2 and fibronectin (Figure 16 and Appendix Table B3).

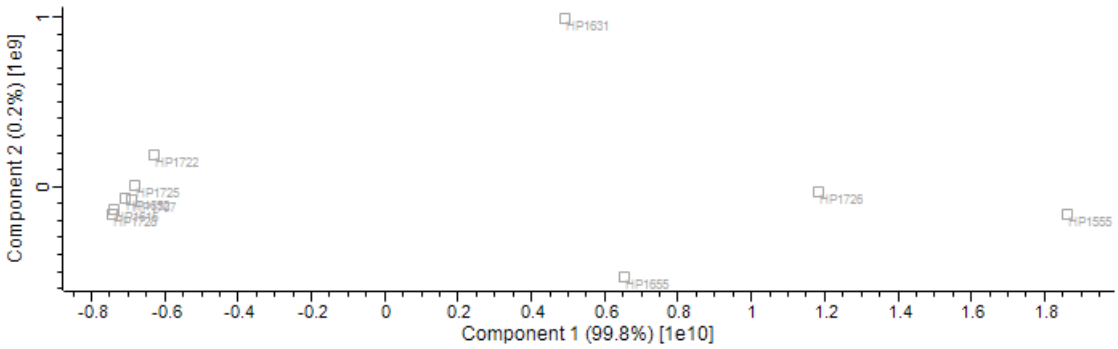


Figure 15: Principle component analysis (PCA) of ECM proteins (n=10)
Scores plot demonstrates the overall composition of the matrisome for 10 donors. 4 donors are separated towards the positive region of PC1.

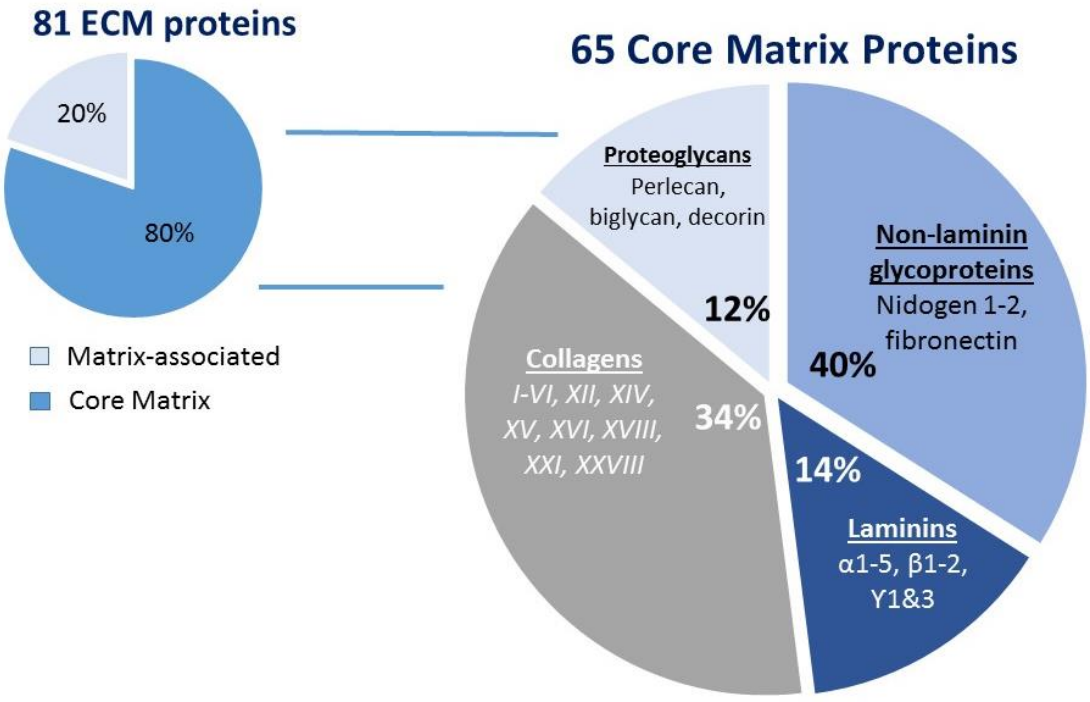


Figure 16: Summary of the 81 ECM proteins detected by proteomics
81 ECM proteins were detected. 20% of these proteins were classified as matrix-associated, which included regulatory and secretory proteins. The remnant 80% formed part of the core matrisome structure. Proteins included 13 collagens and 9 laminin chains. n=6

3.3.2.2 Localisation of Core Matrix proteins to the islet-exocrine interface using immunofluorescence

To determine the distribution of core matrix proteins in relation to islets, double immunofluorescence staining was performed on frozen pancreatic tissue sections. A sub-set of identified ECM proteins were selected for analysis including: collagens I-VI, XVIII and XXVIII, laminins (i.e. total net laminin), and the specific laminin chains: α2, α3, α5, β1, Y1, as well as perlecan, decorin, fibronectin and nidogen-1 (Figure 17). All donors showed a lack of staining for collagens II and XVIII, the laminin chains α3 and β2 and decorin. Although the other 13 proteins were detected, the signals for collagen XXVIII and fibronectin were weak, as compared to the other ECM proteins. For all 13 proteins that stained positively, there was evidence for the ECM being present at the islet-exocrine interface, surrounding the islet periphery. With the exception of

laminin α2 and collagen XXVIII, these 11 proteins also appeared within a second distinct intra-islet network (Figure 17).

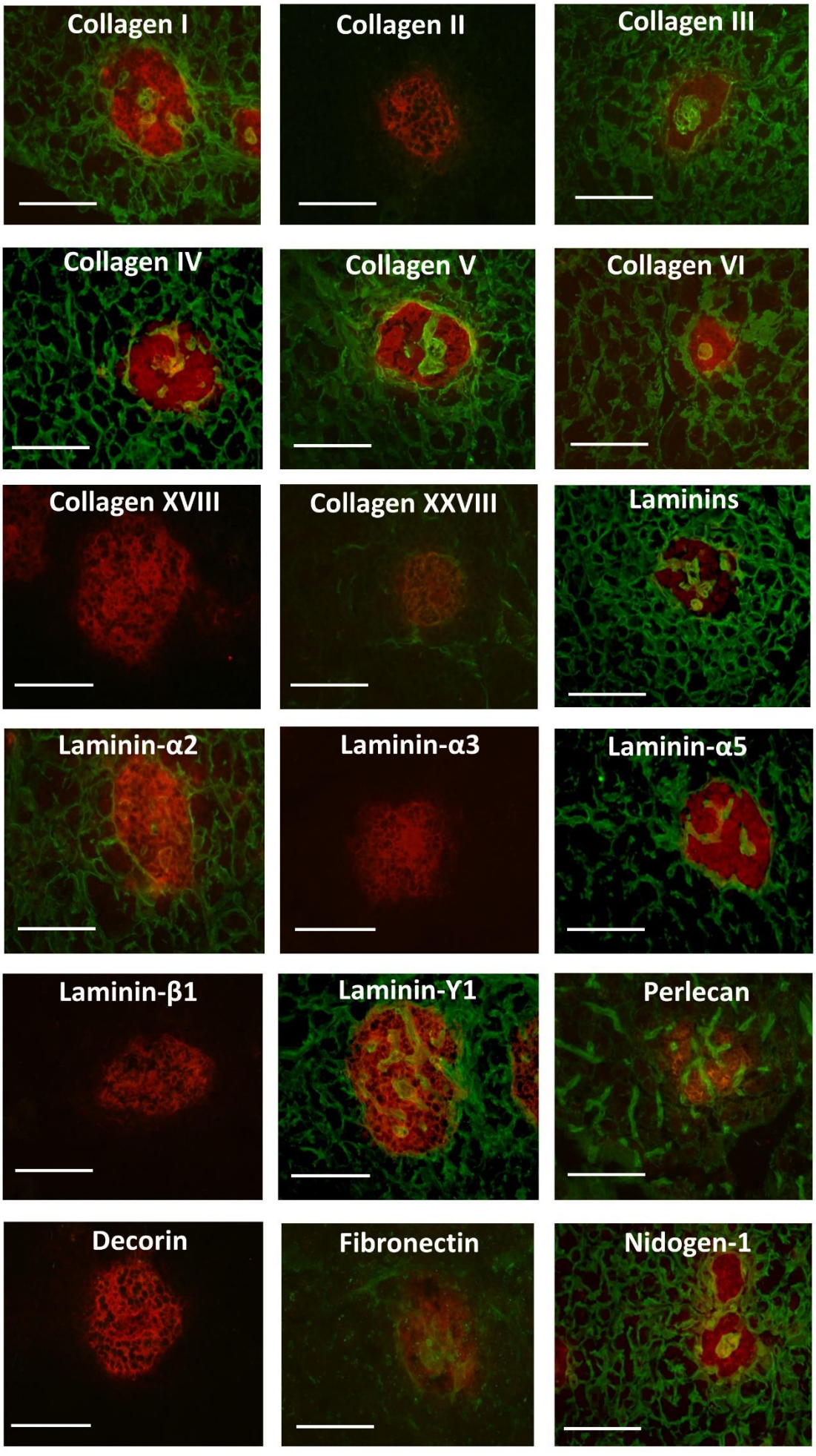

Collagen I
Collagen II
Collagen III
Collagen IV
Collagen V
Collagen VI
Collagen XVIII
Collagen XXVIII
Laminins
Laminin-α2
Laminin-α3
Laminin-α5
Laminin-β1
Laminin-Y1
Perlecan
Decorin
Fibronectin
Nidogen-1

Figure 17: Distribution of ECM proteins in relation to islets
Immunofluorescent detection of islets (*red*) and ECM (*as indicated, in green*). The majority of matrix proteins were detected throughout the tissue section; diffusely throughout the exocrine, as well as localised at the islet-exocrine interface. In addition, there was clear distinct staining pattern within the intra-islet region, where the matrix presumably supports the blood vessels within the islet interior. There was a lack of staining for collagen II and XVIII, laminin α3, β1 and decorin. Staining was weak for collagen XXVIII and fibronectin. Laminin α2 staining was present but was lacking from the intra-islet region. The above images are representative of all donors investigated (n=6). Scale bars = 100μm.

3.3.3 Donor Age-related Differences in the Pancreatic Matrisome

PCA was used to assess the effect of donor age on the pancreatic matrisome. A clear donor age-related cluster separation was visualised on the scores plot for total ECM proteins and for both collagen (22 chains) and laminin (9 chains) (all Figure 18). In all instances the younger donors formed a clear distinct population in the negative regions of the scores plots, along the principle component 1, which accounted for over 80% of the explained variation (Figure 18). Statistical analysis was performed on individual proteins to identify those responsible for this age-related separation. In total, 20 proteins were found to be significantly differentially expressed between the two donor groups, and with the exception of fibrinogen, all proteins were significantly more highly expressed in the younger donor group (Figure 19 a and Appendix Table B3 for full list). 74% (14/19) of these proteins were classified as collagens, and included chains that made up collagen I, II, III, IV, V, XV, XVIII and XXVIII. The laminin chains α2, 3 and Y1, and the non-laminin glycoproteins nidogen-1 and nephronectin were also differentially expressed. The fold increase in the younger donor group was examined (Figure 19 a). The proteins displaying the highest fold increase were the α4 and 5 chains of collagen IV. The α5 chain was increased by 11.5 fold in the younger donor group. Proteins that were not significantly affected by age included 4 of the chains comprising the collagen VI molecule (α1-3 and 6), collagens XVI and XXI, fibronectin, nidogen-2 and the heparan sulphate proteoglycans perlecan and decorin (Figure 19 b and Appendix Table B3 for full list).

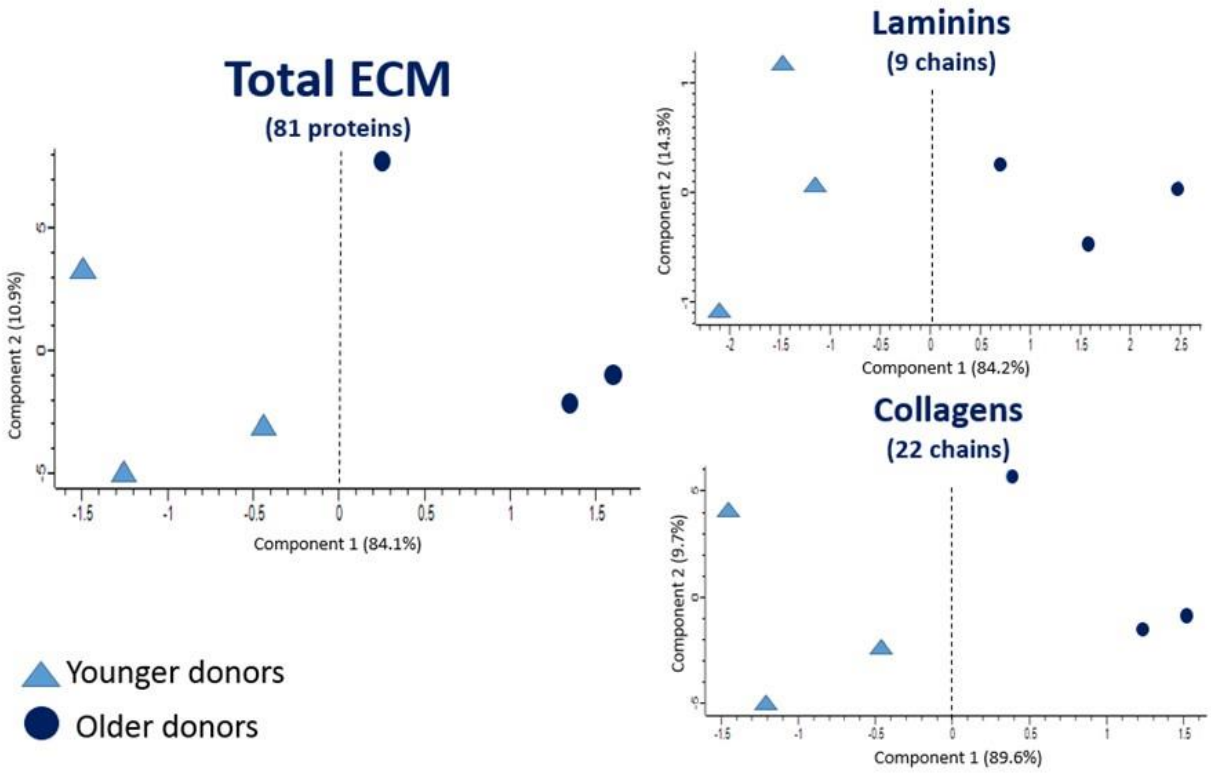


Figure 18: Donor age-related differences in the pancreatic matrisome, as detected by Principle Component Analysis (PCA)

PCA was used to visualise the overall effect of donor age on the expression of the ECM proteome, including, specifically, the collagen and laminin chains. In all instances the younger donors form a clear separate population in the negative region of the plots, suggesting that donor age influences the composition of the pancreatic matrisome.

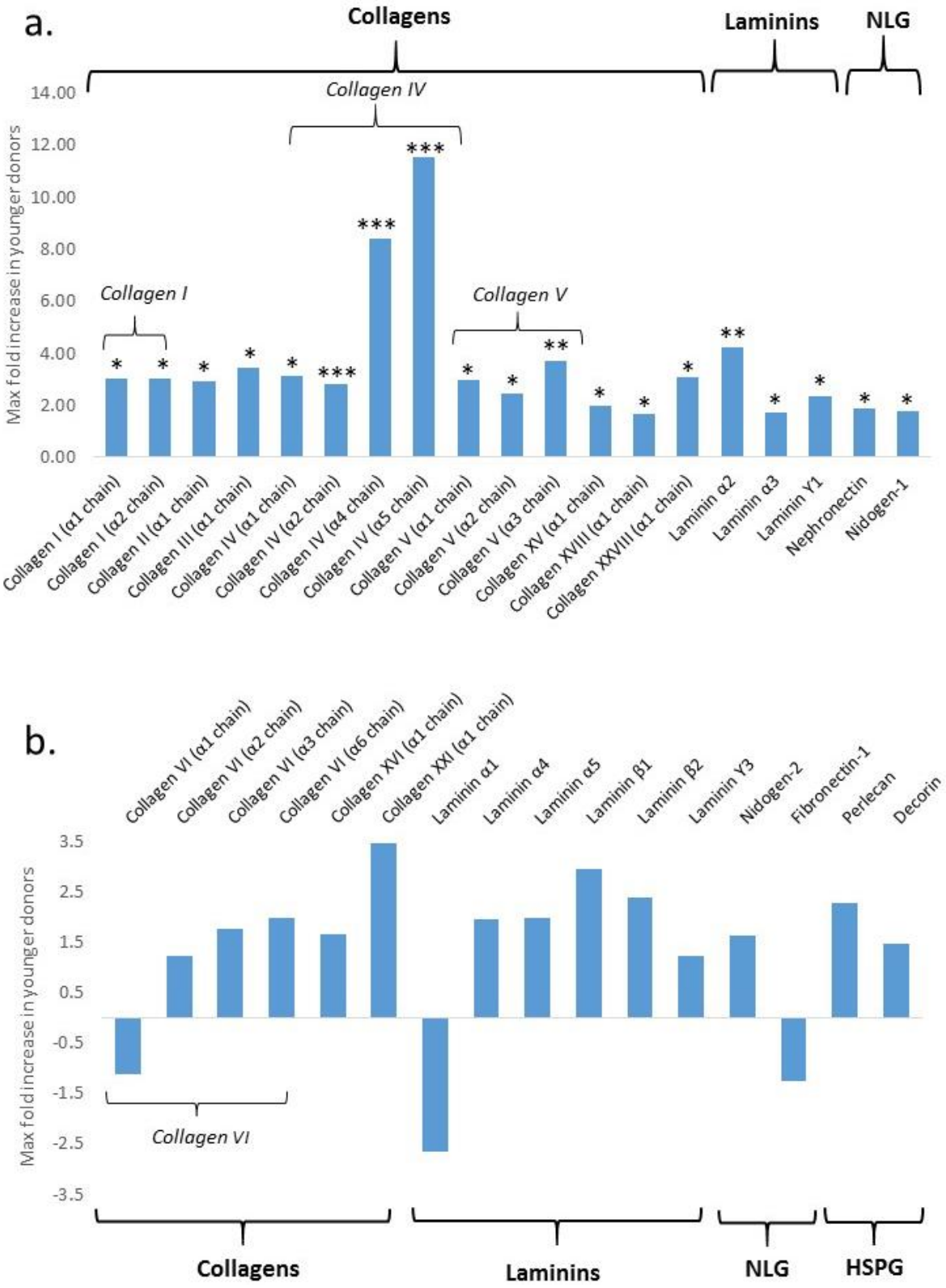


Figure 19: Proteomic detected age-related changes in the pancreatic ECM
a. 19 ECM proteins were significantly more highly expressed in the younger donor group.
b. A selection of the proteins that were not significantly affected by age. The full list of proteins can be found in the thesis Appendix (Table B3).
Both graphs demonstrate the maximum fold increase in the younger donor group, compared with the older donor group. Therefore, a negative value indicates that the protein is more highly

expressed in older donors. Proteins are grouped by class (i.e. collagens, laminins) and by protein (i.e. collagen IV chains).
Collagen IV was the protein most affected by age, with almost a 12-fold increase in the α5 chain in younger donors. The α1 chain of collagen VI was more highly expressed in older donors, though this did not reach statistical significance.
Data were analysed by ANOVA , using Progenesis.
* $p<0.05$, ** $p<0.01$, *** $p<0.001$
NLG; Non-laminin glycoproteins
HSPG; Heperan sulphate proteoglycans

3.3.4 ELISA Validation of Donor Age-related Changes in ECM Expression

The results of the LC-MS/MS experiments were validated on a larger cohort using ECM specific ELISAs. The ELISAs were able to confirm the lack of significant age-related change in the expression of collagen VI, perlecan, total laminin content and laminin α5 (Figure 20 a-d). However, they were unable to support a significant age-related decline in laminin-α2, collagen V, collagen I and nidogen-1 (Figure 20 e-h). In line with the LC-MS/MS results, the ELISA detected a significant age-related decline in collagen IV. In the younger donor group the concentration of collagen IV was 38.7±5.1 ng/ml, which decreased to 22.4±4.9 ng/ml in the older donor group (Figure 20 i).

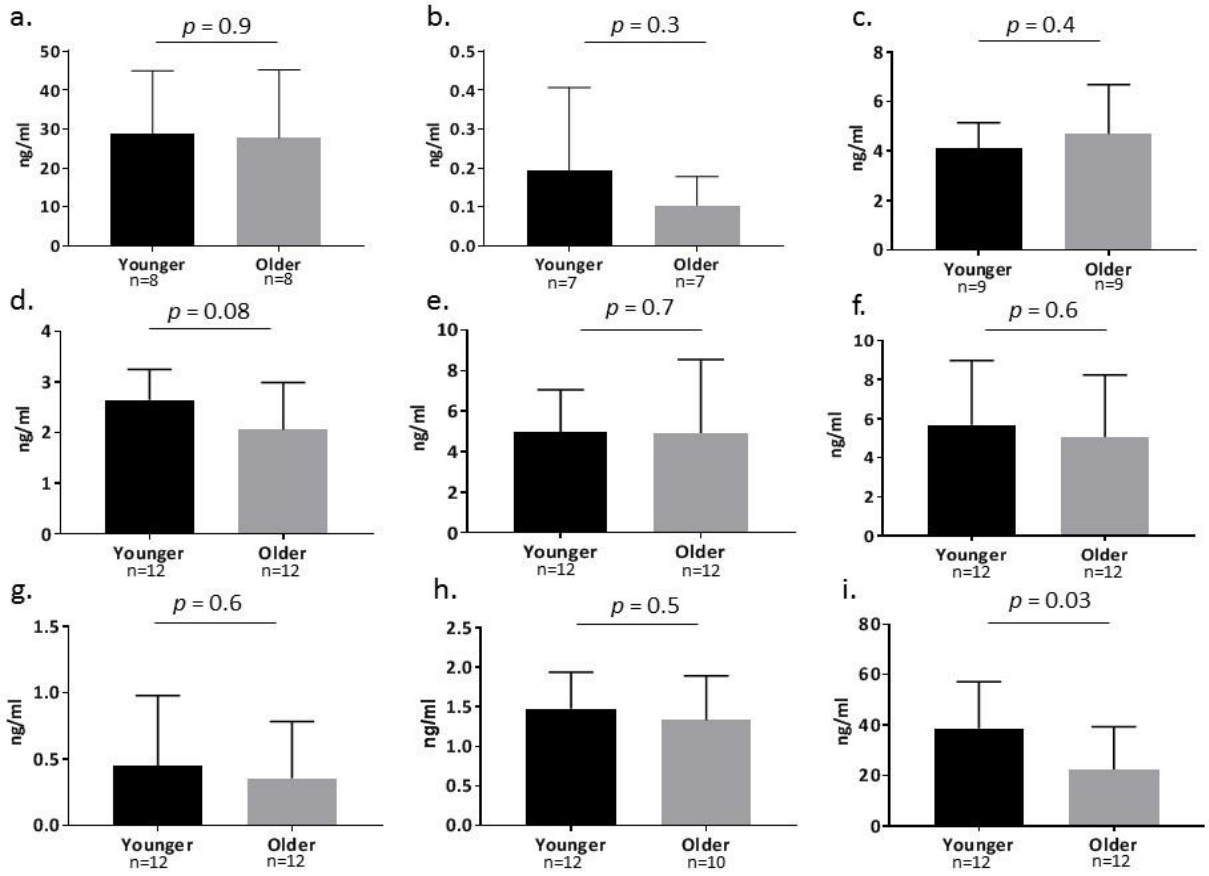


Figure 20: Quantification of pancreatic ECM proteins by ECM specific ELISAs
The age-related difference in the selection of proteins detected by LC-MS/MS were validated on a larger cohort using ECM specific ELISAs. The ELISAs confirmed the proteomics results by showing that there is no significant age-related change in a) collagen VI, b) perlecan, c) total laminin, or d) laminin α5. The ELISAs were unable to confirm that there is a significant age-related decline in e) laminin α2, f) collagen V, g) collagen I, or h) nidogen-1. However, ELISA confirmed that there is a significant loss of i) collagen IV with age. Graphs display mean ± SEM.
Data were analysed by independent samples t-test.

3.4 Discussion

LC-MS/MS identified 81 ECM proteins in the decellularised human pancreas. Of these proteins 80% were classified as core matrisome proteins, which included 22 collagen chains, 9 laminin chains, 8 heparan sulphate proteoglycans and 26 non-laminin glycoproteins. The expression of 20 ECM proteins were significantly affected by age. With the exception of fibrinogen, all proteins were more highly expressed in the younger donor group, and the alpha chains comprising the collagen IV molecule were the most affected, which was confirmed on a larger cohort using ELISA.

The importance of defining pancreatic architecture, within the context of pancreas dissociation, was first discussed in the 1980s [315]. Following this, a number of studies successfully used antibody based detection methods to begin characterising the human pancreatic matrisome, leading to the identification of a number of collagens, laminins and other non-laminin glycoproteins [167, 171, 173, 210]. However, the opportunity to perform a large-scale analysis of the pancreatic matrix has only recently been realised, with the rise of high-throughput 'omics' based technologies [311].

Overall, the data presented within this Chapter support the recent investigation by Sackett *et al*., which details the identification of 120 matrix and matrix affiliated proteins within the decellularised human pancreas [163]. Of the additional 39 matrix proteins that were identified in Sackett's study, only 7 were classified as core matrix proteins. Differences existed in the detection of collagen, with the detection of an additional 11 chains to those presented here. However, their identification of laminin chains was poorer (7 vs 9 chains; full comparison of the two studies is available in Appendix Table B3). These differences in matrix detection likely result for two reasons. Firstly, different ECM extraction methodologies were used. Where Sackett *et al.* utilised an in-house developed ECM extraction method [163], the ECM extraction method used within this Chapter was commercially produced by Millipore. Although both methods involved incubating the tissue in buffers containing sodium deoxycholate, it was not possible to obtain the exact composition of buffers within the commercial kit, on the grounds of proprietary. Secondly, differences in matrix detection may arise from the data analysis methods used. In the current study, a positive protein identification was only made if there were two or more unique peptide matches. This ensures that protein identifications are made with a degree of confidence. Although it is standard to implement a minimum sequence match when analysing proteomic data sets, it is not clear from their manuscript if Sackett *et al*. utilised this approach. Adding this extra requirement decreased the number of positive protein identifications in the current dataset and led to the removal of 9 collagen chains (including those from collagens IX, X, XI, XXIII, XXV and XXVII).

The majority of the 18 proteins studied by immunostaining were present at the islet-exocrine interface, supporting previous reports [99, 112, 167, 171, 210]. For the first time these studies confirm the presence of laminin α2 and collagen XXVIII at the islet-exocrine interface of the human pancreas. 5 proteins that were not detected included: collagens II and VXIII, the laminin chains α3 and β1, and decorin. Expression of collagen II is usually restricted to cartilage [311], and although detected in both the data here, and that presented by Sackett *et al.* [163], the levels within the pancreas may fall outside the detection limits for the utilised antibody. The lack of collagen XVIII staining may result from its intracellular localisation [204]. Although detected, expression of collagen XXVIII and fibronectin were weak as compared to the other ECM proteins.

In the current study, the distribution of laminins α2, 3, 5, β1 and γ1 were studied. Laminins α2, α5 and γ1 were detected, whereas α3 and β1 were absent. Human pancreatic laminin distribution has been studied previously by Virtanen *et al.* [167]. In support of the current study, the authors reported the presence of laminin α5 and γ1 in the peri-islet region, as well as the absence of laminin α3 [167]. However, unlike in this study, the authors successfully detected laminin β1. In addition, they reported that laminin α2 was only present in the exocrine, and absent from the peri-islet region, which is different to what is shown in this Chapter. Such variations in protein detection likely arise from differences in the primary antibodies utilised. Indeed, it would be good practice to utilise an additional primary antibody, directed at a different epitope, to confirm the absence of specific proteins. However, such studies are restricted by the availability of commercially available antibodies.

There have been a limited number of studies that have investigated the impact of age on the composition of the ECM. Bedossa *et al.*, showed that overall pancreatic collagen content significantly increases with age [274]. This contradicts the data presented in this Chapter, which demonstrated a significant age-related reduction in the expression of 14 collagen chains. However, Bedossa *et al*. used a restricted age range of donors, and the youngest donor included was 48 years

old. In addition, the authors assess collagen content based on the ratio of Sirius red staining (detects collagenous proteins) to fast green staining (detects non-collagenous proteins). Therefore, as the authors point out, it cannot be excluded that the increase in collagen ratio did not result from a decrease in non-collagenous proteins [274]. In a more recent study, Tons *et al.* came to a similar conclusion as Bedossa *et al*., whilst using the same method to detect collagen [275]. However, this study was not supported by any form of statistical analysis [275]. By using a hydroxyproline assay to assess total pancreatic collagen content, Longanathan and colleagues found that there was a trend towards reduced collagen in donors over 35 years old, but this did not reach significance [99]. In addition, the authors used ECM specific antibodies to semi-quantify collagens I, III, IV, VI, laminin and fibronectin, via morphometrical assessment. Although the majority of proteins were not affected by age, there was a significant age-related decline in collagen IV and total laminin [99]. Hughes *et al.* confirmed the lack of significant age-related change in collagen VI content, this time specifically within the peri-islet region [171]. The work by Longanathan *et al.* and Hughes *et al*. partially support the data presented in this chapter, specifically with regards to the significant decline in collagen IV with age, and the lack of change in collagen VI. However, differences in the results (i.e. collagens I, III) most likely arise from the relative sensitivities of the methods used; as proteomics offers a much more sensitive quantification than antibody-based detection, not all of the perceived differences may translate to immunostaining.

Differences in method sensitivities may also explain why the ELISAs were unable to fully validate the proteomic results. Although they were able to confirm a significant age-related decline in collagen IV content (the protein that displayed the highest age-related decline in the proteomics) they were unable to support an age-related reduction in nidogen-1, collagen I, collagen V and laminin α2. However, ELISAs do enable an absolute assessment of protein concentration to be performed, which is not made possible in proteomics when using label-free quantification. As well as allowing the quantities of different proteins to be compared, absolute quantification confirms the prevalence of each protein within the pancreatic matrix. Of all the proteins assayed by ELISA,

collagen IV was the most abundant. In fact, the expression of collagen IV was around 75-fold higher than collagen I (Figure 20). Although collagen VI expression was similar to collagen IV, all of the other proteins were expressed below 6ng/ml. Due to its high prevalence, this data highlights the importance of collagen IV in the pancreas digestion process, especially in pancreases from younger donors, where expression is significantly higher.

One criticism of the current study is that the pancreatic matrisome was defined on the basis of a whole tissue homogenate, as opposed specifically characterising the matrix associated with islet tissue. Although immunostaining was used to partially overcome this limitation, it was not feasible to study all 65 core matrix proteins in this manner. As islets only make up around 2% of the overall pancreatic mass, it can be argued that the proteome defined here does not fully represent the composition of the matrix located at the islet-exocrine interface. Whilst extracting islets enzymatically to enable specific characterisation of the islet matrix would be a counter-indication, there are other strategies that could be used to address this limitation. Firstly, it is possible to isolate islets from pancreatic tissue sections using laser capture microdissection (LCM). Islets are located (via Toluidine blue staining or antibody labelling) and excised using a high-energy laser source, coupled to a microscope [307]. This technique allows proteomic profiles to be generated specifically from islet tissue, under conditions that are comparable to their native environment. Zhang and colleagues used this technology to compare the proteomic profiles of LCM prepared human islet and exocrine tissue. 1104 and 706 proteins were detected in the islet and exocrine tissue respectively, with an overlap of 612 proteins [307]. Of the 5 collagen types that were identified, only the expression of collagen VI was significantly affected by location, and distribution was significantly higher in the islet tissue (Table 13).

	Exocrine (n=6)	Islet (n=9)	*p*-value
Collagen I α1	26.58±0.26	26.57±0.25	0.98
Collagen I α2	26.12±0.24	26.55±0.19	0.18
Collagen IV α1	18.75±3.8	23.66±0.10	0.13
Collagen IV α2	20±4.0	24.45±0.18	0.19
Collagen VI α1	23.61±0.65	25.67±0.10	0.002**
Collagen VI α2	23.48±0.36	25.8±0.12	0.001***
Collagen VI α3	26.49±0.19	27.45±0.12	0.0007***

Table 13: Relative abundance of matrix proteins detected in the exocrine and islet proteome by Zhang *et al.* [307]
Data represents the accumulation of ion counts following label free quantification. This raw data was obtained from the online supplementary materials (Table S1), which accompany the Zhang *et al.* article [307]. T-tests were performed in Prism. Only collagen VI expression was significantly affected by location and was higher in the islet tissue than the acinar. Collagen III and XIV were also identified, but this was limited to a single islet sample. Data were analysed by paired samples t-test. ** $p<0.01$, *** $p<0.001$

Although this does highlight potential differences in matrix expression between the exocrine and endocrine pancreas, these differences were not reflected in the immunostaining images, presented in this Chapter. In addition, the low number of matrix proteins detected in the study by Zhang *et al.* further emphasise the importance of performing ECM extraction prior to proteomics [307]. Finally, next generation mass spec imaging platforms may also provide a sophisticated alternative for characterising the matrix within the islet-exocrine interface. Within these workflows, matrix-assisted laser desorption/ionisation imaging mass spectrometry (MALDI-IMS) is used to directly ionise peptides within a defined tissue area, which are then desorbed and analysed by MS [316]. The resulting MS output can be arranged into heat maps and aligned against histological features, resulting in a high degree of spatial resolution [316]. The technique has been used to characterise a number of tissues including that from the liver and aorta [316] and provides an interesting avenue for studying the islet matrix.

3.5 Conclusions

Proteomics identified 81 core matrix and matrix-affiliated proteins in the decellularised human pancreas. Label-free quantification was able to demonstrate that 19 proteins were significantly more highly expressed in pancreases from younger donors. Collagen IV was most affected, which was confirmed using ECM specific ELISAs. This is the first large scale protein analysis study aimed at characterising pancreatic matrix expression in different donor types. The significant age-related decline of key ECM proteins in the human pancreas may explain why current enzyme blends are ineffective at digesting the ECM in younger donors. Although tailoring enzyme blends to compensate for the increased level of matrix proteins in younger donors should enhance digestion outcomes from this donor type, it is first important to understand how these differences impact matrix digestion by collagenase-based blends. The next Chapter describes the development of a novel glass slide-based digestion assay that allows multiple enzyme blends to be tested on the pancreas of any one donor.

CHAPTER 4

Development and Validation of a Slide-based Assay for Monitoring Enzyme Digestion of Pancreatic Tissue

4.1 Introduction

The islet isolation process remains highly variable, and relatively non-specific. This is in large part due to the variability of the pancreas digestion phase of the procedure, where collagenase-based blends digest the ECM proteins located at the islet-exocrine interface to liberate 'free' (devoid of exocrine) islets for purification. In addition to the variability of commercially available collagenases [135], the success of pancreas digestion is also heavily influenced by donor factors, as explored in Chapter 2. Analysis of the UK dataset identified donor age as one of the major influencing factors. Lower isolation yields from younger donors is supported by previous reports [136, 215, 222].

As successful human islet isolation is dependent upon the effective separation of islets from their surrounding exocrine tissue, a more detailed knowledge of the composition of the peri-islet pancreatic matrix, on which collagenase is acting, is vital. In the previous Chapter, high-throughput proteomics identified 81 ECM related proteins in the human pancreas. Critically, these experiments also revealed that 19 core matrix proteins are significantly more highly expressed in younger donors. Understanding how these changes in pancreatic structure influence the susceptibility of each matrix component to digestion will enable the development of novel, tailored enzyme blends. This will help to optimise islet isolation outcomes from the full range of donor pancreases.

However, the limited availability of donor pancreases makes it undesirable to use full-scale islet isolation procedures when conducting detailed experiments aimed at characterising pancreas digestion in different donor types and by specific enzyme components. This is also apparent in the batch testing of new enzyme lots, which is complicated by the presence of inter-pancreatic variability between individual donors, when the testing is completed across different organs. Instead, what is required is a simple method that enables multiple enzyme components and combinations of components to be tested on any one pancreatic sample. This chapter describes the development of such a research method.

4.2 Methods

4.2.1 Sampling Technique

With appropriate consent and ethical approval, clinical grade human pancreases from older (≥45 years old; n=7) and younger (≤35 years old; n=8) multi-organ donors were procured for islet isolation. Organs were transported in UW solution (Bridge to Life, London, UK) on ice to the DRWF Human Islet Isolation Facility, at the Churchill Hospital in Oxford. 0.5cm^3 tissue samples were taken from the head of the pancreas and snap frozen in liquid nitrogen. Frozen tissue sections (10µm thickness) were prepared using a Cryostat (Leica, Milton Keynes, UK) and collected onto Superfrost Plus glass slides (Thermo-Fisher Scientific, Loughborough, UK), before storage at -25°C until use.

4.2.2 Enzymatic Treatment and Immunolabelling of Tissue Sections

Pancreas cryosections were thawed in HBSS (Lonza, Basel, Switzerland) before undergoing incubation for 5 minutes at 37°C with HBSS (control), collagenase NB1 alone, neutral protease (NP) alone (both Serva, Heidelberg, Germany) or a combination of the two enzymes, at clinically relevant concentrations (collagenase 7.2 PZU/ml, NP 0.14 DMCU/ml). Following treatment, enzymatic activity was quenched by placing slides in cold running water. Sections were fixed with 2.5% paraformaldehyde (Sigma, Poole, UK) and then blocked with 10% normal goat serum or 5% normal swine serum (Vector Laboratories, Peterborough, UK), for laminin α5 and collagen IV staining respectively, for 30 minutes at room temperature (r.t). Sections then underwent double immunofluorescent labelling. Incubation with primary antibodies: polyclonal guinea pig anti-insulin (1:100; A0564, Dako, Ely, UK), and either monoclonal mouse anti-laminin α5 (1:100; ab77175, Abcam, Cambridge, UK) or polyclonal goat anti-collagen IV (1:100; 134001, BioRad, Oxford, UK) was for 1.5 hours at r.t. Sections were then incubated with secondary antibodies for 30 minutes at r.t.: Texas Red conjugated goat anti-guinea pig (1:100; TI-7000, Vector Laboratories) and AMCA conjugated horse anti-mouse (1:100; CI-2000, Vector Laboratories) for laminin α5 detection, or

AlexaFluor 594 conjugated donkey anti-guinea pig (1:500; 706-585-178, Jackson Immunoresearch, PA, USA) and AlexaFluor 405 conjugated donkey anti-goat (1:100; 175664, Abcam) for collagen IV detection. Slides were mounted with ProLong Diamond Antifade mounting media without DAPI (Thermo-Fisher Scientific) and cured overnight at 4°C.

Non-specific binding of the secondary antibodies was tested by omitting primary antibodies. Negative control sections were incubated with normal host IgG (Santa Cruz Biotechnology, TX, USA) in place of the primary antibodies at appropriate concentrations, to test for non-specific binding of primary antibodies.

4.2.3 Quantitative Analysis of Digestion

Islets were identified by immunofluorescent labelling of insulin. A minimum of ten islets were imaged per donor, per treatment, using an Axioskop 40 microscope and Axiovision software (Carl Zeiss, Jena, Germany), in 8-bit format. The corresponding field of protein staining (laminin α5 or collagen IV) was also imaged in the same format. Image settings during capture remained constant with respect to those used for the control images, including exposure time. The images were imported into Image J, where the immunolabelled protein that encapsulated the islet and penetrated into the intra-islet region was semi-quantified morphometrically, using a purpose built semi-automated macro. Briefly, the outline of the islet was selected by drawing around the insulin positive region. The images were converted to 32-bit, before the area of the islet was automatically recorded. This region of interest was then superimposed onto a 32-bit version of the corresponding protein image, and the area and intensity of protein staining within this islet region was measured. A threshold value was set to a standard 25, which removed any positive regions that were likely to have occurred due to background staining, rather than the presence of protein (Figure 21). The results were imported to Excel (Microsoft Corporation, USA, 2016), where the threshold area of the protein staining was normalised against the whole islet area, to take into account islet size, and

then multiplied by the mean signal threshold intensity. The data generated from the treatment conditions were normalised to the control, to indicate the percentage of protein loss compared to control.

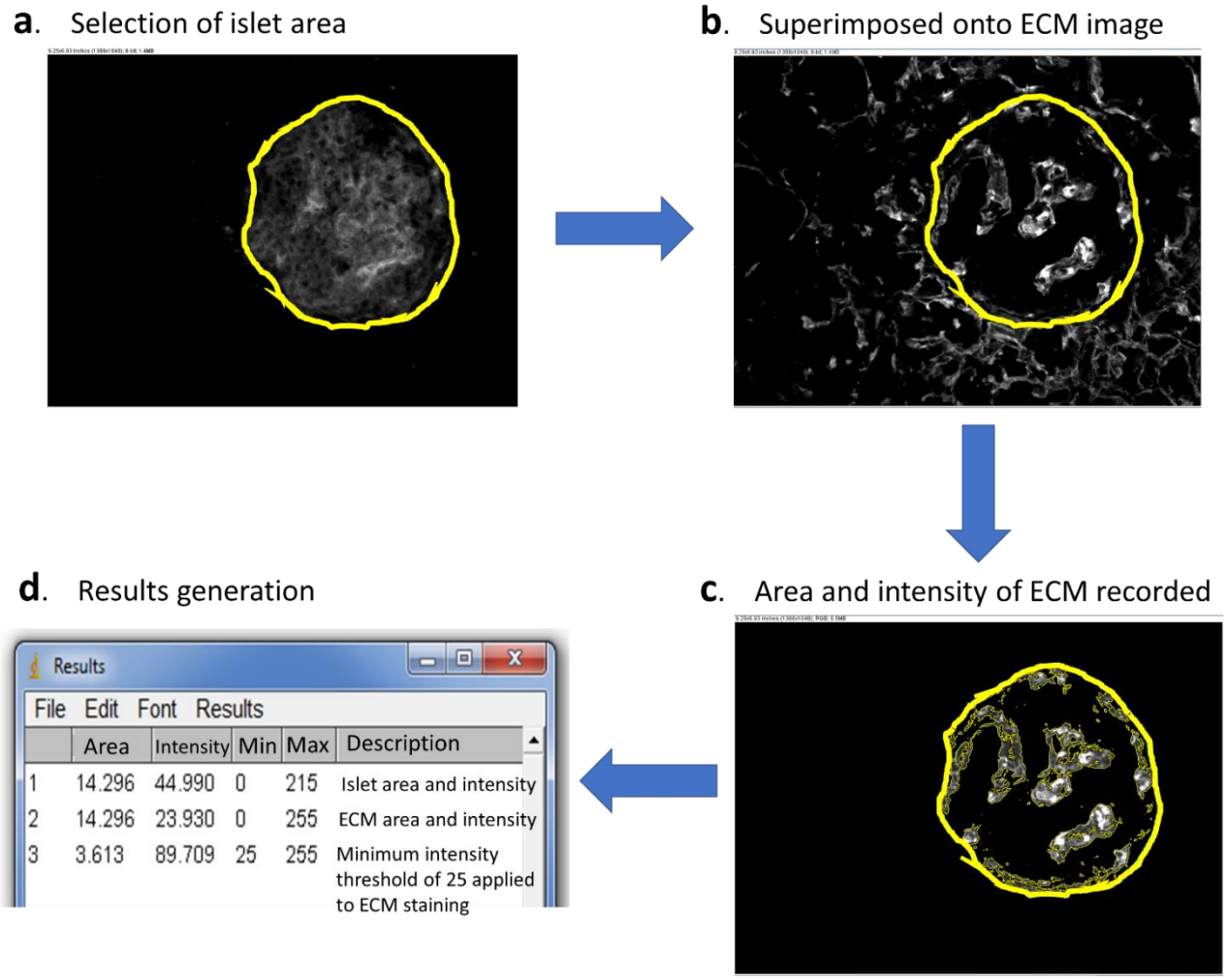


Figure 21: Overview of the tasks performed by the semi-automated macro, for the measurement of peri islet ECM staining

ECM protein is semi-quantified within the islet area, using image J and a purpose built semi-automated macro. The sequence of commands is as follows:

a. The islet is identified by insulin positive staining and selected by free hand drawing. The area of the islet is recorded (line 1 in image d.)

b. The islet area is superimposed onto a 32-bit version of the ECM image and the area and intensity of the staining within this area is recorded (line 2 in image d.)

c. An intensity threshold is set to 25, to eliminate any background staining, and the intensity of the staining within the ECM positive region is recorded (line 3 in image d.)

d. Three lines of results are generated; a description of each result is outlined above in a-c.

4.2.4 Assay Reproducibility

To demonstrate the reproducibility of the technique, complete image sets from five randomly selected donors for each protein were independently analysed by an additional researcher, on a different computer system, using the semi-automated macro described above.

4.2.5 Statistical Analysis

Digestion data were analysed using mixed linear modelling, to determine both enzyme component and donor age effects on protein digestion. Linear modelling requires that the dependent (i.e. response variable) is normally distributed. Box-cox transformation was used to test the normality of the response variable, which was then transformed as appropriate. The fit of each model was tested by performing quantile-quantile (Q-Q) normality plots and completing Shapiro-Wilk tests on the residuals. A Shapiro-Wilk *p* value of greater than 0.05 indicates an appropriate fitting model. Q-Q plots and Shapiro-Wilk tests were incorporated, as a standard, into all mixed linear modelling performed in Chapters 4 and 5, to confirm that the models were appropriately fitted to the data. Data are expressed as mean ± SEM. Wilcox paired sign rank test was used to determine if there was a significant difference in the results obtained from the two independent researchers. All statistical analyses were performed in R (R Core Team (2016). R: A language and environment for statistical computing. R Foundation for Statistical Computing, Vienna, Austria.) For all analyses performed, a *p* value of less than 0.05 was considered significant.

4.3 Results

4.3.1 Donor Demographics

Studies were performed on tissue biopsies obtained from both older (≥45 years) and younger (≤35 years) donor pancreases, accepted for clinical islet isolation (Table 14). The mean donor age was 30±1 years and 54±2 years, in the younger and older groups respectively. BMI, cold ischemia time

(CIT) and gender ratio were statistically matched between the two groups. Retrieval of the organs either occurred after donor cardiac death (DCD) or after donor brain death (DBD). Although three pancreatic biopsies in the younger group were obtained from DCD donors, compared to no donors of this type in the older donor group, this did not reach statistical significance (*p*=0.07).

	Younger Donors ≤ 35 years (n=8)	**Older Donors ≥ 45 years (n=7)**	***p* value**
Age, y (Mean ± SEM)	30±1	54±2	<0.001
Age, y (Median (Range))	31 (25-35)	53 (46-60)	<0.001
Gender (M:F)	6:2	5:2	0.876
BMI (Mean ± SEM)	26±1	27±1	0.29
CIT, h (Mean ± SEM)	5.6±0.5	7.0±1.4	0.089
Donor Type (DBD:DCD)	5:3	7:0	0.07

Table 14: Donor and pancreas characteristics for Chapter 4
CIT, cold ischaemia time; DBD, donation after brain death; DCD, donation after cardiac death
Statistical analysis was performed by an independent samples t-test.

4.3.2 Mixed Linear Modelling

Mixed linear modelling was used to determine both enzyme component and donor age effects on protein digestion, with the semi-quantified protein content as the response (or dependent) variable. This type of model takes into consideration the influence of random effects (i.e. the individual donors) on the response variable, as well as fixed effects (i.e. the age of the donor). For the model to be valid, the response variable must be normally distributed. To achieve normality each of the response variables were transformed by box-cox transformation. The final model fit was confirmed using the appropriate diagnostics, including the generation of Q-Q plots. Examples of a Q-Q plots for collagen IV and laminin α5, which demonstrate the normal fit of the models, are available in the thesis Appendix (Figure C1). Testing the residuals via Shapiro-Wilk produced *p* values of 0.15 and 0.10 for collagen IV and laminin α5, confirming normality (data not shown).

4.3.3 Quantitative Analysis of Digestion

The developed slide-based digestion assay was able to successfully demonstrate differential digestion of peri-islet ECM proteins collagen IV (Figure 22 a) and laminin α5 (Figure 22 b), when utilising individual components of clinical islet isolation enzyme blends. These proteins were selected based on their identification in Chapter 3, as well as their know prevalence in the human pancreas. The assay also identified donor age-related differences in the digestion of these proteins. Loss of matrix proteins following time-controlled digestion was detected by the reduction in the signal intensity of the immunofluorescent staining.

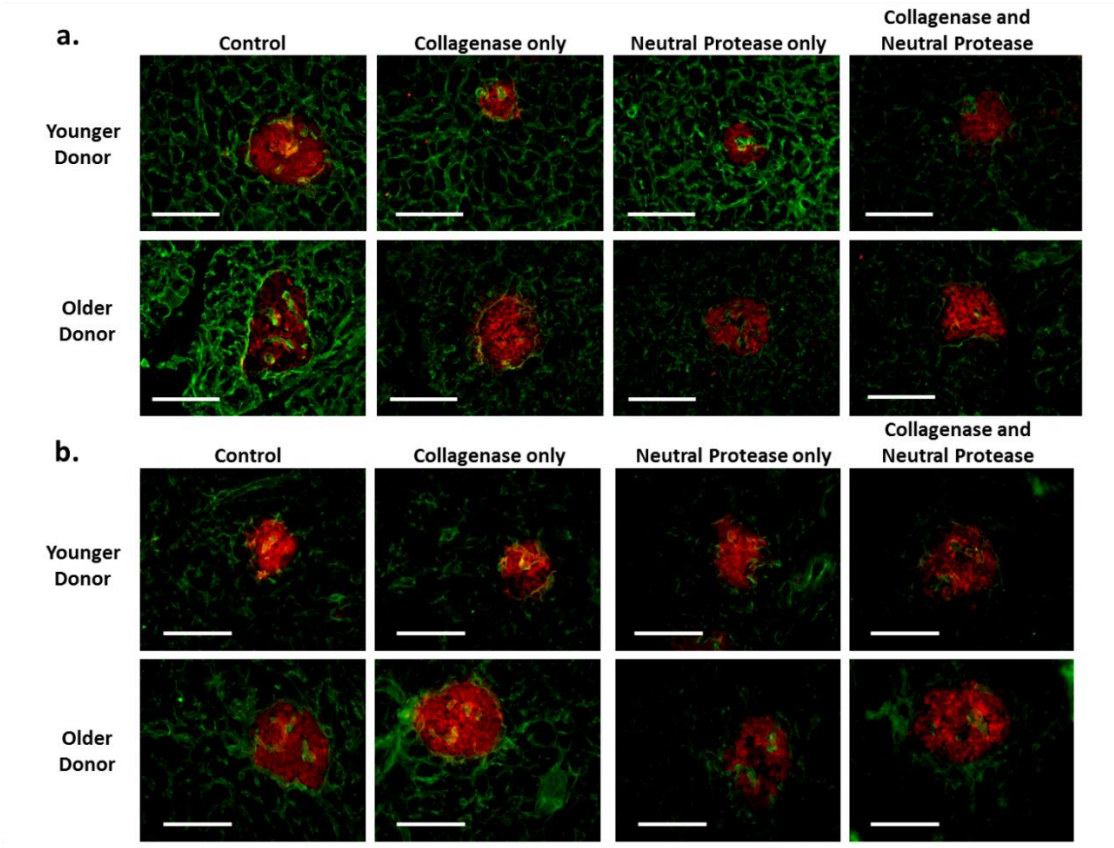


Figure 22: Immunofluorescence labelling of collagen IV and laminin α5 digestion at the islet-exocrine interface of younger and older donors
Representative images of pancreas sections following treatment with HBSS (control), collagenase, neutral protease or a combination of both enzymes for 5 minutes. Digestion of a. collagen IV and b. laminin α5 (both *green*) is seen around and within the islet (*red*, insulin labelling of β-cells). Loss of signal for both proteins was significantly greater in the older donor group, than the younger group, when treated with neutral protease. There was no significant loss of laminin α5 when treated with collagenase alone in either group, though this treatment was effective at digesting collagen IV in both donor groups. The loss of collagen IV by collagenase was more effective in older donors. The combination of enzymes ameliorated the significant age-related digestion differences in both proteins. Scale bars = 100µm.

When sections were treated for 5 minutes with collagenase alone there was a 32±5% reduction in collagen IV in the older donor group (p<0.001 compared to control, Figure 23 a), but only a 19±5% loss of collagen IV in the younger donor group (p<0.001 compared to control, Figure 23 a). Despite the significant collagenase mediated loss of collagen IV in both groups, there was significantly more loss in the older donor group (p<0.05, Figure 23 a). NP was ineffective at digesting collagen IV in younger donors (4±5% loss compared to control; NS, Figure 23 a) whereas significant digestion occurred in the older donor group (36±4% loss compared to control; p<0.001, Figure 23 a). NP was therefore significantly more effective at digesting collagen IV in the older donor group (p<0.001, Figure 23 a). Despite the enhanced resistance of collagen IV to digestion in the younger donors when treated with collagenase or NP independently, combining the two enzymes ameliorated these significant differences and led to a 57±4% and 58±3% reduction in collagen IV, in the younger and older donor groups respectively (both p<0.001, compared to respective control, Figure 23 a).

When treated with collagenase alone, digestion of laminin α5 was not significant in either donor group (loss of 10±6% and 5±6% for younger and older groups respectively, as compared to respective controls; both NS, Figure 23 b). However, laminin α5 was significantly digested by NP in both donor groups (loss of 24±5% and 40±3% for younger and older groups respectively, as compared to respective controls; p<0.01 and p<0.001, Figure 23 b). Therefore, the digestion of laminin α5 by NP was significantly greater in the older donors (p=0.05, Figure 23 b). Again, the significant age-related differences in digestion were lost when collagenase and NP were combined. This combined treatment lead to a loss of 44±5% and 43±4% in the amount of laminin α5 for the younger and older groups, respectively (both p<0.001, compared to respective control, Figure 23 b).

No non-specific binding of either primary or secondary antibodies was detected by the control staining (data not shown).

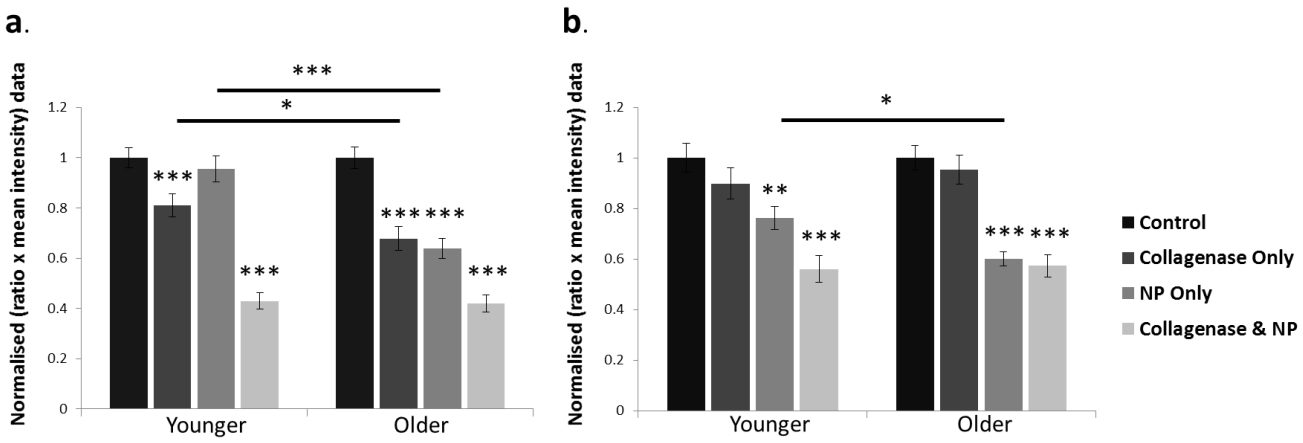


Figure 23: Quantitative analysis of collagen IV and laminin α5 digestion
The area and intensity of immunofluorescent staining for a. collagen IV and b. laminin α5 was normalised to the control, post digestion with specific enzyme components, and the efficiency of digestion was compared between two donor age groups. Independent use of neutral protease lead to significantly more loss of both collagen IV and laminin α5 in the older donor group, than in the younger group. There was no significant loss of laminin α5 when treated with collagenase alone in either group. Collagenase significantly digested collagen IV in both donors groups, but was more effective on older donors. The combination of enzymes ameliorated the significant age related digestion differences in both proteins.
Data represent the mean±SEM from n=6 each donor group (collagen IV) and n=7 each donor group (laminin α5). Data were analysed by mixed linear modelling.
**p* <0.05, ***p*<0.01, ****p*<0.001 vs control, or as indicated by solid bars.
NP, neutral protease.

4.3.4 Assay Reproducibility

To assess the reproducibility of the assay, complete image sets obtained from five donors for each protein were analysed by an independent operator, as per the method described. There was no significant variation in the data obtained from the image analysis between the two operators for either collagen IV (Figure 24 a) or laminin α5 (Figure 24 b), as seen via dot plot of all individual values. In addition, correlation curves demonstrated that the data points from Operator 1 were closely correlated to those from Operator 2 (Figure 25).

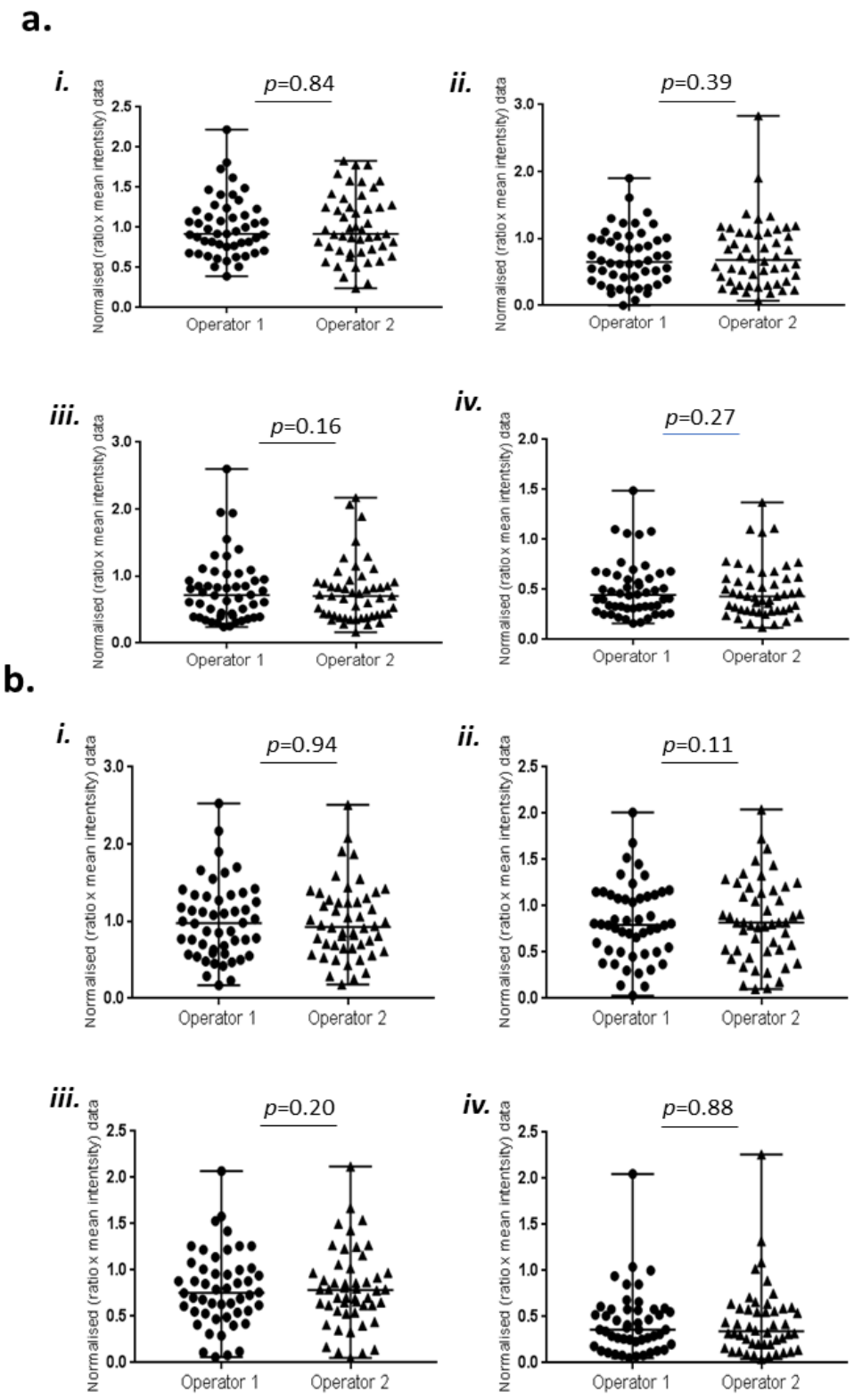


Figure 24: Assay Reproducibility

To assess assay reproducibility, complete image sets for both a. collagen IV and b. laminin α5, from five randomly selected donors, were independently analysed by a second operator. Data represent the ratio of positive protein labelling to that of the insulin stained region. This ratio was then

multiplied by the mean intensity of the labelling. All treatment data was normalised to the respective control. There was no significant variation in the measurements obtained from control (i), collagenase only (ii), neutral protease (NP) only (iii), or collagenase and NP (iv). Graphs display all data points, as measured by both operators (n=5 donors for each protein), along with the median and range. Data were analysed by Wilcox paired sign rank test.

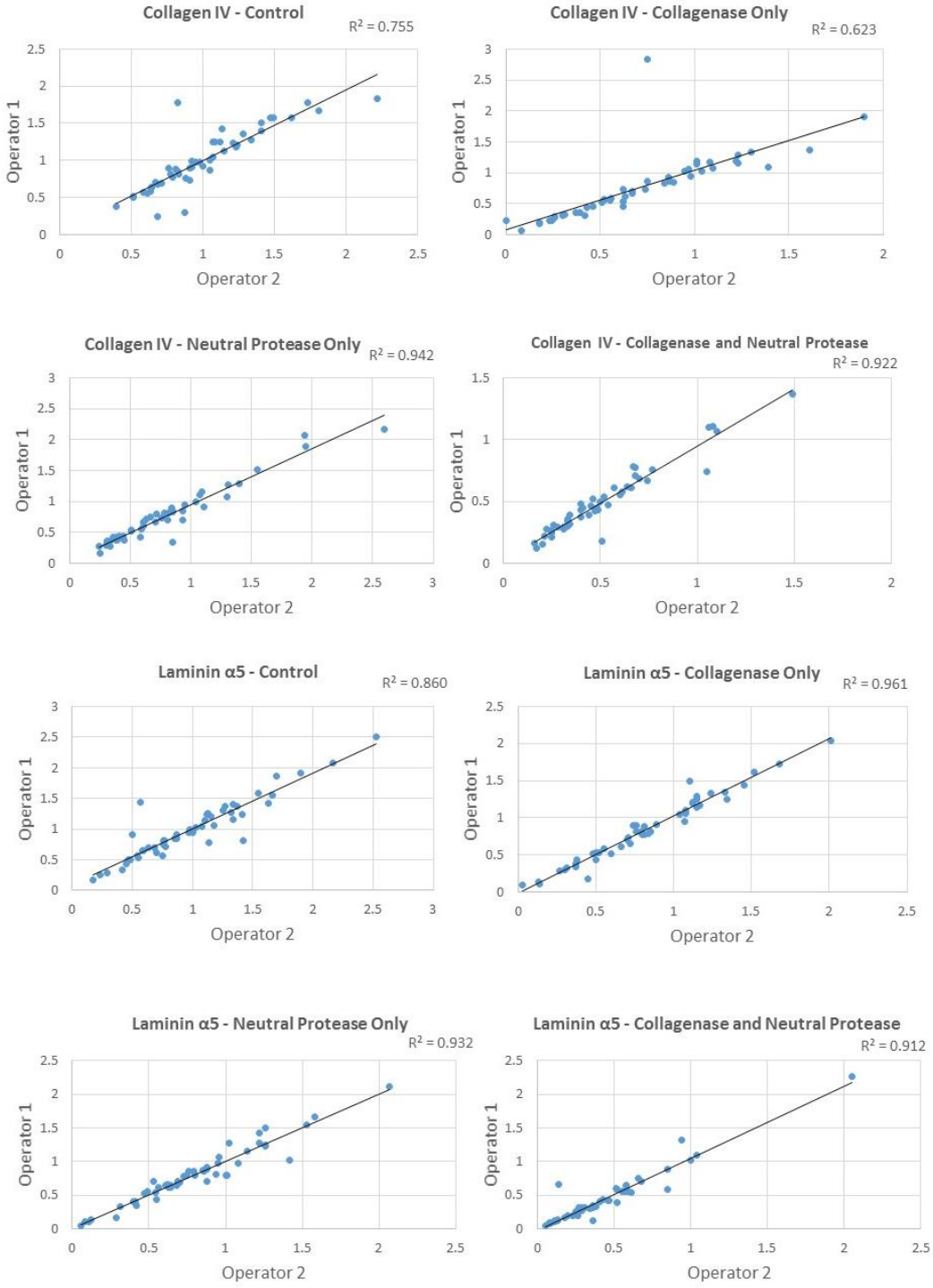


Figure 25: Correlation of Independent Operator Results
Following image analysis, the results from Operator 1 were correlated against that from Operator 2. Each data point represents the ratio of positive protein labelling to that of the insulin stained region, multiplied by the mean intensity of the protein labelling. All treatment data were normalised to the respective controls.
Data from n=5 donors are displayed.

4.4 Discussion

A simple, slide-based digestion assay was developed in order to characterise digestion of the pancreatic matrix by collagenase and NP enzymes used in clinical islet isolation. This enables multiple experiments on any one donor pancreas whilst controlling for inter-pancreatic donor variability. In these experiments, the assay was used to investigate the influence of donor age and the role of specific components of enzyme blends in the digestion of ECM proteins comprising the islet-exocrine interface.

As donor pancreases are presently the only source of islets for clinical transplantation, optimising human islet isolation remains a research priority. In particular, understanding human pancreas digestion at the molecular level is paramount. In order to do this, it is important to characterise the pancreatic matrix in detail, and to develop targeted enzyme blends that optimally digest the profile of matrix proteins found in different donor types. As demonstrated in Chapter 2, islet isolation success if dependent on a wide range of different pancreas donor variables, including BMI, past medical and social history. In particular, donor age was identified to have a significant impact on isolation outcome. High-throughput proteomics demonstrated that donor age significantly influences pancreatic matrix protein composition. In turn this may impact on the effectiveness of digestion by collagenase-based enzyme blends.

The *in vitro* digestion technique described in this Chapter was first proposed by members of the Oxford Islet Transplant Research Group in 2007 [317]. It allows characterisation of the effect of collagenase and supplementary protease enzymes on digestion of specific substrates. It enables

testing of multiple enzyme batches and components on any one human pancreas, in addition to the analysis of collagenase components individually and in combination, using pancreases from the full range of donors accepted for islet transplantation. The reproducibility of the technique was demonstrated, as analysis of digestion can be compared using multiple slides from the same donor pancreas sample, and between different researchers using the same slides.

The data presented within this Chapter demonstrates that there is variability in the digestion efficiencies of collagenase and NP on individual components of the islet-exocrine interface, which is further influenced by the age of the pancreatic donor. The normalisation of data to a control tissue section, which was treated with HBSS alone, eliminates the potential interference from endogenous proteolytic enzymes and ensures that any digestion seen is as result of the exogenously added enzymes only.

The method was tested by studying the digestion of two islet BM proteins – collagen IV and laminin α5. These proteins were selected on the basis of their prevalence, and important functions, within the islet BM. Collagen IV is the major structural component of BMs and forms the islet BM scaffold [174]. Laminin α5 is found in both layers of the human islet BM [167], making it a valuable tool for monitoring BM integrity following islet isolation [112].

The assay demonstrated that the digestion of peri-islet laminin α5 is dependent on NP. Furthermore, NP was significantly more effective in digesting this protein in donors ≥45 years of age, when compared to a younger donor group of ≤35 years of age. The digestion of collagen IV was also significantly influenced by the age of the donor. Although NP was ineffective at digesting collagen IV in younger donors, significant digestion occurred in the older donor group. Collagenase digestion of collagen IV was also significantly greater in the older donor group. The ability of the technique to detect such important differences substantiates its usefulness and practicality.

There have been previous attempts to develop simple assays to enable the batch-testing of enzymes. These methods involve incubating small samples of pancreatic tissue with different

enzymes at 37°C followed by sampling of the digested and undigested tissue, and the isolation of small numbers of islets [318]. An alternative approach involves division of the pancreas into sections, each of which is infused via the pancreatic duct with a different enzyme, followed by a small-scale islet isolation procedure using each section [99, 319]. Attempts have also been made to incubate rat tissue sections with enzymes, followed by the fixation and sectioning of the tissue. Digestion of specific ECM proteins can then be examined by immunostaining [320]. The main limitations to these methods are the requirement for greater volumes of enzyme and the necessity for larger pieces of pancreatic tissue, in addition to the additional time and labour required. There is also a limit to the number of enzymes and combinations that can be tested on any one pancreatic sample, as it is not possible to obtain large biopsies from pancreases received for clinical isolation. In contrast, the described slide-based assay is high-throughput and as it uses frozen sections of tissue there is no requirement for fresh samples. Small tissue samples ($0.5cm^3$) can be taken from pancreases received for clinical islet isolation, without compromising efficient distension of the pancreas with enzyme during the islet isolation procedure, and stored long term. This provides an important resource, enabling the testing of enzyme batches on the same pancreas, therefore eliminating errors caused by inter-pancreatic variability during testing. Furthermore, it also supports the ongoing investigation of pancreatic structure, as demonstrated by these data. More specifically, this is a valuable method for identifying donor related differences in the digestion of ECM proteins, and has the potential aid in the development of novel, tailored enzyme blends specific for different donor types.

One potential criticism of this slide-based assay is that it does not replicate delivery of digestion enzymes into the pancreas by ductal infusion. Indeed, it is well known that efficient delivery of collagenase enzyme blends to the islet-exocrine interface using intraductal administration is crucial for optimal large-scale pancreas digestion and release of well-cleaved, but intact islets [60]. However, the aim was not to use the technique to liberate islets, but to use it as a tool to determine the impact of specific enzyme components on the digestion of ECM proteins. It is also worth noting

that cryosectioning the pancreatic tissue may increase the exposure of the ECM surrounding the islet to the enzyme solution, creating a larger surface area for digestion than is present in the actual human islet isolation procedure. However, the simplicity and speed of the method allows for the rapid, simultaneous evaluation of enzyme batches using samples from a wide range of donor types. This would not be possible to do using full-scale islet isolation protocols. This method can therefore be used as an important evaluation tool for assessing multiple enzymes and enzyme combinations on any one pancreas.

4.5 Conclusion

This novel, slide-based digestion assay allows for the assessment of peri- and intra-islet ECM digestion by specific components of commercially available tissue dissociation enzymes, as well as determining the influence of donor factors on protein digestibility. As the assay utilises small amounts of both enzyme and human tissue, it is an ideal technique for batch testing enzymes, or for investigating variations in the digestion of the pancreatic ECM between donor types, such as the younger and older donor, which will facilitate the development of tailored enzyme blends for islet isolation.

CHAPTER 5

The Impact of Donor Age on Enzymatic Digestion of ECM proteins; a Study Using Slide-based Digestion and Conventional Immuno-labelling

5.1 Introduction

Previous studies have identified the importance of attenuating the ratio of collagenase and NP for enhancing islet isolation outcomes from younger donors [98, 99]. However, such attenuations are made without first understanding how age influences the action of these specific enzyme components when digesting the pancreatic ECM.

The previous Chapter focused on the development and validation of a simple slide-based digestion assay, suitable for investigating the effects of donor specific inter-pancreatic variability on the enzymatic digestion of ECM components. The assay successfully demonstrated how the key basement membrane (BM) proteins collagen IV and laminin α5 are digested by specific enzyme components. Enzyme mediated protein loss was also shown to be affected by donor age.

Using high-throughput proteomics Chapter 3 demonstrated that the pancreatic ECM is a highly complex structure, containing 81 matrix and matrix-affiliated proteins. 19 of these matrix proteins were more highly expressed in younger donors. Therefore, in addition to collagen IV and laminin α5, donor age may impact the enzymatic digestibility of other ECM proteins in the human pancreas.

The aim of this next study was to use this developed assay to investigate the substrate specificity of the enzyme components comprising clinical isolation blends, and determine how donor age influences the digestion of these key ECM proteins. Proteins selected for investigation in this current study include the interstitial matrix (IM) proteins: collagens I, V, VI and the BM proteins laminin, nidogen-1 and perlecan. Proteins were selected on the basis of their identification in Chapter 3. Investigation was not limited to those proteins that were found to be significantly differentially expressed between the two groups. This was to ensure that potential differences in protein digestion, which are irrespective of protein quantity, are not overlooked. Where possible, the action of specific enzyme components on individual matrix proteins was validated by western blotting, using purified matrix proteins treated with enzymes.

5.2 Methods

5.2.1 Sampling Technique

With appropriate consent and ethical approval, human pancreases from older (≥45 years old; n=9) and younger (≤35 years old; n=8) multi-organ donors were procured for islet isolation (Table 15). Organs were transported in UW solution (Bridge to Life, London, UK) on ice to the DRWF Human Islet Isolation Facility, at the Churchill Hospital in Oxford. 0.5cm^3 tissue samples were taken from the head of the pancreas and snap frozen in liquid nitrogen, and stored at -80°C. Frozen tissue sections (10µm thickness) were prepared using a Cryostat (Leica, Milton Keynes, UK) and collected onto Superfrost Plus glass slides (Thermo-Fisher Scientific, Loughborough, UK), before storage at -20ºC until use.

5.2.2 Quantitative Analysis of ECM Digestion Using Slide-based Digestion and Immunostaining

The slide-based digestion assay protocol, developed and validated in Chapter 4, was used to assess age related effects on the enzyme component based digestion of further key ECM proteins. Digestion and the immunofluorescent detection of proteins were performed (as per the method described in Chapter 4 - Section 4.2.2 - 4.2.3). Collagens I, V and VI, pan-laminin, nidogen-1 and perlecan were investigated (n=7 donors for each age group). Briefly, tissue sections were incubated for 5 minutes at 37ºC with HBSS (control), collagenase NB1 alone, neutral protease NB (NP) alone, or a combination of the two enzymes, at clinically relevant concentrations (collagenase 7.2 PZU/ml, NP 0.14 DMCU/ml; both Serva, Heidelberg, Germany). Following digestion, and treatment with blocking serum, slides were incubated for 1.5 hours at room temperature (r.t) with the optimal dilution of the primary antibody, followed by a 30 minute incubation with the secondary antibody at r.t. The experimental parameters for the detection of each protein can be found in Appendix Table D1. Negative control sections were incubated with normal host IgG (Santa Cruz Biotechnology, TX, USA) in place of the primary antibodies at appropriate concentrations, to test for non-specific binding of primary antibodies. Primary antibodies were also omitted to test for

non-specific binding of secondary antibodies. Images were acquired in 8-bit format and analysed using the semi-automated macro described in Chapter 4 – Section 4.2.3. A minimum of ten islets were imaged per donor, per treatment.

5.2.3 Statistical Analysis for Slide-based Digestion Assay Experiments

Digestion data were analysed by mixed linear modelling, as per Chapter 4 (Section 4.2.5). For each protein box-cox transformations were performed and the response variable transformed accordingly. Quantile-quantile (Q-Q) normality plots and Shapiro-Wilk testing of the residuals were used to determine the overall fit of the model for each of the proteins. The mean ± SEM are displayed.

5.2.4 Purified Protein Digestion

5µg of protein were used for each incubation. Although protein concentration is provided by the manufacturer, the concentration of each protein was confirmed upon receipt via BCA assay, as per the manufacturer's instructions (Pierce BCA protein assay kit, Thermo-Fisher Scientific, Loughborough, UK). All samples were assayed in quadruplicate, and the final protein concentration was considered as the average BCA measurement, as opposed to that provided by the manufacturer (Appendix Table D2). The proteins were incubated at a volume to volume ratio of 1:2 (enzyme:protein) with HBSS (control), collagenase NB1 alone, NP alone or a combination of the two enzymes, at clinically relevant concentrations (collagenase 7.2 PZU/ml, NP 0.14 DMCU/ml). For the control samples the purified proteins were replaced by the appropriate diluent solution (Appendix Table D2). Incubation took place in 0.5ml Eppendorf tubes (Thermo-Fisher Scientific) for 30 minutes, 2 hours, or overnight at 37˚C. At the end of the reaction time, the tubes were removed and chilled on wet ice, followed by the addition of a protease cocktail inhibitor (7X concentrate, cOmplete™ Mini Protease Inhibitor Cocktail, Roche). The digests were centrifuged at 2,000g for 2 minutes, and then frozen at -20˚C until analysis. Collagens I, IV and VI, pan-laminin and nidogen-1

were investigated. All experiments were completed in triplicate. The concentration of each protein and the supplier information can be found in Appendix Table D2.

5.2.5 Sample Loading and Protein Electrophoresis

The samples were thawed to r.t, followed by the addition of LDS buffer (4X) and sample reducing agent (10X) (both NuPAGE, Thermo-Fisher Scientific). The volume of each digest was corrected to 20µl using deionised water. Each sample was heated for 10 minutes at 70˚C. The entire sample volume was then loaded onto a 3-8% Tris-Acetate mini gel (NuPAGE, Thermo-Fisher Scientific). 10µl of HiMark pre-stained protein standard (Thermo-Fisher Scientific) was loaded in at least 1 lane per gel. The tank was prepared by the addition of 1X Tris acetate running buffer (Thermo-Fisher Scientific) and the introduction of 500µl of antioxidant (Thermo-Fisher Scientific) to the middle compartment. Electrophoresis was performed at 150V for 60 minutes (instrument model: CS-300V, Thermo-Fisher Scientific). The gel was removed from the plastic cassette and submerged in 20% ethanol (Thermo-Fisher Scientific) for 10 minutes.

5.2.6 Gel Transfer to Nitrocellulose Membrane

Proteins were transferred from the gel to a nitrocellulose membrane using the iBlot dry transfer system (Invitrogen, Thermo-Fisher Scientific), according to the manufacturer's instructions. Briefly, the gel was placed onto the nitrocellulose membrane, located on top of the anode. Filter paper, pre-soaked in deionised water, was placed on top of the gel and bubbles removed by gentle rolling, followed by the addition of the cathode. The completed stack was transferred to the iBlot transfer system, where the transfer was completed on program 3 (20V for 7 minutes).

5.2.7 Membrane Blocking and Immunostaining

Proteins were detected using the WesternBreeze system with chromogenic detection (Thermo-Fisher Scientific), along with the appropriate primary antibodies, at optimised dilutions (Appendix Table D2). All membrane washes and incubations were completed at r.t on a rotary platform. Post-transfer, the membranes were washed twice with deionised water and blocked for 30 minutes with the blocking buffer contained within the WesternBreeze kit, as per the manufacturer's instructions. The membrane was washed twice with deionised water, followed by incubation with the primary antibodies, diluted in blocking solution, for 1 hour. The membrane was washed 4 times, for 5 minutes each, with the WesternBreeze washing solution, followed by the addition of the WesternBreeze secondary antibody solution specific to the primary antibody (Appendix Table D2). After 30 minutes the secondary antibody was removed, and the washing steps repeated. Finally, the membrane was exposed to the chromogen solution, with the exposure time dependent on the protein (Appendix Table D2). The reaction was stopped by the addition of deionised water, once all bands were visible. The membrane was washed twice with deionised water, before being left to air dry. In addition to emitting the purified protein from the digest mixture, further control staining was completed for each protein by emitting the primary antibody and checking for any non-specific binding of the secondary antibody.

5.2.8 Densitometry

To determine the extent of protein loss with enzyme treatment densitometry was performed. The method was adapted from the protocol "Analyzing gels and western blots with Image J", written by Professor Luke Miller (San Jose State University; November 2010):

http://lukemiller.org/index.php/2010/11/analyzing-gels-and-western-blots-with-image-j/.

Briefly, the membranes were scanned (CanoScan, Cannon, Middlesex, UK) and the TIFF files imported to image J. The background was removed, followed by the manual alignment of bands by image rotation. Finally, the images were converted to 8-bit. The subsequent bands for each

condition were selected and the 'analyse' tool within image J used to determine the density of the band. The total density of all bands was calculated, and the density of each band determined as a proportion of this total. The relative density to the control (set to 100%) was calculated for all bands.

5.3 Results

5.3.1 Donor Demographics

Studies were performed on tissue biopsies obtained from both older (≥45 years) and younger (≤35 years) donor pancreases, accepted for clinical islet isolation (Table 15). The mean donor age was 29±1 years and 54±2 years, in the younger and older groups respectively. BMI, cold ischemia time (CIT), gender ratio and donor type (DBD or DCD; donation after brain or cardiac death, respectively) were statistically matched between the two groups.

	Younger Donors ≤ 35 years (n=8)	**Older Donors ≥ 45 years (n=9)**	***p* value**
Age, y (Mean ± SEM)	29±1	54±2	<0.001
Age, y (Median (Range))	29.5 (25-32)	56 (46-60)	<0.001
Gender (M:F)	7:1	7:2	0.60
BMI (Mean ± SEM)	26±1	28±1	0.37
CIT, h (Mean ± SEM)	5.45±0.5	6.45±0.5	0.24
Donor Type (DBD:DCD)	7:1	9:0	0.27

Table 15: Donor demographics for Chapter 5
CIT, cold ischaemia time; DBD, donation after brain death; DCD, donation after cardiac death. Statistical analysis was performed by independent samples t-test.

5.3.2 Mixed Linear Modelling for Slide-based Digestion Assay Experiments

Pancreatic tissue digestion data for each protein were analysed by mixed linear modelling, post-transformation of the response variable to normality. Transformation was performed in response to the box-cox transformation results, based on the value of lambda. Diagnostics were performed

to validate model fit, via Shapiro-Wilk test and the production of Q-Q plots of the residuals. The fit of each model was sufficiently validated for all proteins (data not shown).

5.3.3 Digestion of ECM Proteins in Native Pancreatic Tissue and Purified Form

The slide-based digestion assay, developed and validated in Chapter 4, was used to investigate the substrate specificity of enzymes used in the clinical isolation of islets, and to determine the impact of donor age on protein digestion. The BM proteins: perlecan, nidogen-1, and pan-laminin were investigated, as well as the IM proteins: Collagens I, V and VI (for all proteins n=7 donors, in each age group). The component based digestion of nidogen-1, pan-laminin and collagens I and VI were validated by western blotting, using purified proteins treated with the same exogenous enzymes. In addition, the digestion of purified collagen IV was also investigated. The tissue digestion results for this BM protein were previously reported in Chapter 4, where they served to validate the developed slide-based digestion assay method. Table 16 provides a summary of protein digestion within the tissue. A summary of purified protein digestion is present in the thesis appendix (Table D3), for the slide-based digestion assay, and purified protein experiments, respectively. No non-specific binding of either primary or secondary antibodies was detected by the control staining in both the slide-based tissue and purified protein digest experiments (data not shown).

	Younger Donors			Older Donors		
	Collagenase Only	NP Only	Collagenase & NP	Collagenase Only	NP Only	Collagenase & NP
Laminin	7±5% (NS)	13±5% (*)	33±3% (***)	7±6% (NS)	9±6% (*)	28±5% (***)
Laminin-α5	10±6% (NS)	24±5% (**)	44±5% (***)	5±6% (NS)	40±3% (***)	43±4% (***)
Collagen IV	19±5% (***)	4±5% (NS)	57±4% (***)	32±5% (***)	36±4% (***)	58±3% (***)
Nidogen-1	5±6% (NS)	64±5% (***)	30±8% (***)	21±10% (NS)	10±9% (NS)	16±7% (*)
Perlecan	88±4% (***)	97±1% (***)	98±0% (***)	78±5% (***)	92±2% (***)	99±0% (***)
Collagen I	9±6% (NS)	0±6% (NS)	11±7% (NS)	16±5% (*)	6±5% (NS)	14±5% (NS)
Collagen V	4±5% (NS)	22±5% (***)	13±4% (*)	7±4% (NS)	5±5% (NS)	12±4% (NS)
Collagen VI	23±7% (***)	17±6% (**)	30±6% (***)	1±5% (NS)	9±4% (NS)	15±4% (**)

No change from control	
0%	
Loss from control	
1-20%	
21-40%	
41-60%	
61-80%	
81-100%	
Increase from control	
1-20%	
21-40%	
41-60%	
61-80%	
81-100%	

Table 16: Summary of enzyme mediated protein digestion, within the pancreatic tissue, using slide-based digestion

Displayed is the percentage change of protein (± SEM) with each enzyme treatment, compared to the respective controls, for the two age groups. Collagen IV and laminin-α5 are data presented in Chapter 4.

NP; Neutral Protease

Statistical analysis was performed by mixed linear modelling

NS; Not significant

*; $p<0.05$

**; $p<0.01$

***; $p<0.001$

5.3.3.1 Interstitial Proteins

Within the pancreatic tissue, the IM protein collagen I was largely resistant to digestion in both donor age groups (Figure 26 a-b). Although treatment with collagenase alone resulted in a significant reduction of collagen I in the older donor group (16±5%, $p<0.05$, compared to control), protein loss in the younger donor group did not reach significance (9±6% reduction compared to control, NS). Treatment with NP alone did not cause significant loss of collagen I in either donor group (0±6% and 6±5%, in the younger and older donor group respectively, NS compared to controls). Combining the two enzymes improved digestion of collagen I as compared to NP treatment alone, resulting in reductions of 11±7% and 14±5%, in the younger and older groups respectively, although this digestion did not reach significance in either group (p=0.058 and p=0.056, for younger and older respectively, compared to controls). For the digestion of purified collagen I the band at 120KDa was investigated (Figure 26 c-d). Although digestion of purified collagen I was more pronounced than that observed within the tissue, the experiments supported that digestion of this protein is mainly facilitated by collagenase. When purified collagen I was treated with collagenase alone there was a reduction of 44±20%, 58±5% and 59±6% as compared to control, for 30 minutes (30 min), 2 hour (2Hr), and overnight (o/n) treatments, respectively. NP treatment was less effective and reduced collagen I by 17±6%, 25±13%, 10±19% (30 min, 2Hr, o/n respectively, as compared to control). When the treatments were combined the digestion pattern was similar to that observed with collagenase treatment alone (53±4% 53±8% and 59±7% reduction in collagen I for 30 min, 2Hr and o/n respectively, compared to control).

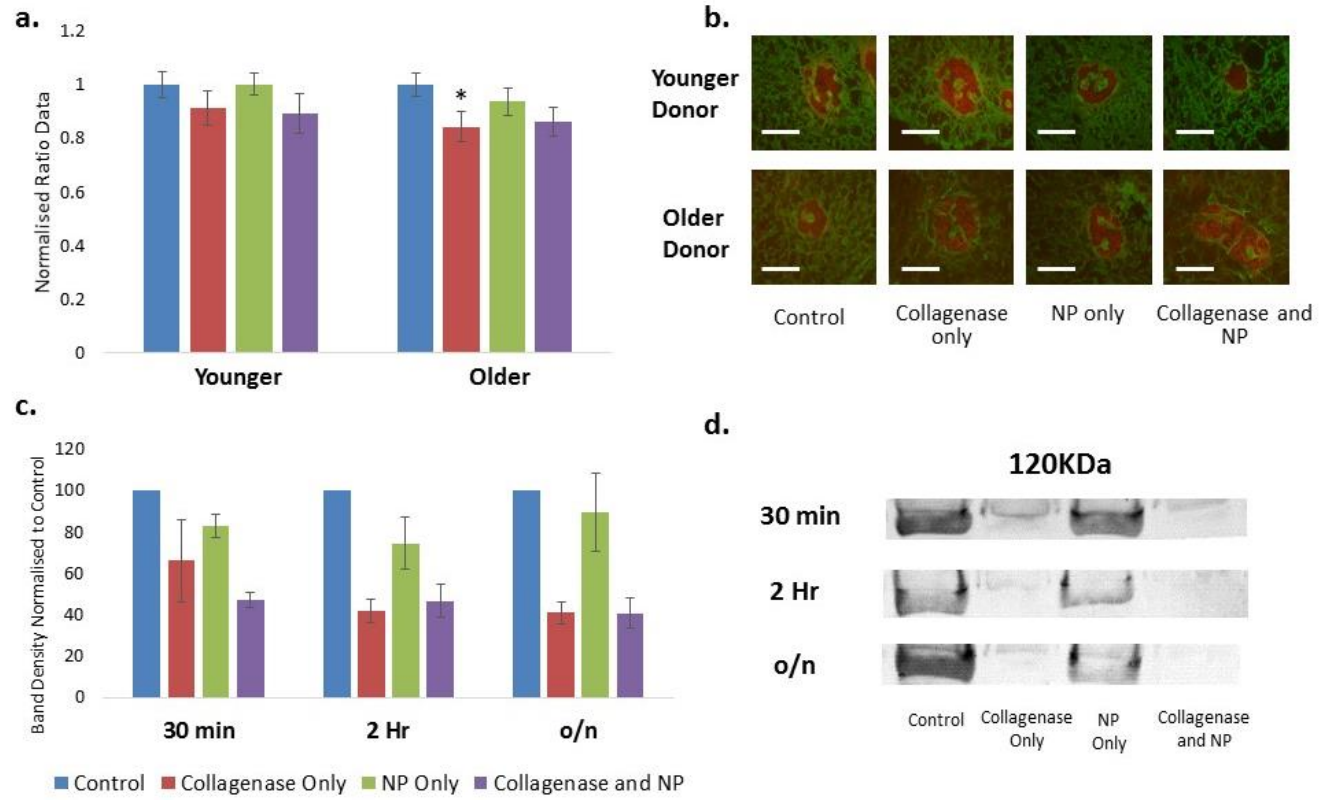


Figure 26: Enzyme mediated digestion of collagen I

a. The area and intensity of collagen I staining in the peri-islet region was normalised to the control (HBSS treated), post-treatment with collagenase, neutral protease or a combination of both enzymes for 5 minutes. The efficiency of digestion was compared between two donor age groups; b. Representative images of the pancreas sections following treatment with each enzyme component. Collagen I (*green*) is seen around and within the islet (*red*, insulin labelling of β-cells); c. Densitometry of collagen I band at 120KDa, after treatment with the same enzyme components over a time course;

d. Representative image of this band, from the three experiments performed for each time point. Experiments demonstrate that collagen I digestion is mainly facilitated by collagenase, but the extent of digestion is greater for the purified protein, than in the tissue.

Graphs show mean ± SEM.

NP; Neutral protease

O/n; overnight

Data were analysed by mixed linear modelling

* p <0.05 as compared to control

Scale bars 100µm

Collagen V was resistant to digestion in the older donor group (loss of 7±4%, 5±5% and 12±4% for collagenase, NP, and the two combined respectively; all NS from control, Figure 27 a-b). Although collagenase was also unsuccessful in digesting collagen V in the younger donor group (increase in 4±5% compared to control; NS), significant digestion was achieved post-NP treatment (22±5% reduction compared to control, p<0.001). Despite the enhanced efficiency of NP to digest collagen

V in the younger donor group, this age related difference did not reach significant (p=0.08 younger vs older). Combining the treatments resulted in a reduction of 13±4% in the younger donor group (p<0.05, compared to control). However, this loss was not significantly different from the older group, following the combined treatment. Due to the lack of commercial availability of a purified collagen V protein, it was not possible to perform the validation western blots on this protein.

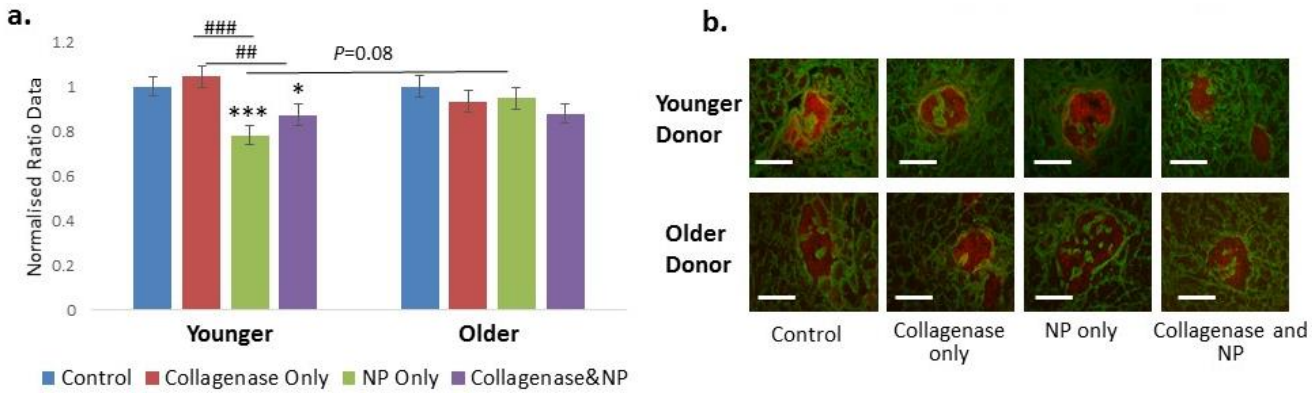


Figure 27: Enzyme mediated digestion of collagen V
a. The area and intensity of collagen V staining in the peri-islet region was normalised to the control (HBSS treated), post treatment with collagenase, neutral protease or a combination of both enzymes for 5 minutes. The efficiency of digestion was compared between two donor age groups; b. Representative images of the pancreas sections following treatment with each enzyme component. Collagen V (*green*) is seen around and within the islet (*red*, insulin labelling of β-cells). These data demonstrate that collagen V is resistant to digestion in the older donor group, with all three enzyme treatments. NP was successful in facilitating collagen V digestion in the younger donor group, and to a lesser extent, as was the combination of collagenase and NP.
Graphs show mean ± SEM
NP; Neutral protease
O/n; overnight
Significant difference from control is indicated by *
Significant difference between two groups is indicated by #
Data were analysed by mixed linear modelling
* p<0.05
p<0.01
***/### p<0.001
Scale bars 100µm

Within the pancreatic tissue, the digestion of collagen VI was significantly affected by donor age (Figure 28 a-b). In the younger donor group there was a significant increase in collagen VI signal, which coincided with all three enzyme treatments (increase of 23±7%, 17±6%, 30±6% for

collagenase, NP and the two combined respectively; $p<0.01$ for NP and $p<0.001$ for both collagenase and the two enzymes combined, compared to control.) In the older donor group collagenase treatment produced a 1±5% increase in collagen VI signal (NS from control), but treatment with NP and collagenase + NP resulted in a reduction (loss of 9±4% and 15±4% respectively, compared to control). Although NP did not significantly digest collagen VI alone, treatment with the enzyme combination resulted in a significant loss ($p<0.01$, compared to control). Therefore, the ability for a combination of collagenase and NP to digest collagen VI was affected by donor age ($p<0.001$), and was significantly more effective in the older donor group.

Interestingly, in purified protein form collagen VI (band at 100KDa, Figure 28 c-d) was successfully digested by collagenase (loss of 63±7%, 67±5% and 74±3%, compared to control, for 30 min, 2Hr and o/n respectively). Loss of collagen VI following NP treatment was minimal (loss of 1±11%, 10±12% and 13±4%, compared to control, for 30 min, 2Hr and o/n respectively). Treating collagen VI with a combination of collagenase and NP produced similar protein loss to that observed with collagenase treatment alone (loss of 71±2%, 69±6% and 72±2%, compared to control, for 30 min, 2Hr and o/n respectively).

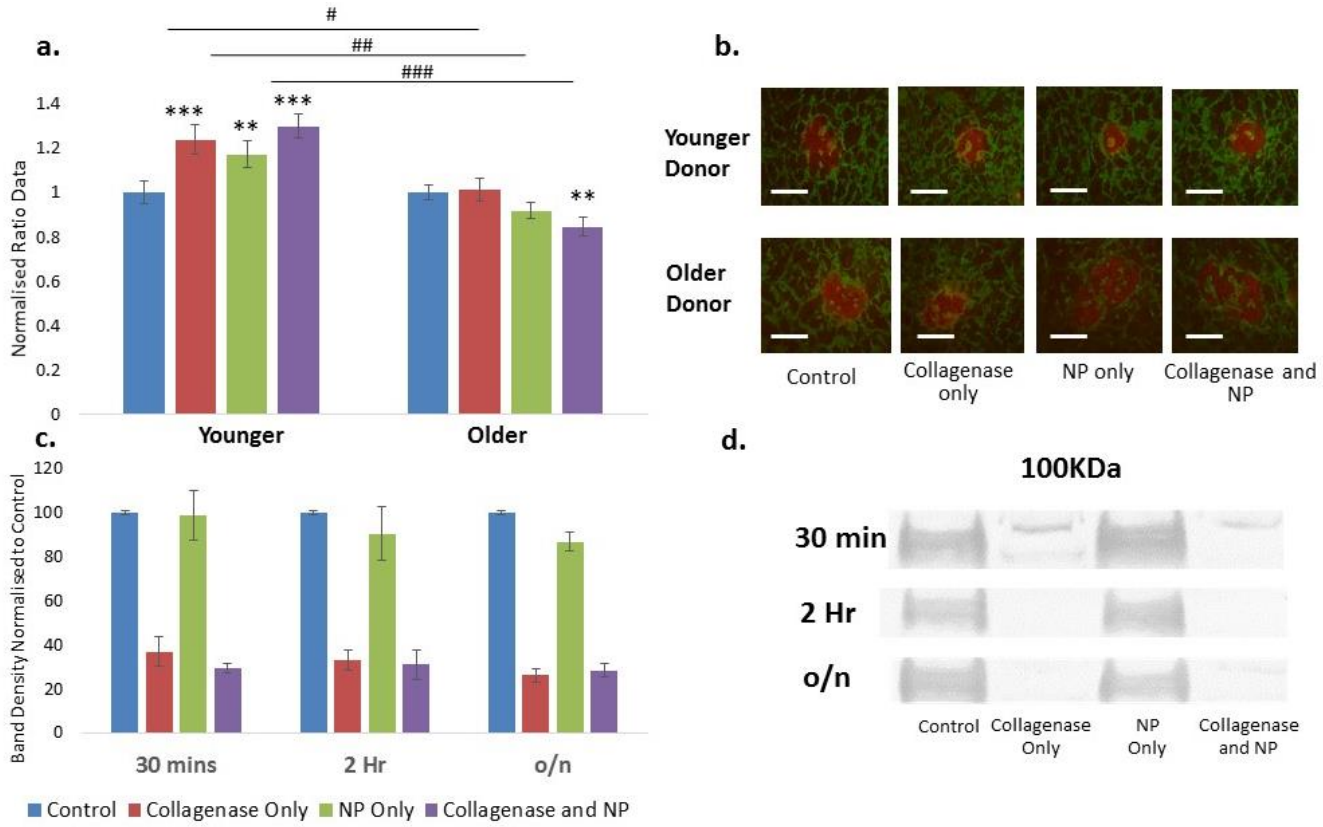


Figure 28: Enzyme mediated digestion of collagen VI

a. The area and intensity of collagen VI staining in the peri-islet region was normalised to the control (HBSS treated), post treatment with collagenase, neutral protease or a combination of both enzymes for 5 minutes. The efficiency of digestion was compared between two donor age groups;
b. Representative images of the pancreas sections following treatment with each enzyme component. Collagen VI (*green*) is seen around and within the islet (*red*, insulin labelling of β-cells);
c. Densitometry of collagen VI band at 100KDa, after treatment with the same enzyme components over a time course;
d. Representative image of this band, from the three experiments performed for each time point. Experiments demonstrate that collagen VI digestion is significantly affected by age, with significant digestion in the older donor group. Although there is a significant increase in collagen VI signal in the younger donor group, it is assumed that the signal increases due to loss of other proteins within the matrix. The purified protein digests suggested that collagen VI was digested by collagenase; this was not supported by the tissue digestion data.
Graphs show mean ± SEM
NP; Neutral protease
O/n; overnight
Significant difference from control is indicated by *
Significant difference between two groups is indicated by #
Data were analysed by mixed linear modelling
# $p<0.05$
**/## $p<0.01$
***/### $p<0.001$
Scale bars 100µm

5.3.3.2 Basement Membrane Proteins

Within pancreatic tissue, laminin digestion was investigated using an antibody unrestricted by laminin subtype specificity ('pan-laminin'; Figure 29 a-b). As with the specific laminin subtype α5 (Chapter 4), laminin was not significantly digested by collagenase alone in either donor group (7±5% and 7±6%, for younger and older respectively, NS compared to control). However, independent treatment with NP reduced laminin significantly, resulting in protein loss of 13±5% (p<0.05) and 9±6% (p=0.05), in the younger and older donor groups respectively. Combining the enzymes enhanced digestion leading to a 33±3% and 28±5% reduction in laminin for the younger and older donors respectively (both p<0.001). Although laminin digestion using the enzyme combination was greater in the younger donors, this age related difference did not reach significance (p=0.14, for younger vs older). For investigating the digestion of purified laminin the band at 170KDa was selected (Figure 29 c-d). Enzyme component based treatment supported greater digestion with NP (loss of 26±22%, 63±24% and 43±20% for 30 min, 2Hr and o/n respectively) than with collagenase (loss of 20±6%, 36±2% and 9±5% for 30 min, 2Hr and o/n respectively). Combining the enzymes led to a reduction of 35±13%, 42±14% and 30±11%, for 30 min, 2Hr and o/n enzyme treatment.

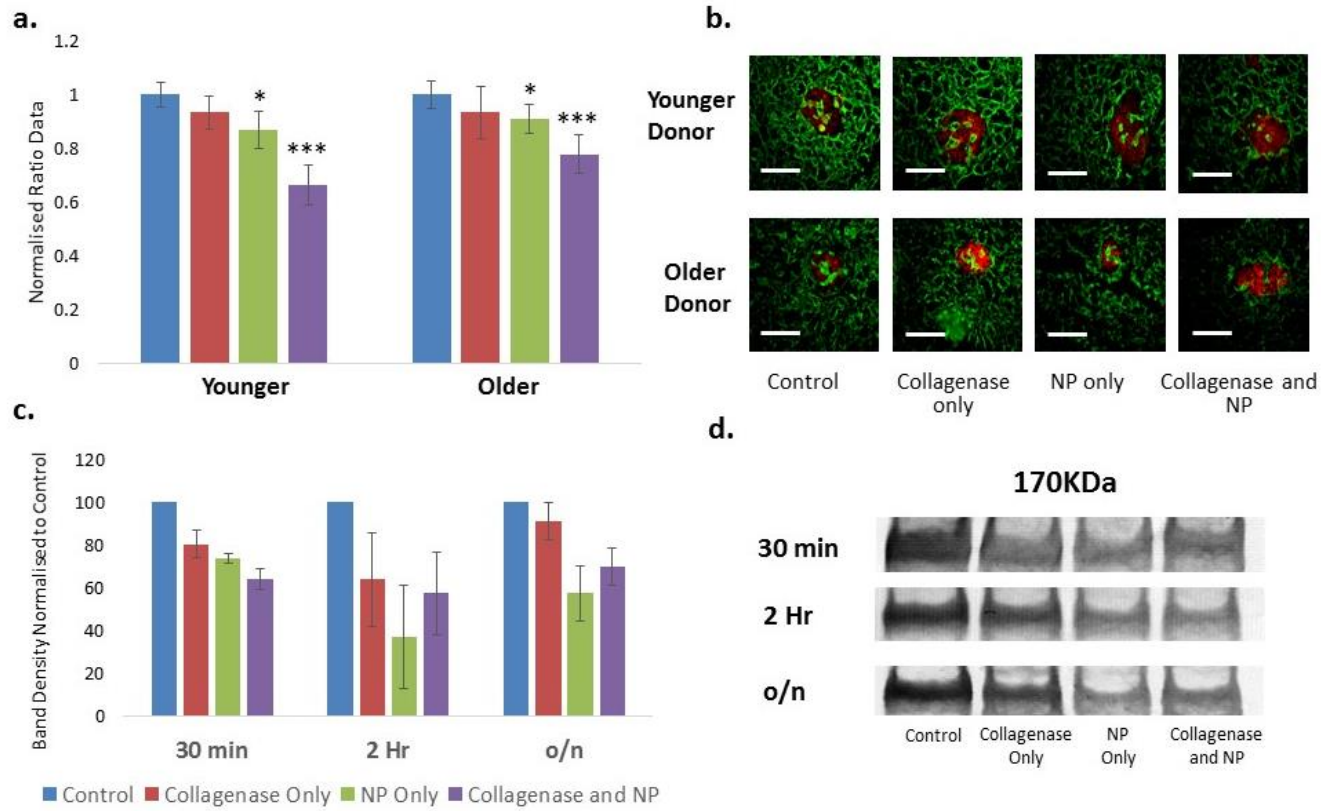


Figure 29: Enzyme mediated digestion of pan-laminin
For these experiments, a laminin antibody not restricted by subtype specificity was used ('pan-laminin'; from here within referred to as laminin)
a. The area and intensity of laminin staining in the peri-islet region was normalised to the control (HBSS treatment), post treatment with HBSS (control), collagenase, neutral protease or a combination of both enzymes for 5 minutes. The efficiency of digestion was compared between two donor age groups;
b. Representative images of the pancreas sections following treatment with each enzyme component. Laminin (*green*) is seen around and within the islet (*red*, insulin labelling of β-cells);
c. Densitometry of the laminin band at 170KDa, after treatment with the same enzyme components over a time course;
d. Representative image of this band, from the three experiments performed for each time point.
Experiments demonstrate that laminin digestion is mainly facilitated by NP, and is not influenced by donor age.
Graphs show mean ± SEM
NP; Neutral protease
O/n; overnight
Data were analysed by mixed linear modelling
* p <0.05 compared to control
*** p <0.001 compared to control
Scale bars 100µm

As with laminin, independent collagenase treatment was unsuccessful in significantly digesting nidogen-1 within the donor tissue, in both age groups (loss of 5±6% and increase of 21±10% in the younger and older groups respectively; Figure 30 a-b). NP treatment significantly digested nidogen-

1 in younger donors (64±5% $p<0.001$ compared to control) but did not cause significant digestion in the older donor group (loss of 10±9%; NS). NP was therefore significantly more effective at digesting nidogen-1 in the younger donor group ($p<0.001$). Combining the enzymes ameliorated the significant age dependent effects on protein digestion and led to a loss of 30±8% and 16±7% in the younger and older groups respectively ($p<0.001$ and $p<0.05$, for younger and older respectively, compared to control). Therefore, in the younger donor group, treatment with NP alone was superior at facilitating nidogen-1 digestion than the enzyme combination ($p<0.001$). Treatment of purified nidogen-1 with the same enzyme components effectively reduced the principle nidogen-1 band at 130KDa (Figure 30 c, d). However, a lower molecular weight band appeared at 80KDa, which was associated with enzyme treatment (Figure 30 e, f). The intensity of this smaller band generally decreased in a time dependent manner, but displayed heightened association with collagenase treatment (increase of 409±95%, 444±104% and 245±5%, for 30 min, 2 Hr and o/n respectively, compared to control, for collagenase treatment alone). The band was less prominent following treatment with NP (increase of 38±11% and decreases of 13±17% and 57±1%, for 30 min, 2 Hr and o/n respectively, compared to control). Combining the two enzymes increased the density of this band to 328±83% and 133±85% for 30 min and 2 Hr, respectively, as compared to control. However, following o/n digestion the density of this band decreased by 57±1% (as compared to control).

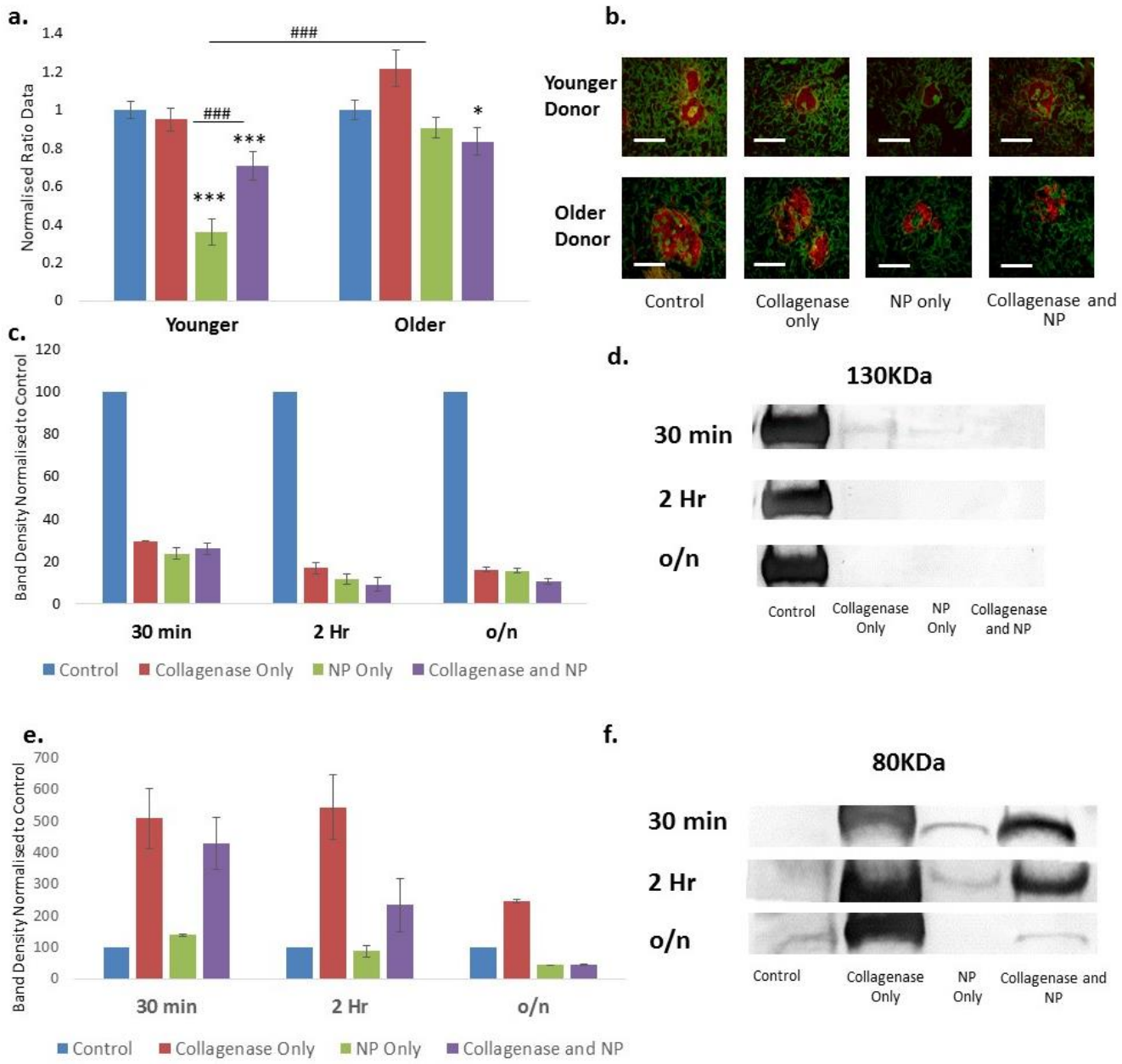


Figure 30: Enzyme mediated digestion of nidogen-1

a. The area and intensity of nidogen-1 staining in the peri-islet region was normalised to the control, post digestion with HBSS (control), collagenase, neutral protease or a combination of both enzymes for 5 minutes and the efficiency of digestion was compared between two donor age groups; b. Representative images of the pancreas sections following treatment with each enzyme component. Nidogen-1 (*green*) is seen around and within the islet (*red*, insulin labelling of β-cells); c. Densitometry of the nidogen-1 band at 130KDa, and e) at 80kDa, after treatment with the same enzyme components over a time course;

d. Representative image of the band at 130KDa and f) 80KDa, from the three experiments performed for each time point.

The data suggests that NP is primarily responsible for the digestion of nidogen-1, and is significantly more effective at digesting this protein in the younger donor group.

Graphs show mean ± SEM

NP; Neutral protease

O/n; overnight

Significant difference from control is indicated by *
Significant difference between two groups is indicated by #
Data were analysed by mixed linear modelling
* $p<0.05$
***/### $p<0.001$
Scale bars 100µm

Perlecan within the donor tissue was substantially digested with all three enzyme treatments in both age groups (Figure 31 a-b). Treatment with collagenase alone led to an 88±4% and 78±5% reduction in perlecan in the younger and older groups respectively (both $p<0.001$, compared to control). Treatment with NP resulted in a 97±1% and 92±2% reduction in perlecan in the younger and older groups respectively (both $p<0.001$, compared to control). Therefore, in both age groups, NP was significantly more effective than collagenase for digesting perlecan (both $p<0.001$; collagenase vs NP). Combining the enzymes further enhanced perlecan loss (98±0% and 99±0%, for younger and older donors, respectively, both $p<0.001$ compared to control) but was not significantly more efficient that utilising NP treatment alone. With all three enzyme treatments, perlecan loss was not influenced by donor age. As human perlecan was not available as a purified protein, it was not possible to perform the validation Western blots.

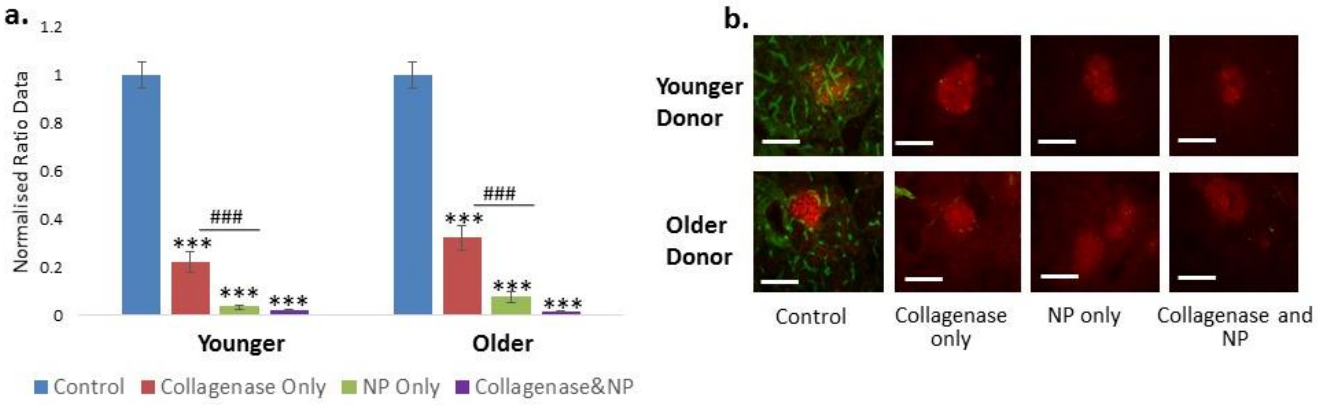


Figure 31: Enzyme mediated digestion of perlecan
a. The area and intensity of perlecan staining in the peri-islet region was normalised to the control, post digestion with HBSS (control), collagenase, neutral protease or a combination of both enzymes for 5 minutes and the efficiency of digestion was compared between two donor age groups; b. Representative images of the pancreas sections following treatment with each enzyme

component. Perlecan (*green*) is seen around and within the islet (*red*, insulin labelling of β-cells). Extensive loss of perlecan was observed with all three treatments; digestion was significantly greater with NP than collagenase. Digestion of perlecan was not influenced by the age of the donor.
Graphs show mean ± SEM
NP; Neutral protease
O/n; overnight
Data were analysed by mixed linear modelling
*** p <0.001 compared to control
p <0.001 between indicated conditions
Scale bars 100µm

The enzyme mediated digestion of collagen IV, investigated within the pancreatic tissue in Chapter 4, was validated using purified collagen IV. The band present at 160KDa was investigated (Figure 32 a-b). Unlike the other BM proteins, loss of collagen IV was greater with collagenase treatment than NP treatment, with the combination of enzyme producing similar digestion to collagenase alone. For all three enzyme treatments, protein loss occurred in a time dependent manner (the percentage loss of protein from 30 min, 2 Hr, o/n treatment respectively, with: collagenase alone 50±13%, 62±4%, 72±4%; NP alone 17±14%, 41±8%, 49±5%; collagenase and NP 40±17%, 77±3%, 81±0%).

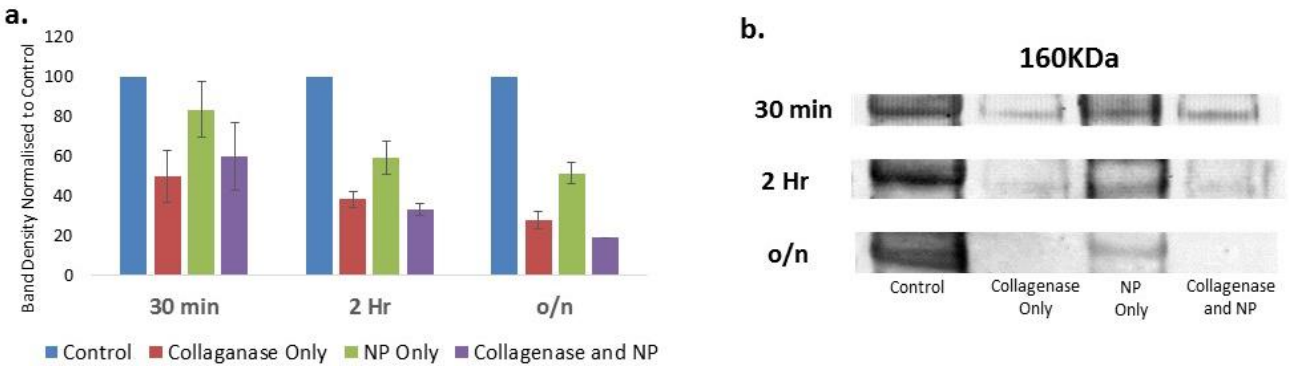


Figure 32: Enzyme mediated digestion of purified collagen IV
a. Densitometry of the collagen IV band at 160KDa, after treatment with HBSS (control), collagenase, NP, or the two enzymes combined, over a time course;
b. Representative image of this band, from the three experiments performed for each time point.
The data demonstrates that the digestion of purified collagen IV is mainly facilitated by collagenase.
Graphs show mean ± SEM
NP; Neutral protease
O/n; overnight

5.4 Discussion

In this current study, the enzymatic digestion of specific pancreatic ECM was shown to be affected by both individual enzyme components and donor age. NP primarily facilitated the digestion of key islet BM proteins. When NP was combined with collagenase, mimicking the enzyme combination utilised in clinical islet isolation, the IM protein collagen VI was significantly more resistant to digestion in younger donors, as compared with their older counterparts.

The current variability of the collagenase-digestion phase of human islet isolation hinders the ability to routinely isolate transplantable islet yields from the full range of donor pancreases. To improve pancreas digestion, during the 1990s researchers in Groningen began to characterise the substrate specificity of certain enzyme subtypes [149, 321]. Although restricted to the rat pancreas, these experiments first introduced the concept of investigating the enzyme mediated digestion of the pancreas at the level of the ECM. In a more recent study, Miyazaki and colleagues aimed to create targeted enzyme blends for different breeds of rat, by examining the quantity of matrix proteins in each strain. The substrate targets for specific collagenase sub-types were also investigated [322]. Our group are the first to investigate pancreas digestion in the human pancreas at the molecular level. The concept of tailoring enzymes to specific matrix substrates is a particularly attractive option for pancreases that are obtained from younger donors, where high numbers of exocrine 'trapped' islets are produced post-digestion [101, 249]. Current strategies to improve pancreas digestion in this donor type are limited to the empirical attenuation of enzyme blends [98, 247], as opposed to characterising important variabilities at the matrix level. Furthermore, substrate targeted enzymes would provide an opportunity to selectively target the IM for digestion, without compromising the integrity of the essential double layered islet BM, which is important for islet function and survival [183]. This Chapter aimed to determine the enzymatic digestion of specific BM and IM proteins, both located within the pancreatic tissue of different aged donors, and in a purified form.

Post-isolation loss of the islet BM has been confirmed in a number of species, including canines [323, 324], mice [325], and most recently, humans [112]. In this study, Cross *et al*. showed that both layers of the double islet BM are substantially disrupted during human islet isolation, when utilising collagenase and NP enzyme blends. Post-isolation islets were completely devoid of perlecan and laminin α5, which did not recover during islet culture (up to 72 hours). Although pan-laminin and collagen IV were present on isolated islets, the amount of pan-laminin decreased significantly overtime in culture [112]. The data presented within this Chapter supports the substantial disruption of the BM following enzyme treatment. Furthermore, it also demonstrates that NP plays a greater role than collagenase in digesting the non-collagenous components of the BM; laminin, laminin α5, and nidogen-1 were resistant to collagenase digestion, but were significantly digested by NP (younger group only for nidogen-1). Perlecan loss within the tissue was facilitated by both enzymes, but the loss was significantly greater with NP than collagenase. Collagen IV was the only BM protein studied that displayed greater loss when treated with collagenase compared to NP (for younger donors only). Interestingly, the addition of collagenase to NP resulted in significantly less nidogen-1 digestion in younger donors than treatment with NP alone. Combining collagenase with the NP also reduced the digestion of a purified nidogen-1 fragment (at 80KDa), following enzyme treatment for 30 minutes and 2 hours. At these two time points, digestion of this fragment was therefore less effective with the two enzymes combined, than if NP was used alone. One possible explanation for this result is that collagenase cleaves nidogen-1 to produce a modified product of lower molecular weight (80KDa), which NP has a decreased affinity for, in comparison to the intact molecule (130KDa). However, following overnight treatment of purified nidogen-1 with collagenase and NP, the fragment at 80KDa was digested to the same extent as treatment with NP alone, suggesting that NP is able digest this fragment, albeit at a slower rate.

The islet BM has important roles in conferring structural support and preventing anoikis; a type of cell death mediated through matrix detachment [326]. In addition, the BM provides vital signalling

functions to adjacent cells, and as such islets that remain partially embedded in exocrine tissue post-isolation display reduced apoptosis and improved *in vitro* function over those completely devoid of matrix [104]. Laminins, via interaction with their transmembrane integrin and Lutheran glycoprotein receptors that are expressed on islets [167, 170], have shown to be crucial in the regulation of insulin gene expression and proliferation [166]. The heperan sulfate side chains of perlecan have also been shown to be essential for normal insulin secretion in mice [327]. Although the role of nidogen-1 in β-cell function remains unknown, it plays a pivotal role in BM assembly; linking collagen IV and laminin [193]. The destruction of these proteins, shown here to be primarily facilitated by NP, is likely to induce islet damage and reduce function. This theory is supported by studies determining the effect of NP concentration on isolation outcome, which have shown that increasing levels of NP induce islet fragmentation [149, 328, 329], and decrease viability [330] and insulin secretory capacity [330], in a dose dependent manner. The data presented within this Chapter demonstrate significant islet BM loss after treatment with what is equivalent to 50 Units of NP. However, some centres have reported using concentrations of 8 fold this amount [161]; ranges that are likely to leave islets completely devoid of these key BM proteins, detrimentally impacting islet function and survival.

Optimal pancreas digestion would preserve the integrity of the islet BM, and selectively digest the IM to release the islets from the surrounding exocrine tissue. Collagen I, V and VI have previously been identified as prominent interstitial matrix proteins within the human pancreas [171, 210]. The digestion of purified collagen I by collagenase has been reported previously [211], and supports our data, which shows collagen I expression is reduced by 59% after overnight collagenase treatment. Although the amount of collagen I was also decreased within the pancreatic tissue following 5 minutes of collagenase treatment, the reduction was modest in comparison to the loss of purified protein (9% and 16% for the younger and older donors respectively). This discrepancy is likely due to structural differences in purified collagen I, compared to that present in the tissue. *In situ* collagen I fibres form part of a highly organised, integrated network with other ECM components,

particularly collagen V [331, 332]. The structure of this network may prevent the triple helical region of collagen from being readily accessible, averting it from interacting with the collagen binding domains of collagenase, required for collagen cleavage [333]. It is therefore unsurprising that collagen I contained within pancreatic tissue is more resistant to digestion than an isolated purified protein. Similarly, it has been shown that purified collagen V is a substrate for class I collagenase [334], whereas our data demonstrates that collagen V is resistant to collagenase digestion within the pancreatic tissue. The action of NP on collagen V digestion has not been reported previously, but our data demonstrates significant digestion of collagen V following NP treatment, however this was restricted to the younger donor group. Like collagen I, the digestion of purified collagen VI was facilitated by collagenase. These data are in contradiction to previous reports, which show that collagen VI is resistant to collagenase digestion [211, 212]. In contrast, within the tissue, collagen VI was resistant to collagenase digestion in both donor groups, in line with these previous reports. Indeed, the explanation for this discrepancy is based on the method used to produce the purified collagen VI, which was achieved using pepsin treatment. Unlike fully intact collagen VI, which contains collagenase resistant segments due to a high degree of regional disulphide bonding, pepsin extracted collagen VI is susceptible to collagenase degradation [212]. Although the effect of NP treatment on collagen VI digestion has not been previously studied, the tissue digestion data suggests that NP plays a greater role in digesting collagen VI than collagenase.

The digestion of collagen VI was also affected by donor age. In the younger donor group enzyme treatment was associated with a significant increase in collagen VI signal compared to the control tissue. Indeed, as the natural variations in the protein content around individual islets were controlled for in these experiments by incorporating random effects into the statistical modelling process, it can be assumed that collagen VI is resistant to digestion in the younger donor group. Put differently, the 'increase' in protein concentration likely results from the enzyme mediated loss of other proteins within the matrix. This loss likely exposes the remaining collagen VI and leads to increased antibody recognition, despite the overall net content of collagen VI remaining unchanged

from the control. In contrast, in older donors the treatment of tissue with collagenase and NP (at the combination utilised clinically), significantly reduced the amount of collagen VI. Therefore, although the enzyme treatment was significantly more effective at digesting collagen VI in older donors, this should be interpreted with caution, given that there is only a 15% difference in the loss of collagen VI between the two groups (when assuming that the content of collagen VI in younger donors remains unchanged from the control). Nonetheless, these experiments highlight collagen VI as a potential target for improving digestion from younger donors.

Interestingly, the data presented within this thesis, and previously, have demonstrated that the quantity of collagen VI in the pancreas is not significantly affected by age [171]. Age-related differences in the digestion of collagen VI are therefore unlikely to be caused by quantitative differences, but perhaps differences in protein structure resulting from the natural aging process. The key role collagen VI plays in linking the BM to the underlying exocrine [208] further justifies the importance for improving its digestion, as it is likely to be instrumental in allowing the separation of the islet from the general exocrine, whilst preserving the islet BM. In addition to collagen VI, age affected the digestion of BM proteins collagen IV, laminin α5 and nidogen-1. Treatment with NP alone was significantly more effective at digesting collagen IV and laminin α5 in younger donors (Chapter 4), whereas for nidogen-1 the older donors were significantly more resistant. Digestion of collagen IV was also significantly reduced in pancreatic tissue sections from younger donors that had been treated with collagenase. Despite these differences, when collagenase and NP were combined, mimicking the composition of enzyme blends that are utilised clinically, these significant age-related differences in protein digestion were ameliorated. Therefore, when utilising the preferred clinical islet isolation enzyme composition, donor age only affected the digestion of collagen VI.

Indeed, the fact that donor age only affected the digestion of one of the studied proteins is somewhat surprising, given the poorer pancreas digestion outcomes observed clinically for

younger donors, when compared to their older counterparts [101, 249]. Furthermore, as shown in Chapter 3, a large subset of ECM proteins displayed significantly higher expression in younger donors. Of these proteins, collagen IV quantity was most considerably affected by age, with the α5 chain displaying an 11.5 fold increase in the younger donors, as well as significant increases in 3 of the other collagen IV chains. The absence of further anticipated age-related differences in enzyme mediated protein digestion may result from the method used for protein measurement; the use of antibodies restricts the detection of the protein to the specific region recognised by the antibody (the 'epitope'). As such, the digestion identified by the antibody may not be representative of the overall state of protein digestion throughout the rest of the protein structure. Thus, by utilising conventional immunolabelling, important age-related differences in protein digestion may be overlooked. Therefore, an alternative method is required to support these data, ideally a technique that can identify proteins at the molecular level, and is not restricted by the use of 'labels' for protein detection.

5.5 Conclusion

The treatment of pancreatic tissue sections and purified ECM proteins with enzyme components found in clinical enzyme blends revealed that the digestion of the islet BM is primarily facilitated by NP. NP should be used with caution, to avoid excessive loss of BM integrity. Proteins located in the pancreatic IM were more resistant to enzyme digestion than those found in the BM, and further investigation is warranted to enhance the digestion of these proteins (i.e. collagens I and VI). A key finding was that Collagen VI was resistant to digestion in younger donors, but was significantly reduced in older donors when utilising a standard clinical collagenase and NP blend. These findings need to be further investigated using a label-free detection approach, unrestricted by specific antibody binding. This was the aim of the study described in the next Chapter.

CHAPTER 6

Raman Microspectroscopy: a Novel Approach for Comparing Digestion of the Pancreatic ECM in Different Aged Donors

6.1 Introduction

In the previous Chapter, the developed slide-based digestion assay was used to determine donor age-related differences in the digestion of key ECM proteins. Importantly, these studies not only revealed the principle role of neutral protease in the digestion of the integral islet basement membrane (BM), but also demonstrated that the interstitial matrix (IM) protein collagen VI is resistant to digestion in younger donors. For the first time, these studies provide evidence for donor age-related differences in the digestion of the human pancreas at the molecular level, which may help to explain the poorer digestion outcomes from younger donors.

The developed slide-based assay is a powerful screening tool, which utilises small amounts of both tissue and enzyme, with loss of specific ECM proteins detected by simple antibody-based detection methods. Conventional immunolabelling offers a straightforward approach for studying the protein networks within tissues, and to date, has been largely responsible for characterising the pancreatic ECM [99, 112, 167, 171]. Although this research has provided insight into the unique spatial distribution of the specific ECM proteins within the islet region [167], identification has been limited to a pre-selected subset of proteins. In addition, when using immunolabelling to assess protein digestion, it is assumed that there is uniform digestion between the regional epitopes recognised by the antibodies, and the rest of the protein molecule. It is therefore important that data produced from this method are supported using a label-free method for assessing protein digestion, unrestricted by antibody binding.

Raman spectroscopy is a non-contact, label-free laser-based technology that has recently gained increasing interest in the field of biomedical research, after originating as an analytical tool for characterising chemical components in the pharmaceutical industry. Raman spectra provide information regarding the unique identifiable molecular composition of a sample, allowing for the characterisation of complex molecular structures. As such, the technology has been successfully employed in a number of biomedical fields including: in microbiology; to identify and discriminate

bacterial spores [335, 336], in stem cell research; to characterise cell state and monitor differentiation capabilities [337, 338] and in medical pathology; to monitor the pathological status of tissues and cells [339, 340]. Raman has the clinical potential to be used in the diagnosis of cancer [341], in addition to being used as a tool to accurately define the border of tumours, prior to surgical removal [342].

Raman spectroscopy operates by exploiting the inelastic scattering of monochromatic light. Following the lights interaction with a sample an incident photon is absorbed and another emitted simultaneously. The vast majority of the photons are emitted at the same frequency as the incident photon, which is commonly termed 'Rayleigh scattering'. However, approximately 1 in 10^6-10^8 incident photons undergo inelastic scattering, which results in the emitted photon that has a distinct electronic ground state [343]. The majority of the inelastic scattering occurs as a 'Stokes shift', which is characterised by a loss of photon energy following interaction with the sample (caused by the samples molecules absorbing energy). Photons can also gain energy following sample interaction, known as anti-Stokes scattering (caused by the sample molecules losing energy), though this is much less common [343] (Figure 33). As energy shifts are unique to the vibrational frequency of specific molecular bonds, Raman spectroscopy enables the identification of molecular groups and compositions in complex samples. To resolve complex molecular shifts multivariate analysis methods are employed. Principle component analysis (PCA) is commonly used in the analysis of spectroscopic data and allows differences and similarities in spectral data sets to be explored [344].

The concept of coupling a conventional microscope to a Raman spectrometer was first proposed in 1990 [345]. Raman microspectroscopy (RMS) increased the spatial resolution of standard Raman spectroscopy, facilitating targeted Raman measurements to be obtained from specific morphological areas of tissue or single cells [339, 346]. This approach was used to assess the integrity of the collagen networks in aortic leaflets following heart valve cryopreservation. The

coupled microscope allowed the Raman measurements to be obtained from the antibody detected collagen rich areas of the aortic leaflets, with spectral variations revealing that standard cryopreservation was detrimental to collagen structure [346]. This particular study also featured proof of principle experiments, where heart valves were treated with collagenase *in vitro* and collagen degradation characterised by RMS [346]. Collagenase mediated loss of collagen was detected by the changes in the spectra representative of collagen [346]. As a single Raman spectrum represents the overall composition of the targeted tissue area, it is theoretically possible to identify multiple ECM proteins from one spectrum. Obtaining spectra from purified proteins can allow unique identifiable peaks for each protein to be determined, which can be used to detect the presence of the protein in spectra obtained from the tissue [347]. Previous work has shown that the spectra procured from purified collagens I and IV are distinguishable based on a higher content of both proline and hydroxyproline in collagen I. Furthermore, a high extent disulphide bridging was detected in purified collagen IV [347]. Peaks representative of both proteins were detected in a human skin sample [347]. This demonstrates the high-throughput capabilities of Raman; it is possible to generate information regarding multiple ECM proteins from a single measurement, without the requirement of labels.

Next generation Raman instruments are capable of incorporating powerful spectroscopic imaging functions. Multivariate analysis tools are used to map biochemical constituents of a defined sample area onto a compositional image. Raman spectral information can be collectively transferred into a false colour code. Resulting spectroscopic images have good spatial resolution, allowing the localisation of ECM proteins within complex tissues to be explored without utilising labels [348, 349]. Previously, Raman imaging has been used to develop complex images of human islets, based on the distinct Raman spectra of insulin and glucagon. The resulting biochemical images were comparable to those generated by conventional fluorescent labelling, and provided the opportunity to study islets in a real-time and label-free manner [348].

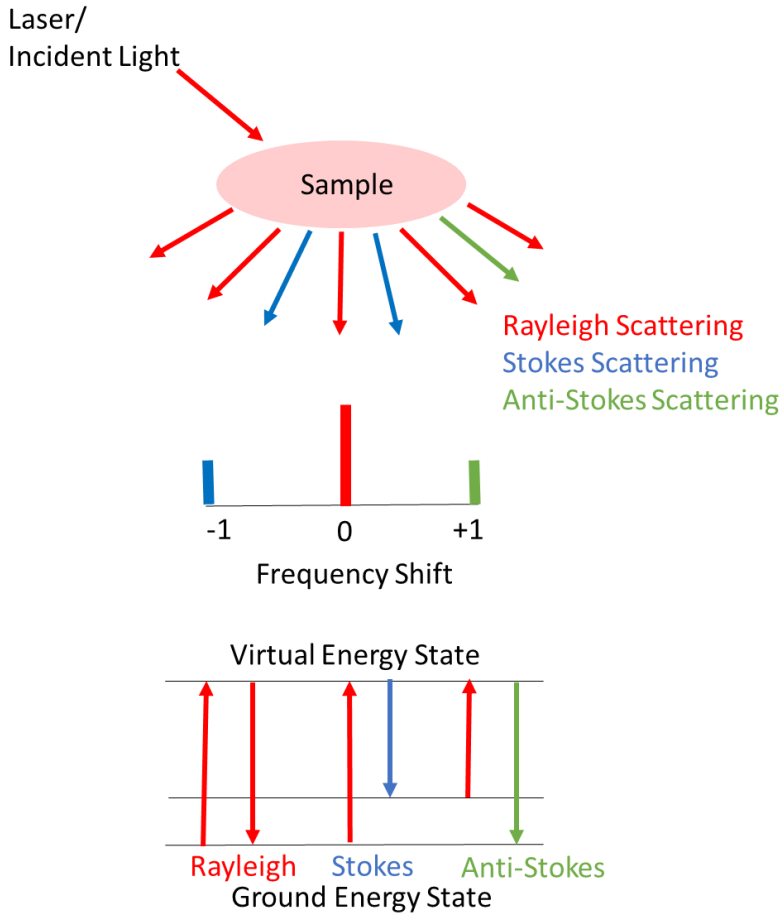


Figure 33: Overview of Raman scattering
Upon interaction with the sample the majority of photons are emitted at the same energy level as the incident laser photons (Rayleigh scattering). However, a small (10^6-10^8) number of photons are shifted to a different frequency, based on the specific vibrations of molecular bonds within the sample (Stokes and anti-Stokes scattering). The resulting scattered photons have a different energy state to the incident photon. The shift in energy is molecularly specific and thus allows sample characterisation. Adapted from Figure 2 in Brauchle *et al.* 2013 [343].

This Chapter aimed to determine if RMS is a suitable tool for characterising age-related changes in the enzyme-mediated digestion of the human pancreas. This was achieved by: i) identifying the Raman spectra for selected ECM proteins, by obtaining reference measurements from purified collagens I, IV VI and laminin, (ii) performing a series of digestion experiments on purified ECM proteins to demonstrate that RMS is capable of detecting ECM protein digestion, and (iii) identifying the unique ECM spectra of human pancreatic tissues, and obtaining Raman

measurements from the tissue following enzyme treatment, to demonstrate the ability of RMS to detect donor age-related differences in ECM digestion.

6.2 Methods

6.2.1 ECM Reference Standards and Digestion

Purified human collagen IV (C533-5mg, 0.7 mg/ml) and laminin (L6274-5mg, 0.5 mg/ml) were purchased from Sigma (Gillingham, UK). Collagens I and VI (ab7533 and ab7538, both 1 mg/ml) were purchased from Abcam (Cambridge, UK). For proof of principle experiments, purified proteins were digested using collagenase NB1 and neutral protease NB (NP) (both Serva, Heidelberg, Germany) at concentrations relevant for human islet isolation (collagenase 7.2 PZU/ml, NP 0.14 DMCU/ml). 50 µg of each reference standard were added at a 1:2 volume ratio to the enzyme solution, and heated at 37°C for 30 minutes, 120 minutes, or overnight. For control samples, the enzyme solution was replaced with HBSS (Lonza, Basel, Switzerland). At the end of the incubation period, the enzyme reaction was ceased by cooling to 4°C, with the addition of protease inhibitor cocktail to all samples, including controls (PIC; cOmplete™ Mini Protease Inhibitor Cocktail, Roche). Samples were stored at -20°C until use.

6.2.2 Human Tissue Sampling and Preparation of Cryosections

With the appropriate research consent and ethical approval, 0.5cm^3 tissue samples were taken from 5 younger (age ≤35) and 5 older (age ≥45) pancreases from multi-organ donors accepted for clinical islet isolation at the Oxford DRWF Human Islet Isolation Facility (Table 17). The biopsies were snap-frozen in liquid nitrogen and stored at -80°C until use. In-house produced silanized coverslips were used for tissue collection. Briefly, coverslips (25mm x 50mm, thickness 1, VWR, Peterborough, UK) were treated with 2% silane (3-aminopropylthirethoxysilane, A3648, Sigma, UK), diluted in 100% acetone for one minute, followed by two separate immersions in 100%

acetone for one minute each. Coverslips were left to air dry in a clean environment for a minimum of 2 hours. The optimal tissue thickness for obtaining Raman measurements was determined to be 10µm. Tissue sections were prepared using a Cryostat (Microm HM 560 cyotome, Thermo Scientific, Loughborough, UK) and collected onto the pre-silanized coverslips. Tissue sections were stored at -20°C until use.

	Younger Donors ≤ 35 years (n=5)	**Older Donors ≥ 45 years (n=5)**	***p* value**
Age, y (Mean ± SEM)	27±1	58±0.7	<0.001
Age, y (Median (Range))	26 (25-30)	58 (56-60)	<0.001
Gender (M:F)	4:1	3:2	0.49
BMI (Mean ± SEM)	26.3±1.7	28.6±0.93	0.28
CIT, h (Mean ± SEM)	6.2±0.7	6.1±0.7	0.92

Table 17: Donor and pancreas characteristics for Chapter 6
CIT; Cold ischemia time
SEM; Standard error of the mean
Statistical analysis was performed by an independent samples t-test.

6.2.3 Digestion of Pancreatic Tissue Sections and Immunofluorescent Labelling

Pancreas cryosections were thawed in HBSS (Lonza). Sections were incubated for 5 minutes at 37°C with HBSS (control), collagenase alone, NP alone (both Serva) or a combination of the two enzymes, at clinically relevant concentrations (collagenase 7.2 PZU/ml, NP 0.14 DMCU/ml). Following treatment, enzymatic activity was quenched by placing slides in cold running water. Sections were fixed with 2.5% paraformaldehyde (Sigma) and then blocked with 5% normal swine serum (Vector Laboratories). Sections then underwent double immunofluorescent labelling. Incubation with primary antibodies: polyclonal guinea pig anti-insulin (1:100; A0564, Dako, Ely, UK), and polyclonal goat anti-collagen IV (1:300; 134001, BioRad, Oxford, UK) was for 1.5 hours at room temperature (r.t). Sections were then incubated with secondary antibodies for 30 minutes at r.t: AlexaFluor 594 conjugated donkey anti-guinea pig (1:500; 706-585-178, Jackson Immunoresearch, PA, USA) and

AlexaFluor A488 conjugated donkey anti-goat (1:500; A11055, Life Technologies). Post removal of the secondary antibodies, the coverslips were immersed in PBS and stored at 4ºC prior to the Raman measurements.

6.2.4 Raman Microspectrometer Set-up

6.2.4.1 Purified Protein Reference Standards and Enzyme-treated Proteins

For measurement of digested and untreated purified proteins, a customised WITec alpha 300R Raman microscope was used (WITec GmbH, Ulm, Germany), equipped with a charged coupled device (CCD) camera (Andor iDus, Belfast, UK). A CCD is a multichannel detector, which contains multiple different detection elements (pixels), whereby each pixel detects light from an individual spectral position. A green laser (532 nm) and a spectrograph with a grating of 600 g/mm were chosen for spectral detection. 20 µl of both the enzyme-treated and control samples for collagens I, IV, VI and laminin were thawed and air dried overnight in separate glass bottom dishes (ibidi, Martinsried, Germany). For each protein, 45 measurements were obtained per condition, with a laser power of 50 mW and an acquisition time of 0.5 seconds per spectrum. Measurements were made with a 63x Apochromat water dipping objective (N.A. 1.0; Carl Zeiss GmbH, Jena, Germany). The enzyme and PIC additives were measured in isolation, to determine their influence on the spectra. Single point Raman measurements of 10 acquisitions of 1 second each were also obtained from the purified proteins prior to incubation, to obtain spectra that were free from these additives.

6.2.4.2 Measurements from Native Human Tissue

The WITec Raman system was used to identify the ECM spectra of human pancreatic tissue. The laser and diffraction grating settings were as described above. Non-digested, rehydrated and Collagen IV/AlexaFluor 488 stained sections of pancreatic tissue were measured with the 63X objective, as per above. Islets were identified according to the immunofluorescence staining and

an area of 200x200 µm was imaged with a scanning step size of 2 µm. The laser power was set to 50 mW and an acquisition time of 0.5 seconds was used per spectrum. Four donors (two from each age group) were selected for the Raman imaging experiments, with two islets imaged per donor.

6.2.4.3 Measurements from Digested Human Tissue

RMS was performed for single spectra acquisition using a custom set-up Raman microspectroscope as described previously [346, 350] coupled to a fluorescence microscope (Olympus, Hamburg, Germany). Briefly, the Raman spectrometer was equipped with a 784 nm diode laser (Toptica Photonics, Munich, Germany), which induced Raman scattering when directed at the sample through the microscopic objective (60x water immersion, NA 1.2, Olympus). The microscope had a secondary camera, for acquiring fluorescent images of the tissue, controlled by CellB software (Olympus). The instrument was calibrated after each start-up, using a silicon wafer with a characteristic Raman shift of 521.74cm^{-1}. Raman spectra were detected using an air-cooled CCD camera (Andor iDus), which was controlled by Andor SOLIS software (Andor iDus). Single point Raman tissue measurements were acquired from pre-treated tissue sections, fully immersed in 1X PBS. For all donors, at least two islets were measured for each treatment. Islets were identified with the microscope camera on the basis of positive insulin labelling, controlled by CellB software (Olympus). For each islet, 15 Raman spectra were taken from the islet peripheral region (peri-islet) and 5 from the intra-islet region. All measurements were restricted to collagen IV positive regions. Spectra were acquired with an integration time of 100 seconds, and a laser output power of 85 mW was used.

6.2.5 Spectral Analysis

Raman images of the native pancreatic tissue were analysed by applying the Project Five 5.1 software (WITec, GmbH). Multivariate analysis allowed for the identification of major spectral components. One component describes pixels of similar spectral information, which can be

projected onto a colour coded intensity distribution image. Analysis of component spectra enables the identification of the respective tissue structure.

For the spectra obtained from pancreatic tissue using the custom Raman set up, processing was performed in OPUS (Bruker Optik GmbH, Ettlingen, Germany). Spectra were obtained from the cover glass and PBS alone after every tenth measurement and subtracted from the sample spectra. Baseline correction (64-point rubberband method) was then performed. To ensure that spectral differences could be attributed to the enzyme treatment, all single-point spectral measurements were normalised to the corresponding control spectra for each donor. This was achieved by averaging the control spectra to the value of 1, before dividing each equivalent spectral position in the enzyme treated spectra by this modified control. Data normalisation was performed in Excel (Microsoft Corporation, USA, 2016). Finally, the spectra were cropped in the region of 480-1680cm^{-1}.

Due to complex molecular patterns of ECM structures, multivariate analysis such as principal component analysis (PCA) is required to resolve complex molecular shifts [344]. PCA is commonly implemented to determine differences and similarities in chemometrics. The principles of PCA for the analysis of Raman data have been explained in detail before [350, 351]. Collectively, the devised principle components (PCs) describe the total information contained within the original data set. The first PC explains the highest amount of variation, and the subsequent PCs explain the next highest amounts of variation chronologically. PCA results are interpreted on a scores plot, where one PC is graphed against another, with every spectrum represented by an individual dot. Whilst similar spectra cluster together on the scores plot, dissimilar spectra are separated. By colour coding spectra (i.e. the dots) that are obtained from different groups (i.e. younger vs older donors) it is possible to determine the PCs that are responsible for the variability between the groups. The corresponding PC loading plot displays the contributions of each spectral region to the overall structure of the scores plot. PCA was completed in Unscrambler X (CAMO Software, Norway). Data

were vector-normalised and smoothed using Savitzky-Golay filtering. The PCs that were most effective at separating the data from different experimental groups were selected, and their subsequent loading spectra were examined. PCA was used to analyse both the digested purified protein experiments and the enzyme treated pancreatic tissue experiments.

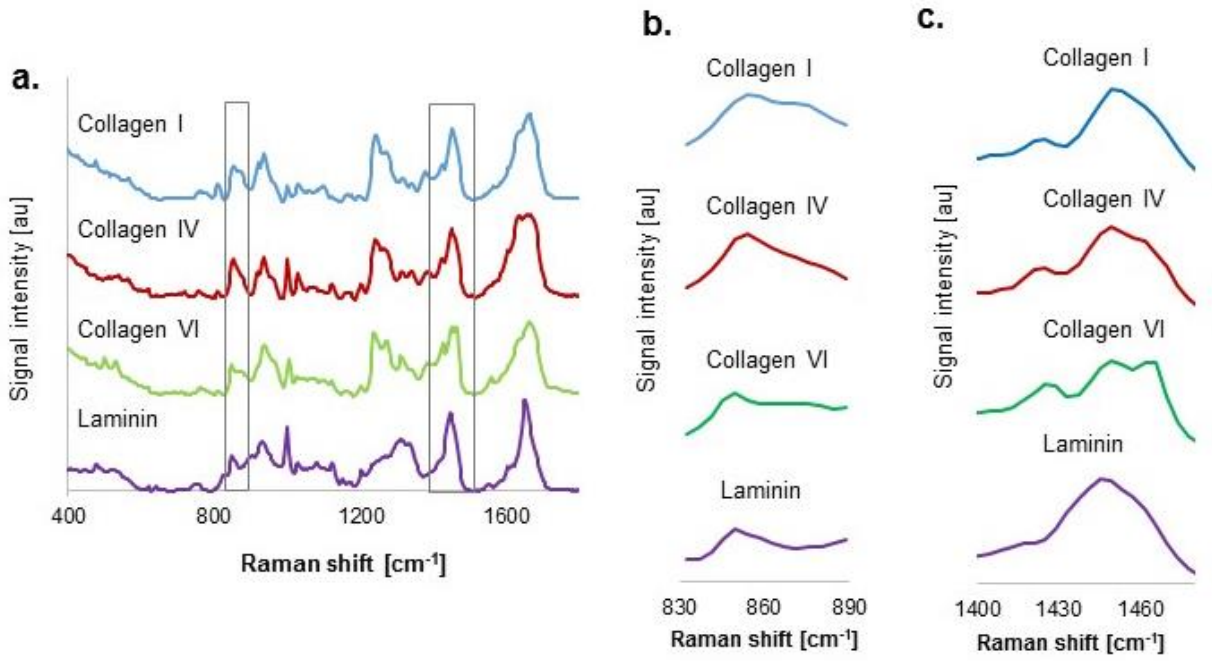
6.2.6 Statistical Analysis

Data are presented as mean ± standard error of the mean (SEM). Data normality was determined by Shapiro Wilk test. Statistical significance of PCA scores was determined by Mann-Whitney U. Statistical analyses were performed in Prism/GraphPad (San Diego, USA). Data with *p*-values of less than 0.05 were identified as statistically significant.

6.3 Results

6.3.1 Raman Spectra for Purified Matrix Proteins

To determine if specific matrix proteins could be distinguished on the basis of their Raman spectra, Raman measurements were first obtained from human purified collagens I, IV, VI and laminin. These proteins were selected based on their identification in Chapter 3, and on their previously reported prevalence in the human pancreas [171, 210]. Figure 34 a displays the Raman reference spectra following baseline correction and normalisation. Anticipated characteristic protein Raman bands were present, such as: proline (854-858cm^{-1}), C-C backbone stretching (938cm^{-1}), phenylalanine (1005cm^{-1}), amide III (1242cm^{-1}), CH_2 deformation (1449-1465cm^{-1}) and amide I (1666cm^{-1}) [352-355]. Although the four proteins displayed a high degree of spectral homogeneity, subtle protein specific characteristics were present. This included shifting of feature peaks, such as proline (Figure 34 b) and CH_2 deformations, where a distinctive double peak was noted for collagen VI (1453 and 1465 cm^{-1}; Figure 34 c). Unlike the collagens, laminin lacked a clearly defined amide III band. Instead a peak was present at 1307cm^{-1} (Figure 34 d).



d.

	Raman Shift [cm^{-1}]			
Molecular consignment	**Collagen I**	**Collagen IV**	**Collagen VI**	**Laminin**
Proline	858	858	854	854
C-C backbone stretch	938	938	938	938
Phenylalanine	1005	1005	1005	1005
Amide III	1242	1242	1242	-
Unassigned peak	-	-	-	1307
CH_2 deformation	1453	1449	1453, 1465	1449
Amide I	1666	1666	1666	1666

Figure 34: Raman spectra for ECM reference standards

a. Spectra display the fingerprint region of purified matrix proteins following baseline correction and normalisation (400-1800cm^{-1}). The four proteins display similar spectra, with a few key variations. Spectral differences are seen in the regions corresponding to **b.** Proline and **c.** CH_2 deformation.

d. General peak assignments for purified ECM proteins. Dashes indicate the absence of a peak. References from Frushour *et al* 1975 [356].

ECM; Extracellular matrix

6.3.2 Changes of ECM Fingerprint Spectra Due to Enzymatic Digestion

The proceeding experiments aimed to determine if Raman was capable of detecting characteristic changes in ECM spectra following enzyme treatment with clinical islet isolation blends over a time

course. Purified matrix proteins were incubated with collagenase and NP at enzyme concentrations clinically relevant for human islet isolation. Reactions were stopped by the addition of a protease inhibitor cocktail (PIC). Protein degradation in response to enzyme treatment was assessed by Raman spectral changes, when compared to a control, using PCA. Spectra obtained from the PIC and enzyme alone revealed major peaks at 880 cm^{-1} (PIC) and 1047 cm^{-1} (enzyme). These peaks were ignored for the purpose of the analysis. Although controls were incorporated for each of the three incubation time points, the duration of heating alone, in the absence of enzyme, did not influence the resulting Raman spectra (data not shown). Therefore, only the overnight control was selected for the analysis. Enzyme treatment affected the overall composition of the Raman spectra obtained from all four ECM proteins, determined on the basis of separated spectral clusterings on the PCA scores plots.

Collagen I separation occurred along the scores plot for PC-3, with the 120 minute and overnight treatment spectra migrating to the negative region of the PC (Figure 35 a). The PC loading displayed Raman bands including 940 cm^{-1} (C-C backbone stretching) and 1453 cm^{-1} (CH_2 deformation) [356] (Figure 35 b). For collagen IV, the 120 minute and overnight treatment spectra migrated towards the negative region of PC-2 (Figure 35 c). Peaks were present at 963 cm^{-1} (general protein assignment) [354] and 1453 cm^{-1} on the loadings for PC-2 (Figure 35 d). Separation of the control and enzyme spectra for Collagen VI was apparent in PC-1 (Figure 35 e). The overnight treated spectra formed a clear population in the negative region of the scores plot. The loading detected feature peaks including 940 cm^{-1} and 1453 cm^{-1} (Figure 35 f). Spectral separation following enzyme incubation of laminin also occurred along PC-1, with the enzyme treated spectra clustering toward the negative region of the PC (Figure 35 g). The characteristic loading pattern for laminin was substantially different from the collagens. Prominent peaks were present at 761 cm^{-1} and 1469 cm^{-1}, which appear to be previously unassigned in the literature (Figure 35 h).

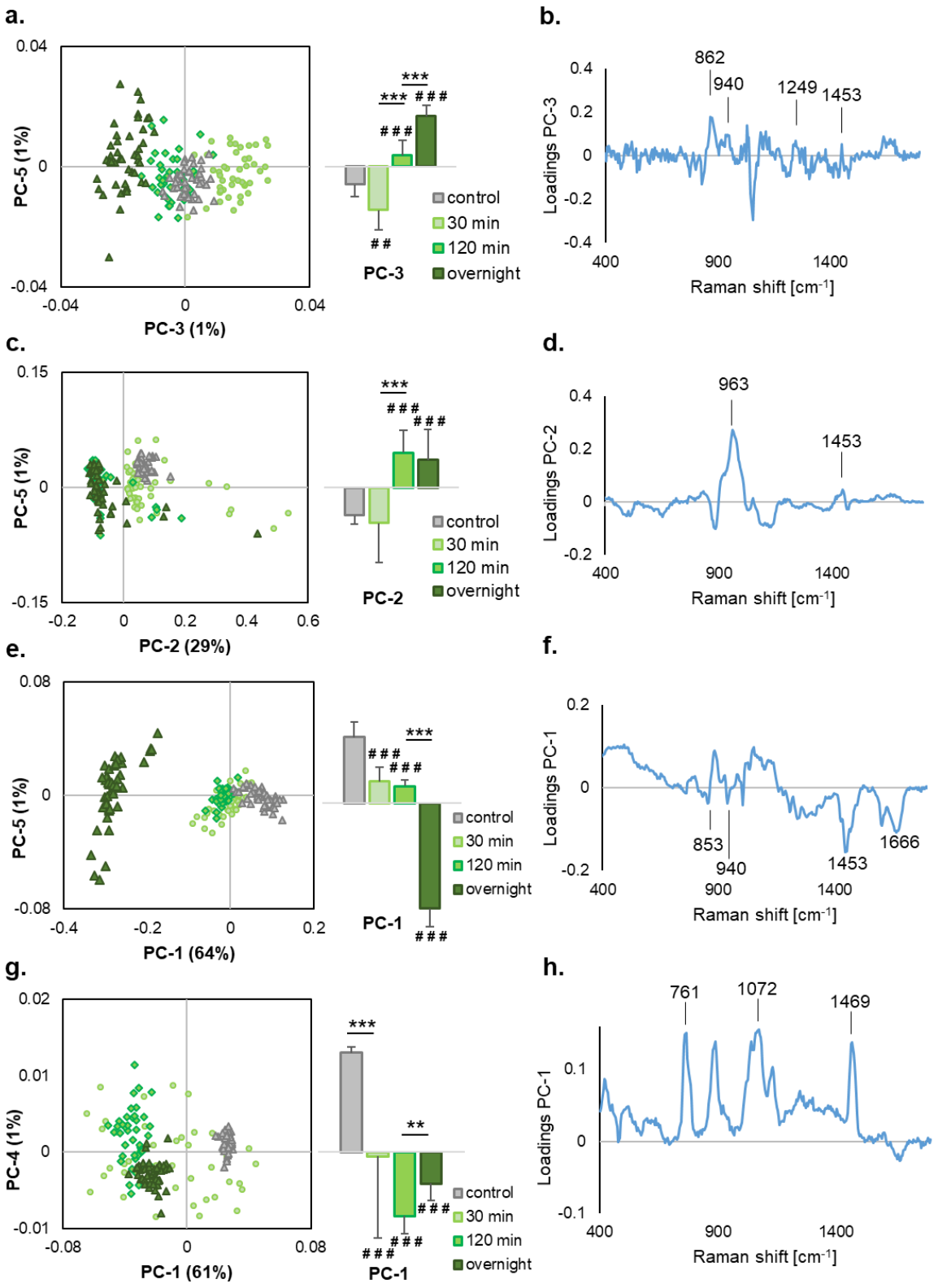
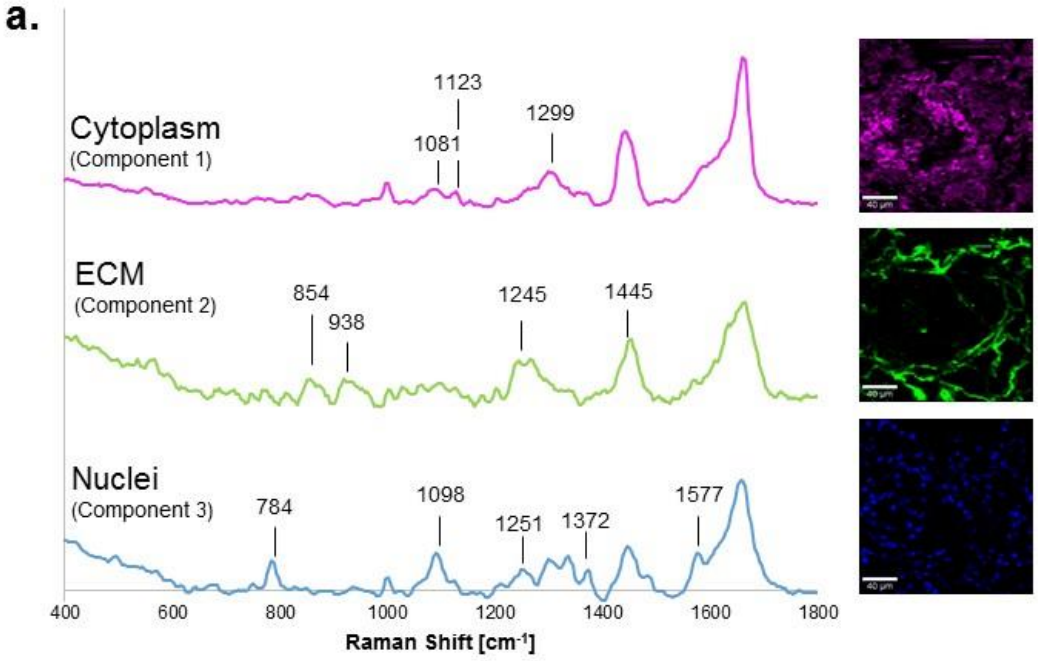


Figure 35: Enzymatic induced changes in Raman biomolecular fingerprint of ECM proteins Principle component analysis (PCA) was performed on spectra obtained from collagenase and neutral protease treated purified proteins. Protein treatment occured for 30 and 120 minutes, or overnight. Control samples were heated overnight in HBSS.

a. Collagen I treatment with enzymes led to separation along PC-3 and **b.** the corresponding PC-3 loading highlighting the main peaks responsible for the separation
c. Collagen IV separation was along PC-2 and **d.** corresponding PC-2 loading
e. Collagen VI separation occured along PC-1 and **f.** corresponding PC-1 loading
g. Laminin separation occured along PC-1 and **h.** corresponding PC-1 loading.
PC; Principle component
Statistical analysis of scores was performed by ANOVA
# Indicates significant difference from control
* Indicates significant difference between the two groups, as indicated by the lines
**/## p<0.01
***/### p<0.001

6.3.3 Identification of the ECM Spectra in Human Pancreatic Tissue

Raman spectroscopic imaging was used to identify the spectra that represented ECM proteins in human pancreatic tissue. A spectral map was generated from a defined area of tissue, which contained an islet. Islets were identified on the basis of the collagen IV labelling pattern. Every pixel within this area corresponded to a single Raman spectrum. Multivariate image analysis was performed to identify pixels that contain spectral information from biochemically similar structures. Each structure can be identified by a specific component spectrum. Intensities for each spectral component are then shown within the image. Three major spectral components were identified in overview scans of the pancreatic tissue (Figure 36 a) and their peak assignments were evaluated to assess their corresponding molecular structures (Figure 36 b). Component 1 described the cytoplasm, and contained peaks assigned to general proteins and lipids such as 1081, 1123 and 1299 cm^{-1}. Component 2 morphologically described the ECM and displayed peaks at 854, 938 and 1245 cm^{-1}. These peaks relate to the Raman scattering of defined molecular bonds in collagens such as vibrations of proline, C-C backbone and amide III. Component 3 correlated to nuclei and showed peaks at 784, 1098 and 1577 cm^{-1} referring to DNA, phosphate backbone and nucleic acid bases. In addition, there was a high degree of homogeneity between the Collagen IV/AlexaFluor488 specific signature (Figure 37 a-c) and the Raman identified ECM component (i.e. Component 2) (Figure 37 d-f), which was observed when merging the images (Figure 37 g-i).



b.

Peak [cm^{-1}]	Cytoplasm	ECM	Nuclei
784			DNA [357]
854		C-C (proline collagen) [356]	
938		C-C (collagen backbone)[356]	
1081	Lipids [358]		
1098			Phosphate [359]
1123	C-N stretch (proteins) [354]		
1245		amide III [356]	
1251			NH_2 G, C [360]
1299	CH_2 deformation (lipids) [357]		
1372			DNA bases [361]
1445		CH_2 deformation (proteins/collagen) [356]	
1577			NADH, G [360]

Figure 36: Raman imaging of pancreatic tissue

a. Multivariate analysis identified three major spectral components. Morphologically the components represented the cytoplasm (Component 1; pink), the ECM (Component 2; green) and nuclei (Component 3; blue).

b. Shows the peak assignment of each component
Scale bar equals 40 µm
ECM; extracellular matrix
NADH; Nicotinamide adenine dinucleotide
G/C; Guanine/Cytosine

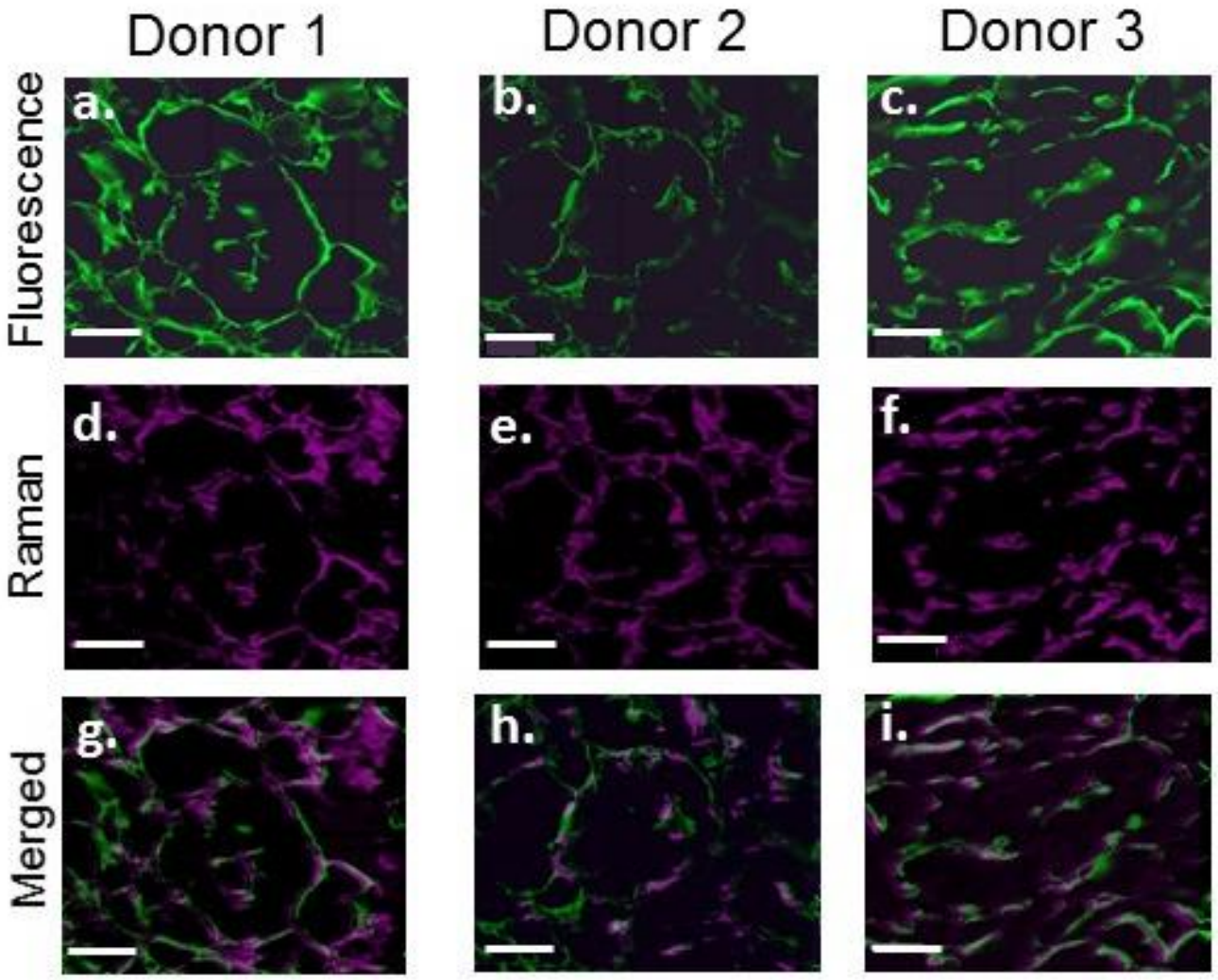


Figure 37: Correlation of Raman imaging and immunofluorescence staining
a-c. Collagen IV immunofluorescent images
d-f. Label-free images of the ECM component identified by multivariate analysis, on the basis of the samples Raman spectra
g-i. Composite images, created by merging the corresponding fluorescent (green) and Raman images (pink), demonstrate a high degree of homogenity between the protein signature identified by the two methods.
Scale bars equal 40 µm

6.3.4 Raman Detects Age-related Differences in the Digestion of the Pancreatic ECM

To induce digestion of the ECM, human pancreatic tissue sections from different aged donors were treated with the enzyme components found in human clinical islet isolation blends: collagenase, NP or the two enzymes in combination. The regional islet-exocrine interface was located by labelling for insulin and collagen IV (Figure 38 a). Following enzyme treatment there was a visible loss of collagen IV signal for both younger and older donors, as compared to the untreated controls. Protein loss was evident in both the peri-islet matrix, and the matrix surrounding the blood vessels in the intra-islet region (Figure 38 b). Reduction in the signal intensity of collagen IV, following 5 minutes of enzyme treatment, was previously semi-quantified morphometrically in Chapter 4 (Section 4.3.3). The collagen IV staining was used to obtain targeted single point Raman measurements (Figure 38 b). Spectra from enzyme-treated sections were normalised to those obtained from control tissue, to enable the investigation of spectral differences that resulted from the administered enzyme treatment. Digestion efficiency was not affected by the matrix location (i.e. peri-islet or intra-islet) and thus measurements were combined (Appendix Figure E1).

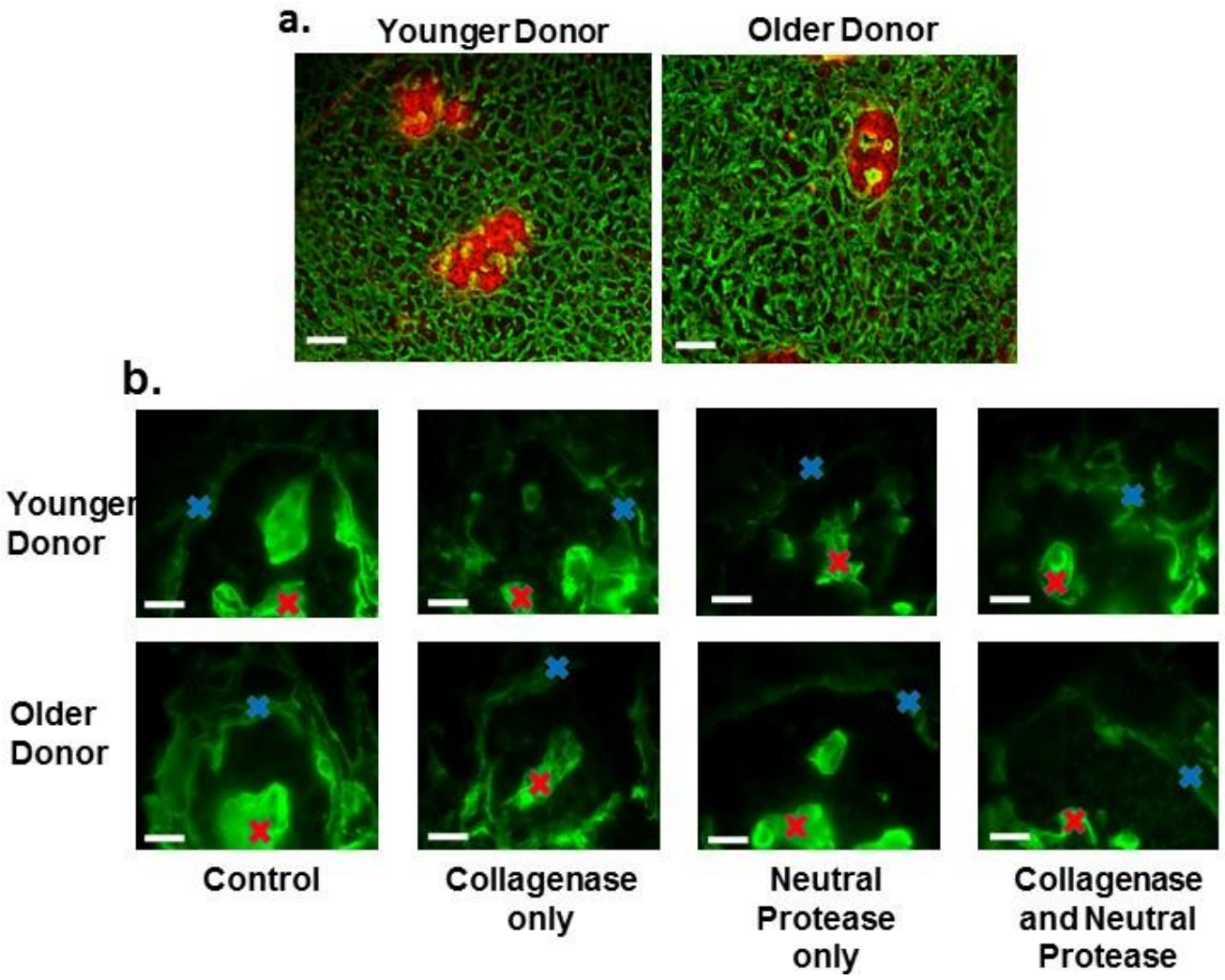


Figure 38: Acquirement of Raman spectra from enzyme treated pancreatic tissue sections

a. Representative immunofluorescent images of control tissue from younger and older donors at 10X, demonstrating identification of islets via positive insulin (red) and collagen IV (green) labelling

b. Representative focus of Raman laser on islet extracellular matrix, as identified by collagen IV, at 60X, following controlled enzyme induced digestion. The crosses depict the areas analysed for one Raman measurement, obtained from the islet peripheral (blue crosses) and the intra-islet region (red crosses). A minimum of 40 measurements were collected for each condition, from a minimum of two islets, for each donor.

Scale bars equal 100 µm (a), 30 µm (b).

RMS successfully revealed age related differences in enzyme induced ECM degradation, which was demonstrated through changes in spectral regions corresponding to ECM proteins (Figure 39). Treatment of pancreatic tissue sections with collagenase alone resulted in spectral changes that

were significantly different across the two age groups. These differences were reflected in the clear cluster separation of the two groups, in the scores displayed for PC-5 (p<0.001 for younger vs older PC-5 scores; Figure 39 a). The corresponding loading spectra included peaks at 758 cm^{-1} (unassigned peak), 1066 cm^{-1} (proline/saccharides), and 1296 cm^{-1} (CH_2 deformation) [352, 356, 362] (Figure 39 b).

Treatment of tissue sections with NP alone resulted in fewer age-related variations in the overall spectral composition. Although the cluster separation between the age groups was less pronounced, it was still significant (p<0.05 for younger vs older PC-5 scores; Figure 39 c). The corresponding PC-5 loading spectra identified peaks at 945 cm^{-1} (C-C backbone stretching) and 1444 cm^{-1} (CH_2 deformations proteins/collagen) [356] (Figure 39 d).

Combining collagenase with NP produced an age-related separation similar to that seen with collagenase treatment alone. The clustering was observed on the scores for PC-4 with the older donors centring towards the negative region of the scores plot (p<0.001 for younger vs older PC-4 scores; Figure 39 e). Peaks featured on the loading spectra included those at 945 cm^{-1}, 1066 cm^{-1}, 1296 cm^{-1} and 1444 cm^{-1} (Figure 39 f).

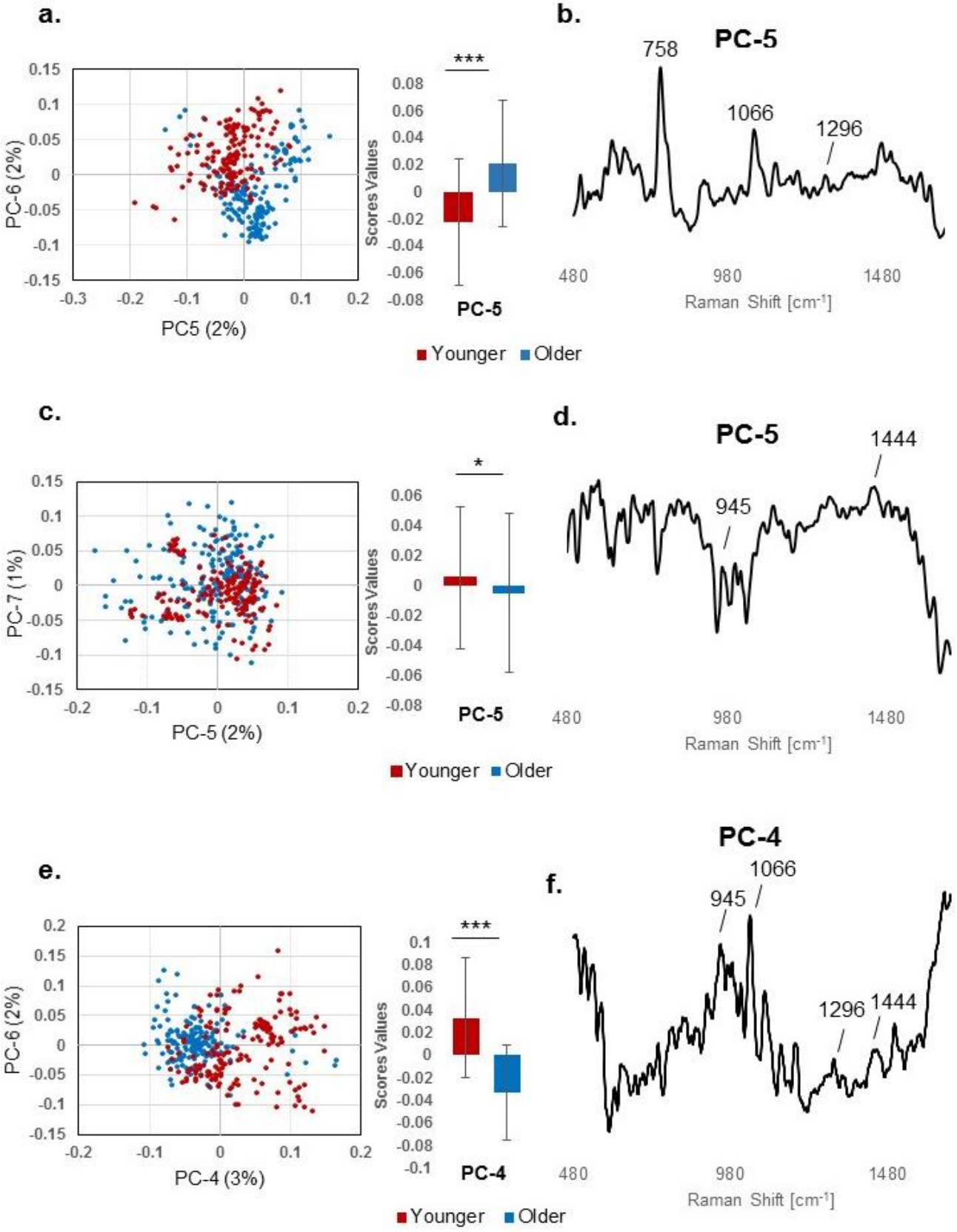


Figure 39: Principle Component Analysis (PCA) of age-related differences in the enzyme digestion of the ECM

a. PCA scores plot demonstrate donor age-related separation in collagenase treated tissues **b**. PC-5 indicates the main differences in the spectra responsible for the separation following collagenase

treatment **c.** donor age separation of Raman spectra acquired from neutral protease treated tissue was poor **d.** corresponding loading spectra for neutral protease treated tissue **e.** PCA scores plot display a good age related separation for tissue treated with collagenase and neutral protease combined **f.** PC-4 indicates main regions of spectral difference following treatment with the enzyme combination
Statistical analysis of scores was performed by Mann-Whitney U
* $p<0.05$
*** $p<0.001$

6.4 Discussion

The data presented in this Chapter demonstrates the feasibility of using RMS to monitor the digestion of the human pancreatic ECM from different aged donors. Donor age significantly affected ECM digestion, with the activity of collagenase altered to a greater extent than NP.

To determine if Raman could be used to resolve distinct matrix proteins on the basis of their distinct biochemical fingerprints, Raman measurements were obtained from purified matrix proteins collagens I, IV, VI and laminin. For collagens, the overall spectral compositions were similar to that described previously [347]. Despite the high degree of homogeneity, subtle spectral variations existed, including a peak shift in the region corresponding to proline. In native collagen, proline often occupies one of the amino acid positions in the tri-peptide repeat that represents the triple helical domain of collagen [209]. Therefore, peak shifts in this region likely result from structural differences in the collagenous domain between the different collagen subtypes. Although proline is present in laminin, its content is lower than in collagen [363]. A similar peak shift was observed in the region corresponding to general CH_2 deformation in proteins.

Subsequently, a series of proof of principle experiments were performed to determine if Raman could detect post-treatment changes in protein composition. This involved incubating the purified matrix proteins with the collagenase and NP blend utilised in the clinical isolation of human islets. The protein treatment occurred over a time course, and with the exception of collagen IV incubation for 30 minutes, all protein treatment spectra were significantly different from the respective controls. In the collagens, spectral regions affected by enzyme treatment corresponded

with CH deformations (1453cm^{-1}) and C-C stretching (940cm^{-1}), which represented general changes in collagen composition due to digestion. The subtle shifts in original peak positions were attributed to the enzyme treatment. Interestingly, post-enzyme treatment, the characteristic changes in the spectral profile of laminin varied drastically from the three collagens. Although this probably reflects differences in the native protein structure, it may also represent key differences in the action of specific enzyme components, as the digestion of laminin has been shown to be mediated by NP (demonstrated in Chapters 4 and 5 of this thesis).

Raman imaging was used to determine the anticipated Raman spectra for the pancreatic ECM associated with human islets. Based on the biochemical profile of the tissue, components that defined nuclei and the cytoplasm were successfully identified, with the corresponding Raman spectra featuring characteristic DNA and general protein/lipid peaks respectively. In addition, an ECM specific component was identified. The optical biochemical fingerprint of this component displayed a remarkable degree of homogeneity to the corresponding collagen IV specific immunostaining. After establishing the anticipated Raman spectra for ECM proteins in the human pancreas, RMS was used to study the effect of donor age on the enzyme induced digestion of the human pancreatic ECM. As previous studies have reported the importance of attenuating the ratio of collagenase and NP for enhancing islet isolation outcomes from younger donors [98, 99], the action of both enzymes was studied separately, as well as in combination. Implementation of a unique spectral processing step, which involved normalising the spectra obtained from the enzyme treated tissues to the respective controls, ensured that differences in ECM biochemical composition following enzyme treatment were attributable to age-related variations in enzyme action. Variations in peak positions between the reference standards and the tissue can be attributed to the structural differences between purified proteins and those found *in vivo* [352].

Treatment of tissue sections with the blends containing collagenase resulted in the most pronounced age-related affects, though independent treatment with NP also resulted in significant

differences in protein digestion between the two age groups. These results suggest that age-related differences in ECM digestion are more dependent on collagenase action, than of NP. Supporting this theory is a study from the Baylor group, which showed that doubling the concentration of collagenase when isolating islets from donors <30 years old leads to a significantly lower proportion of trapped islets [98]. Alternatively, recent data obtained from a trisected pancreas model demonstrated that increasing content of NP, but not collagenase, significantly reduced the number of trapped islets and enhanced post-purification islet recovery in donors aged <35 [99]. However, unlike in the study described in this Chapter, the measurement of age-related digestion based differences did not occur at the level of the ECM. In addition, it should be reiterated that the direct addition of enzyme to slides does not mimic the clinically utilised intra-ductal infusion of collagenase based enzymes [60].

Investigations into the enzymatic digestion of the pancreatic ECM have previously been restricted to immuno-staining methods. This has involved the incubation of small pancreatic tissue sections in various enzyme solutions, followed by cryosectioning and immunolabelling [320], or alternatively, the direct application of enzymes to sectioned tissue, as described in Chapters 4 and 5. Loss of protein is in turn determined based on a reduction in the staining intensity of specific ECM proteins. Antibody-based detection offers a straightforward approach for investigating specific protein molecules. However, when measuring the enzymatic breakdown of proteins, the assessment of digestion is confined to the regional epitope recognised by the antibody, and thus assumes uniform degradation between this region and the rest of the molecule. Although this issue can be at least partially overcome by employing polyclonal antibodies, that are capable of detecting more than one regional epitope, Raman offers a label-free approach for monitoring protein digestion [346]. Immunostaining is utilised, but only for the purpose of directing the laser spot, with measurements obtained based on the presence of ubiquitously expressed molecular bonds within the protein [346]. This molecular-based assessment arguably makes RMS a more robust way for monitoring protein digestion, which is not restricted by local antibody binding. Furthermore, the

data presented within this Chapter substantiate the usefulness of utilising RMS for detecting donor related differences in the digestion of the peri-islet matrix in the context of human islet isolation.

The main limitation of this study is that the digestion of specific ECM proteins could not be studied. This was partly due to the homogeneity of the spectra obtained from the reference standards, which restricted the identification of unique identifying spectral components for each of the four reference proteins. Furthermore, the ECM networks within tissues are highly heterogeneous. *In vivo* the ECM is composed of a highly integrated structure, whereby multiple proteins are intercalated to form tight networks [174]. This makes it technically challenging to target single proteins within this matrix with the laser spot. Indeed, using conventional histology, it has previously been shown that key matrix proteins are differentially digested during human islet isolation [112]. Although this highlights the importance of characterising the digestion of specific proteins, it is first important to characterise the effect of age on the combined matrix, as found *in situ.*

6.5 Conclusion

The experiments outlined in this Chapter have confirmed the feasiblity of using RMS to study the impact of donor-age on the digestion of ECM proteins at the islet-exocrine interface. This is the first study to use RMS in this way. Raman imaging can be successfully used to create biochemical images of the pancreatic ECM, in a label free manner. RMS clearly demonstrated that the ECM at the islet-exocrine interface is differentially digested with respect to donor age. The results indicated that donor age affected the action of collagenase to a greater extent than NP. In contrast to coventional histology, Raman measurements are reflective of the molecular bonds within the tissue. ECM characterisation is therefore not limited to pre-selected proteins, and digestion assessment is not restricted to the protein regions that are recognised by antibodies. Future work should focus on

using RMS to identify specific matrix proteins within the extracellular pancreas. This may be made possible by utilising alternative reference standards.

CHAPTER 7

Conclusions and Proposed Future Research

7.1 Introduction

Only 53% of the pancreases that are processed for clinical islet isolation in the UK result in transplantable islet yields (Chapter 2). Poor isolation outcomes can be partly attributed to the variability of the pancreas digestion phase of the procedure, which relies on the ability of commercially available enzymes to digest the ECM that surrounds islets. The enzyme blends that are used currently have been developed empirically, without a detailed understanding of the structure and composition of the substrate on which they are acting (i.e. the ECM). The creation of substrate-specific enzyme blends has the potential to enhance pancreas digestion and the overall success of islet isolation.

The studies detailed in this thesis aimed to determine how the molecular structure of the human pancreas is influenced by age and how this affects islet isolation, and ultimately islet transplantation, outcomes. To answer this question, the research contained within this thesis was divided into three key parts:

- Firstly, the impact of donor factors on isolation and transplantation outcomes were analysed, using a UK dataset (Chapter 2)

- The significant impact that donor age had on islet yield, prompted detailed investigations into the effect of donor age on molecular structure of the human pancreas. The composition of the native pancreatic ECM was defined using high-throughput proteomics, and age-dependent differences in matrix protein expression were reported (Chapter 3)

- Subsequent studies aimed to define the effect of donor age on the digestion of the human pancreas, following treatment with the specific components of collagenase-based blends. ECM digestion was measured by a novel slide-based digestion assay (Chapters 4 and 5). In addition,

Raman microspectroscopy (RMS) was used as a label-free detection approach to measure age-related differences in matrix digestion (Chapter 6).

The purpose of this Chapter is to combine the findings of each of these topics in a conclusive way, whilst highlighting avenues for future and ongoing research.

7.2 Thesis Conclusions

7.2.1 Overall Thesis Conclusions

The table below summarises the main findings of each thesis Chapter.

Chapter	Main findings
2. Analysis of donor factors on islet isolation and transplantation outcomes in the UK	• In the UK, the outcome of human islet isolation is affected by several donor factors including: age, BMI, the presence of hypertension, and a history of smoking • 8% of the overall variation in yield (IEQ) can be explained by donor/pancreas factors • An increasing donor age has a significantly positive impact on isolation outcome • There is an inverse trend between donor age and post-transplantation graft function • Enhancing isolation outcomes from younger donors will improve the utilisation of these metabolically potent islets for clinical transplantation.
3. The impact of donor age on ECM protein expression in the native pancreas	• The human pancreas contains 81 ECM proteins (core proteins, and matrix affiliated) • Donor age significantly affects the expression of 20 of these proteins. 19 proteins are more highly expressed in younger donors, including collagens I, IV, V, laminins α2-3, Y1 and nidogen-1 • Collagen IV was most significantly affected, as confirmed by ECM specific ELISAs.
4. Development and validation of a slide-based assay for monitoring enzyme digestion of pancreatic tissue	• Development of a slide-based digestion assay allowed age-dependent differences in the digestion of specific ECM proteins at the islet-exocrine interface to be explored • Excellent assay reproducibility was demonstrated; the results of the image analysis were independent of the researcher or operating system • Laminin α5 was resistant to collagenase treatment, but was significantly digested upon treatment with

	neutral protease (NP). Protein loss was significantly greater in older donors. This age-related difference was lost upon combining the two enzymes • Independent treatment with collagenase or NP resulted in a significantly greater loss of collagen IV in the older donor group. These age-related affects were ameliorated upon combining the two enzymes.
5. The impact of donor age on enzymatic digestion of ECM proteins; a study using slide-based digestion and conventional immuno-labelling	• The assay developed and validated in Chapter 4 was used to investigate the impact of age on the digestion of other key pancreatic ECM proteins • Digestion of the islet basement membrane (BM) is primarily facilitated by NP. NP should be used with caution, to avoid excessive loss of BM integrity, which may result in islet fragmentation • Interstitial matrix (IM) proteins (i.e. collagens I, V and VI) were more resistant to digestion than those found in the BM. Further investigation is warranted to enhance the digestion of these proteins • Collagen VI was resistant to digestion in younger donors, but was significantly reduced in older donors, when using a standard collagenase and NP blend.
6. Raman microspectroscopy: a novel approach for comparing digestion of the pancreatic ECM in different aged donors	• Raman microspectroscopy (RMS) can be used to study the impact of donor age on the digestion of ECM proteins at the islet-exocrine interface, in a marker-independent manner • High quality biochemical images of the pancreatic ECM can be generated, in a label-free manner • The pancreatic matrisome is significantly differentially digested with respect to donor age. The action of collagenase is affected to a greater extent than NP.

Table 18: Summary of main thesis findings

7.2.2 The Influence of Donor Factors on Isolation and Transplantation Outcomes

In the UK, the outcome of human islet isolation is affected by several donor factors. In Chapter 2, multivariate models were created to determine which donor factors have the greatest impact on isolation outcome. Outcome was investigated both in terms of obtaining a transplantable yield (≥200K IEQ), in addition to the total number of IEQs that could be recovered. Factors contained within the final multivariate models included: age, BMI, the presence of hypertension and a history of smoking.

Chapter 2 confirmed that there is a significantly positive impact between donor age and isolation outcome [215, 222, 224, 249]. However, there was also an inverse (though non-significant) trend between donor age and post-transplantation graft function, in agreement with previous reports [102, 242]. Improving isolation outcomes from younger donors will improve the utilisation of these metabolically potent islets for clinical transplantation.

Suboptimal pancreas digestion in younger donors is the primary reason for poor isolation outcomes from this donor type. Therefore, the experiments performed within this thesis aimed to confirm if the molecular structure of the human pancreas changes with age, and determine how this affects pancreas digestion with collagenase-based enzymes.

7.2.3 Aging Causes Molecular Changes in the Composition of the Native Human Pancreas

At the time of the study being performed, the data presented in Chapter 3 represented the first use of high-throughput proteomics to characterise the human pancreatic matrix at the molecular level. However, following the completion of these experiments, researchers at the University of Wisconsin published results from their own characterisation of the pancreatic ECM, using high-throughput proteomics [163]. However, Sackett *et al.* did not investigate how ECM composition is influenced by donor age.

Chapter 3 demonstrated that the pancreatic ECM is a highly intricate structure, containing 81 matrix, and matrix affiliated proteins. The complexity of the matrix highlights the pitfalls of selecting individual proteins for investigation [99, 171], prior to understanding how age influences the overall structure of the native pancreas. Although the original experimental design incorporated tissue samples from 10 donors, issues with 4 of the samples reduced the analysis to 3 donors in each age group. To validate the proteomics results, ELISAs were performed on a larger cohort (n=12 in each group). The proteomics studies demonstrated that the expression of 20

proteins were significantly influenced by age, with the α 4 and 5 chains of collagen IV most affected. Although the ELISA validation studies confirmed an age-related decrease in collagen IV content, they failed to corroborate the decline in several other proteins, including collagen I and nidogen. This most likely reflects the reduced sensitivity of ELISAs, as compared to high-throughput proteomics-based methodologies. Ultimately, to increase the statistical power of the experiments, the proteomic cohort should be extended to a minimum of 10 donors, as originally intended.

Although post-translational modifications (PTM) were included in the proteomics run for protein identification purposes, the frequency of these modifications in each donor age group were not examined. PTMs are known to alter the structure and stability of proteins. For example, hydroxylation of the proline residues within collagen increases the overall thermal stability of the triple helix [364]. Indeed, hydroxylation deficiency has been shown to increase susceptibility of proteins to collagenase degradation *in vitro* [365]. Therefore, hydroxylation may also influence the digestibility of the pancreatic ECM during the human islet isolation process. Further work should aim to examine how PTMs in the pancreatic matrisome change overtime, and how this influences protein digestion. The frequency of PTMs can be determined by comparing the ratio of modified peptides to their unmodified counterparts, following LC-MS/MS. Studies involving the assessment of protein crosslinking (i.e. via Lysyl Oxidase [207]) would also be of interest. These suggested investigations would enhance and compliment the current studies, which have focused on age-related changes in protein quantity, by incorporating information regarding changes in protein structure.

Finally, as discussed in Chapter 3, further work should explore technologies that enable characterisation of the ECM in different morphological pancreatic regions. Both laser capture microdissection (LCM) and mass spec imaging could be used for this purpose [307, 316]. The ECM at the islet-exocrine interface is of particular importance for islet isolation, as efficient cleavage of this structure is required to release free islets. Investigations should aim to specifically characterise

the ECM within this region, determining if it is compositionally distinct from the ECM in other areas of the pancreas.

Overall, Chapter 3 demonstrated that the composition of the pancreatic ECM changes with age. Specifically, ageing results in a quantitative decline in a number of key matrix proteins including the highly significant loss of collagen IV. The increased matrix content in younger donors may be responsible for the suboptimal digestion outcomes in donors of this type, when using standard enzyme blends.

7.2.4 The Pancreatic ECM is Differentially Digested Depending on Donor Age

Subsequent experiments aimed to determine how age-related changes in the pancreatic matrix influence its breakdown with collagenase-based enzymes. Chapter 4 describes the development and validation of a simple slide-based digestion assay, which enabled the digestion of specific matrix proteins to be studied. Following the treatment of pancreatic tissue sections with enzyme components at clinically relevant concentrations, the assay uses conventional immunostaining to detect changes in the signal intensity of specific proteins at the islet-exocrine interface. Using this assay, Chapter 5 investigated the influence of collagenase and neutral protease (NP) treatment on a number of basement membrane (BM) and interstitial (IM) proteins. Interestingly, these studies revealed that IM proteins, including collagen I, V and VI, are more resistant to digestion than a number of BM proteins, such as laminins, collagen IV and perlecan. Furthermore, the digestion of most BM proteins is facilitated primarily by NP, as opposed to collagenase. The islet BM has been shown to be important for conferring structural support and regulating insulin secretion [166, 366]. Therefore, excessive loss of BM may result in islet fragmentation, reduced viability and insulin secretion. Interestingly, all three of these factors have been observed in islets, following isolation with increased protease [149, 156, 330]. Use of supplementary proteases, such as NP, varies drastically across different islet centres, with reported doses ranging from 50 to 400 U of NP [112,

161]. For the first time, the data presented within this thesis provides molecular based evidence for why protease dose should be selected with caution.

Although the optimal concentration of protease remains to be determined, islet groups have reported the benefits of using increased protease when extracting islets from younger donors [99, 247]. These attenuations have been based on empirical observations, as opposed to understanding how age influences the enzymatic breakdown of the ECM. This thesis has provided the first evidence to demonstrate that donor age influences the digestion of the human pancreas at the molecular level. Following independent treatment with either collagenase or NP, several age related differences were observed. However, with the exception of collagen VI, these differences were lost upon combining the enzymes to mimic the clinical enzyme composition. Collagen VI was resistant to digestion in younger donors, though it was significantly digested following 5 minutes of treatment in the older donor group. This is somewhat surprising, given the fact that the quantity of collagen VI did not vary with age in the native pancreas (Chapter 3, and Hughes *et al.* [171]). On the other hand, although collagen IV concentrations were significantly elevated in younger donor pancreases, age did not influence the digestion of collagen IV following treatment with collagenase and NP combined. Therefore, these results suggest that age-related differences in protein digestion cannot be explained by protein quantity alone. This further emphasises the need for future research to focus on age-related differences in protein structure.

Chapter 6 explored using Raman microspectroscopy (RMS) as a novel and marker-independent technology for characterising age-related differences in the digestion of the ECM. RMS was intended to be used as a confirmation technique, to validate the results of Chapters from 4 and 5, which had monitored protein digestion on the basis of antibody-based detection. Unlike with immunostaining, RMS identifies proteins at the level of their molecular bonds. RMS detected significant differences in matrix digestion between younger and older donors. Donor age affected the activity of collagenase to a greater extent that NP. However, despite incorporating the

appropriate protein reference standards, RMS was unable to attribute these age-related differences in matrix breakdown to specific proteins.

On the basis of these results, it is advisable for future studies to study how collagenase attenuation may improve islet yields from younger donors, as opposed to restricting investigations to NP. Indeed, increasing collagenase concentration has previously been shown to be a viable strategy when isolating islets from younger donors [98]. By increasing the concentration of collagenase, it may also be possible to decrease (or restrict) the amount of protease used in islet isolation, thus preventing excessive islet fragmentation, caused by the loss of the islet BM. Collagenase was also shown to digest purified collagen VI to a greater extent that NP. Increasing collagenase concentration in younger donors may help to enhance the digestion of collagen VI, which is currently resistant to digestion in this donor type.

7.3 Ongoing work

7.3.1 Development of a Simple '*in vitro*' Islet Isolation Technique

The slide-based digestion assay developed and validated in this thesis allows ECM digestion to be assessed following treatment with specific components of commercially available enzyme blends. By utilising small amounts of tissue and enzymes, multiple enzyme components can be tested on a single pancreas. The technique is therefore invaluable when studying the influence of donor factors on protein digestibility. However, it is important to note that these studies do not replicate the delivery of enzymes into the pancreas by ductal infusion. Although enzymes were used at clinically relevant concentrations, when adding enzyme directly to a cryosection, the tissue surface area exposed to the enzyme is likely higher than what occurs during intra-ductal infusion. It is also not possible to examine the impact that different enzymes combinations have on the number of islets that can be retrieved, or the influence on islet quality.

To overcome these issues, an '*in vitro*' islet isolation technique is currently in development. This procedure enables the isolation of islets from pancreatic tissue segments, following intra-ductal enzyme infusion, and allows different enzyme combinations to be tested on the same pancreas. Unlike previously described techniques, where two or more isolations are performed sequentially [99], multiple isolations can be performed in tandem. Performing simultaneous isolations not only limits the confounding influence of cold ischemic duration, but also substantially reduces the time and labour involved. Importantly, the method has enabled investigations into the effect of different enzyme concentrations on matrix protein digestion.

Briefly, the proposed assay involves dissecting the trimmed pancreas into 30g segments and infusing each section with a distinct enzyme blend (Figure 40 a). Islet isolations on each segment are then performed in tandem. Digestion occurs in 50ml Falcon tubes, as opposed to using a Ricordi chamber and a continuous digestion circuit. HBSS and 3 steel Ricordi balls are placed in each tube, pre-warmed to 37°C with HBSS (Figure 40 b). At specific time points, samples can be taken from the tubes and stained with dithizone, to assess the progression of digestion. Research samples can also be collected, to enable the digestion of specific matrix proteins to be assessed. At regular intervals the digest is passed through a specialised funnel with a wire mesh (Figure 40 c). The wire mesh has a pore size of approximately 500µm, which allows cleaved islets to pass through the funnel and into the collection beaker and chilled human albumin (20%), whereas undigested tissue is returned to the falcon tube. Collected islets are incubated in UW at 4°C for a minimum of 30 minutes.

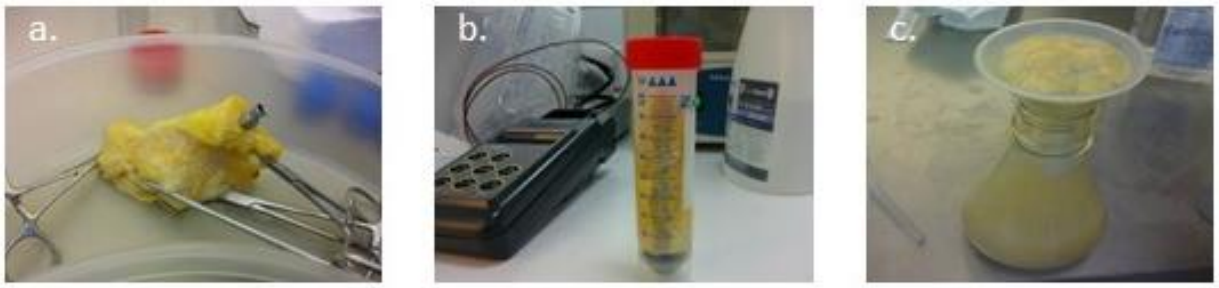


Figure 40: Pancreas infusion and digestion
a) 30g of pancreatic tissue are infused with a specified enzyme blend (2000 Units of collagenase with either 50 or 200 Units of neutral protease)
b) Tissue is cut into smaller pieces and placed into a falcon tube containing Ricordi steel balls and preheated HBSS. Shaking occurs every 1-2 minutes. Samples are taken to monitor digest progression every 3 minutes (via dithizone staining)
c) Periodically, tissue is passed through a mesh filter (500µm). This allows cleaved islets to pass through into the chilled human albumin (20%) below. Undigested tissue is returned to the falcon tube.

Islets are purified on a discontinuous gradient, which uses 4 distinct densities of Biocoll (Figure 41 a). Following centrifugation, layers are separated on a volume basis (Figure 41 b, c) and the purity determined by dithizone assessment. Fractions with the highest purities are combined. The resulting islets are counted, and viability and glucose stimulated insulin secretion (GSIS) assessments are performed. The concentration of ECM proteins within the digestion supernatants (taken from the Falcon tube during pancreas digestion), and on the isolated islets, are determined by ELISA.

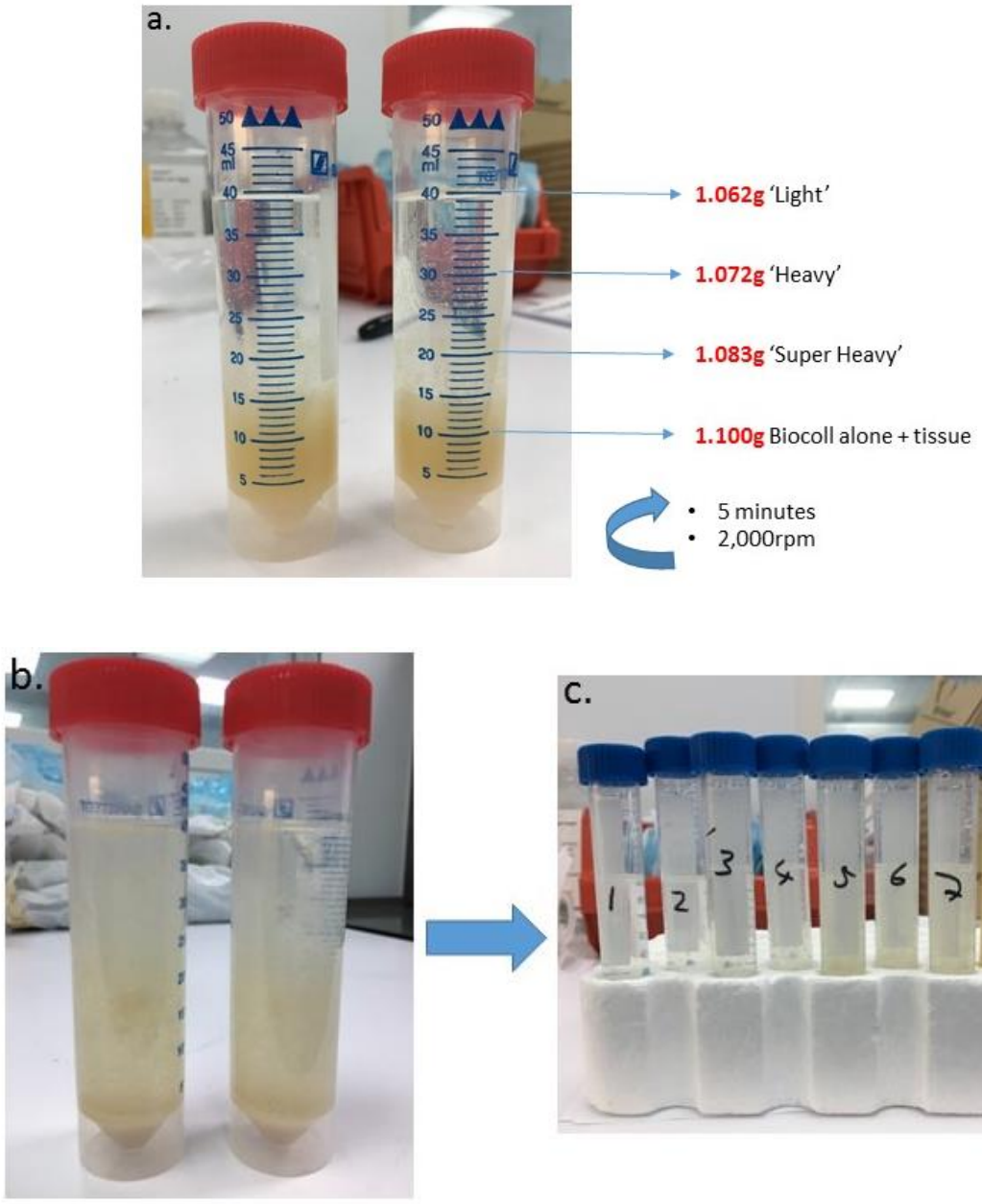


Figure 41: Discontinuous density gradient purification

a) Digest is mixed with Biocoll and layered at the bottom of a falcon tube. 3 additional density gradients are layered on top of this. Specific densities are made by mixing Biocoll (1.1g/ml) with UW

b) Tubes are centrifuged for 5 minutes at 2,000 rpm with no brake. This results in the density related separation observed in the image

c) Post-centrifugation layers were divided, 5ml at a time, and placed into chilled HBSS. Each of the 8 fractions were then sampled for purity assessment, using dithizone. Samples with the optimal purity were combined. Islets were then counted (both IEQ and islet particle) and viability assessment was performed (Ethidium bromide/fluorescein diacetate)

At the time of writing this thesis, islets from 4 donors have been isolated using this technique (Table 19). In all cases, the pancreas had been retrieved but rejected for clinical use, and thus made available for research. For each pancreas, two isolations were performed, with 50 and 200 U of NP respectively. A standard collagenase dose was maintained for both isolations (i.e. approx. 2000 U). For each isolation, the anatomical region of the pancreas receiving each enzyme blend was alternated.

Donor (Oxford Reference)	Age	BMI	Donor type	CIT (hours)	Cause of Death	Reason Declined Clinically
HP1752	37	24	DCD	12	Hypoxic Brain Damage	Small & poorly perfused
HP1758	56	24	DBD	9.5	Intracranial haemorrhage	Pancreas too small for clinical
HP1813	44	36	DCD	6	Hypoxic Brain Damage	Fatty
HP1821	19	21	DBD	8	Hypoxic Brain Damage	Past medical history (Heroin Overdose)

Table 19: Details of current cohort for *in vitro* islet isolation experiments
DBD; Donation after brain death
DCD; Donation after cardiac death

Although experiments are still ongoing, current results suggest that there is a two-fold increase in the number of islets that can be recovered following isolation with 200 U, as opposed to 50 U, of NP (Figure 42 a). However, the overall islet size distribution (i.e. IEQ) is halved following treatment with the elevated NP (Figure 42 b). Although the viability of the preparations was not affected by protease dose (Figure 42 c), purity tended to be higher in the 50 U group (Figure 42 d). Interestingly, after 24 hours of culture, the number of islets recovered was over 50% lower in the 200 U group

(Figure 42 e), and there was a decline in viability (Figure 42 f). The viability in the 50 U group increased after the 24-hour culture period (Figure 42 f). These data suggest that using increased protease results in islet fragmentation (and thus the production of smaller islets). Statistics were performed, however none of the observed differences reached statistical significance, presumably due to currently low sample numbers.

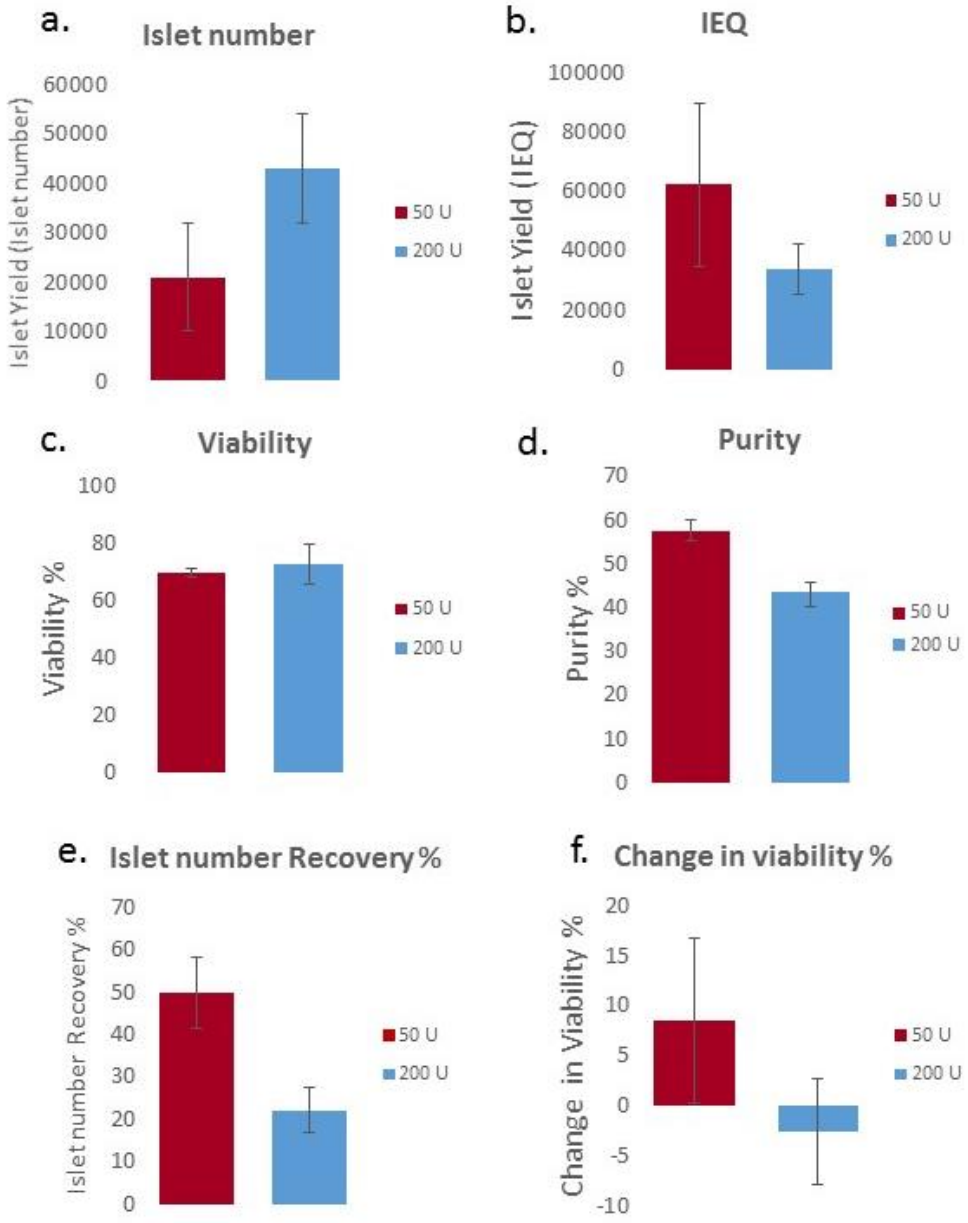


Figure 42: Results from islet isolations using 50 vs 200 Units of neutral protease (NP)
a) The number of islet particles produced following isolation with 200 Units (U) of NP was higher than that produced with 50 U

b) The number of IEQs produced following isolation with 50 U of NP was higher than that produced with 200 U
c) The viability of islets produced when isolating with 50 or 200 U of NP was similar
d) Purity was higher in the 50 U group than the 200 U group
e) After 24 hours of culture, the recovery of islet particles was approx. 30% lower in the 200 U NP group
f) Whilst 24 hours of culture led to an improved viability of the 50 U group, there was a decline in viability in the 200 U group.
Although Witney-Mann U tests were performed, none of the changes noted above reached statistical significance. Mean and standard deviations are displayed (n=4).

So far, increased islet fragmentation with higher protease dose cannot be explained by the enhanced loss of laminin, which was measured from the supernatants collected during pancreas digestion (Figure 43 a). Although the amount of laminin associated with islets decreased after 24 hours of culture, this was independent of the amount of protease used in the isolation process (Figure 43 b). GSIS was performed for all isolations/conditions post-isolation and following 24 hours of islet culture, however, the insulin concentration in each sample is yet to be determined by ELISA.

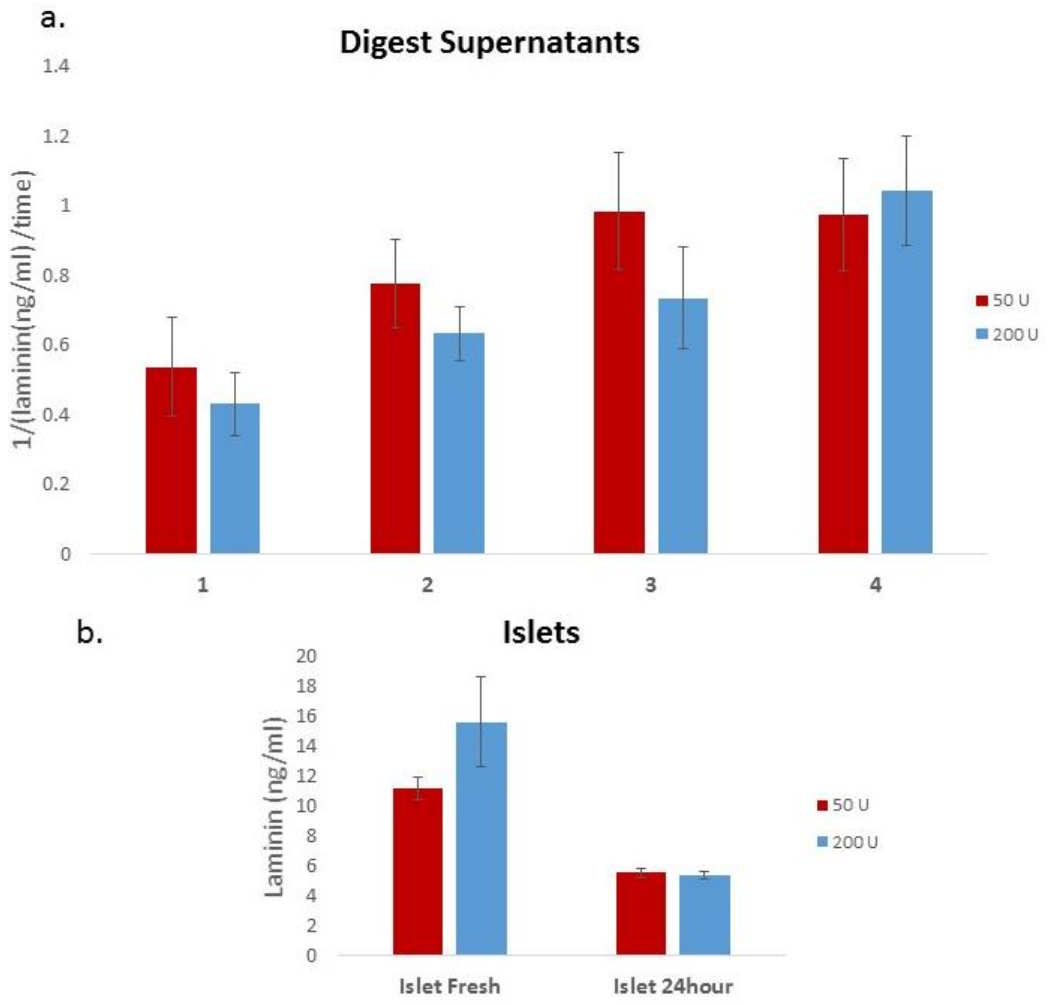


Figure 43: Influence of neutral protease (NP) concentration on the digestion of laminin during islet isolation and on post-isolated islets

a) Digestion samples were collected approximately every 5 minutes (1-4). The laminin concentration in the samples was determined by ELISA and normalised to the time at which the sample was taken (calculated from the commencement of digestion). NP concentration did not significantly affect the amount of laminin released into the digestion supernatant. However, after 15 minutes, digestion of laminin with 50 U of NP appeared to stabilise, where with 200 U it continued to increase up until around 20 minutes

b) More laminin remained on islets following digestion with 200 U of NP. This did not reach statistical significance. By 24 hours, the amount of laminin on islets had reduced, and was comparable between the two protease groups.

Mean and standard deviations are displayed (n=4).

The continuation of this study is restricted by the availability of pancreases for research. Based on organ availability, these experiments aim to determine how different enzyme combinations affect the digestion of pancreases from different aged donors. In addition to the impact on islet yield, the effect of enzyme attenuations on the digestion of specific matrix proteins, in addition to laminin,

are being assessed (through the digest supernatants). The GSIS assays aim to determine how changes to enzyme blends impact islet function.

Based on the molecular digestion data provided within this thesis, these experiments are continuing with a stronger focus on the attenuation of collagenase dose and investigating how increased collagenase could enhance isolation outcomes from younger donors.

7.3.2 Collection of Undigested Pancreatic Tissue from Clinical Isolations

Finally, undigested pancreatic tissue is currently being collected from the Ricordi chamber, at the end of the pancreas digestion phase, of clinical islet isolations. So far, 55 samples have been collected (but only 12 of these samples are from donors ≤35 years old). The aim is to assay this tissue and determine if the matrix that remains following digestion differs between younger and older donors.

7.4 Conclusion

This thesis contains the first study to use high-throughput proteomics to demonstrate that donor age affects the composition of the native pancreatic ECM. Pancreases from younger donors were shown to contain significantly higher amounts of specific matrix proteins, possibly explaining poorer pancreas digestion outcomes from this donor type. Age-related differences in the digestion of matrix proteins at the molecular level were also confirmed. The data suggests that age affects the action of collagenase, to a greater extent than NP. The experiments are the first to investigate the impact of donor factors on the composition and digestion of the human pancreas at the molecular level. These findings, along with the recommendations for future work, will assist the development of novel donor-specific enzymes, thereby increasing the overall success of islet isolation and benefiting many people with Type 1 Diabetes Mellitus worldwide.

References

[1] American Diabetes Association. Diagnosis and classification of diabetes mellitus. Diabetes care 2004;27 Suppl 1:S5-S10.

[2] IDF Diabetes Atlas, 7th edition. Brussels, Belgium: International Diabetes Federation, 2015.

[3] Hex N, Bartlett C, Wright D, Taylor M, Varley D. Estimating the current and future costs of Type 1 and Type 2 diabetes in the UK, including direct health costs and indirect societal and productivity costs. Diabetic medicine : a journal of the British Diabetic Association 2012;29:855-62.

[4] Best CH. The internal secretion of the pancreas. Canadian Medical Association journal 1962;87:1046-51.

[5] Orchard TJ, Costacou T, Kretowski A, Nesto RW. Type 1 diabetes and coronary artery disease. Diabetes care 2006;29:2528-38.

[6] The Diabetes Control and Complications Trial Research Group. The effect of intensive treatment of diabetes on the development and progression of long-term complications in insulin-dependent diabetes mellitus.. The New England journal of medicine 1993;329:977-86.

[7] Langerhans P. Beiträge zur mikroskopichen Anatomie der Bauchspeicheldrüse (dissertation) 1869.

[8] Leung PS, Ip SP. Pancreatic acinar cell: its role in acute pancreatitis. The international journal of biochemistry & cell biology 2006;38:1024-30.

[9] Ionescu-Tirgoviste C, Gagniuc PA, Gubceac E, Mardare L, Popescu I, Dima S, et al. A 3D map of the islet routes throughout the healthy human pancreas. Scientific reports 2015;5:14634.

[10] Pisania A, Weir GC, O'Neil JJ, Omer A, Tchipashvili V, Lei J, et al. Quantitative analysis of cell composition and purity of human pancreatic islet preparations. Laboratory investigation; a journal of technical methods and pathology 2010;90:1661-75.

[11] Cabrera O, Berman DM, Kenyon NS, Ricordi C, Berggren PO, Caicedo A. The unique cytoarchitecture of human pancreatic islets has implications for islet cell function. Proceedings of the National Academy of Sciences of the United States of America 2006;103:2334-9.

[12] In't Veld P, Marichal M. Microscopic anatomy of the human islet of Langerhans. Advances in experimental medicine and biology 2010;654:1-19.

[13] Briant L, Salehi A, Vergari E, Zhang Q, Rorsman P. Glucagon secretion from pancreatic alpha-cells. Upsala journal of medical sciences 2016;121:113-9.

[14] Brereton MF, Vergari E, Zhang Q, Clark A. Alpha-, Delta- and PP-cells: Are They the Architectural Cornerstones of Islet Structure and Co-ordination? The journal of histochemistry and cytochemistry : official journal of the Histochemistry Society 2015;63:575-91.

[15] Brissova M, Shiota M, Nicholson WE, Gannon M, Knobel SM, Piston DW, et al. Reduction in pancreatic transcription factor PDX-1 impairs glucose-stimulated insulin secretion. The Journal of biological chemistry 2002;277:11225-32.

[16] Brissova M, Fowler MJ, Nicholson WE, Chu A, Hirshberg B, Harlan DM, et al. Assessment of human pancreatic islet architecture and composition by laser scanning confocal microscopy. The journal of histochemistry and cytochemistry : official journal of the Histochemistry Society 2005;53:1087-97.

[17] Wang X, Misawa R, Zielinski MC, Cowen P, Jo J, Periwal V, et al. Regional differences in islet distribution in the human pancreas--preferential beta-cell loss in the head region in patients with type 2 diabetes. PloS one 2013;8:e67454.

[18] Lewis MP, Reber HA, Ashley SW. Pancreatic blood flow and its role in the pathophysiology of pancreatitis. The Journal of surgical research 1998;75:81-9.

[19] Jansson L. Glucose stimulation of pancreatic islet blood flow by redistribution of the blood flow within the whole pancreatic gland. Pancreas 1988;3:409-12.

[20] Lifson N, Kramlinger KG, Mayrand RR, Lender EJ. Blood flow to the rabbit pancreas with special reference to the islets of Langerhans. Gastroenterology 1980;79:466-73.

[21] Henderson JR, Moss MC. A morphometric study of the endocrine and exocrine capillaries of the pancreas. Quarterly journal of experimental physiology 1985;70:347-56.

[22] Rodriguez-Diaz R, Abdulreda MH, Formoso AL, Gans I, Ricordi C, Berggren PO, et al. Innervation patterns of autonomic axons in the human endocrine pancreas. Cell metabolism 2011;14:45-54.

[23] Fajans SS, Bell GI, Polonsky KS. Molecular mechanisms and clinical pathophysiology of maturity-onset diabetes of the young. The New England journal of medicine 2001;345:971-80.

[24] Nolan CJ, Prentki M. The islet beta-cell: fuel responsive and vulnerable. Trends in endocrinology and metabolism: TEM 2008;19:285-91.

[25] McCulloch LJ, van de Bunt M, Braun M, Frayn KN, Clark A, Gloyn AL. GLUT2 (SLC2A2) is not the principal glucose transporter in human pancreatic beta cells: implications for understanding genetic association signals at this locus. Molecular genetics and metabolism 2011;104:648-53.

[26] De Vos A, Heimberg H, Quartier E, Huypens P, Bouwens L, Pipeleers D, et al. Human and rat beta cells differ in glucose transporter but not in glucokinase gene expression. The Journal of clinical investigation 1995;96:2489-95.

[27] Matschinsky F, Liang Y, Kesavan P, Wang L, Froguel P, Velho G, et al. Glucokinase as pancreatic beta cell glucose sensor and diabetes gene. The Journal of clinical investigation 1993;92:2092-8.

[28] Ashcroft FM, Harrison DE, Ashcroft SJ. Glucose induces closure of single potassium channels in isolated rat pancreatic beta-cells. Nature 1984;312:446-8.

[29] Rorsman P, Ashcroft FM, Trube G. Single Ca channel currents in mouse pancreatic B-cells. Pflugers Archiv : European journal of physiology 1988;412:597-603.

[30] Ammala C, Eliasson L, Bokvist K, Larsson O, Ashcroft FM, Rorsman P. Exocytosis elicited by action potentials and voltage-clamp calcium currents in individual mouse pancreatic B-cells. The Journal of physiology 1993;472:665-88.

[31] Meier JJ, Veldhuis JD, Butler PC. Pulsatile insulin secretion dictates systemic insulin delivery by regulating hepatic insulin extraction in humans. Diabetes 2005;54:1649-56.

[32] Tokarz VL, MacDonald PE, Klip A. The cell biology of systemic insulin function. The Journal of cell biology 2018;217:2273-89.

[33] Diabetes Complications Trial /Epidemiology of Diabetes Complications Study Research. Intensive Diabetes Treatment and Cardiovascular Outcomes in Type 1 Diabetes: The DCCT/EDIC Study 30-Year Follow-up. Diabetes care 2016;39:686-93.

[34] Campbell L, Pepper T, Shipman K. HbA1c: a review of non-glycaemic variables. Journal of clinical pathology 2019;72:12-9.

[35] The Diabetes Control and Complications Trial Research Group. Hypoglycemia in the Diabetes Control and Complications Trial. Diabetes 1997;46:271-86.

[36] Heller S, White D, Lee E, Lawton J, Pollard D, Waugh N, et al. A cluster randomised trial, cost-effectiveness analysis and psychosocial evaluation of insulin pump therapy compared with multiple injections during flexible intensive insulin therapy for type 1 diabetes: the REPOSE Trial. Health technology assessment 2017;21:1-278.

[37] Garg SK, Weinzimer SA, Tamborlane WV, Buckingham BA, Bode BW, Bailey TS, et al. Glucose Outcomes with the In-Home Use of a Hybrid Closed-Loop Insulin Delivery System in Adolescents and Adults with Type 1 Diabetes. Diabetes technology & therapeutics 2017;19:155-63.

[38] Kovatchev BP, Renard E, Cobelli C, Zisser HC, Keith-Hynes P, Anderson SM, et al. Safety of outpatient closed-loop control: first randomized crossover trials of a wearable artificial pancreas. Diabetes care 2014;37:1789-96.

[39] Esposito S, Santi E, Mancini G, Rogari F, Tascini G, Toni G, et al. Efficacy and safety of the artificial pancreas in the paediatric population with type 1 diabetes. Journal of translational medicine 2018;16:176.

[40] Russell SJ, Hillard MA, Balliro C, Magyar KL, Selagamsetty R, Sinha M, et al. Day and night glycaemic control with a bionic pancreas versus conventional insulin pump therapy in preadolescent children with type 1 diabetes: a randomised crossover trial. The lancet Diabetes & endocrinology 2016;4:233-43.

[41] Basu A, Dube S, Slama M, Errazuriz I, Amezcua JC, Kudva YC, et al. Time lag of glucose from intravascular to interstitial compartment in humans. Diabetes 2013;62:4083-7.

[42] Berg AK, Norgaard K, Thyssen JP, Zachariae C, Hommel E, Rytter K, et al. Skin Problems Associated with Insulin Pumps and Sensors in Adults with Type 1 Diabetes: A Cross-Sectional Study. Diabetes technology & therapeutics 2018;20:475-82.

[43] Johnson PR, Jones KE. Pancreatic islet transplantation. Seminars in pediatric surgery 2012;21:272-80.

[44] Mittal S, Johnson P, Friend P. Pancreas transplantation: solid organ and islet. Cold Spring Harbor perspectives in medicine 2014;4:a015610.

[45] Kelly WD, Lillehei RC, Merkel FK, Idezuki Y, Goetz FC. Allotransplantation of the pancreas and duodenum along with the kidney in diabetic nephropathy. Surgery 1967;61:827-37.

[46] Lillehei RC, Simmons RL, Najarian JS, Goetz FC. Pancreatico-duodenal and renal allotransplantation in juvenile onset, insulin dependent, diabetes mellitus with terminal nephropathy. Studium generale; Zeitschrift fur die Einheit der Wissenschaften im Zusammenhang ihrer Begriffsbildungen und Forschungsmethoden 1970;23:392-408.

[47] NHSBT. Annual Report on Pancreas and Islet Transplantation. Report for 2017/2018. 2018.

[48] Gruessner AC, Gruessner RW. Pancreas transplant outcomes for United States and non United States cases as reported to the United Network for Organ Sharing and the International Pancreas Transplant Registry as of December 2011. Clinical transplants 2012:23-40.

[49] Gaba RC, Garcia-Roca R, Oberholzer J. Pancreatic islet cell transplantation: an update for interventional radiologists. Journal of vascular and interventional radiology : JVIR 2012;23:583-94; quiz 94.

[50] Scharp DW, Lacy PE, Santiago JV, McCullough CS, Weide LG, Falqui L, et al. Insulin independence after islet transplantation into type I diabetic patient. Diabetes 1990;39:515-8.

[51] Brooks AM, Walker N, Aldibbiat A, Hughes S, Jones G, de Havilland J, et al. Attainment of metabolic goals in the integrated UK islet transplant program with locally isolated and transported preparations. American journal of transplantation 2013;13:3236-43.

[52] Moassesfar S, Masharani U, Frassetto LA, Szot GL, Tavakol M, Stock PG, et al. A Comparative Analysis of the Safety, Efficacy, and Cost of Islet Versus Pancreas Transplantation in Nonuremic Patients With Type 1 Diabetes. American journal of transplantation 2016;16:518-26.

[53] Shapiro AM, Pokrywczynska M, Ricordi C. Clinical pancreatic islet transplantation. Nature reviews Endocrinology 2017;13:268-77.

[54] Hellerstroem C. A Method for the Microdissection of Intact Pancreatic Islets of Mammals. Acta endocrinologica 1964;45:122-32.

[55] Moskalewski S. Isolation and Culture of the Islets of Langerhans of the Guinea Pig. General and comparative endocrinology 1965;5:342-53.

[56] Lacy PE, Kostianovsky M. Method for the isolation of intact islets of Langerhans from the rat pancreas. Diabetes 1967;16:35-9.

[57] Lindall A, Steffes M, Sorenson R. Immunoassayable insulin content of subcellular fractions of rat islets. Endocrinology 1969;85:218-23.

[58] Scharp DW, Kemp CB, Knight MJ, Ballinger WF, Lacy PE. The use of ficoll in the preparation of viable islets of langerhans from the rat pancreas. Transplantation 1973;16:686-9.

[59] Horaguchi A, Merrell RC. Preparation of viable islet cells from dogs by a new method. Diabetes 1981;30:455-8.

[60] Gray DW, McShane P, Grant A, Morris PJ. A method for isolation of islets of Langerhans from the human pancreas. Diabetes 1984;33:1055-61.

[61] Scharp DW, Lacy PE, Finke E, Olack B. Low-temperature culture of human islets isolated by the distention method and purified with Ficoll or Percoll gradients. Surgery 1987;102:869-79.

[62] Alderson D, Kneteman NM, Scharp DW. The isolation of purified human islets of Langerhans. Transplantation proceedings 1987;19:916-7.

[63] Ricordi C, Finke EH, Dye ES, Socci C, Lacy PE. Automated isolation of mouse pancreatic islets. Transplantation 1988;46:455-7.

[64] Faradji A, Andreu G, Pillier-Loriette C, Bohbot A, Nicod A, Autran B, et al. Separation of mononuclear bone marrow cells using the Cobe 2997 blood cell separator. Vox sanguinis 1988;55:133-8.

[65] Vesilind GW, Simpson MB, Shifman MA, Colman RE, Kao KJ. Evaluation of a centrifugal blood cell processor for washing platelet concentrates. Transfusion 1988;28:46-51.

[66] Lake SP, Bassett PD, Larkins A, Revell J, Walczak K, Chamberlain J, et al. Large-scale purification of human islets utilizing discontinuous albumin gradient on IBM 2991 cell separator. Diabetes 1989;38 Suppl 1:143-5.

[67] Robertson GS, Chadwick DR, Contractor H, James RF, London NJ. The optimization of large-scale density gradient isolation of human islets. Acta diabetologica 1993;30:93-8.

[68] Ballinger WF, Lacy PE. Transplantation of intact pancreatic islets in rats. Surgery 1972;72:175-86.

[69] Kemp CB, Knight MJ, Scharp DW, Ballinger WF, Lacy PE. Effect of transplantation site on the results of pancreatic islet isografts in diabetic rats. Diabetologia 1973;9:486-91.

[70] Kretschmer GJ, Sutherland DE, Matas AJ, Steffes MW, Najarian JS. The dispersed pancreas: transplantation without islet purification in totally pancreatectomized dogs. Diabetologia 1977;13:495-502.

[71] Scharp DW, Murphy JJ, Newton WT, Ballinger WF, Lacy PE. Transplantation of islets of Langerhans in diabetic rhesus monkeys. Surgery 1975;77:100-5.

[72] Sutherland DE, Matas AJ, Goetz FC, Najarian JS. Transplantation of dispersed pancreatic islet tissue in humans: autografts and allografts. Diabetes 1980;29 Suppl 1:31-44.

[73] Warnock GL, Kneteman NM, Ryan E, Seelis RE, Rabinovitch A, Rajotte RV. Normoglycaemia after transplantation of freshly isolated and cryopreserved pancreatic islets in type 1 (insulin-dependent) diabetes mellitus. Diabetologia 1991;34:55-8.

[74] Socci C, Falqui L, Davalli AM, Ricordi C, Braghi S, Bertuzzi F, et al. Fresh human islet transplantation to replace pancreatic endocrine function in type 1 diabetic patients. Report of six cases. Acta diabetologica 1991;28:151-7.

[75] Shapiro AM, Lakey JR, Ryan EA, Korbutt GS, Toth E, Warnock GL, et al. Islet transplantation in seven patients with type 1 diabetes mellitus using a glucocorticoid-free immunosuppressive regimen. The New England journal of medicine 2000;343:230-8.

[76] Shapiro AM, Ricordi C, Hering BJ, Auchincloss H, Lindblad R, Robertson RP, et al. International trial of the Edmonton protocol for islet transplantation. The New England journal of medicine 2006;355:1318-30.

[77] Reno CM, Litvin M, Clark AL, Fisher SJ. Defective counterregulation and hypoglycemia unawareness in diabetes: mechanisms and emerging treatments. Endocrinology and metabolism clinics of North America 2013;42:15-38.

[78] Leitao CB, Tharavanij T, Cure P, Pileggi A, Baidal DA, Ricordi C, et al. Restoration of hypoglycemia awareness after islet transplantation. Diabetes care 2008;31:2113-5.

[79] O'Connell PJ, Holmes-Walker DJ, Goodman D, Hawthorne WJ, Loudovaris T, Gunton JE, et al. Multicenter Australian trial of islet transplantation: improving accessibility and outcomes. American journal of transplantation 2013;13:1850-8.

[80] Hering BJ, Clarke WR, Bridges ND, Eggerman TL, Alejandro R, Bellin MD, et al. Phase 3 Trial of Transplantation of Human Islets in Type 1 Diabetes Complicated by Severe Hypoglycemia. Diabetes care 2016;39:1230-40.

[81] Thompson DM, Meloche M, Ao Z, Paty B, Keown P, Shapiro RJ, et al. Reduced progression of diabetic microvascular complications with islet cell transplantation compared with intensive medical therapy. Transplantation 2011;91:373-8.

[82] CITR. CITR 10th Annual Report. 2017. p. 328.

[83] Lablanche S, Borot S, Wojtusciszyn A, Bayle F, Tetaz R, Badet L, et al. Five-Year Metabolic, Functional, and Safety Results of Patients With Type 1 Diabetes Transplanted With Allogenic Islets Within the Swiss-French GRAGIL Network. Diabetes care 2015;38:1714-22.

[84] Barbaro B, Salehi P, Wang Y, Qi M, Gangemi A, Kuechle J, et al. Improved human pancreatic islet purification with the refined UIC-UB density gradient. Transplantation 2007;84:1200-3.

[85] Ichii H, Pileggi A, Molano RD, Baidal DA, Khan A, Kuroda Y, et al. Rescue purification maximizes the use of human islet preparations for transplantation. American journal of transplantation 2005;5:21-30.

[86] Miyagi-Shiohira C, Kobayashi N, Saitoh I, Watanabe M, Noguchi Y, Matsushita M, et al. The Evaluation of Islet Purification Methods That Use Large Bottles to Create a Continuous Density Gradient. Cell medicine 2017;9:45-51.

[87] Ricordi C, Alejandro R, Zeng Y, Tzakis A, Casavilla A, Jaffe R, et al. Human islet isolation and purification from pediatric-age donors. Transplantation proceedings 1991;23:783-4.

[88] Miki A, Ricordi C, Messinger S, Yamamoto T, Mita A, Barker S, et al. Toward improving human islet isolation from younger donors: rescue purification is efficient for trapped islets. Cell transplantation 2009;18:13-22.

[89] Brandhorst D, Brandhorst H, Acreman S, Schive SW, Bjornson Scholz H, Johnson PRV. Hypoxia-Induced Damage in Human Islets Is Reduced With the Use of Mesenchymal Stem Cell-Preconditioned Medium. Transplantation proceedings 2017;49:2330-2.

[90] Noguchi H, Miyagi-Shiohira C, Kurima K, Kobayashi N, Saitoh I, Watanabe M, et al. Islet Culture/Preservation Before Islet Transplantation. Cell medicine 2015;8:25-9.

[91] Daoud J, Petropavlovskaia M, Rosenberg L, Tabrizian M. The effect of extracellular matrix components on the preservation of human islet function in vitro. Biomaterials 2010;31:1676-82.

[92] Arzouni AA, Vargas-Seymour A, Rackham CL, Dhadda P, Huang GC, Choudhary P, et al. Mesenchymal stromal cells improve human islet function through released products and extracellular matrix. Clinical science 2017;131:2835-45.

[93] Ludwig B, Reichel A, Steffen A, Zimerman B, Schally AV, Block NL, et al. Transplantation of human islets without immunosuppression. Proceedings of the National Academy of Sciences of the United States of America 2013;110:19054-8.

[94] Syed F, Bugliani M, Novelli M, Olimpico F, Suleiman M, Marselli L, et al. Conformal coating by multilayer nano-encapsulation for the protection of human pancreatic islets: In-vitro and in-vivo studies. Nanomedicine : nanotechnology, biology, and medicine 2018;14:2191-203.

[95] Teramura Y, Kaneda Y, Iwata H. Islet-encapsulation in ultra-thin layer-by-layer membranes of poly(vinyl alcohol) anchored to poly(ethylene glycol)-lipids in the cell membrane. Biomaterials 2007;28:4818-25.

[96] Marek N, Krzystyniak A, Ergenc I, Cochet O, Misawa R, Wang LJ, et al. Coating human pancreatic islets with CD4(+)CD25(high)CD127(-) regulatory T cells as a novel approach for the local immunoprotection. Annals of surgery 2011;254:512-8; discussion 8-9.

[97] Krzystyniak A, Golab K, Witkowski P, Trzonkowski P. Islet cell transplant and the incorporation of Tregs. Current opinion in organ transplantation 2014;19:610-5.

[98] Shimoda M, Noguchi H, Naziruddin B, Fujita Y, Chujo D, Takita M, et al. Improved method of human islet isolation for young donors. Transplantation proceedings 2010;42:2024-6.

[99] Loganathan G, Venugopal S, Narayanan S, Tweed B, Goedde MA, Gunaratnam B, et al. Improved recovery of human islets from young donor pancreases utilizing increased protease dose to collagenase for digesting peri-islet extracellular matrix. American journal of transplantation 2019;19:831-43.

[100] Stahle M, Foss A, Gustafsson B, Lempinen M, Lundgren T, Rafael E, et al. Clostripain, the Missing Link in the Enzyme Blend for Efficient Human Islet Isolation. Transplantation direct 2015;1:e19.

[101] Balamurugan AN, Naziruddin B, Lockridge A, Tiwari M, Loganathan G, Takita M, et al. Islet product characteristics and factors related to successful human islet transplantation from the Collaborative Islet Transplant Registry (CITR) 1999-2010. American journal of transplantation 2014;14:2595-606.

[102] Niclauss N, Bosco D, Morel P, Demuylder-Mischler S, Brault C, Milliat-Guittard L, et al. Influence of donor age on islet isolation and transplantation outcome. Transplantation 2011;91:360-6.

[103] Webb MA, Illouz SC, Pollard CA, Gregory R, Mayberry JF, Tordoff SG, et al. Islet auto transplantation following total pancreatectomy: a long-term assessment of graft function. Pancreas 2008;37:282-7.

[104] Thomas FT, Contreras JL, Bilbao G, Ricordi C, Curiel D, Thomas JM. Anoikis, extracellular matrix, and apoptosis factors in isolated cell transplantation. Surgery 1999;126:299-304.

[105] Shimoda M, Itoh T, Iwahashi S, Takita M, Sugimoto K, Kanak MA, et al. An effective purification method using large bottles for human pancreatic islet isolation. Islets 2012;4:398-404.

[106] Shimoda M, Itoh T, Sugimoto K, Takita M, Chujo D, Iwahashi S, et al. An effective method to release human islets from surrounding acinar cells with agitation in high osmolality solution. Transplantation proceedings 2011;43:3161-6.

[107] Kerr-Conte J, Pattou F, Xia Y, Proye C, Lefebvre J. Simple Dithizone-Stained Multilayer Test for Selection of Density Gradient before Human Islet Mass Purification. Transplantation proceedings 1994;26:3413-5.

[108] Noguchi H, Naziruddin B, Shimoda M, Chujo D, Takita M, Sugimoto K, et al. A Combined Continuous Density/Osmolality Gradient for Supplemental Purification of Human Islets. Cell medicine 2012;3:33-41.

[109] Kin T, Senior P, O'Gorman D, Richer B, Salam A, Shapiro AM. Risk factors for islet loss during culture prior to transplantation. Transplant international : official journal of the European Society for Organ Transplantation 2008;21:1029-35.

[110] Ichii H, Sakuma Y, Pileggi A, Fraker C, Alvarez A, Montelongo J, et al. Shipment of human islets for transplantation. American journal of transplantation 2007;7:1010-20.

[111] Bucher P, Bosco D, Mathe Z, Matthey-Doret D, Buhler AL, Morel P, et al. Human islet culture before transplantation: Influence of medium on islet apoptosis and function. Transplantation 2003;76:S65-S6.

[112] Cross SE, Vaughan RH, Willcox AJ, McBride AJ, Abraham AA, Han B, et al. Key matrix proteins within the pancreatic islet basement membrane are differentially digested during human islet isolation. American journal of transplantation 2016;17:451-61.

[113] Kerr-Conte J, Vandewalle B, Moerman E, Lukowiak B, Gmyr V, Arnalsteen L, et al. Upgrading pretransplant human islet culture technology requires human serum combined with media renewal. Transplantation 2010;89:1154-60.

[114] Avgoustiniatos ES, Scott WE, 3rd, Suszynski TM, Schuurman HJ, Nelson RA, Rozak PR, et al. Supplements in human islet culture: human serum albumin is inferior to fetal bovine serum. Cell transplantation 2012;21:2805-14.

[115] Itoh T, Sugimoto K, Takita M, Shimoda M, Chujo D, SoRelle JA, et al. Low temperature condition prevents hypoxia-induced islet cell damage and HMGB1 release in a mouse model. Cell transplantation 2012;21:1361-70.

[116] Noguchi H, Naziruddin B, Jackson A, Shimoda M, Ikemoto T, Fujita Y, et al. Low-temperature preservation of isolated islets is superior to conventional islet culture before islet transplantation. Transplantation 2010;89:47-54.

[117] Sezai S, Sakurabayashi S, Yamamoto Y, Morita T, Hirano M, Oka H. Hepatic arterial and portal venous oxygen content and extraction in liver cirrhosis. Liver 1993;13:31-5.

[118] Llacua A, de Haan BJ, Smink SA, de Vos P. Extracellular matrix components supporting human islet function in alginate-based immunoprotective microcapsules for treatment of diabetes. Journal of biomedical materials research Part A 2016;104:1788-96.

[119] Llacua LA, de Haan BJ, de Vos P. Laminin and collagen IV inclusion in immunoisolating microcapsules reduces cytokine-mediated cell death in human pancreatic islets. Journal of tissue engineering and regenerative medicine 2018;12:460-7.

[120] Yeung TY, Seeberger KL, Kin T, Adesida A, Jomha N, Shapiro AM, et al. Human mesenchymal stem cells protect human islets from pro-inflammatory cytokines. PloS one 2012;7:e38189.

[121] Schive SW, Mirlashari MR, Hasvold G, Wang M, Josefsen D, Gullestad HP, et al. Human Adipose-Derived Mesenchymal Stem Cells Respond to Short-Term Hypoxia by Secreting Factors Beneficial for Human Islets In Vitro and Potentiate Antidiabetic Effect In Vivo. Cell medicine 2017;9:103-16.

[122] Desai T, Shea LD. Advances in islet encapsulation technologies. Nature reviews Drug discovery 2017;16:367.

[123] Issa F, Robb RJ, Wood KJ. The where and when of T cell regulation in transplantation. Trends Immunol 2013;34:107-13.

[124] Vignali DAA, Collison LW, Workman CJ. How regulatory T cells work. Nat Rev Immunol 2008;8:523-32.

[125] Xiao F, Ma L, Zhao M, Huang G, Mirenda V, Dorling A, et al. Ex vivo expanded human regulatory T cells delay islet allograft rejection via inhibiting islet-derived monocyte chemoattractant protein-1 production in CD34+ stem cells-reconstituted NOD-scid IL2rgammanull mice. PloS one 2014;9:e90387.

[126] Golab K, Kizilel S, Bal T, Hara M, Zielinski M, Grose R, et al. Improved coating of pancreatic islets with regulatory T cells to create local immunosuppression by using the biotin-polyethylene glycol-succinimidyl valeric acid ester molecule. Transplantation proceedings 2014;46:1967-71.

[127] Schuetz C, Markmann JF. Islet cell transplant: Update on current clinical trials. Current transplantation reports 2016;3:254-63.

[128] Carlsson PO, Espes D, Sedigh A, Rotem A, Zimerman B, Grinberg H, et al. Transplantation of macroencapsulated human islets within the bioartificial pancreas betaAir to patients with type 1 diabetes mellitus. American journal of transplantation 2018;18:1735-44.

[129] Tomei AA, Manzoli V, Fraker CA, Giraldo J, Velluto D, Najjar M, et al. Device design and materials optimization of conformal coating for islets of Langerhans. Proceedings of the National Academy of Sciences of the United States of America 2014;111:10514-9.

[130] Chicheportiche D, Reach G. In vitro kinetics of insulin release by microencapsulated rat islets: effect of the size of the microcapsules. Diabetologia 1988;31:54-7.

[131] Buchwald P, Tamayo-Garcia A, Manzoli V, Tomei AA, Stabler CL. Glucose-stimulated insulin release: Parallel perifusion studies of free and hydrogel encapsulated human pancreatic islets. Biotechnology and bioengineering 2018;115:232-45.

[132] Salvay DM, Rives CB, Zhang X, Chen F, Kaufman DB, Lowe WL, Jr., et al. Extracellular matrix protein-coated scaffolds promote the reversal of diabetes after extrahepatic islet transplantation. Transplantation 2008;85:1456-64.

[133] Weber LM, Anseth KS. Hydrogel encapsulation environments functionalized with extracellular matrix interactions increase islet insulin secretion. Matrix biology 2008;27:667-73.

[134] Bandiera A. Transglutaminase-catalyzed preparation of human elastin-like polypeptide-based three-dimensional matrices for cell encapsulation. Enzyme and microbial technology 2011;49:347-52.

[135] Barnett MJ, Zhai X, LeGatt DF, Cheng SB, Shapiro AM, Lakey JR. Quantitative assessment of collagenase blends for human islet isolation. Transplantation 2005;80:723-8.

[136] Hanley SC, Paraskevas S, Rosenberg L. Donor and isolation variables predicting human islet isolation success. Transplantation 2008;85:950-5.

[137] Harrington DJ. Bacterial collagenases and collagen-degrading enzymes and their potential role in human disease. Infection and immunity 1996;64:1885-91.

[138] Woolley DE, Glanville RW, Roberts DR, Evanson JM. Purification, characterization and inhibition of human skin collagenase. The Biochemical journal 1978;169:265-76.

[139] Gross J, et al. Animal Collagenases: Specificity Of Action, And Structures Of The Subsrate Cleavage Site. Biochemical and biophysical research communications 1974;61:605-12.

[140] French MF, Mookhtiar KA, Van Wart HE. Limited proteolysis of type I collagen at hyperreactive sites by class I and II Clostridium histolyticum collagenases: complementary digestion patterns. Biochemistry 1987;26:681-7.

[141] Maclennan JD, Mandl I, Howes EL. Bacterial digestion of collagen. The Journal of clinical investigation 1953;32:1317-22.

[142] Bond MD, Van Wart HE. Purification and separation of individual collagenases of Clostridium histolyticum using red dye ligand chromatography. Biochemistry 1984;23:3077-85.

[143] Eckhard U, Schonauer E, Nuss D, Brandstetter H. Structure of collagenase G reveals a chew-and-digest mechanism of bacterial collagenolysis. Nature structural & molecular biology 2011;18:1109-14.

[144] Chung L, Dinakarpandian D, Yoshida N, Lauer-Fields JL, Fields GB, Visse R, et al. Collagenase unwinds triple-helical collagen prior to peptide bond hydrolysis. The EMBO journal 2004;23:3020-30.

[145] Stultz CM. Localized unfolding of collagen explains collagenase cleavage near imino-poor sites. Journal of molecular biology 2002;319:997-1003.

[146] Nerenberg PS, Salsas-Escat R, Stultz CM. Do collagenases unwind triple-helical collagen before peptide bond hydrolysis? Reinterpreting experimental observations with mathematical models. Proteins 2008;70:1154-61.

[147] Fields GB. A model for interstitial collagen catabolism by mammalian collagenases. Journal of theoretical biology 1991;153:585-602.

[148] Overall CM. Molecular determinants of metalloproteinase substrate specificity: matrix metalloproteinase substrate binding domains, modules, and exosites. Molecular biotechnology 2002;22:51-86.

[149] Wolters GH, Vos-Scheperkeuter GH, van Deijnen JH, van Schilfgaarde R. An analysis of the role of collagenase and protease in the enzymatic dissociation of the rat pancreas for islet isolation. Diabetologia 1992;35:735-42.

[150] Johnson PR, White SA, London NJ. Collagenase and human islet isolation. Cell transplantation 1996;5:437-52.

[151] Toledo-Pereyra LH, Zammit M, Malcom S, Cromwell P. Inconsistency of collagenase activity for isolation of islet cells for transplantation. Transplantation 1979;27:222.

[152] Boehringer. A purified mixture of collagenase and two other proteases obtained from Clostridium histolyticum Patent number: WO 96/00283. 1995.

[153] Fetterhoff TJ, Cavanagh TJ, Wile KJ, Wright MJ, Dwulet FE, Gill J, et al. Human pancreatic dissociation using a purified enzyme blend. Transplantation proceedings 1995;27:3282-3.

[154] Lakey JR, Cavanagh TJ, Zieger MA, Wright M. Evaluation of a purified enzyme blend for the recovery and function of canine pancreatic islets. Cell transplantation 1998;7:365-72.

[155] Linetsky E, Bottino R, Lehmann R, Alejandro R, Inverardi L, Ricordi C. Improved human islet isolation using a new enzyme blend, liberase. Diabetes 1997;46:1120-3.

[156] Bucher P, Mathe Z, Morel P, Bosco D, Andres A, Kurfuest M, et al. Assessment of a novel two-component enzyme preparation for human islet isolation and transplantation. Transplantation 2005;79:91-7.

[157] Caballero-Corbalan J, Friberg AS, Brandhorst H, Nilsson B, Andersson HH, Felldin M, et al. Vitacyte collagenase HA: a novel enzyme blend for efficient human islet isolation. Transplantation 2009;88:1400-2.

[158] Goto M, Eich TM, Felldin M, Foss A, Kallen R, Salmela K, et al. Refinement of the automated method for human islet isolation and presentation of a closed system for in vitro islet culture. Transplantation 2004;78:1367-75.

[159] Brandhorst H, Raemsch-Guenther N, Raemsch C, Friedrich O, Huettler S, Kurfuerst M, et al. The ratio between collagenase class I and class II influences the efficient islet release from the rat pancreas. Transplantation 2008;85:456-61.

[160] Kin T, Zhai X, Murdoch TB, Salam A, Shapiro AM, Lakey JR. Enhancing the success of human islet isolation through optimization and characterization of pancreas dissociation enzyme. American journal of transplantation 2007;7:1233-41.

[161] Balamurugan AN, Breite AG, Anazawa T, Loganathan G, Wilhelm JJ, Papas KK, et al. Successful Human Islet Isolation and Transplantation Indicating the Importance of Class 1 Collagenase and Collagen Degradation Activity Assay. Transplantation 2010;89:954-61.

[162] Brandhorst H, Kurfurst M, Johnson PR, Korsgren O, Brandhorst D. Comparison of Neutral Proteases and Collagenase Class I as Essential Enzymes for Human Islet Isolation. Transplantation direct 2016;2:e47.

[163] Sackett SD, Tremmel DM, Ma F, Feeney AK, Maguire RM, Brown ME, et al. Extracellular matrix scaffold and hydrogel derived from decellularized and delipidized human pancreas. Scientific reports 2018;8:10452.

[164] Cheng JY, Raghunath M, Whitelock J, Poole-Warren L. Matrix components and scaffolds for sustained islet function. Tissue engineering Part B, Reviews 2011;17:235-47.

[165] Halfter W, Candiello J, Hu H, Zhang P, Schreiber E, Balasubramani M. Protein composition and biomechanical properties of in vivo-derived basement membranes. Cell adhesion & migration 2013;7:64-71.

[166] Nikolova G, Jabs N, Konstantinova I, Domogatskaya A, Tryggvason K, Sorokin L, et al. The vascular basement membrane: a niche for insulin gene expression and Beta cell proliferation. Developmental cell 2006;10:397-405.

[167] Virtanen I, Banerjee M, Palgi J, Korsgren O, Lukinius A, Thornell LE, et al. Blood vessels of human islets of Langerhans are surrounded by a double basement membrane. Diabetologia 2008;51:1181-91.

[168] Takada Y, Ye X, Simon S. The integrins. Genome biology 2007;8:215.

[169] Ris F, Hammar E, Bosco D, Pilloud C, Maedler K, Donath MY, et al. Impact of integrin-matrix matching and inhibition of apoptosis on the survival of purified human beta-cells in vitro. Diabetologia 2002;45:841-50.

[170] Wang RN, Paraskevas S, Rosenberg L. Characterization of integrin expression in islets isolated from hamster, canine, porcine, and human pancreas. The journal of histochemistry and cytochemistry : official journal of the Histochemistry Society 1999;47:499-506.

[171] Hughes SJ, Clark A, McShane P, Contractor HH, Gray DW, Johnson PR. Characterisation of collagen VI within the islet-exocrine interface of the human pancreas: implications for clinical islet isolation? Transplantation 2006;81:423-6.

[172] Kennedy RH, Bockman DE, Uscanga L, Choux R, Grimaud JA, Sarles H. Pancreatic extracellular matrix alterations in chronic pancreatitis. Pancreas 1987;2:61-72.

[173] Korpos E, Kadri N, Kappelhoff R, Wegner J, Overall CM, Weber E, et al. The peri-islet basement membrane, a barrier to infiltrating leukocytes in type 1 diabetes in mouse and human. Diabetes 2013;62:531-42.

[174] Timpl R, Brown JC. Supramolecular assembly of basement membranes. BioEssays : news and reviews in molecular, cellular and developmental biology 1996;18:123-32.

[175] Ninomiya Y, Kagawa M, Iyama K, Naito I, Kishiro Y, Seyer JM, et al. Differential expression of two basement membrane collagen genes, COL4A6 and COL4A5, demonstrated by immunofluorescence staining using peptide-specific monoclonal antibodies. The Journal of cell biology 1995;130:1219-29.

[176] Ortega N, Werb Z. New functional roles for non-collagenous domains of basement membrane collagens. Journal of cell science 2002;115:4201-14.

[177] Kuhn K, Glanville RW, Babel W, Qian RQ, Dieringer H, Voss T, et al. The structure of type IV collagen. Annals of the New York Academy of Sciences 1985;460:14-24.

[178] Dixit SN, Mainardi CL, Beachey EH, Kang AH. 7S domain constitutes the amino-terminal end of type IV collagen: an immunochemical study. Collagen and related research 1983;3:263-9.

[179] Timpl R, Wiedemann H, van Delden V, Furthmayr H, Kuhn K. A network model for the organization of type IV collagen molecules in basement membranes. European journal of biochemistry 1981;120:203-11.

[180] Kalluri R. Basement membranes: structure, assembly and role in tumour angiogenesis. Nature reviews Cancer 2003;3:422-33.

[181] Kaido T, Yebra M, Cirulli V, Montgomery AM. Regulation of human beta-cell adhesion, motility, and insulin secretion by collagen IV and its receptor alpha1beta1. The Journal of biological chemistry 2004;279:53762-9.

[182] Vandenberg P, Kern A, Ries A, Luckenbill-Edds L, Mann K, Kuhn K. Characterization of a type IV collagen major cell binding site with affinity to the alpha 1 beta 1 and the alpha 2 beta 1 integrins. The Journal of cell biology 1991;113:1475-83.

[183] Stendahl JC, Kaufman DB, Stupp SI. Extracellular matrix in pancreatic islets: relevance to scaffold design and transplantation. Cell transplantation 2009;18:1-12.

[184] Engel J, Odermatt E, Engel A, Madri JA, Furthmayr H, Rohde H, et al. Shapes, domain organizations and flexibility of laminin and fibronectin, two multifunctional proteins of the extracellular matrix. Journal of molecular biology 1981;150:97-120.

[185] Burgeson RE, Chiquet M, Deutzmann R, Ekblom P, Engel J, Kleinman H, et al. A new nomenclature for the laminins. Matrix biology 1994;14:209-11.

[186] Aumailley M, Bruckner-Tuderman L, Carter WG, Deutzmann R, Edgar D, Ekblom P, et al. A simplified laminin nomenclature. Matrix biology 2005;24:326-32.

[187] Hohenester E, Yurchenco PD. Laminins in basement membrane assembly. Cell adhesion & migration 2013;7:56-63.

[188] Paulsson M, Deutzmann R, Timpl R, Dalzoppo D, Odermatt E, Engel J. Evidence for coiled-coil alpha-helical regions in the long arm of laminin. The EMBO journal 1985;4:309-16.

[189] Timpl R, Tisi D, Talts JF, Andac Z, Sasaki T, Hohenester E. Structure and function of laminin LG modules. Matrix Biology 2000;19:309-17.

[190] Ott U, Odermatt E, Engel J, Furthmayr H, Timpl R. Protease resistance and conformation of laminin. European journal of biochemistry 1982;123:63-72.

[191] Kohfeldt E, Sasaki T, Gohring W, Timpl R. Nidogen-2: a new basement membrane protein with diverse binding properties. Journal of molecular biology 1998;282:99-109.

[192] Hogan BL, Cooper AR, Kurkinen M. Incorporation into Reichert's membrane of laminin-like extracellular proteins synthesized by parietal endoderm cells of the mouse embryo. Developmental biology 1980;80:289-300.

[193] Fox JW, Mayer U, Nischt R, Aumailley M, Reinhardt D, Wiedemann H, et al. Recombinant nidogen consists of three globular domains and mediates binding of laminin to collagen type IV. The EMBO journal 1991;10:3137-46.

[194] Reinhardt D, Mann K, Nischt R, Fox JW, Chu ML, Krieg T, et al. Mapping of nidogen binding sites for collagen type IV, heparan sulfate proteoglycan, and zinc. The Journal of biological chemistry 1993;268:10881-7.

[195] Irving-Rodgers HF, Ziolkowski AF, Parish CR, Sado Y, Ninomiya Y, Simeonovic CJ, et al. Molecular composition of the peri-islet basement membrane in NOD mice: a barrier against destructive insulitis. Diabetologia 2008;51:1680-8.

[196] Bader BL, Smyth N, Nedbal S, Miosge N, Baranowsky A, Mokkapati S, et al. Compound genetic ablation of nidogen 1 and 2 causes basement membrane defects and perinatal lethality in mice. Molecular and cellular biology 2005;25:6846-56.

[197] Sarrazin S, Lamanna WC, Esko JD. Heparan sulfate proteoglycans. Cold Spring Harbor perspectives in biology 2011;3.

[198] Murdoch AD, Dodge GR, Cohen I, Tuan RS, Iozzo RV. Primary structure of the human heparan sulfate proteoglycan from basement membrane (HSPG2/perlecan). A chimeric molecule with multiple domains homologous to the low density lipoprotein receptor, laminin, neural cell adhesion molecules, and epidermal growth factor. The Journal of biological chemistry 1992;267:8544-57.

[199] Gubbiotti MA, Neill T, Iozzo RV. A current view of perlecan in physiology and pathology: A mosaic of functions. Matrix biology 2017;57-58:285-98.

[200] Rupp F, Payan DG, Magill-Solc C, Cowan DM, Scheller RH. Structure and expression of a rat agrin. Neuron 1991;6:811-23.

[201] Groffen AJ, Ruegg MA, Dijkman H, van de Velden TJ, Buskens CA, van den Born J, et al. Agrin is a major heparan sulfate proteoglycan in the human glomerular basement membrane. The journal of histochemistry and cytochemistry : official journal of the Histochemistry Society 1998;46:19-27.

[202] Halfter W, Dong S, Schurer B, Cole GJ. Collagen XVIII is a basement membrane heparan sulfate proteoglycan. The Journal of biological chemistry 1998;273:25404-12.

[203] O'Reilly MS, Boehm T, Shing Y, Fukai N, Vasios G, Lane WS, et al. Endostatin: an endogenous inhibitor of angiogenesis and tumor growth. Cell 1997;88:277-85.

[204] Simeonovic CJ, Popp SK, Starrs LM, Brown DJ, Ziolkowski AF, Ludwig B, et al. Loss of intra-islet heparan sulfate is a highly sensitive marker of type 1 diabetes progression in humans. PloS one 2018;13:e0191360.

[205] Choong FJ, Freeman C, Parish CR, Simeonovic CJ. Islet heparan sulfate but not heparan sulfate proteoglycan core protein is lost during islet isolation and undergoes recovery post-islet transplantation. American journal of transplantation 2015;15:2851-64.

[206] Potter KJ, Werner I, Denroche HC, Montane J, Plesner A, Chen Y, et al. Amyloid formation in human islets is enhanced by heparin and inhibited by heparinase. American journal of transplantation 2015;15:1519-30.

[207] Herchenhan A, Uhlenbrock F, Eliasson P, Weis M, Eyre D, Kadler KE, et al. Lysyl Oxidase Activity Is Required for Ordered Collagen Fibrillogenesis by Tendon Cells. Journal of Biological Chemistry 2015;290:16440-50.

[208] Kuo HJ, Maslen CL, Keene DR, Glanville RW. Type VI collagen anchors endothelial basement membranes by interacting with type IV collagen. The Journal of biological chemistry 1997;272:26522-9.

[209] Gelse K, Poschl E, Aigner T. Collagens--structure, function, and biosynthesis. Advanced drug delivery reviews 2003;55:1531-46.

[210] Van Deijnen JH, Van Suylichem PT, Wolters GH, Van Schilfgaarde R. Distribution of collagens type I, type III and type V in the pancreas of rat, dog, pig and man. Cell and tissue research 1994;277:115-21.

[211] Shi L, Ermis R, Garcia A, Telgenhoff D, Aust D. Degradation of human collagen isoforms by Clostridium collagenase and the effects of degradation products on cell migration. International wound journal 2010;7:87-95.

[212] Aumailley M, von der Mark H, Timpl R. Size and domain structure of collagen VI produced by cultured fibroblasts. FEBS letters 1985;182:499-502.

[213] Kaido T, Perez B, Yebra M, Hill J, Cirulli V, Hayek A, et al. Alphav-integrin utilization in human beta-cell adhesion, spreading, and motility. The Journal of biological chemistry 2004;279:17731-7.

[214] Pinkse GG, Bouwman WP, Jiawan-Lalai R, Terpstra OT, Bruijn JA, de Heer E. Integrin signaling via RGD peptides and anti-beta1 antibodies confers resistance to apoptosis in islets of Langerhans. Diabetes 2006;55:312-7.

[215] Lakey JR, Warnock GL, Rajotte RV, Suarez-Alamazor ME, Ao Z, Shapiro AM, et al. Variables in organ donors that affect the recovery of human islets of Langerhans. Transplantation 1996;61:1047-53.

[216] Wang LJ, Kin T, O'Gorman D, Shapiro AM, Naziruddin B, Takita M, et al. A Multicenter Study: North American Islet Donor Score in Donor Pancreas Selection for Human Islet Isolation for Transplantation. Cell transplantation 2016;25:1515-23

[217] Toso C, Oberholzer J, Ris F, Triponez F, Bucher P, Demirag A, et al. Factors affecting human islet of Langerhans isolation yields. Transplantation proceedings 2002;34:826-7.

[218] Berkova Z, Saudek F, Girman P, Zacharovova K, Kriz J, Fabryova E, et al. Combining Donor Characteristics with Immunohistological Data Improves the Prediction of Islet Isolation Success. Journal of diabetes research 2016;4214328.

[219] Liu X, Matsumoto S, Okitsu T, Iwanaga Y, Noguchi H, Yonekawa Y, et al. Analysis of donor- and isolation-related variables from non-heart-beating donors (NHBDs) using the Kyoto islet isolation method. Cell transplantation 2008;17:649-56.

[220] Hubert T, Strecker G, Gmyr V, Arnalsteen L, Garrigue D, Ezzouaoui R, et al. Acute insulin response to arginine in deceased donors predicts the outcome of human islet isolation. American journal of transplantation 2008;8:872-6.

[221] Zeng Y, Torre MA, Karrison T, Thistlethwaite JR. The correlation between donor characteristics and the success of human islet isolation. Transplantation 1994;57:954-8.

[222] Nano R, Clissi B, Melzi R, Calori G, Maffi P, Antonioli B, et al. Islet isolation for allotransplantation: variables associated with successful islet yield and graft function. Diabetologia 2005;48:906-12.

[223] Sakuma Y, Ricordi C, Miki A, Yamamoto T, Pileggi A, Khan A, et al. Factors that affect human islet isolation. Transplantation proceedings 2008;40:343-5.

[224] Kaddis JS, Danobeitia JS, Niland JC, Stiller T, Fernandez LA. Multicenter analysis of novel and established variables associated with successful human islet isolation outcomes. American journal of transplantation 2010;10:646-56.

[225] Kim SC, Han DJ, Kang CH, We YM, Back JH, Kim YH, et al. Analysis on donor and isolation-related factors of successful isolation of human islet of Langerhans from human cadaveric donors. Transplantation proceedings 2005;37:3402-3.

[226] Benhamou PY, Watt PC, Mullen Y, Ingles S, Watanabe Y, Nomura Y, et al. Human islet isolation in 104 consecutive cases. Factors affecting isolation success. Transplantation 1994;57:1804-10.

[227] Yeh CC, Wang LJ, McGarrigle JJ, Wang Y, Liao CC, Omami M, et al. Effect of Manufacturing Procedures on Human Islet Isolation From Donor Pancreata Standardized by the North American Islet Donor Score. Cell transplantation 2017;26:33-44.

[228] Jansson L. The regulation of pancreatic islet blood flow. Diabetes/metabolism reviews 1994;10:407-16.

[229] Ricordi C, Fraker C, Szust J, Al-Abdullah I, Poggioli R, Kirlew T, et al. Improved human islet isolation outcome from marginal donors following addition of oxygenated perfluorocarbon to the cold-storage solution. Transplantation 2003;75:1524-7.

[230] Ponte GM, Pileggi A, Messinger S, Alejandro A, Ichii H, Baidal DA, et al. Toward maximizing the success rates of human islet isolation: influence of donor and isolation factors. Cell transplantation 2007;16:595-607.

[231] Witkowski P, Liu Z, Guo Q, Poumian-Ruiz E, Cernea S, Herold K, et al. Two-layer method in short-term pancreas preservation for successful islet isolation. Transplantation proceedings 2005;37:3398-401.

[232] Tsujimura T, Kuroda Y, Avila JG, Kin T, Oberholzer J, Shapiro AM, et al. Influence of pancreas preservation on human islet isolation outcomes: impact of the two-layer method. Transplantation 2004;78:96-100.

[233] Mosteller RD. Simplified calculation of body-surface area. The New England journal of medicine 1987;317:1098.

[234] Matsumoto I, Sawada T, Nakano M, Sakai T, Liu B, Ansite JD, et al. Improvement in islet yield from obese donors for human islet transplants. Transplantation 2004;78:880-5.

[235] Kin T, Murdoch TB, Shapiro AM, Lakey JR. Estimation of pancreas weight from donor variables. Cell transplantation 2006;15:181-5.

[236] Mizukami H, Takahashi K, Inaba W, Osonoi S, Kamata K, Tsuboi K, et al. Age-associated changes of islet endocrine cells and the effects of body mass index in Japanese. Journal of diabetes investigation 2014;5:38-47.

[237] Wang Y, Danielson KK, Ropski A, Harvat T, Barbaro B, Paushter D, et al. Systematic analysis of donor and isolation factor's impact on human islet yield and size distribution. Cell transplantation 2013;22:2323-33.

[238] Olehnik SK, Fowler JL, Avramovich G, Hara M. Quantitative analysis of intra- and inter-individual variability of human beta-cell mass. Scientific reports 2017;7:16398.

[239] Saisho Y, Butler AE, Manesso E, Elashoff D, Rizza RA, Butler PC. beta-cell mass and turnover in humans: effects of obesity and aging. Diabetes care 2013;36:111-7.

[240] Muller DC, Elahi D, Tobin JD, Andres R. Insulin response during the oral glucose tolerance test: the role of age, sex, body fat and the pattern of fat distribution. Aging 1996;8:13-21.

[241] Shimokata H, Muller DC, Fleg JL, Sorkin J, Ziemba AW, Andres R. Age as independent determinant of glucose tolerance. Diabetes 1991;40:44-51.

[242] Ihm SH, Matsumoto I, Sawada T, Nakano M, Zhang HJ, Ansite JD, et al. Effect of donor age on function of isolated human islets. Diabetes 2006;55:1361-8.

[243] Maedler K, Schumann DM, Schulthess F, Oberholzer J, Bosco D, Berney T, et al. Aging correlates with decreased beta-cell proliferative capacity and enhanced sensitivity to apoptosis: a potential role for Fas and pancreatic duodenal homeobox-1. Diabetes 2006;55:2455-62.

[244] Lyon J, Manning Fox JE, Spigelman AF, Kim R, Smith N, O'Gorman D, et al. Research-Focused Isolation of Human Islets From Donors With and Without Diabetes at the Alberta Diabetes Institute IsletCore. Endocrinology 2016;157:560-9.

[245] Sharma A, Zangen DH, Reitz P, Taneja M, Lissauer ME, Miller CP, et al. The homeodomain protein IDX-1 increases after an early burst of proliferation during pancreatic regeneration. Diabetes 1999;48:507-13.

[246] Reers C, Erbel S, Esposito I, Schmied B, Buchler MW, Nawroth PP, et al. Impaired islet turnover in human donor pancreata with aging. European journal of endocrinology 2009;160:185-91.

[247] Szot GL, Lee MR, Tavakol MM, Lang J, Dekovic F, Kerlan RK, et al. Successful clinical islet isolation using a GMP-manufactured collagenase and neutral protease. Transplantation 2009;88:753-6.

[248] Brandhorst D, Hering BJ, Brandhorst H, Federlin K, Bretzel RG. Influence of donor data and organ procurement on human islet isolation. Transplantation proceedings 1994;26:592-3.

[249] Meier RP, Sert I, Morel P, Muller YD, Borot S, Badet L, et al. Islet of Langerhans isolation from pediatric and juvenile donor pancreases. Transplant international : official journal of the European Society for Organ Transplantation 2014;27:949-55.

[250] Takita MM, S.; Noguchi, H.; Shimoda, M.; Chujo, D.; Sugimoto, K.; Itoh, T.; Lamon, J.; Lara, L.; Onaca, N.; Naziruddin, B.; Klintmalm, G.; Levy, M. One hundred human pancreastic islet isolations at Baylor Research Institute. Proceedings 2010;23:341-8.

[251] Matsumoto S, Zhang G, Qualley S, Clever J, Tombrello Y, Strong DM, et al. Analysis of donor factors affecting human islet isolation with current isolation protocol. Transplantation proceedings 2004;36:1034-6.

[252] Briones RM, Miranda JM, Mellado-Gil JM, Castro MJ, Gonzalez-Molina M, Cuesta-Munoz AL, et al. Differential analysis of donor characteristics for pancreas and islet transplantation. Transplantation proceedings 2006;38:2579-81.

[253] Hawthorne W, Chew YV, Haron C, Williams L, Hitos K, Mariana L, et al. Outcomes for Islet Transplantation in Donation After Circulatory Death compared with Donation after Brain Death in Australia. Transplantation 2018;102:S76-S.

[254] Andres A, Kin T, O'Gorman D, Livingstone S, Bigam D, Kneteman N, et al. Clinical islet isolation and transplantation outcomes with deceased cardiac death donors are similar to neurological determination of death donors. Transplant international : official journal of the European Society for Organ Transplantation 2016;29:34-40.

[255] Clayton HA, Swift SM, Turner JM, James RF, Bell PR. Non-heart-beating organ donors: a potential source of islets for transplantation? Transplantation 2000;69:2094-8.

[256] Markmann JF, Vataminiuk M. The use of non-heart-beating donors for isolated pancreatic islet transplantation (vol 75, pg 1423, 2003). Transplantation 2003;76:1009.

[257] Chetboun M, Kerr-Conte JA, Gmyr V, Thuillier D, Ezzouaoui R, Hubert T, et al. Tobacco Smoking Results in Reduced Pancreatic Islet Mass in Humans. Diabetes 2018;67.

[258] Frantz C, Stewart KM, Weaver VM. The extracellular matrix at a glance. Journal of cell science 2010;123:4195-200.

[259] Chung AW, Booth AD, Rose C, Thompson CR, Levin A, van Breemen C. Increased matrix metalloproteinase 2 activity in the human internal mammary artery is associated with ageing, hypertension, diabetes and kidney dysfunction. J Vasc Res 2008;45:357-62.

[260] McNulty M, Spiers P, McGovern E, Feely J. Aging is associated with increased matrix metalloproteinase-2 activity in the human aorta. Am J Hypertens 2005;18:504-9.

[261] Glenn JV, Beattie JR, Barrett L, Frizzell N, Thorpe SR, Boulton ME, et al. Confocal Raman microscopy can quantify advanced glycation end product (AGE) modifications in Bruch's membrane

leading to accurate, nondestructive prediction of ocular aging. FASEB journal : official publication of the Federation of American Societies for Experimental Biology 2007;21:3542-52.

[262] Hofmann B, Jacobs K, Santos AN, Wienke A, Silber RE, Simm A. Relationship between cardiac tissue glycation and skin autofluorescence in patients with coronary artery disease. Diabetes Metab 2015;41:410-5.

[263] Sell DR, Biemel KM, Reihl O, Lederer MO, Strauch CM, Monnier VM. Glucosepane is a major protein cross-link of the senescent human extracellular matrix. Relationship with diabetes. The Journal of biological chemistry 2005;280:12310-5.

[264] Araki N, Ueno N, Chakrabarti B, Morino Y, Horiuchi S. Immunochemical evidence for the presence of advanced glycation end products in human lens proteins and its positive correlation with aging. The Journal of biological chemistry 1992;267:10211-4.

[265] Reigle KL, Di Lullo G, Turner KR, Last JA, Chervoneva I, Birk DE, et al. Non-enzymatic glycation of type I collagen diminishes collagen-proteoglycan binding and weakens cell adhesion. Journal of cellular biochemistry 2008;104:1684-98.

[266] Tsilibary EC, Charonis AS, Reger LA, Wohlhueter RM, Furcht LT. The effect of nonenzymatic glucosylation on the binding of the main noncollagenous NC1 domain to type IV collagen. The Journal of biological chemistry 1988;263:4302-8.

[267] Lan KC, Chiu CY, Kao CW, Huang KH, Wang CC, Huang KT, et al. Advanced glycation end-products induce apoptosis in pancreatic islet endothelial cells via NF-kappaB-activated cyclooxygenase-2/prostaglandin E2 up-regulation. PloS one 2015;10:e0124418.

[268] Stitt A, Gardiner TA, Alderson NL, Canning P, Frizzell N, Duffy N, et al. The AGE inhibitor pyridoxamine inhibits development of retinopathy in experimental diabetes. Diabetes 2002;51:2826-32.

[269] Gardiner TA, Anderson HR, Stitt AW. Inhibition of advanced glycation end-products protects against retinal capillary basement membrane expansion during long-term diabetes. The Journal of pathology 2003;201:328-33.

[270] Dworatzek E, Baczko I, Kararigas G. Effects of aging on cardiac extracellular matrix in men and women. Proteomics Clinical applications 2016;10:84-91.

[271] Eikmans M, Baelde HJ, de Heer E, Bruijn JA. Effect of age and biopsy site on extracellular matrix mRNA and protein levels in human kidney biopsies. Kidney international 2001;60:974-81.

[272] Karttunen T, Risteli J, Autio-Harmainen H, Risteli L. Effect of age and diabetes on type IV collagen and laminin in human kidney cortex. Kidney international 1986;30:586-91.

[273] Singh K, Masuda K, Thonar EJ, An HS, Cs-Szabo G. Age-related changes in the extracellular matrix of nucleus pulposus and anulus fibrosus of human intervertebral disc. Spine 2009;34:10-6.

[274] Bedossa P, Lemaigre G, Bacci J, Martin E. Quantitative estimation of the collagen content in normal and pathologic pancreas tissue. Digestion 1989;44:7-13.

[275] Tons HA, Terpstra OT, Bouwman E. Heterogeneity of human pancreata in perspective of the isolation of the islets of langerhans. Transplantation proceedings 2008;40:367-9.

[276] Debessa CRG, Maifrino LBM, de Souza RR. Age related changes of the collagen network of the human heart. Mech Ageing Dev 2001;122:1049-58.

[277] Carrino DA, Sorrell JM, Caplan AI. Age-related changes in the proteoglycans of human skin. Archives of biochemistry and biophysics 2000;373:91-101.

[278] Shuster S, Black MM, McVitie E. The influence of age and sex on skin thickness, skin collagen and density. The British journal of dermatology 1975;93:639-43.

[279] Uspenskaia O, Liebetrau M, Herms J, Danek A, Hamann GF. Aging is associated with increased collagen type IV accumulation in the basal lamina of human cerebral microvessels. Bmc Neurosci 2004;5.

[280] Oxlund BS, Ortoft G, Bruel A, Danielsen CC, Bor P, Oxlund H, et al. Collagen concentration and biomechanical properties of samples from the lower uterine cervix in relation to age and parity in non-pregnant women. Reproductive biology and endocrinology : RB&E 2010;8:82.

[281] Balamurugan AN, Chang Y, Bertera S, Sands A, Shankar V, Trucco M, et al. Suitability of human juvenile pancreatic islets for clinical use. Diabetologia 2006;49:1845-54.

[282] Socci C, Davalli AM, Vignali A, Pontiroli AE, Maffi P, Magistretti P, et al. A significant increase of islet yield by early injection of collagenase into the pancreatic duct of young donors. Transplantation 1993;55:661-3.

[283] Shimoda M, Itoh T, Sugimoto K, Iwahashi S, Takita M, Chujo D, et al. Improvement of collagenase distribution with the ductal preservation for human islet isolation. Islets 2012;4:130-7.

[284] Takita M, Itoh T, Shimoda M, Kanak MA, Shahbazov R, Kunnathodi F, et al. Pancreatic Ductal Perfusion at Organ Procurement Enhances Islet Yield in Human Islet Isolation. Pancreas 2014;43:1249-55.

[285] Matsumoto S, Noguchi H, Naziruddin B, Onaca N, Jackson A, Nobuyo H, et al. Improvement of pancreatic islet cell isolation for transplantation. Proceedings 2007;20:357-62.

[286] Golebiewska JE, Bachul PJ, Wang LJ, Matosz S, Basto L, Kijek MR, et al. Validation of a New North American Islet Donor Score for Donor Pancreas Selection and Successful Islet Isolation in a Medium-Volume Islet Transplant Center. Cell transplantation 2019;28:185-94.

[287] O'Gorman D, Kin T, Murdoch T, Richer B, McGhee-Wilson D, Ryan E, et al. The standardization of pancreatic donors for islet isolation. Transplantation proceedings 2005;37:1309-10.

[288] Goto M, Johansson U, Eich TM, Lundgrem T, Engkvist M, Felldin M, et al. Key factors for human islet isolation and clinical transplantation. Transplantation proceedings 2005;37:1315-6.
[289] Forbes S, Oram RA, Smith A, Lam A, Olateju T, Imes S, et al. Validation of the BETA-2 Score: An Improved Tool to Estimate Beta Cell Function After Clinical Islet Transplantation Using a Single Fasting Blood Sample. American journal of transplantation 2016;16:2704-13.
[290] Rickels MR, Naji A, Teff KL. Acute insulin responses to glucose and arginine as predictors of beta-cell secretory capacity in human islet transplantation. Transplantation 2007;84:1357-60.
[291] Ryan EA, Paty BW, Senior PA, Bigam D, Alfadhli E, Kneteman NM, et al. Five-year follow-up after clinical islet transplantation. Diabetes 2005;54:2060-9.
[292] Ryan EA, Paty BW, Senior PA, Lakey JR, Bigam D, Shapiro AM. Beta-score: an assessment of beta-cell function after islet transplantation. Diabetes care 2005;28:343-7.
[293] Golebiewska J, Solomina J, Kijek MR, Kotukhov A, Basto L, Golab K, et al. External Validation of the Newly Developed BETA-2 Scoring System for Pancreatic Islet Graft Function Assessment. Transplantation proceedings 2017;49:2340-6.
[294] Spiliotis IB, C.; Gough, S.; Crookston, R.; Ravanan, R.; Casey, J.; Forbes, S.; Choudhary, P.; Rosenthal M.; Rutter, M. Use of the Glucose-Dependent Insulin Secretion Rate (GDISR) as a novel predictor of islet graft function. Journal of the Society for Biomedical Diabetes Research 2017;14:141-2.
[295] Krishnan RK, D.; Tucker, T.; Opara, E.; Foster, E.; Imagawa, D.; Stamos, M.; Lakey, J. Strategies to Combat Hypoxia in Encapsulated Islet Transplantation. Surgery: Current Research 2016;6:1-10.
[296] Komatsu H, Cook C, Wang CH, Medrano L, Lin H, Kandeel F, et al. Oxygen environment and islet size are the primary limiting factors of isolated pancreatic islet survival. PloS one 2017;12.
[297] German AK. Effect of Tobacco Smoking on the Oxygen Balance of the Tissues. Vrachebnoe Delo 1991:86-9.
[298] Lakey JRT, Warnock GL, Shapiro AMJ, Korbutt GS, Ao ZL, Kneteman NM, et al. Intraductal collagenase delivery into the human pancreas using syringe loading or controlled perfusion. Cell transplantation 1999;8:285-92.
[299] Brandhorst H, Friberg A, Nilsson B, Andersson HH, Felldin M, Foss A, et al. Large-Scale Comparison of Liberase HI and Collagenase NB1 Utilized for Human Islet Isolation. Cell transplantation 2010;19:3-8.
[300] Shimoda M, Noguchi H, Naziruddin B, Fujita Y, Chujo D, Takita M, et al. Assessment of human islet isolation with four different collagenases. Transplantation proceedings 2010;42:2049-51.
[301] Ferrannini E, Camastra S, Gastaldelli A, Maria Sironi A, Natali A, Muscelli E, et al. beta-cell function in obesity: effects of weight loss. Diabetes 2004;53 Suppl 3:S26-33.

[302] Polonsky KS, Given BD, Hirsch L, Shapiro ET, Tillil H, Beebe C, et al. Quantitative study of insulin secretion and clearance in normal and obese subjects. The Journal of clinical investigation 1988;81:435-41.

[303] Henquin JC. Influence of organ donor attributes and preparation characteristics on the dynamics of insulin secretion in isolated human islets. Physiological reports 2018;6.

[304] Uscanga L, Kennedy RH, Stocker S, Grimaud JA, Sarles H. Immunolocalization of collagen types, laminin and fibronectin in the normal human pancreas. Digestion 1984;30:158-64.

[305] Naba A, Clauser KR, Mani DR, Carr SA, Hynes RO. Quantitative proteomic profiling of the extracellular matrix of pancreatic islets during the angiogenic switch and insulinoma progression. Scientific reports 2017;7.

[306] Waanders LF, Chwalek K, Monetti M, Kumar C, Lammert E, Mann M. Quantitative proteomic analysis of single pancreatic islets. Proceedings of the National Academy of Sciences of the United States of America 2009;106:18902-7.

[307] Zhang L, Lanzoni G, Battarra M, Inverardi L, Zhang Q. Proteomic profiling of human islets collected from frozen pancreata using laser capture microdissection. Journal of proteomics 2017;150:149-59.

[308] Karpievitch YV, Polpitiya AD, Anderson GA, Smith RD, Dabney AR. Liquid Chromatography Mass Spectrometry-Based Proteomics: Biological and Technological Aspects. The annals of applied statistics 2010;4:1797-823.

[309] Twyman RM. Principles of Proteomics. Advanced Texts: Taylor & Francis; 2004.

[310] Zhang Y, Fonslow BR, Shan B, Baek MC, Yates JR, 3rd. Protein analysis by shotgun/bottom-up proteomics. Chemical reviews 2013;113:2343-94.

[311] Naba A, Clauser KR, Ding H, Whittaker CA, Carr SA, Hynes RO. The extracellular matrix: Tools and insights for the "omics" era. Matrix biology 2016;49:10-24.

[312] Clerc O, Deniaud M, Vallet SD, Naba A, Rivet A, Perez S, et al. MatrixDB: integration of new data with a focus on glycosaminoglycan interactions. Nucleic acids research 2019;47:D376-D81.

[313] Petyuk VA, Qian WJ, Hinault C, Gritsenko MA, Singhal M, Monroe ME, et al. Characterization of the mouse pancreatic islet proteome and comparative analysis with other mouse tissues. Journal of proteome research 2008;7:3114-26.

[314] Naba A, Clauser KR, Hynes RO. Enrichment of Extracellular Matrix Proteins from Tissues and Digestion into Peptides for Mass Spectrometry Analysis. Journal of visualized experiments : JoVE 2015:e53057.

[315] van Suylichem PT, Pasma A, Wolters GH, van Schilfgaarde R. Microscopic aspects of the structure and collagen content of the pancreas from the perspective of islet isolation. Transplantation proceedings 1987;19:3958-9.

[316] Angel PM, Comte-Walters S, Ball LE, Talbot K, Mehta A, Brockbank KGM, et al. Mapping Extracellular Matrix Proteins in Formalin-Fixed, Paraffin-Embedded Tissues by MALDI Imaging Mass Spectrometry. Journal of proteome research 2018;17:635-46.

[317] Hughes S, Gray D, Clark A, Johnson P. Development of an assay for the detailed study of collagenase-digestion within the islet-exocrine interface of the human pancreas Xenotransplantation 2007;14:485.

[318] Johnson PR, Van Suylichem PT, Roberts DL, Vos-Scheperkeuter GH, White SA, Van Schilfgaarde R, et al. A simple in vitro method for evaluating the efficacy of different batches of crude Clostridium histolyticum collagenase for islet isolation. Transplantation proceedings 1995;27:3284-5.

[319] Balamurugan AN, Green ML, Breite AG, Loganathan G, Wilhelm JJ, Tweed B, et al. Identifying Effective Enzyme Activity Targets for Recombinant Class I and Class II Collagenase for Successful Human Islet Isolation. Transplantation direct 2016;2:e54.

[320] Dendo M, Maeda H, Yamagata Y, Murayama K, Watanabe K, Imura T, et al. Synergistic Effect of Neutral Protease and Clostripain on Rat Pancreatic Islet Isolation. Transplantation 2015;99:1349-55.

[321] Vos-Scheperkeuter GH, van Suylichem PT, Vonk MW, Wolters GH, van Schilfgaarde R. Histochemical analysis of the role of class I and class II Clostridium histolyticum collagenase in the degradation of rat pancreatic extracellular matrix for islet isolation. Cell transplantation 1997;6:403-12.

[322] Miyazaki Y, Murayama K, Fathi I, Imura T, Yamagata Y, Watanabe K, et al. Strategy towards tailored donor tissue-specific pancreatic islet isolation. PloS one 2019;14:e0216136.

[323] Wang RN, Rosenberg L. Maintenance of beta-cell function and survival following islet isolation requires re-establishment of the islet-matrix relationship. The Journal of endocrinology 1999;163:181-90.

[324] Rosenberg L, Wang R, Paraskevas S, Maysinger D. Structural and functional changes resulting from islet isolation lead to islet cell death. Surgery 1999;126:393-8.

[325] Irving-Rodgers HF, Choong FJ, Hummitzsch K, Parish CR, Rodgers RJ, Simeonovic CJ. Pancreatic islet basement membrane loss and remodeling after mouse islet isolation and transplantation: impact for allograft rejection. Cell transplantation 2014;23:59-72.

[326] Thomas F, Wu J, Contreras JL, Smyth C, Bilbao G, He J, et al. A tripartite anoikis-like mechanism causes early isolated islet apoptosis. Surgery 2001;130:333-8.

[327] Takahashi I, Noguchi N, Nata K, Yamada S, Kaneiwa T, Mizumoto S, et al. Important role of heparan sulfate in postnatal islet growth and insulin secretion. Biochemical and biophysical research communications 2009;383:113-8.

[328] Brandhorst H, Johnson PRV, Korsgren O, Brandhorst D. Quantifying the Effects of Different Neutral Proteases on Human Islet Integrity. Cell transplantation 2017;26:1733-41.

[329] Bucher P, Bosco D, Mathe Z, Matthey-Doret D, Andres A, Kurfuerst M, et al. Optimization of neutral protease to collagenase activity ratio for islet of Langerhans isolation. Transplantation proceedings 2004;36:1145-6.

[330] Brandhorst H, Brendel MD, Eckhard M, Bretzel RG, Brandhorst D. Influence of neutral protease activity on human islet isolation outcome. Transplantation proceedings 2005;37:241-2.

[331] Niyibizi C, Eyre DR. Bone type V collagen: chain composition and location of a trypsin cleavage site. Connective tissue research 1989;20:247-50.

[332] Birk DE. Type V collagen: heterotypic type I/V collagen interactions in the regulation of fibril assembly. Micron 2001;32:223-37.

[333] Matsushita O, Jung CM, Minami J, Katayama S, Nishi N, Okabe A. A study of the collagen-binding domain of a 116-kDa Clostridium histolyticum collagenase. The Journal of biological chemistry 1998;273:3643-8.

[334] Shima H, Inagaki A, Imura T, Yamagata Y, Watanabe K, Igarashi K, et al. Collagen V Is a Potential Substrate for Clostridial Collagenase G in Pancreatic Islet Isolation. Journal of diabetes research 2016;2016:4396756.

[335] Esposito AP, Talley CE, Huser T, Hollars CW, Schaldach CM, Lane SM. Analysis of single bacterial spores by micro-Raman spectroscopy. Applied spectroscopy 2003;57:868-71.

[336] De Gelder J, Scheldeman P, Leus K, Heyndrickx M, Vandenabeele P, Moens L, et al. Raman spectroscopic study of bacterial endospores. Analytical and bioanalytical chemistry 2007;389:2143-51.

[337] Schulze HG, Konorov SO, Caron NJ, Piret JM, Blades MW, Turner RF. Assessing differentiation status of human embryonic stem cells noninvasively using Raman microspectroscopy. Analytical chemistry 2010;82:5020-7.

[338] Ichimura T, Chiu LD, Fujita K, Kawata S, Watanabe TM, Yanagida T, et al. Visualizing Cell State Transition Using Raman Spectroscopy. PloS one 2014;9.

[339] Brauchle E, Kasper J, Daum R, Schierbaum N, Falch C, Kirschniak A, et al. Biomechanical and biomolecular characterization of extracellular matrix structures in human colon carcinomas. Matrix Biology 2018;68-69:180-93.

[340] Daniel A, Prakasarao A, Ganesan S. Near-infrared Raman spectroscopy for estimating biochemical changes associated with different pathological conditions of cervix. Spectrochimica acta Part A, Molecular and biomolecular spectroscopy 2018;190:409-16.

[341] Nijssen A, Maquelin K, Santos LF, Caspers PJ, Bakker Schut TC, den Hollander JC, et al. Discriminating basal cell carcinoma from perilesional skin using high wave-number Raman spectroscopy. Journal of biomedical optics 2007;12:034004.

[342] Zhang J, Fan Y, He M, Ma X, Song Y, Liu M, et al. Accuracy of Raman spectroscopy in differentiating brain tumor from normal brain tissue. Oncotarget 2017;8:36824-31.

[343] Brauchle E, Schenke-Layland K. Raman spectroscopy in biomedicine - non-invasive in vitro analysis of cells and extracellular matrix components in tissues. Biotechnology journal 2013;8:288-97.

[344] Votteler M, Carvajal Berrio DA, Pudlas M, Walles H, Schenke-Layland K. Non-contact, label-free monitoring of cells and extracellular matrix using Raman spectroscopy. Journal of visualized experiments : JoVE 2012.

[345] Puppels GJ, de Mul FF, Otto C, Greve J, Robert-Nicoud M, Arndt-Jovin DJ, et al. Studying single living cells and chromosomes by confocal Raman microspectroscopy. Nature 1990;347:301-3.

[346] Votteler M, Carvajal Berrio DA, Pudlas M, Walles H, Stock UA, Schenke-Layland K. Raman spectroscopy for the non-contact and non-destructive monitoring of collagen damage within tissues. Journal of biophotonics 2012;5:47-56.

[347] Nguyen TT, Gobinet C, Feru J, Brassart-Pasco S, Manfait M, Piot O. Characterization of Type I and IV Collagens by Raman Microspectroscopy: Identification of Spectral Markers of the Dermo-Epidermal Junction. Spectrosc-Int J 2012;27:421-7.

[348] Hilderink J, Otto C, Slump C, Lenferink A, Engelse M, van Blitterswijk C, et al. Label-Free Detection of Insulin and Glucagon within Human Islets of Langerhans Using Raman Spectroscopy. PloS one 2013;8.

[349] Albro MB, Bergholt MS, St-Pierre JP, Vinals Guitart A, Zlotnick HM, Evita EG, et al. Raman spectroscopic imaging for quantification of depth-dependent and local heterogeneities in native and engineered cartilage. NPJ Regenerative medicine 2018;3:3.

[350] Pudlas M, Brauchle E, Klein TJ, Hutmacher DW, Schenke-Layland K. Non-invasive identification of proteoglycans and chondrocyte differentiation state by Raman microspectroscopy. Journal of biophotonics 2013;6:205-11.

[351] Pudlas M, Koch S, Bolwien C, Thude S, Jenne N, Hirth T, et al. Raman spectroscopy: a noninvasive analysis tool for the discrimination of human skin cells. Tissue engineering Part C, Methods 2011;17:1027-40.

[352] Frank CJ, McCreery RL, Redd DC. Raman spectroscopy of normal and diseased human breast tissues. Analytical chemistry 1995;67:777-83.

[353] Cheng WT, Liu MT, Liu HN, Lin SY. Micro-Raman spectroscopy used to identify and grade human skin pilomatrixoma. Microscopy research and technique 2005;68:75-9.

[354] Huang Z, McWilliams A, Lui H, McLean DI, Lam S, Zeng H. Near-infrared Raman spectroscopy for optical diagnosis of lung cancer. International journal of cancer 2003;107:1047-52.

[355] Gniadecka M, Wulf HC, Mortensen NN, Nielsen OF, Christensen DH. Diagnosis of basal cell carcinoma by Raman spectroscopy. J Raman Spectrosc 1997;28:125-9.

[356] Frushour BG, Koenig JL. Raman scattering of collagen, gelatin, and elastin. Biopolymers 1975;14:379-91.

[357] Stone N, Kendall C, Smith J, Crow P, Barr H. Raman spectroscopy for identification of epithelial cancers. Faraday discussions 2004;126:141-57.

[358] Krafft C, Neudert L, Simat T, Salzer R. Near infrared Raman spectra of human brain lipids. Spectrochimica acta Part A, Molecular and biomolecular spectroscopy 2005;61:1529-35.

[359] Dukor RK. Vibrational Spectroscopy in the Detection of Cancer. Handbook of Vibrational Spectroscopy: John Wiley & Sons, Ltd; 2006.

[360] Ruiz-Chica AJ, Medina MA, Sanchez-Jimenez F, Ramirez FJ. Characterization by Raman spectroscopy of conformational changes on guanine-cytosine and adenine-thymine oligonucleotides induced by aminooxy analogues of spermidine. J Raman Spectrosc 2004;35:93-100.

[361] Chan JW, Taylor DS, Zwerdling T, Lane SM, Ihara K, Huser T. Micro-Raman spectroscopy detects individual neoplastic and normal hematopoietic cells. Biophys J 2006;90:648-56.

[362] O Faolain E, Hunter MB, Byrne JM, Kelehan P, McNamara M, Byrne HJ, et al. A study examining the effects of tissue processing on human tissue sections using vibrational spectroscopy. Vib Spectrosc 2005;38:121-7.

[363] Timpl R, Rohde H, Robey PG, Rennard SI, Foidart JM, Martin GR. Laminin--a glycoprotein from basement membranes. The Journal of biological chemistry 1979;254:9933-7.

[364] Shoulders MD, Raines RT. Collagen structure and stability. Annual review of biochemistry 2009;78:929-58.

[365] Gottlieb AA, Kaplan A, Udenfriend S. Further Evidence for Accumulation of a Hydroxyproline-Deficient Collagenase-Degradable Protein during Collagen Biosynthesis in Vitro. Journal of Biological Chemistry 1966;241:1551.

[366] Llacua LA, Faas MM, de Vos P. Extracellular matrix molecules and their potential contribution to the function of transplanted pancreatic islets. Diabetologia 2018;61:1261-72.

[367] Khoshnoodi J, Pedchenko V, Hudson BG. Mammalian collagen IV. Microscopy research and technique 2008;71:357-70.

[368] Patel TR, Bernards C, Meier M, McEleney K, Winzor DJ, Koch M, et al. Structural elucidation of full-length nidogen and the laminin-nidogen complex in solution. Matrix Biology 2014;33:60-7.

[369] Aumailley M. The laminin family. Cell adhesion & migration 2013;7:48-55.

Publications and Awards Arising from DPhil

Full length Publications

Spiers, R. M., *et al.* "Development of a Simple in Vitro Assay to Assess Digestion of the Extracellular Matrix of the Human Pancreas by Collagenase Based Enzyme Blends." Cell Transplantation **27** (7): 1039-1046 (2018).

Spiers, R. M., *et al*. "Donor age significantly influences the Raman spectroscopic biomolecular fingerprint of human pancreatic extracellular matrix proteins following collagenase-based digestion" Manuscript submitted.

Conference Papers (selected)

Spiers, R, M., *et al*. "The novel 'Glucose-Dependent Insulin Secretion Rate' (GDISR) detects a time-dependent deterioration in islet graft function following first transplant". 17th IPITA World Congress (July 2019) Lyon, France (Oral presentation)

Spiers, R, M., *et al*. "Donor age-related difference in the digestibility of key pancreatic extracellular matrix proteins may help to explain poorer islet isolation outcomes from younger human donors". 17th IPITA World Congress (July 2019) Lyon, France (Oral presentation)

Spiers, R, M., *et al*. "Raman microspectroscopy: a powerful tool for understanding donor age-related differences in extracellular matrix protein digestion during human islet isolation". 17th IPITA World Congress (July 2019) Lyon, France (Oral presentation)

Spiers, R. M., *et al*. "High-throughput proteomics to characterise donor age-related changes in the extracellular matrix of the human pancreas". 9th EPITA Symposium & 38th AIDPIT Workshop (January 2019) Igls, Austria (Oral presentation)

Spiers, R, M., *et al*. "Investigating the feasibility of using Raman microspectroscopy as a non-invasive technology to characterise the extracellular matrix at the islet-exocrine interface of the human pancreas". 16th IPITA World Congress (June 2017) Oxford, UK (Poster presentation)

Spiers, R. M., *et al*. "Donor age significantly impacts on the success of human islet isolation". NHSBT Congress (May 2016) Warwick, UK (Poster presentation)

Spiers, R. M., *et al*. "Neutral protease levels impact more on peri-islet laminin loss in older donors than younger donors" 5th EPITA Symposium & 34th AIDPIT Workshop (January 2016) Igls, Austria (Poster presentation)

Awards

Nuffield Department of Surgical Sciences 'Citizen of the Year' annual award (2017)
Awarded for substantial contributions towards the Departments public engagement and outreach programme, in the field of Islet Isolation and Transplantation Research

EMBO Short-Term Fellowship (2018)
Awarded to facilitate my travel to the laboratory of Professor Katja Schenke-Layland in Tubingen, Germany. Project title: "Utilising Raman Microspectroscopy to determine the impact of donor age related extracellular matrix variations on the digestion of the human pancreas during islet isolation".
Award number: 7224

Acknowledgements

I am immensely grateful to those who have supported me through the development of this thesis. I am especially thankful to my supervisors, Professor Paul Johnson and Dr Sarah Cross, who have mentored me throughout my studies. They have both provided continuous guidance, support and never-ending enthusiasm, whilst allowing me the freedom to develop my research.

Thank you to Professor Rutger Ploeg, Dr Maria Kaiser, Dr Sarah Bonham, Dr Roman Fischer and Dr Honglei Huang, who provided invaluable advice and expertise for the proteomic studies.

I am indebted to Professor Katja Schenke-Layland and her research group at the University of Tubingen, for hosting me in Germany. I am especially grateful to Dr Eva Brauchle for the supervision and support that she provided for the Raman studies, and Ms Julia Marzi for providing superb technical and analytical assistance. Thank you to all the members of the group who included me in social events, and for introducing me to the wonders of the German Christmas market! I am also grateful to the European Molecular Biology Organisation who funded this research visit, by awarding me with a prestigious Travel Fellowship.

Many thanks to the Juvenile Diabetes Research Foundation, who funded my salary throughout my studies. I am grateful to the donors and their families who consented for the use of the tissue samples in these studies.

Thank you to colleagues (past and present), who have both supported my research, and whom I have worked alongside in the DRWF Human Islet Isolation Facility: Steve Hughes, Rebecca Vaughan, Paul Bateman, John Spiliotis, Yukari Kimura, Helen Brown, Sam Acreman, Anju Abraham, Heide and Daniel Brandhorst, Rebecca Miller and Phoebe Tsou. Thank you for the continued support and for making the Johnson Lab such an enjoyable place to work.

Finally, I would like to thank my parents, for their never-ending support and encouragement.

APPENDICES

Appendix A

(Chapter 2)

Factor (units)	N	Variable type	Descriptive statistics ***Continuous variable:*** ***1) Mean ± SD*** ***2) Median + (range)*** ***Categorical variable:*** ***Number + (percentage)***
Age (years)	732	Continuous	1. 45.7 ± 9.8 2. 47 (17 - 64)
Sex (M/F)	732	Categorical	Male: 397 (54.2%) Female: 335 (47.5%)
Height (cm)	732	Continuous	1. 171.3 ± 9.9 2. 172 (142 - 200)
Weight (Kg)	732	Continuous	1. 83.2 ± 14.9 2. 81.4 (49 - 150)
BMI (Kg/m^2)	732	Continuous	1. 28.3 ± 4.4 2. 28 (18 – 42)
Body surface area (BSA) **(As per Mosteller [233])**	732	Continuous	1. 2.0 ± 9.9 2. 2.0 (1 – 3)
Abdominal girth (cm)	707	Continuous	1. 98.7 ± 14.2 2. 99 (35 – 154)
Past hypertension (Y/N)	721	Categorical	Yes: 174 (23.7%) No: 547 (74.6%)
Past alcohol abuse (Y/N)	475	Categorical	Yes: 50 (10.5%) No: 425 (89.5%)
Past smoker (Y/N)	728	Categorical	Yes: 406 (55.4%) No: 322 (44.2%)
Past smoker amount (cigarettes/day)	691	Continuous	1. 8.6 ± 10.9 2. 2 (0 – 70)
Traumatic cause of death (Y/N)	731	Categorical	Yes: 37 (5.1%) No: 694 (94.9%)
Cardiac arrest? (Y/N)	728	Categorical	Yes: 406 (55.8%) No: 322 (44.2%)
Cardiac arrest duration (minutes)	197	Continuous	1. 24.1 ± 18.5 2. 20 (1 – 99)
Hypoxia related cause of death (Y/N)	732	Categorical	Yes: 117 (16%) No: 615 (84%)
Donor type (DCD/DBD)	732	Categorical	DBD: 613 (83.7%) DCD: 119 (16.3%)
Blood Urea (mmol/l)	654	Continuous	1. 5.3 ± 2.5 2. 4.9 (1 – 24)
Alanine aminotransferase (ALT; iu/l)	606	Continuous	1. 74.2 ± 134.4 2. 34 (4 – 1937)
Amylase (iu/l)	440	Continuous	1. 89.2 ± 108.3 2. 58 (7 – 978)
Aspartate aminotransferase (AST; iu/l)	197	Continuous	1. 71.8 ± 107.6 2. 36 (6 – 785)

Factor (units)	N	Variable type	Descriptive statistics ***Continuous variable:*** ***1) Mean ± SD*** ***2) Median + (range)*** ***Categorical variable:*** ***Number + (percentage)***
Bilirubin (µmol/l)	647	Continuous	1. 11.5 ± 9.3 2. 9 (1 – 80)
Glucose (mmol/l)	487	Continuous	1. 8.3 ± 2.8 2. 7.7 (4 – 35)
Insulin (Y/N)	38	Categorical	Yes: 24 (63.2%) No: 14 (36.8%)
Methylprednisolone administered? (Y/N)	596	Categorical	Yes: 416 (69.8%) No: 180 (30.2%)
Dopamine administered? (Y/N)	202	Categorical	Yes: 3 (1.5%) No: 199 (98.5%)
Dobutamine administered? (Y/N)	589	Categorical	Yes: 22 (3.7%) No: 567 (96.3%)
Adrenaline administered? (Y/N)	590	Categorical	Yes: 25 (4.2%) No: 565 (95.8%)
Noradrenaline administered? (Y/N)	604	Categorical	Yes: 476 (78.8%) No: 128 (21.2%)
Vasopressin administered? (Y/N)	598	Categorical	Yes: 401 (67.1%) No: 197 (32.9%)
Triliodotryronine administered? (Y/N)	583	Categorical	Yes: 98 (16.8%) No: 485 (83.2%)
Duration in intensive treatment unit (ITU) (days)	211	Continuous	1. 3.3 ± 3.0 2. 2.4 (1 – 27)
Pancreas cold ischemia time (CIT) (hours)	578	Continuous	1. 6.9 ± 2.1 2. 7 (1 – 12)
Pancreas weight (g)	604	Continuous	1. 96.1 ± 26.2 2. 92 (45 – 237)
Pancreas fibrosis (Y/N)	630	Categorical	Yes: 23 (3.7%) No: 607 (96.3%)
Pancreas nodular (Y/N)	632	Categorical	Yes: 8 (1.3%) No: 624 (98.7%)
Pancreas haematomas (Y/N)	643	Categorical	Yes: 87 (13.5%) No: 556 (86.5%)
Pancreas oedema (Y/N)	644	Categorical	Yes: 6 (0.9%) No: 638 (99.1%)
Pancreas inflammation (Y/N)	646	Categorical	Yes: 6 (0.9%) No: 640 (99.1%)
Pancreas fatty (Y/N)	649	Categorical	Yes: 396 (61%) No: 253 (39%)
Capsular damage (Y/N)	643	Categorical	Yes: 41 (6.4%) No: 602 (93.6%)
Parenchymal damage (Y/N)	642	Categorical	Yes: 30 (4.7%) No: 612 (95.3%)
Islet yield K (IEQ)	732	Continuous	1. 223.4 ± 26.2 2. 200 (0 – 1100)

Factor (units)	N	Variable type	Descriptive statistics ***Continuous variable:*** ***1) Mean ± SD*** ***2) Median + (range)*** ***Categorical variable:*** ***Number + (percentage)***
'Transplantable' yield ≥ 200 K IEQ (Y/N)	732	Categorical	Yes: 389 (53.1%) No: 343 (46.9%)

Table A1: Descriptive statistics of donors accepted for clinical islet isolation in the UK

		<200K IEQ 'Not transplantable'	**≥200K IEQ 'Transplantable'**
Age (years)		44.5±10.0	46.7±9.5
Sex	*Male*	198 (49.9%)	199 (50.1%)
	Female	145 (43.4%)	190 (56.7%)
Height (cm)		171.6±9.9	171.0±10.0
Weight (Kg)		81.77±15.4	84.4±14.4
BMI (Kg/m^2)		27.7±4.4	28.9±4.4
Body surface area (BSA) (As per Mosteller [233]**)**		1.97±2.2	2.0±2.1
Abdominal girth (cm)		97.0±14.9	100.3±13.3
Past hypertension	*Yes*	66 (37.9%)	108 (62.1%)
	No	274 (50.1%)	273 (49.9%)
Past alcohol abuse	*Yes*	23 (46%)	27 (54%)
	No	182 (42.8%)	243 (57.2%)
Past smoker	*Yes*	208 (51.2%)	198 (48.8%)
	No	134 (41.6%)	188 (58.4%)
Past smoker amount (cigarettes/day)		9.0±11.0	8.3±11.0
Traumatic cause of death	*Yes*	19 (51.4%)	18 (48.6%)
	No	323 (46.5%)	371 (53.5%)
Cardiac arrest	*Yes*	104 (50.7%)	101 (49.3%)
	No	220 (45.8%)	260 (54.2%)
Cardiac arrest duration (minutes)		25.2±18.4	23.0±18.6
Hypoxic related cause of death	*Yes*	68 (58.1%)	49 (41.9%)
	No	275 (44.7%)	340 (55.3%)
Donor type	*DBD*	277 (45.2%)	336 (54.8%)
	DCD	66 (55.5%)	53 (44.5%)

		<200K IEQ 'Not transplantable'	≥200K IEQ 'Transplantable'
Blood Urea (mmol/l)		5.2±2.1	5.4±2.8
Alanine aminotransferase (ALT; iu/l)		75.7±150.6	73.5±116.2
Amylase (iu/l)		90.1±103.2	88.5±112.6
Aspartate aminotransferase (AST; iu/l)		69.9 ±98.0	73.5±116.2
Bilirubin (µmol/l)		11.5±10.3	11.5±8.4
Glucose (mmol/l)		8.4±3.2	8.3±2.5
Insulin	*Yes*	5 (20.8%)	19 (79.2%)
	No	8 (57.1%)	6 (42.9%)
Methylprednisolone administered	*Yes*	195 (46.9%)	221 (53.1%)
	No	88 (48.9%)	92 (51.1%)
Dopamine administered	*Yes*	2 (66.7%)	1 (33.3%)
	No	110 (55.3%)	89 (44.7%)
Dobutamine administered	*Yes*	12 (54.5%)	10 (45.5%)
	No	263 (46.4%)	304 (53.6%)
Adrenaline administered	*Yes*	12 (48%)	13 (52%)
	No	263 (46.5%)	302 (53.5%)
Noradrenaline administered	*Yes*	229 (48.1%)	247 (51.9%)
	No	56 (43.8%)	72 (56.3%)
Vasopressin administered	*Yes*	194 (48.4%)	207 (51.6%)
	No	87 (44.2%)	110 (55.8%)
Triliodotryronine administered	*Yes*	47 (48.0%)	51 (52.0%)
	No	223 (46.0%)	262 (54.0%)
Duration in intensive treatment unit (ITU) (days)		3.4±3.5	3.1±2.2
Pancreas cold ischemia time (CIT) (hours)		6.9±2.0	6.8±2.2
Pancreas weight (g)		97.5±28.1	94.8±24.4
Pancreas fibrosis	*Yes*	15 (65.2%)	8 (34.8%)
	No	273 (45.0%)	334 (55.0%)
Pancreas nodular	*Yes*	5 (62.5%)	3 (37.5%)
	No	282 (45.2%)	342 (54.8%)
Pancreas haematomas	*Yes*	54 (62.1%)	33 (37.9%)
	No	231 (41.5%)	325 (58.5%)
Pancreas oedema	*Yes*	3 (50.0%)	3 (50.0%)

		<200K IEQ 'Not transplantable'	≥200K IEQ 'Transplantable'
	No	283 (44.4%)	355 (55.6%)
Pancreas inflammation	*Yes*	2 (33.3%)	4 (66.7%)
	No	286 (44.7%)	354 (55.3%)
Pancreas fatty	*Yes*	171 (43.2%)	225 (56.8%)
	No	119 (47.0%)	134 (53.0%)
Capsular damage	*Yes*	16 (39.0%)	25 (61.0%)
	No	274 (45.5%)	328 (54.5%)
Parenchymal damage	*Yes*	11 (36.7%)	19 (63.3%)
	No	275 (44.9%)	337 (55.1%)

Table A2 Descriptive statistics for explanatory variables within the non-transplantable and transplantable groups

Recipient	1-month	3-months	6-months	9-months	12-months	Total
BR101	X	X				2
ED001	X					1
ED002		X				1
ED003	X*					1
ED007			X		X	2
ED008	X$^{\&}$					1
ED010	X	X				2
ED011	X	X				2
ED022		X				1
ED023	X	X				2
MA002	X	X	X			3
NE002	X	X				1
NE007		X		X	X	3
NE008	X	X				2
NE011		X	X			2
NE013	X		X*		X*	3
NE019	X	X				2
NE020	X	X				2
NE021	X*	X*				2
NE024	X					1
NE025	X					1
NE028		X$^{£,\&}$				1
NE031	X$^{\&}$	X$^{\&}$				2
NE034	X	X				2
OX001	X	X	X			3
OX004	X					1
OX006	X	X	X	X	X	5

Recipient	1-month	3-months	6-months	9-months	12-months	Total
OX007			X			1
OX008	X	X[£]				2
OX009	X					1
OX011			X[£]			1
OX014	X	X				2
OX017	X	X*				2
OX020	X			X		2
OX021	X	X	X			3
OX022	X	X	X			3
OX023		X				1
RF003	X					1
RF004	X					1
RF006				X	X	2
RF007			X			1
RF009		X	X		X	3
RF012		X[&]	X[&]			2
RF013	X	X				2
RF015	X[£]	X[£]				2
Total	32	29	13	4	6	84

Table A3: List of recipients whom attended each specified follow-up clinical visit

*Insulin independent,

[£] Failed graft (90-minute stimulated C-peptide <50pmol/L),

[&] No improvement in hypoglycaemia

Factor (units)	N	Variable type	Descriptive statistics ***Continuous variable:*** ***1) Mean ± SD*** ***2) Median + (range)*** ***Categorical variable:*** ***Number + (percentage)***
Age (years)	84	Continuous	1. 45.9 ± 10.1 2. 48 (17 - 63)
Sex (M/F)	71	Categorical	Male: 34 (48%) Female: 37 (52%)
BMI (Kg/m^2)	84	Continuous	1. 29.4 ± 4.6 2. 29.6 (19 – 37)
Donor type (DBD/DCD)	82	Categorical	DBD: 67 (82%) DCD: 15 (18%)
Cold ischemia time (hours)	36	Continuous	1. 7.1 ± 1.9 2. 7 (4-11)
Islet preparation purity (%)	62	Continuous	1. 73.4 ± 16.1 2. 75 (36-90)
Islet preparation viability (%)	77	Continuous	1. 88.4 ± 5.7 2. 90 (70-97)

Factor (units)	N	Variable type	Descriptive statistics ***Continuous variable:*** ***1) Mean ± SD*** ***2) Median + (range)*** ***Categorical variable:*** ***Number + (percentage)***
Recipient weight (Kg)	84	Continuous	1. 67.9 ± 10.1 2. 66.8 (49.1-98.5)
IEQs transplanted per Kg of recipient body weight (IEQ/Kg)	84	Continuous	1. 6153.6 ± 1825.8 2. 5773.5 (3108-11429)
90-minute stimulated C-peptide (pmol/L)	84	Continuous	1. 502.0 ± 514.8 2. 310 (9-2760)
Glucose Dependent Insulin Secretion Rate (GDISR) score	84	Continuous	1. 0.261 ± 0.326 2. 0.117 (0-1.401)
Beta-2 Score*	66	Continuous	1. 6.102 ± 5.188 2. 4.785 (0.022-27.830)

Table A4: Descriptive statistics for UK clinical islet transplants

* Note: missing daily insulin dosage data for 18 recipients prevented the Beta-2 score from being calculated for all of the 84 visits

Factor	*B* (+95% CI)	*P* Value
Donor Age (years)	-0.0061 (-0.0157 – 0.0035)	0.206
Donor Sex (Female)	0.0294 (-0.2067 – 0.2656)	0.801
Donor BMI (Kg/m^2)	0.0131 (-0.0118 – 0.0381)	0.292
Donor type (DCD)	0.0957 (-0.1977 – 0.3891)	0.513
Pancreas cold ischemia time (hours)	0.0161 (-0.0604 – 0.0928)	0.664
Preparation viability (%)	-0.0065 (-0.1767 – 0.1637)	0.938
Preparation purity (%)	-0.0351 (-0.1899 – 0.1197)	0.646
Time since transplantation (months)	-0.0157 (-0.0290 - -0.0024)	0.023
Number of islets transplanted/Kg of recipient (IEQ/Kg)	0.00008 (0.00003 – 0.00012)	0.003

Table A5: Univariate analysis for factors influencing transplantation outcome, measured using the GDISR score. Analysis restricted to the 66 clinical visits for which the Beta-2 score was calculated

Appendix B

(Chapter 3)

Protein	Blocking buffer; host, dilution, supplier and catalogue	ECM primary antibody; host, dilution, supplier and catalogue	ECM secondary antibody; host, dilution, supplier and catalogue	Insulin primary antibody; host, dilution, supplier and catalogue	Insulin secondary antibody; host, dilution, supplier and catalogue
Collagen I	Goat serum 10%; Vector Laboratories; S-1000	Collagen I polyclonal; Raised in rabbit; 1:300; Abcam, ab34710	Goat anti-rabbit A488; 1:500; Life Technologies, A-110088	Insulin polyclonal; Raised in guinea-pig; 1:100; Dako, A0564	Goat-anti guinea pig Texas Red; 1:100; Vector Laboratories, TI-7000
Collagen II	Goat serum 10%; Vector Laboratories; S-1000	Collagen II polyclonal; Raised in rabbit; 1:300; Abcam, ab34712	Goat anti-rabbit A488; 1:500; Life Technologies, A-110088	Insulin polyclonal; Raised in guinea-pig; 1:100; Dako, A0564	Goat-anti guinea pig Texas Red; 1:100; Vector Laboratories, TI-7000
Collagen III	Goat serum 10%; Vector Laboratories; S-1000	Collagen III polyclonal; Raised in rabbit; 1:300; Abcam, ab7778	Goat anti-rabbit A488; 1:500; Life Technologies, A-110088	Insulin polyclonal; Raised in guinea-pig; 1:100; Dako, A0564	Goat-anti guinea pig Texas Red; 1:100; Vector Laboratories, TI-7000
Collagen IV	Swine serum 5%; Vector Laboratories; S-4000	Collagen IV polyclonal; Raised in goat; 1:100; BioRad, 134001	Donkey anti-goat A488; 1:500; Life Technologies, A-11055	Insulin polyclonal; Raised in guinea-pig; 1:100; Dako, A0564	Donkey anti-guinea pig AlexaFluor 594; 1:500; Jackson ImmunoResearch, 706-585-178
Collagen V	Swine serum 5%; Vector Laboratories; S-4000	Collagen V polyclonal; Raised in goat; 1:300; Abcam, ab189285	Donkey anti-goat A488; 1:500; Life Technologies, A-11055	Insulin polyclonal; Raised in guinea-pig; 1:100; Dako, A0564	Donkey anti-guinea pig AlexaFluor 594; 1:500; Jackson ImmunoResearch, 706-585-178
Collagen VI	Goat serum 10%; Vector Laboratories; S-1000	Collagen VI polyclonal; Raised in rabbit; 1:300; Abcam, ab6588	Goat anti-rabbit A488; 1:500; Life Technologies, A-110088	Insulin polyclonal; Raised in guinea-pig; 1:100; Dako, A0564	Goat-anti guinea pig Texas Red; 1:100; Vector Laboratories, TI-7000
Collagen XVIII	Goat serum 10%; Vector Laboratories; S-1000	Collagen XVIII polyclonal; Raised in rabbit; 1:200; Abcam, ab202973	Goat anti-rabbit A488; 1:500; Life Technologies, A-110088	Insulin polyclonal; Raised in guinea-pig; 1:100; Dako, A0564	Goat-anti guinea pig Texas Red; 1:100; Vector Laboratories, TI-7000
Collagen XXVIII	Goat serum 10%; Vector	Collagen XXVIII polyclonal; Raised in rabbit;	Goat anti-rabbit A488; 1:500; Life	Insulin polyclonal; Raised in guinea-pig;	Goat-anti guinea pig Texas Red; 1:100;

Protein	Blocking buffer; host, dilution, supplier and catalogue	ECM primary antibody; host, dilution, supplier and catalogue	ECM secondary antibody; host, dilution, supplier and catalogue	Insulin primary antibody; host, dilution, supplier and catalogue	Insulin secondary antibody; host, dilution, supplier and catalogue
	Laboratories; S-1000	1:300; Abcam, ab188533	Technologies, A-110088	1:100; Dako, A0564	Vector Laboratories, TI-7000
Pan-Laminin	Goat serum 10%; Vector Laboratories; S-4000	Pan-laminin polyclonal; Raised in rabbit; 1:500; BioRad, AHP420	Goat anti-rabbit A488; 1:500; Life Technologies, A-110088	Insulin polyclonal; Raised in guinea-pig; 1:100; Dako, A0564	Goat-anti guinea pig Texas Red; 1:100; Vector Laboratories, TI-7000
Laminin-α2	Goat serum 10%; Vector Laboratories; S-4000	Laminin-α2 [4H8-2] monoclonal; Raised in rat; 1:100; Abcam, ab11576	Goat anti-rat A488; 1:500; Life Technologies, A-11006	Insulin polyclonal; Raised in guinea-pig; 1:100; Dako, A0564	Goat-anti guinea pig Texas Red; 1:100; Vector Laboratories, TI-7000
Laminin-α3	Goat serum 10%; Vector Laboratories; S-4000	Laminin-α3 [EPR8266] monoclonal; Raised in rabbit; 1:100; Abcam, ab151715	Goat anti-rabbit A488; 1:500; Life Technologies, A-110088	Insulin polyclonal; Raised in guinea-pig; 1:100; Dako, A0564	Goat-anti guinea pig Texas Red; 1:100; Vector Laboratories, TI-7000
Laminin-α5	Goat serum 10%; Vector Laboratories; S-4000	Laminin-α2 [4B12] monoclonal; Raised in mouse; 1:100; Abcam, ab77175	Goat anti-mouse CFL; 1:100; Santa-Cruz, sc-362257	Insulin polyclonal; Raised in guinea-pig; 1:100; Dako, A0564	Goat-anti guinea pig Texas Red; 1:100; Vector Laboratories, TI-7000
Laminin-β1	Goat serum 10%; Vector Laboratories; S-4000	Laminin-β1 polyclonal; Raised in rabbit; 1:100; Abcam, ab69633	Goat anti-rabbit A488; 1:500; Life Technologies, A-110088	Insulin polyclonal; Raised in guinea-pig; 1:100; Dako, A0564	Goat-anti guinea pig Texas Red; 1:100; Vector Laboratories, TI-7000
Laminin-Y1	Goat serum 10%; Vector Laboratories; S-4000	Laminin-Y1 [A5] monoclonal; Raised in rat; 1:100; Abcam, ab80580	Goat anti-rat A488; 1:500; Life Technologies, A-11006	Insulin polyclonal; Raised in guinea-pig; 1:100; Dako, A0564	Goat-anti guinea pig Texas Red; 1:100; Vector Laboratories, TI-7000
Perlecan	Goat serum 10%; Vector Laboratories; S-4000	Perlecan monoclonal; Raised in mouse (against amino acids 4092-4391); 1:300; Santa Cruz, sc-377219	Goat anti-mouse CFL; 1:100; Santa-Cruz, sc-362257	Insulin polyclonal; Raised in guinea-pig; 1:100; Dako, A0564	Goat-anti guinea pig Texas Red; 1:100; Vector Laboratories, TI-7000

Protein	Blocking buffer; host, dilution, supplier and catalogue	ECM primary antibody; host, dilution, supplier and catalogue	ECM secondary antibody; host, dilution, supplier and catalogue	Insulin primary antibody; host, dilution, supplier and catalogue	Insulin secondary antibody; host, dilution, supplier and catalogue
Decorin	Goat serum 10%; Vector Laboratories; S-4000	Decorin polyclonal; Raised in rabbit; 1:100; Abcam, ab137508	Goat anti-rabbit A488; 1:500; Life Technologies, A-110088	Insulin polyclonal; Raised in guinea-pig; 1:100; Dako, A0564	Goat-anti guinea pig Texas Red; 1:100; Vector Laboratories, TI-7000
Nidogen-1	Goat serum 10%; Vector Laboratories; S-4000	Nidogen-1 monoclonal; Raised in mouse; 1:300; Thermo Scientific, 302117	Goat anti-mouse CFL; 1:100; Santa-Cruz, sc-362257	Insulin polyclonal; Raised in guinea-pig; 1:100; Dako, A0564	Goat-anti guinea pig Texas Red; 1:100; Vector Laboratories, TI-7000
Fibronectin	Goat serum 10%; Vector Laboratories; S-4000	Fibronectin polyclonal; Raised in rabbit; 1:100; Abcam, ab23750	Goat anti-rabbit A488; 1:500; Life Technologies, A-110088	Insulin polyclonal; Raised in guinea-pig; 1:100; Dako, A0564	Goat-anti guinea pig Texas Red; 1:100; Vector Laboratories, TI-7000

Table B1: Details of the antibodies and dilutions used in the immunofluorescent staining experiments

Protein	Supplier and (catalogue number)
Collagen I	Cloud-Clone Corp. (SEA350Hu)
Collagen IV	Cloud-Clone Corp. (SEA180Hu)
Collagen V	Cloud-Clone Corp. (SEC152Hu)
Collagen VI	Cloud-Clone Corp. (SED123Hu)
Total laminin	Abcam (ab119599)
Laminin-α2	Cloud-Clone Corp. (SEC074Hu)
Laminin-α5	Cloud-Clone Corp. (SEC078Hu)
Perlecan	Cloud-Clone Corp. (SEA565Hu)
Nidogen-1	Invitrogen (EHNID1)

Table B2: Details of ECM ELISAs

Protein Group	Type	Protein	Identified in Chapter 3 Data Set	Highest mean	Max fold change	*p* value (ANOVA)	Identified by Sackett *et al.*? [163]
Core matrisome	Collagens	Collagen Type 1 Alpha 1 Chain	X	Younger Donors	3.013	0.043	X
Core matrisome	Collagens	Collagen Type 1 Alpha 2 Chain	X	Younger Donors	3.049	0.047	X
Core matrisome	Collagens	Collagen Type 2 Alpha 1 Chain	X	Younger Donors	2.909	0.034	
Core matrisome	Collagens	Collagen Type 2 Alpha 2 Chain		N/A	N/A	N/A	X
Core matrisome	Collagens	Collagen Type 3 Alpha 1 Chain Isoform 1	X	Younger Donors	3.448	0.021	X
Core matrisome	Collagens	Collagen Type 3 Alpha 1 Chain Isoform 2		N/A	N/A	N/A	X
Core matrisome	Collagens	Collagen Type 3 Alpha 2 Chain		N/A	N/A	N/A	X
Core matrisome	Collagens	Collagen Type 4 Alpha 1 Chain	X	Younger Donors	3.146	0.004	X
Core matrisome	Collagens	Collagen Type 4 Alpha 2 Chain	X	Younger Donors	2.804	0.000	X
Core matrisome	Collagens	Collagen Type 4 Alpha 4 Chain	X	Younger Donors	8.414	0.000	X
Core matrisome	Collagens	Collagen Type 4 Alpha 5 Chain	X	Younger Donors	11.547	0.000	X
Core matrisome	Collagens	Collagen Type 5 Alpha 1 Chain	X	Younger Donors	2.957	0.023	X
Core matrisome	Collagens	Collagen Type 5 Alpha 2 Chain	X	Younger Donors	2.454	0.024	X
Core matrisome	Collagens	Collagen Type 5 Alpha 3 Chain	X	Younger Donors	3.705	0.005	X
Core matrisome	Collagens	Collagen Type 6 Alpha 1 Chain	X	Older Donors	1.127	0.685	X
Core matrisome	Collagens	Collagen Type 6 Alpha 2 chain Isoform 2C2	X	Younger Donors	1.215	0.476	X
Core matrisome	Collagens	Collagen Type 6 Alpha 2 chain Isoform 2C2A		N/A	N/A	N/A	X
Core matrisome	Collagens	Collagen Type 6 Alpha 3 Chain	X	Younger Donors	1.748	0.187	X
Core matrisome	Collagens	Collagen Type 6 Alpha 6 Chain	X	Younger Donors	1.982	0.614	X
Core matrisome	Collagens	Collagen Type 7 Alpha 1 Chain		N/A	N/A	N/A	X
Core matrisome	Collagens	Collagen Type 8 Alpha 1 Chain		N/A	N/A	N/A	X
Core matrisome	Collagens	Collagen Type 8 Alpha 2 Chain		N/A	N/A	N/A	X

Protein Group	Type	Protein	Identified in Chapter 3 Data Set	Highest mean	Max fold change	*p* value (ANOVA)	Identified by Sackett *et al.*? [163]
Core matrisome	Collagens	Collagen Type 9 Alpha 3 Chain		N/A	N/A	N/A	X
Core matrisome	Collagens	Collagen Type 10 Alpha 1 Chain		N/A	N/A	N/A	X
Core matrisome	Collagens	Collagen Type 11 Alpha 1 Chain		N/A	N/A	N/A	X
Core matrisome	Collagens	Collagen Type 11 Alpha 2 Chain		N/A	N/A	N/A	X
Core matrisome	Collagens	Collagen Type 12 Alpha 1 Chain	X	Younger Donors	1.738	0.190	X
Core matrisome	Collagens	Collagen Type 13 Alpha 1 Chain		N/A	N/A	N/A	X
Core matrisome	Collagens	Collagen Type 14 Alpha 1 Chain	X	Younger Donors	1.288	0.859	X
Core matrisome	Collagens	Collagen Type 15 Alpha 1 Chain	X	Younger Donors	1.980	0.024	X
Core matrisome	Collagens	Collagen Type 16 Alpha 1 Chain	X	Younger Donors	1.651	0.891	X
Core matrisome	Collagens	Collagen Type 18 Alpha 1 Chain	X	Younger Donors	1.665	0.030	X
Core matrisome	Collagens	Collagen Type 21 Alpha 1 Chain	X	Younger Donors	3.457	0.128	X
Core matrisome	Collagens	Collagen Type 28 Alpha 1 Chain	X	Younger Donors	3.071	0.014	X
		Total collagens	22				33
Core matrisome	Laminins	Laminin α1	X	Older Donors	2.669	0.067	
Core matrisome	Laminins	Laminin α2	X	Younger Donors	4.250	0.005	X
Core matrisome	Laminins	Laminin α3	X	Younger Donors	1.692*	0.047	
Core matrisome	Laminins	Laminin α4	X	Younger Donors	1.936	0.075	X
Core matrisome	Laminins	Laminin α5	X	Younger Donors	1.966	0.120	X
Core matrisome	Laminins	Laminin β1	X	Younger Donors	2.951	0.082	X
Core matrisome	Laminins	Laminin β2	X	Younger Donors	2.386	0.090	X
Core matrisome	Laminins	Laminin γ1	X	Younger Donors	2.363	0.031	X
Core matrisome	Laminins	Laminin γ3	X	Younger Donors	1.218	0.677	X
		Total laminins	9				7
Core matrisome	Non-laminin glycoproteins	Elastin	X	Younger Donors	1.119	0.915	
Core matrisome	Non-laminin glycoproteins	EGF-containing fibulin-like	X	Younger Donors	1.419	0.337	

Protein Group	Type	Protein	Identified in Chapter 3 Data Set	Highest mean	Max fold change	*p* value (ANOVA)	Identified by Sackett *et al.*? [163]
		extracellular matrix protein 1					
Core matrisome	Non-laminin glycoproteins	Fibrillin 1	X	Younger Donors	1.510	0.322	X
Core matrisome	Non-laminin glycoproteins	Agrin	X	Younger Donors	1.280	0.233	X
Core matrisome	Non-laminin glycoproteins	Nidogen-1	X	Younger Donors	1.783	0.031	X
Core matrisome	Non-laminin glycoproteins	Nidogen-2	X	Younger Donors	1.620	0.284	X
Core matrisome	Non-laminin glycoproteins	Fibronectin 1	X	Older Donors	1.255	0.611	X
Core matrisome	Non-laminin glycoproteins	Tubulointerstitial nephritis antigen-like	X	Younger Donors	1.902	0.063	X
Core matrisome	Non-laminin glycoproteins	Extracellular matrix protein FRAS1	X	Younger Donors	1.559	0.056	X
Core matrisome	Non-laminin glycoproteins	FRAS1-related extracellular matrix protein 2	X	Older Donors	1.041	0.981	
Core matrisome	Non-laminin glycoproteins	Fibrinogen alpha Chain	X	Older Donors	4.133	0.047	X
Core matrisome	Non-laminin glycoproteins	Fibrinogen beta Chain	X	Older Donors	5.102	0.062	X
Core matrisome	Non-laminin glycoproteins	Fibrinogen gamma Chain	X	Older Donors	6.260	0.058	X
Core matrisome	Non-laminin glycoproteins	Vitronectin	X	Older Donors	1.044	0.537	X
Core matrisome	Non-laminin glycoproteins	Milk fat globule- EGF Factor 8 protein		N/A	N/A	N/A	X
Core matrisome	Non-laminin glycoproteins	Dermatopontin	X	Younger Donors	2.856	0.211	X
Core matrisome	Non-laminin glycoproteins	Elastin microfibril interfactor 1/ EMILIN 1	X	Older Donors	1.332	0.246	X
Core matrisome	Non-laminin glycoproteins	Elastin microfibril interfactor 2/ EMILIN 2	X	Older Donors	1.203	0.800	
Core matrisome	Non-laminin glycoproteins	Tenascin XB	X	Older Donors	7.213	0.214	X
Core matrisome	Non-laminin glycoproteins	Periostin	X	Older Donors	1.427	0.407	X
Core matrisome	Non-laminin glycoproteins	Transforming growth factor Beta induced	X	Younger Donors	1.457	0.885	X
Core matrisome	Non-laminin glycoproteins	Insulin like growth factor binding protein 7		N/A	N/A	N/A	X
Core matrisome	Non-laminin glycoproteins	von Willebrand factor A domain-containing protein 1	X	Younger Donors	1.050	0.992	X

Protein Group	Type	Protein	Identified in Chapter 3 Data Set	Highest mean	Max fold change	*p* value (ANOVA)	Identified by Sackett *et al.*? [163]
Core matrisome	Non-laminin glycoproteins	Thrombospondin 1		N/A	N/A	N/A	X
Core matrisome	Non-laminin glycoproteins	Nephronectin	X	Younger Donors	1.849	0.017	X
Core matrisome	Non-laminin glycoproteins	Fibulin 1		N/A	N/A	N/A	X
Core matrisome	Non-laminin glycoproteins	Fibulin 2	X	Younger Donors	1.164	0.903	
Core matrisome	Non-laminin glycoproteins	Insulin like growth factor binding protein 2		N/A	N/A	N/A	X
Core matrisome	Non-laminin glycoproteins	Latent transforming growth factor beta binding protein	X	Older Donors	1.733	0.403	X
Core matrisome	Non-laminin glycoproteins	Olfactomedin-like protein 1	X	Younger Donors	1.161	0.522	
Core matrisome	Non-laminin glycoproteins	Olfactomedin-like protein 3	X	Younger Donors	1.669	0.097	
		Total non-laminin glycoproteins	26				24
Core matrisome	Proteoglycans	Perlecan	X	Younger Donors	2.263	0.082	X
Core matrisome	Proteoglycans	Biglycan	X	Younger Donors	1.054	0.705	X
Core matrisome	Proteoglycans	Prolargin	X	Younger Donors	1.335	0.717	X
Core matrisome	Proteoglycans	Decorin	X	Younger Donors	1.466	0.324	X
Core matrisome	Proteoglycans	Asporin	X	Younger Donors	1.922	0.160	X
Core matrisome	Proteoglycans	Lumican	X	Younger Donors	1.692	0.176	X
Core matrisome	Proteoglycans	Osteoglycan/Mimecan	X	Younger Donors	1.245	0.317	X
Core matrisome	Proteoglycans	Fibromodulin		N/A	N/A	N/A	X
Core matrisome	Proteoglycans	Versican	X	Older Donors	1.626	0.330	
		Total proteoglycans	8				8
Matrix-associated	ECM regulators	Protease serine 1		N/A	N/A	N/A	X
Matrix-associated	ECM regulators	Protease serine 2		N/A	N/A	N/A	X
Matrix-associated	ECM regulators	Protease serine 3		N/A	N/A	N/A	X
Matrix-associated	ECM regulators	Chymotrypsin Like Elastase Family Member 2A		N/A	N/A	N/A	X

Protein Group	Type	Protein	Identified in Chapter 3 Data Set	Highest mean	Max fold change	*p* value (ANOVA)	Identified by Sackett *et al.*? [163]
Matrix-associated	ECM regulators	Chymotrypsin Like Elastase Family Member 2B	X	Older Donors	1.303	0.610	X
Matrix-associated	ECM regulators	Chymotrypsin Like Elastase Family Member 3A		N/A	N/A	N/A	X
Matrix-associated	ECM regulators	Chymotrypsin Like Elastase Family Member 3B		N/A	N/A	N/A	X
Matrix-associated	ECM regulators	Chymotrypsin C	X	Older Donors	3.331	0.394	
Matrix-associated	ECM regulators	Chymotrypsin-like protease CTRL-1	X	Younger Donors	2.489	0.547	
Matrix-associated	ECM regulators	Transglutaminase 2		N/A	N/A	N/A	X
Matrix-associated	ECM regulators	Cathespin D		N/A	N/A	N/A	X
Matrix-associated	ECM regulators	Alpha-1-microglobulin/Bikunin precursor		N/A	N/A	N/A	X
Matrix-associated	ECM regulators	Serine family A member 1		N/A	N/A	N/A	X
Matrix-associated	ECM regulators	Serine family A member 3		N/A	N/A	N/A	X
Matrix-associated	ECM regulators	Serine family B member 1		N/A	N/A	N/A	X
Matrix-associated	ECM regulators	Serine family G member 1		N/A	N/A	N/A	X
Matrix-associated	ECM regulators	Serine family H member 1/ Serpin H1	X	Younger Donors	1.613	0.416	X
Matrix-associated	ECM regulators	Serine family 1 member 2		N/A	N/A	N/A	X
Matrix-associated	ECM regulators	Cystatin B		N/A	N/A	N/A	X
Matrix-associated	ECM regulators	Cystatin C		N/A	N/A		X
Matrix-associated	ECM regulators	Cathespin B	X	Older Donor	1.558	0.336	X
Matrix-associated	ECM regulators	Alpha-2-macroglobulin		N/A	N/A		X
Matrix-associated	ECM regulators	Inter-alpha-trypsin inhibitor heavy chain H5	X	Older Donor	2.208	0.341	X
Matrix-associated	ECM regulators	Kininogen 1		N/A	N/A		X
		Total ECM regulatory	6				22
Matrix-associated	ECM-affiliated proteins	Annexin 1	X	Older Donors	1.902	0.300	X

Protein Group	Type	Protein	Identified in Chapter 3 Data Set	Highest mean	Max fold change	*p* value (ANOVA)	Identified by Sackett *et al.*? [163]
Matrix-associated	ECM-affiliated proteins	Annexin 2	X	Older Donors	1.896	0.209	X
Matrix-associated	ECM-affiliated proteins	Annexin 3		N/A	N/A		X
Matrix-associated	ECM-affiliated proteins	Annexin 4	X	Younger Donors	1.249	0.242	X
Matrix-associated	ECM-affiliated proteins	Annexin 5		N/A	N/A		X
Matrix-associated	ECM-affiliated proteins	Annexin 6	X	Younger Donors	1.246	0.730	X
Matrix-associated	ECM-affiliated proteins	Annexin 7		N/A	N/A		X
Matrix-associated	ECM-affiliated proteins	Annexin 11	X	Older Donors	1.556	0.169	X
Matrix-associated	ECM-affiliated proteins	Regenerating family member 1 alpha		N/A	N/A		X
Matrix-associated	ECM-affiliated proteins	Regenerating family member 3 alpha		N/A	N/A		X
Matrix-associated	ECM-affiliated proteins	Regenerating family member 1 beta		N/A	N/A		X
Matrix-associated	ECM-affiliated proteins	Lectin, Mannose binding 1		N/A	N/A		X
Matrix-associated	ECM-affiliated proteins	Galectin 1	X	Older Donors	1.512	0.317	X
Matrix-associated	ECM-affiliated proteins	Galectin 2		N/A	N/A		X
Matrix-associated	ECM-affiliated proteins	Galectin 3	X	Older Donors	4.288	0.127	X
Matrix-associated	ECM-affiliated proteins	Galectin 4	X	Older Donors	3.793	0.073	X
Matrix-associated	ECM-affiliated proteins	Galectin 8		N/A	N/A		X
Matrix-associated	ECM-affiliated proteins	Ciq And TNF Related 2		N/A	N/A		X
Matrix-associated	ECM-affiliated proteins	Ciq And TNF Related 5		N/A	N/A		X
Matrix-associated	ECM-affiliated proteins	Hemopexin		N/A	N/A		X
Matrix-associated	ECM-affiliated proteins	Extracellular superoxide dismutase [Cu-Zn]	X	Younger Donors	1.164	0.772	
		Total ECM affiliated	9				20
Matrix-associated	Secreted factors	S100 Calcium Binding Protein A10	X	Older Donors	3.761	0.212	X
Matrix-associated	Secreted factors	S100 Calcium Binding Protein A11		N/A	N/A	N/A	X
Matrix-associated	Secreted factors	S100 Calcium Binding Protein A13		N/A	N/A	N/A	X

Protein Group	Type	Protein	Identified in Chapter 3 Data Set	Highest mean	Max fold change	*p* value (ANOVA)	Identified by Sackett *et al.*? [163]
Matrix-associated	Secreted factors	Hornerin		N/A	N/A	N/A	X
Matrix-associated	Secreted factors	CFC1B		N/A	N/A	N/A	X
Matrix-associated	Secreted factors	Host cell factor C1		N/A	N/A	N/A	X
		Total secretory proteins	1				6
		FINAL TOTAL (Core matrix + Matrix associated)	**81**				**120**

Table B3: List of ECM proteins identified in the decellularised human pancreas
The *p* values highlighted in red indicate those that were statistically significant when comparing protein quantities between younger and older donors. In total, the expression of 20 ECM proteins were significantly affected by age.
Data in final column lists the proteins that were identified in the 2018 study by Sackett *et al*. [163]
N/A; represents the proteins that were only detected in the Sackett et al study (and not this thesis). Therefore, this information was not applicable to these columns.

Appendix C
(Chapter 4)

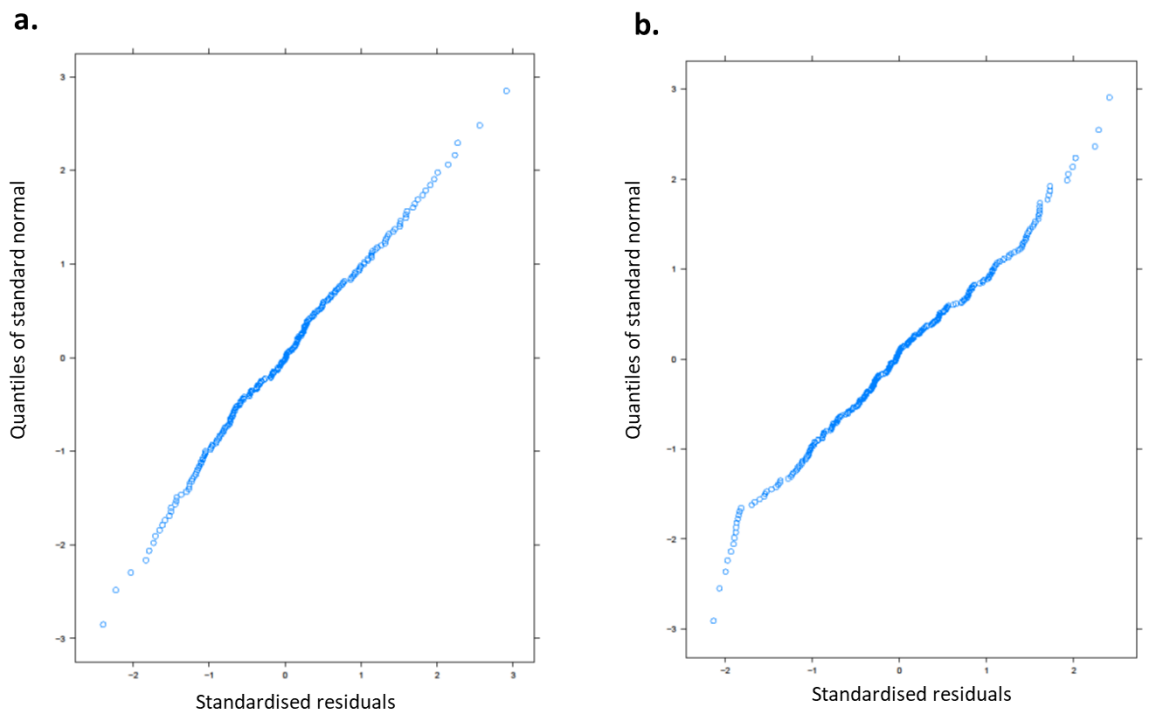


Figure C1: Q-Q normality plots of residuals for transformed semi-quantified measurements of collagen IV and laminin α5

The normality of the a. collagen IV and b. laminin α5 residuals were tested post transformation using Q-Q plots. The standardised residuals (i.e. as determined from the model) are plotted against residuals that come from a theoretical normal distribution (i.e. the quantiles of standard normal). The formation of a straight line indicates that the model residuals come from a normal distribution.

Q-Q; quantile-quantile

Appendix D

(Chapter 5)

Protein	Blocking buffer; host, dilution, supplier and catalogue	ECM primary antibody; host, dilution, supplier and catalogue	ECM secondary antibody; host, dilution, supplier and catalogue	Insulin primary antibody; host, dilution, supplier and catalogue	Insulin secondary antibody; host, dilution, supplier and catalogue
Collagen I	Goat serum 10%; Vector Laboratories; S-1000	Collagen I polyclonal; Raised in rabbit; 1:300; Abcam, ab34710	Goat anti-rabbit A488; 1:500; Life Technologies, A-110088	Insulin polyclonal; Raised in guinea-pig; 1:100; Dako, A0564	Goat-anti guinea pig Texas Red; 1:100; Vector Laboratories, TI-7000
Collagen V	Swine serum 5%; Vector Laboratories; S-4000	Collagen V polyclonal; Raised in goat; 1:300; Abcam, ab189285	Donkey anti-Goat A488; 1:500; Life Technologies, A-11055	Insulin polyclonal; Raised in guinea-pig; 1:100; Dako, A0564	Donkey anti-guinea pig AlexaFluor 594; 1:500; Jackson ImmunoResearch, 706-585-178
Collagen VI	Goat serum 10%; Vector Laboratories; S-1000	Collagen VI polyclonal; Raised in rabbit; 1:300; Abcam, ab6588	Goat anti-rabbit A488; 1:500; Life Technologies, A-110088	Insulin polyclonal; Raised in guinea-pig; 1:100; Dako, A0564	Goat-anti guinea pig Texas Red; 1:100; Vector Laboratories, TI-7000
Pan-laminin	Goat serum 10%; Vector Laboratories; S-4000	Pan-laminin polyclonal; Raised in rabbit; 1:500; BioRad, AHP420	Goat anti-rabbit A488; 1:500; Life Technologies, A-110088	Insulin polyclonal; Raised in guinea-pig; 1:100; Dako, A0564	Goat-anti guinea pig Texas Red; 1:100; Vector Laboratories, TI-7000
Nidogen-1	Goat serum 10%; Vector Laboratories; S-4000	Nidogen-1 monoclonal; Raised in mouse; 1:300; Thermo Scientific, 302117	Goat anti-mouse CFL; 1:100; Santa-Cruz, sc-362257	Insulin polyclonal; Raised in guinea-pig; 1:100; Dako, A0564	Goat-anti guinea pig Texas Red; 1:100; Vector Laboratories, TI-7000
Perlecan	Goat serum 10%; Vector Laboratories; S-4000	Perlecan monoclonal; Raised in mouse (against amino acids 4092-4391); 1:300; Santa Cruz, sc-377219	Goat anti-mouse CFL; 1:100; Santa-Cruz, sc-362257	Insulin polyclonal; Raised in guinea-pig; 1:100; Dako, A0564	Goat-anti guinea pig Texas Red; 1:100; Vector Laboratories, TI-7000

Table D1: Summary of the materials used in the slide-based digestion experiments

Protein	Expected band (KDa) and *reference*	Protein supplier and catalogue	Concentration (supplied by manufacturer)	Concentration (as determined by BCA)	µl required for 5µg	Purified Protein Diluent	Primary antibody; supplier and catalogue	Primary antibody host species and dilution	WesternBreeze kit and catalogue	Chromogen development time (mins)	Band examined (KDa)
Collagen IV	α1-6; all 160 *[211, 367]*	Sigma; C5533-5mg	Made to 2.5mg/ml upon receipt	0.77mg/ml	6.5	1 X PBS	BioRad; 134001	Goat; 1:1500 Polyclonal	Goat (WB7107)	10	160
Collagen I	α1; 139 α2; 129	Abcam; ab7533	1mg/ml	0.77mg/ml	6.5	4.1% sodium acetate	Abcam; ab34710	Rabbit; 1:2000 Polyclonal	Rabbit (WB7105)	10	120
Collagen VI	α1,2; 140 α3; 240 *[211]*	Abcam; ab7538	1mg/ml	0.9mg/ml	5.5	0.6% acetic acid	Abcam; ab6588	Rabbit; 1:2000 Polyclonal	Rabbit (WB7105)	4	100
Nidogen-1	139 *[368]*	R&D Systems; MA5-23911	Made to 0.5mg/ml upon receipt	0.77mg/ml	6.5	1 X PBS	ThermoFisher; MA5-23911	Mouse; 1:2000 Monoclonal	Mouse (WB7103)	7	1. 130 2. 80
Pan-laminin	α1; 337 α2; 343 α3(A);189 (B);366 α4; 202 α5; 399 β1; 198 β2; 195 β3; 129 ϒ1; 177 ϒ2; 130 ϒ3; 171 *[369]*	Sigma; L6274-5mg	0.6mg/ml (lot specific)	0.66mg/ml	7.5	1 X TBS	BioRad; AHP420	Rabbit; 1:1500 Polyclonal	Rabbit (WB7105)	20	170

Table D2: Summary of materials and methods used for the purified protein digestion and western blotting experiments

The expected band represents that referenced in the literature, for the specific chains that make up the protein. The band examined is taken from the manufacturer's recommendation, which was also the most prominent band on the blot.

	Molecular Weight of protein band investigated	Collagenase Only	NP Only	Collagenase & NP
Laminin	170KDa	30 min; 20±6%, 2 Hour; 36±2% O/n; 9±5%	30 min; 26±22% 2 Hour; 63±24% O/n; 43±20%	30 min; 35±13%, 2 Hour; 42±14% O/n; 30±11%
Collagen IV	160KDa	30 min; 50±13%, 2 Hour; 62±4%, O/n; 72±4%;	30 min; 17±14% 2 Hour; 41±8% O/n; 49±5%	30 min; 40±17% 2 Hour; 77±3% O/n; 81±0%
Nidogen-1	130KDa	30 min; 70±0%, 2 Hour; 83±3%, O/n; 84±1%;	30 min; 76±3%, 2 Hour; 88±3%, O/n; 84±2%;	30 min; 74±3%, 2 Hour; 91±3%, O/n; 89±1%;
Nidogen-1	80KDa	30 min; + 409±95% 2 Hour; +444±104% O/n; + 245±5%,	30 min; + 38±11%, 2 Hour; 13±17% O/n; 57±1%	30 min; + 328±83% 2 Hour; + 133±85% O/n; 57±1%
Collagen I	120KDa	30 min; 44±20%, 2 Hour; 58±5% O/n; 59±6%	30 min; 17±6%, 2 Hour; 25±13%, O/n; 10±19%	30 min; 53±4% 2 Hour; 53±8% O/n; 59±7%
Collagen VI	100KDa	30 min; 63±7% 2 Hour; 67±5% O/n; 74±3%	30 min; 1±11% 2 Hour; 10±12% O/n; 13±4%	30 min; 71±2% 2 Hour; 69±6% O/n; 72±2%

Table D3: Summary of enzyme mediated protein digestion, of purified proteins, detected using western blotting

Displayed is the percentage loss of protein (± SEM) with each enzyme treatment, compared to the respective controls. The '+', seen in the treatment of nidogen, indicates an increase as compared to control.

NP; Neutral Protease

O/n; overnight

Appendix E

(Chapter 6)

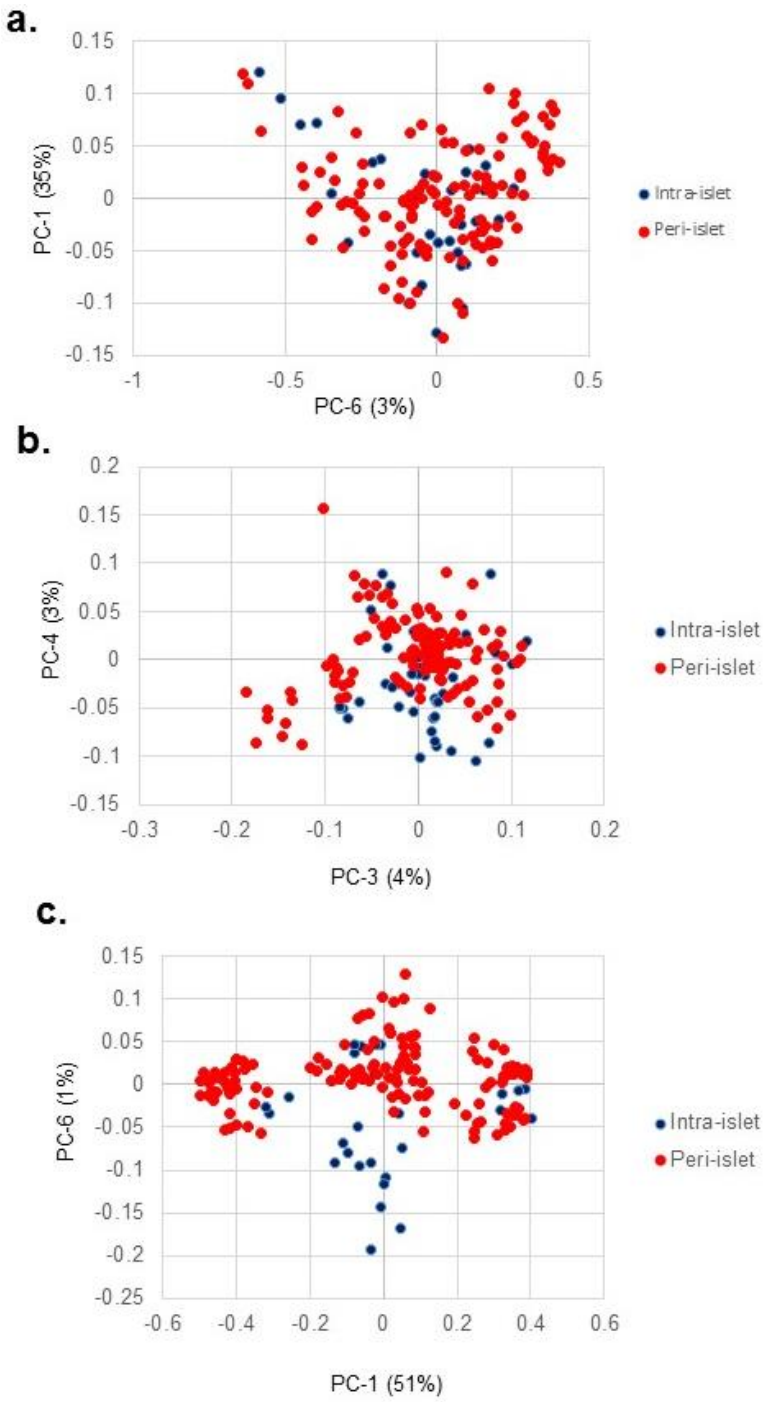


Figure E1: PCA of Raman spectra obtained from the intra- and peri-islet ECM
a. Collagenase treated tissue, **b.** neutral protease treated tissue, **c.** collagenase and neutral protease treated tissue. For all enzyme treatments ECM location did not influence ECM digestion. This led to the measurements from the two locations being combined.
Peri-islet; Islet peripheral
PCA; Principle component analysis
PC; Principle component